



# BULLETIN OF THE MINERAL RESEARCH AND EXPLORATION

<http://bulletin.mta.gov.tr>

BULLETIN OF THE MINERAL RESEARCH AND EXPLORATION	
CONTENTS	
NEOGENE STRATIGRAPHY OF THE İZMİR -OUTER- BAY ISLANDS	Fikret GÖKTAŞ <sup>a*</sup>
Research Article	

## NEOGENE STRATIGRAPHY OF THE İZMİR -OUTER- BAY ISLANDS

Fikret GÖKTAŞ<sup>a\*</sup>

<sup>a</sup>119/8 Sok., 6/5, K.3, D.9, Evka-3, Bornova, İZMİR

Research Article

### Keywords:

Gulf of Izmir, Neogene Stratigraphy, Middle Miocene Deposition, Alkaline Basic Volcanism, K/Ar Geochronology

### ABSTRACT

The volcanoclastics, derived from calcalkaline acidic-intermediate volcanism in the region during late Early Miocene, and lacustrine deposits of Middle Miocene and alkaline volcanics are exposed on Uzun Island, Hekim Island, Çiçek Island and Karantina Island in the Outer Gulf of Izmir. Kocadağ volcanoclastics derived from Kocadağ volcanism, by extruding mainly calcalkaline andesitic-dacitic products during Late Early Miocene, represents the exposed oldest rock unit. The volcanoclastic succession extending in the north of Uzun Island is composed of pyroclastics in ignimbrite and blocky ash flow facieses, and epiclastics in volcanic mass flow (lahar) facies. Foça tuff, represented by rhyolitic ignimbrites, originated from an area around Foça and moving to an area around Uzun Island, emplaced onto the Kocadağ volcanoclastics in two main explosive stages. The Değirmen-tepe Member alluvial deposits composed of coarse volcanic detritus were deposited during a inactive period between the explosion stages. A K/Ar age of 16.0 Ma was obtained from a rhyolite dome, which shows lateral relationship with the correlant ignimbrites in Foça Peninsula, and so it is considered that Foça tuff emplaced onto the region at the end of late Early Miocene. Lacustrine-dominated Middle Miocene succession, which overlies the Foça tuff unconformably, differentiated as the Urla group. Urla group consists of alluvial Beşik-tepe Formation, the Pırnallı Island volcanoclastics, which is composed of sublacustrine volcanic density-flow deposits and felsic ignimbrites, Hekim Island basalt comprising basic volcanics and lacustrine Urla limestone, respectively from bottom to top. Beşik-tepe formation only exposed on Uzun Island, overlies the Foça tuff with an unconformity indicating a basin margin deposition during the Middle Miocene. Pırnallı Island volcanoclastic succession, which its lower boundary does not expose within the area on Hekim Island and Çiçek Islands, is mainly composed of epiclastics deposited by the dynamics of sublacustrine gravity flow and includes trachytic ignimbrite layers in various welding degrees. The main lithologic components of Pırnallı Island volcanoclastics derived from alkaline trachytic volcanism, which was active during the Middle Miocene in Menteş Peninsula. The eruption center of Hekim Island basalt intruding as a sill to the bottom of Urla limestone succession is on Hekim Island. Along the upper contact of the basalt intruding backshore deposits at the bottom of Urla limestone, the peperites occurred reflecting the interaction between molten lava and unconsolidated sediment. A K/Ar age of 14,8±0,8 Ma is obtained from the basic lavas called as trachybasalt and basaltic trachyandesite according to the major element composition. Hekim Island basalt, which exposed at the center of Foça Depression, can be correlated with both the Ilpınar basalt in Foça Peninsula and the Ovacık basalt in Urla basin with respect to chrono- and lithostratigraphy. Urla limestone succession, which progressively overlies Hekim Island basalt, begins with backshore mudstones, continues with foreshore deposits comprising stromatolitic oncooids and algal bioclasts and lasts with cherty limestones.

Received: 28.08.2015

Accepted: 19.11.2015

## 1. Introduction

This study is towards the stratigraphy of the Neogene rock units outcropping in the İzmir outer bay islands of Uzun Island, Hekim Island, Çiçek Islands and Karantina Island and their correlation with the units in the Foça Depression (Kaya, 1979, 1981). The Foça Depression mainly represents continuous lake sedimentation all along Miocene-Early Pliocene and it is known that with the development of İzmir Bay the Foça Depression has lost its unity. (Figure1A). Foça

and Urla parts and eastern shore section of Karaburun are the parts of the Foça Depression, which is above the sea level to day. The rock units in the islands group had not been studied in the concept of correlating them with the Foça Depression. So it was considered that the islands group would be a good place to study the rock units to correlate them with the Foça depression (Figure 1 B). Summaries of proposed Neogene stratigraphies for different parts are given in (Figure 2). Stratigraphy of the study area, relative sizes have been

\*Corresponding author: Fikret Göktas, [fikretgoktas50@gmail.com](mailto:fikretgoktas50@gmail.com)  
<http://dx.doi.org/10.19111/bmre.86643>

studied in the Uzun Island and Hekim Island as they are high enough from the sea level and provide good outcrops to study. Volcanoclastic facieses described in the text have been classified according to Cas and Wright (1987).

## 2. Stratigraphy

Main rock units cropping out in the islands group are continental Miocene sediments and volcanics. Stratigraphic succession consists of Early Miocene felsic-mafic-intermediate volcanoclastics and dominant Middle Miocene lake sediments and laterally associated felsic-mafic volcanics. Andezitic-dasitic Kocadağ volcanoclastics are associated with the Kocadağ volcanics (Türkecan et al., 1998). Rhyolitic Foça tuffs generated from the Foça volcanic centre (Kaya, 1979, 1981). Kocadağ volcanics and Foça tuffs are the units of Early Miocene calk alkali volcanisms outcropping in the study area. Middle Miocene sedimentation has been studied within the Urla group. Foça tuffs mainly consist of lake sediments overlie the Middle Miocene sediments with an unconformity starting with alluvial fan deposits Between Urla basin and Hekim Island bimodal Middle Miocene volcanisms were active (Helvacı et al., 2009; Göktaş, 2011). They are represented with felsic volcanoclastics participating with lake sedimentations and mafic volcanics (Figure 3).

### 2.1. Kocadağ Volcanoclastics

The succession consisting of mainly andeziric, less dacitic volcanics origin sediments is considered to be related to the Kocadağ volcanics. The farthest away extended unit of the Kocadağ volcanics crop out only in Uzun Island (Figure 4). Göktaş (2011) reported the presence of volcanoclastics in Uzun Island generated from the Kocadağ volcanic complex.

The succession consists of pyroclastic and epiclastic sediments displaying typical scarlet-brown colour on the alteration surfaces. Pyroclastic flow sediments consist of ignimbrite and blocky ash flow facieses mainly of andesitic-dacitic volcanic origin. Ignimbrites consisting with different size lava blocks of the same origin differ from blocky ash flow levels. Epiclastic sediments in the blocky volcanic flow (lahar) facieses consist of andesitic, dacitic coarse fragments (Figure 5A). Levels represented

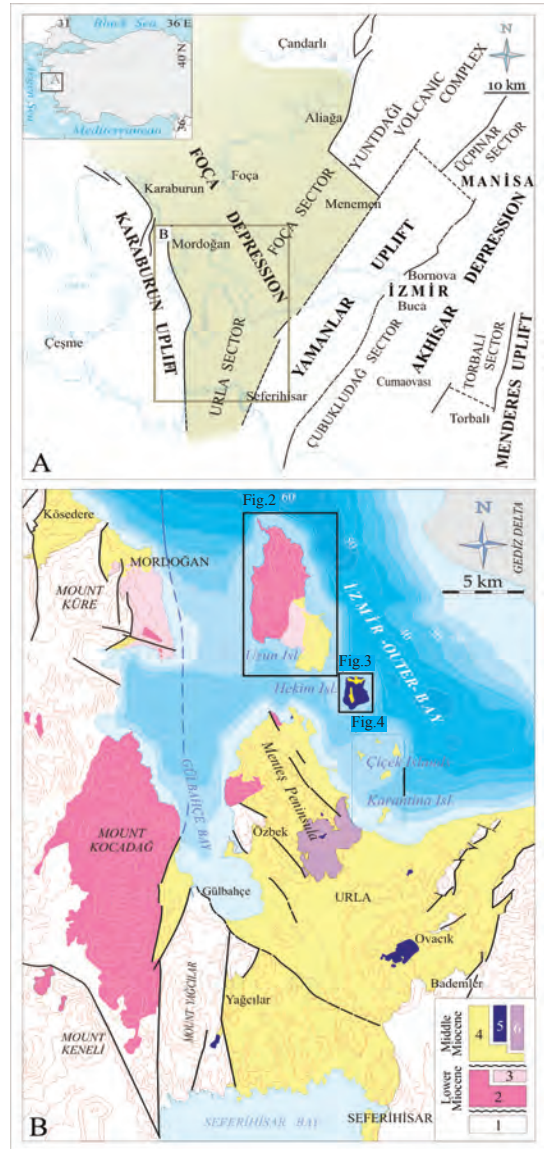


Figure 1- Position of the study area within the Foça Depression (modified from Kaya, 1979) (A) and in the Outer Gulf of İzmir (B). 1. Pre-Neogene basement, 2. Kocadağ volcanics, 3. Foça tuff, 4. Middle Miocene deposits, 5. Alkaline basic volcanics, 6. Alkaline acidic volcanics ("Menteş trachyte": Kaya, 1979). Bathymetry of the Outer Gulf is taken from Sayın (2003).

with matrix supported inhomogeneous pebble stones and pebbly sandstones are massive. Size rate of most of semi rounded pebbles and blocks (most 90 cm) vary vertical and lateral directions. Matrix is made of badly graded coarse-very coarse grained volcanic sands and mainly consists of granules of volcanic materials. In the succession thickness of felsic tuff interlayer's consisting base surge and/or ash fall facieses materials are most 12 m thick. Centimeter-decimeter thick parallel tuff layers

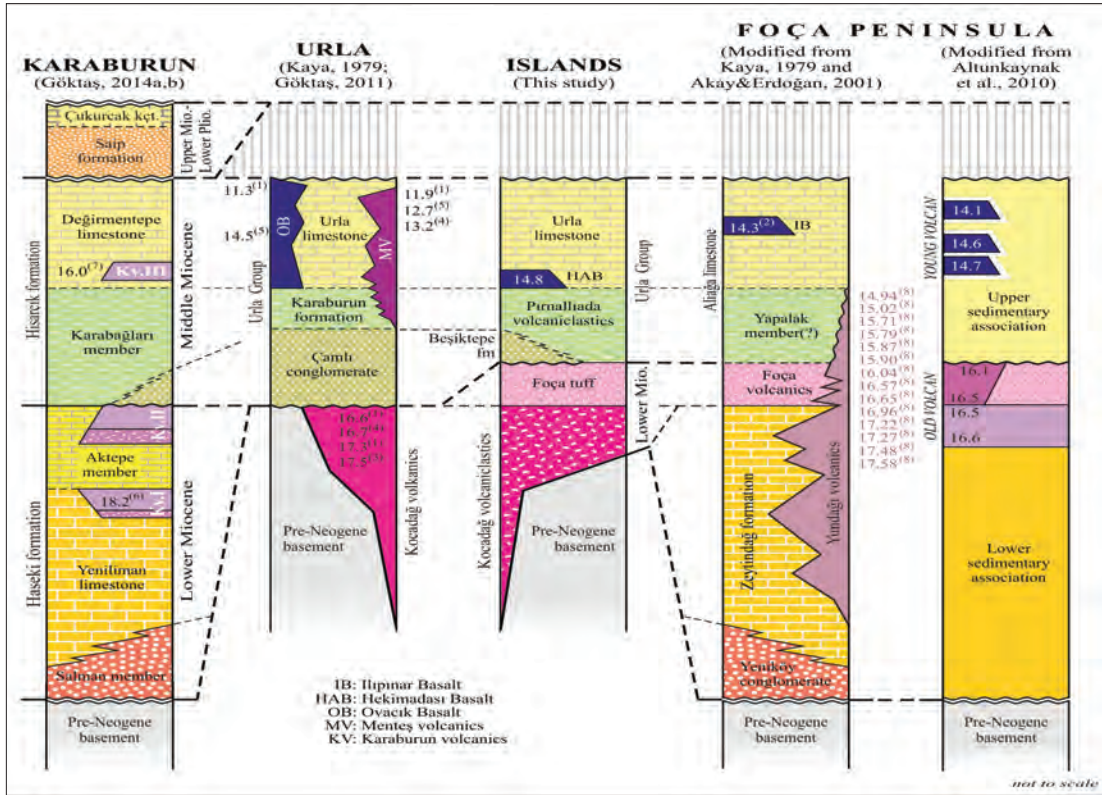


Figure 2- Correlation of proposed stratigraphic sequences for different parts of Foça depression basin. (1)Borsi et al. (1972), (2) Ercan et al. (1996), (3)Helvacı et al. (2009), (4)Karacık et al. (2013), (5)Göktaş (2011), (6)Göktaş (2014a), (7) Göktaş (2014b), (8) Seghedi et al. (2015).

seldom are made of accretionary lapillies. Within the succession there are laterally discontinuous lacustrine sediment intercalations (Figure 5B). Carbonate containing clay stone and fine-medium size grained sandstone are the units of the temporary lake sediments consisting of volcanic materials. Massive or normal graded sandstone intecalations have characteristic fossils indicating local bio turbulences. Some of the typically parallel thin bedded/laminated claystones-siltstones have been subjected to soft sedimentary deformation (Figure 5C).

## 2.2. Foça Tuff

Pyroclastic successions represented with rhyolitic ignimbrites in the Foça Peninsula have been described first time by Kaya (1979). Since Kaya (1979) the ignimbrites in the Foça Peninsula have been studied by Kaya, 1981, Kaya and Savaşçın, 1981; Akay, 2000; Altunkaynak and Yılmaz, 2000; Akay and Erdoğan, 2001, 2004; Altunkaynak et al., 2006, 2010; Agostini

et al., 2010 and indicated that their extensions in the study area are represented by ignimbrites. Within the succession presence of discontinuous alluvium fan intercalations have been described as Değirmentepe member. The succession crops out only in Uzun Island and with the Değirmentepe member the thickness is maximum about 250 metres.

Whitish, light gray unwelded ignimbrites show exfoliations (Figure 6A). Main body of metric scale thick ignimbrites has centimeter-decimeter thick parallel tuff beds with ash falls and/or pyroclastic surge levels. With the overlying flows they have been mostly reduced and the succession in general has been protected only in some local areas (Figure 6B). Centimetric scale juvenile clasts, found in the main body of ignimbrites are represented by round cornered-semi round pumice and lava fragments of same origin. Same origin lithic rhyolites are mainly bluish dark gray and burgundy coloured and have aphyric or porphyritic textures.



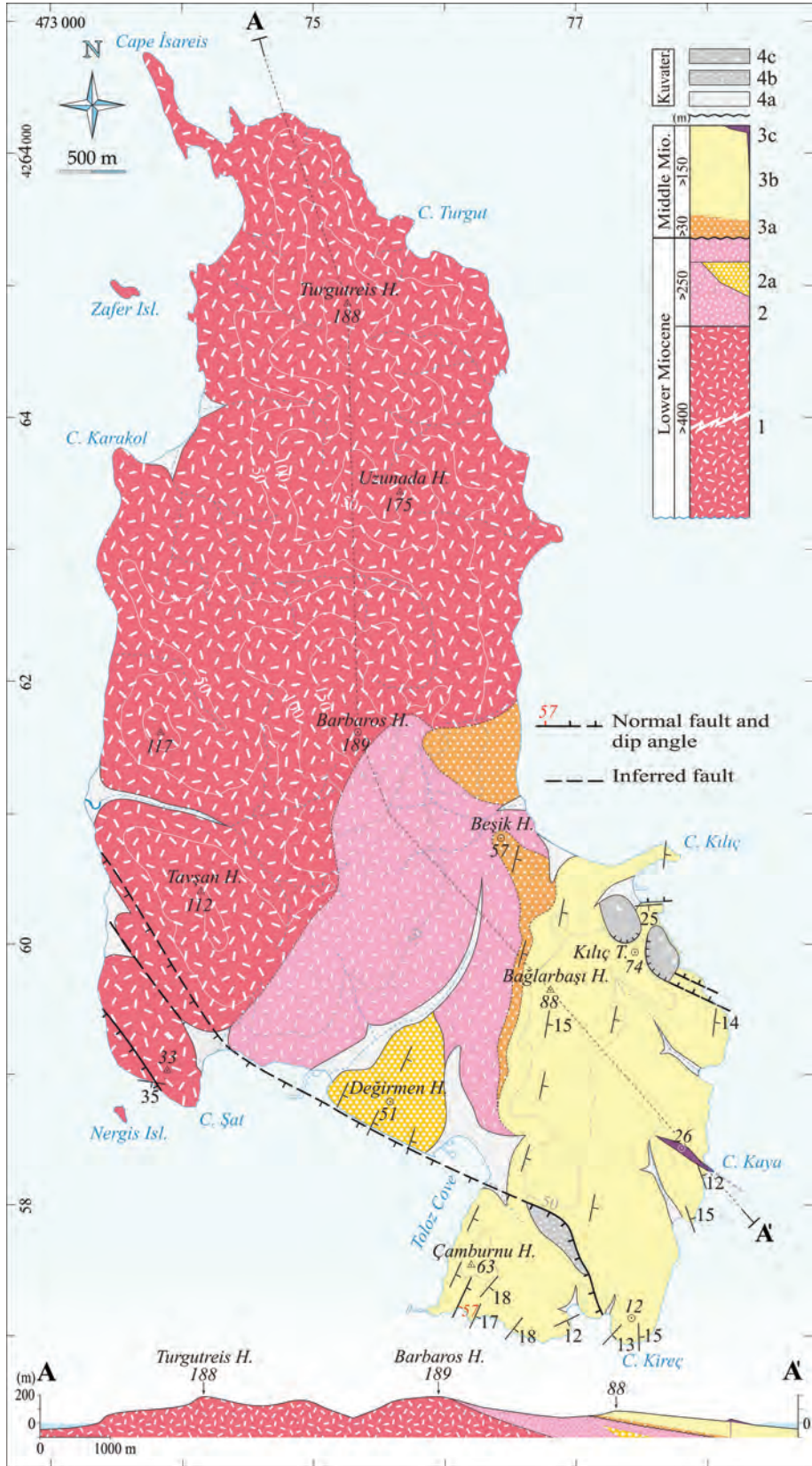


Figure 4- Geological map of Uzun Island. 1. Kocadağ volcanoclastics, 2. Foça tuff (a: Değirmen H. member), 3. Urla group (a: Beşiktepe fm., b: Urla limestone, c: Hekim Island basalt), 4. Quaternary deposits (a: Alluvium, b: Slope debris, c: Landslide debris).



Figure 5- A) Volcanic mass flow (lahar) levels. B) Planar parallel thin bedded-laminated lacustrine deposits. C) Green coloured laminated claystone level within the lacustrine succession was fluidized and subjected to a ductile deformation by flexural flow probably as a result of seismic shocks of a volcanic explosion.

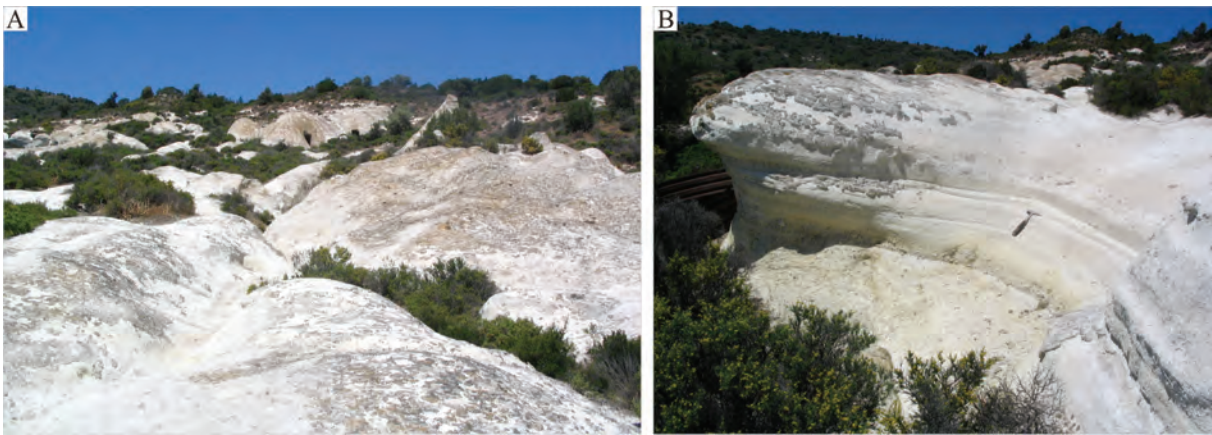


Figure 6- Foça tuff. A) General view. B) Ignimbrite units distinguished by possible base surge levels.

### 2.2.1. Değirmen-tepe Member

Volcanic pebble stone–pebbly sandstone succession present within the Foça tuffs as an interlayer has been named as Değirmen-tepe member (Figures 3 and 4). The thickness is maximum 150 metres.

Sedimentary succession mainly consists of blocky pebble stones with large pebbles. The beds are decimetre-meter thick, basal contacts in many places are eroded and are irregular. Pebbles are matrix supported of coarse-very coarse fragmented volcanic sand and granule matrix. In places where percentage of pebble fragments is increased, matrix material is still present in between the pebble fragments. Rock types present have been generated from the Kocadağ volcanoclastics. Rickety felsic pyroclastites derived from the Foça tuffs have mostly been ground and they are mostly seen in the matrix. They are mainly scarlet-burgundy coloured and are porphyritic andesitic-

dacitic lava pebbles and blocks and are in general semi rounded or rounded. Degree of roundness has been inherited from the original rocks. Volcanic sandstones are faded yellow coloured and are not well graded, have small pebbles, with the decimetre thick massive levels, they separate multiple bedded pebble stones or they are laterally discontinuous intercalations.

Sedimentary succession represents block flow dominated alluvium fan deposition. Levels with high pebble-block rates display disorganized texture and it is mainly related to the debris flow facieses. Massive sandstones have also been sedimented by block flow dynamics.

### 2.3. Urla Group

Urla group was first defined by Gökteş (2011) in the Urla basin. The group includes Miocene dominantly lake sedimentation and laterally associated

alkali volcanics. In the study area The Urla group is represented by alluvial Beşiktepe formation, Pınallı Island lake volcanoclastics, Hekim Island basalts and Urla lake limestones (Figure 3)

### 2.3.1. Beşiktepe Formation

The succession consisting of pebblestone-sandstone has first time been studied in detail within the formation level. Known thickness of the succession cropping out in the Uzun Island is about 50-150 metres (Figure 3, 4).

The succession is orange coloured and consists of laterally discontinuous pebblestones and mainly sandstones. Materials mainly derived from the Kocadağ volcanoclastics and Foça tuffs. Pebbles of the pebblestones are within the limits of small round-semi round pebbles and have coarse volcanic sand matrix support. In places coarse sandstones containing small pebbles and granules display cross bedding. Sandy mudstone levels are rare in the succession and are not well graded.

The unit represents sedimentation of alluvium fan deposits where plaited running water dynamics were dominantly effective. The unit defines the sedimentation of the Urla group in the Middle Miocene basin at the edge of Uzun Island.

### 2.3.2. Pınallı Island Volcanoclastics

Volcanoclastic succession consisting intercalations of epiclastics of felsic pyroclastics which developed in sublacustrine conditions and fed by eruptions and sedimented by gravity flows has been studied in detail and for the first time in this study defined in the formation level. Upper sections of the succession can be seen above sea level in some of the islands; in Hekim Island and Çiçek Island, namely in İncirli Island and Pınarlı Island (Figure 7A, 7B). The thickness of the succession is about 50m and extensive outcrops are in the Hekim Island .

Epiclastic sediment facieses form the largest portion of the succession. They have regular parallel beddings consisting sandstones with massive or graded felsic volcanic materials and with less pebble stone levels. In Pınallı Island along the NE coast, coarse grained, normal graded metric scale thick beds are laterally followed in the order of tens of metres (Figure 8A). Matrix supported beds starting with

coarse pebbles grades down to sand size through small size pebbles. Base of the beds are either planer or eroded. Main elements of the rock types are trachytic lava clasts. In the NW coast of the Pınallı Island a 2 m thick blocky pebblestone level has same rock type clasts (Figure 8B-b, 8C-b). The base is sharp and planer. Coarse clasts consist of porphyritic trachyte lavas with coarse feldspar phenocryst show reverse grading at the base but normal grading at the top. Reverse grading starting from the boundary of coarse sand-granule size ends at the base with 60 cm coarse blocks. Matrix supported coarse clasts are semi rounded, less with blunt corners. Matrix consists of coarse-very coarse sand and also has granule size materials. Below the pebble stone level, 2m thick part observable a suspended sediments level is present (Figure 8B-a, 8C-a). The succession with centimeter thick planer bedded siltstone-claystone alternations has most 1 cm size rim-type lapillies containing fine-medium size volcanic sandstone and 1-3 cm thick micritic limestone interbeds. The epiclastic succession outcropping in the Hekim Island from base to the top consists of sandstones with volcanic elements and also less amount claystone-siltstone intercalations (Figure 8D-b). Centimeter-decimeter thick planer beddings are typical. Beddings are laterally continuous and thickness does not vary much. Coarse-very coarse grained sandstone beds are decimetre thick, massive or normal graded. They have matrix support of reverse graded sandstones with coarse ash, rare lapilli size white pumice and trachytic lava fragments. Reverse grading developed from fine sand to coarse sand form centimetre-decimetre thick parallel undulated bedding groups (Figure 8E, F, G). In rare cases Enlarged lapillies and sandstone interlayers with charred wood pieces are observed (Figure 8H).

Each of the pyroclastic interlayers marked with trachytic ignimbrite units in the epiclastic succession are the products of one volcanic (explosion) activity (Figure 9). 2-4 m thick separate levels of welded ignimbrite facieses can be seen in the western coastal part of the Hekim Island (Figure 8D-a, 9A, B, C). At the bottom two levels of the unit, dark scarlet-brown colour representing operative thermal oxidation is typical (Figure 8D-a). Third level is yellowish light brown coloured (Figure 9B). Coarse pumices containing sanidine phenocryst are centimetre, locally decimetre thick. Pumices of first two layers are dark coloured. Apart

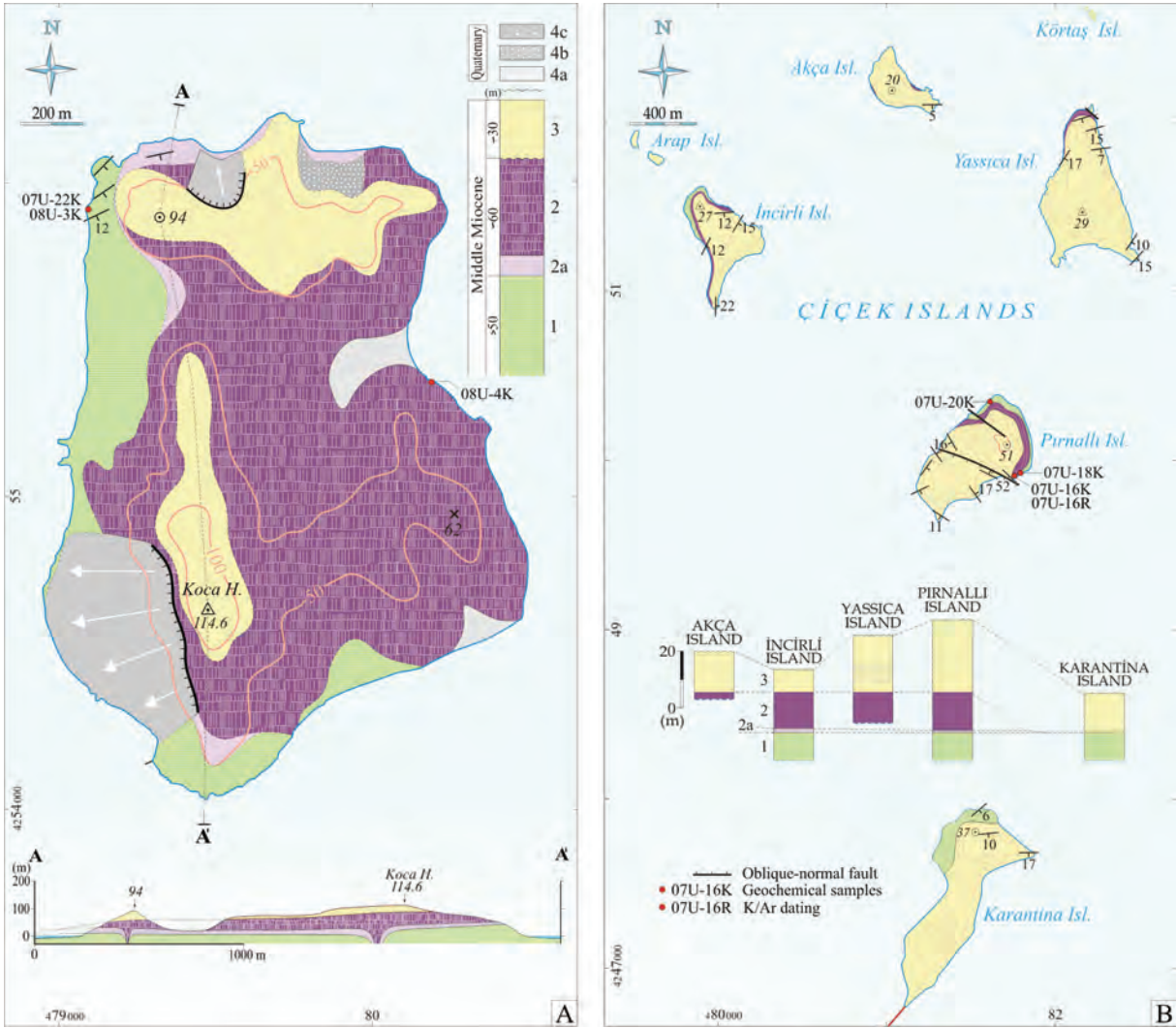


Figure 7- A) Geological map of Hekim Island. 1. Pirnalı Island volcanics, 2. Hekim Island basalt (a: Base surge deposits), 3. Urla limestone, 4. Quaternary deposits (a: Alluvium, b: Slope debris, c: Landslide debris). B) Geological map of Çiçek Islands and Karantina Island. 1. Pirnalı Island volcanics, 2. Hekim Island basalt (a: Base surge deposits), 3. Urla limestone.

from the second level from the bottom (Figure 10A) elongation and orientation of the elements in the pumices are not noticeable. Thin section study of the matrix of the pumices indicated elongation of the elements and less noticeably development of fiyam (?) structure. Lithic fragments are made of trachytic lava clasts. At the base, below the fourth level there are big mammal fossils remains. At this part in a zone where white pumices becomes more showing less distinct elongations (Figure 9C, D). Following the route of the ignimbrite flow planer bedded turbiditic succession developed at the bottom of the turbiditic succession cross bedded volcanic sandstone facieses is present. Small pebbles and granule containing coarse grained sandstone succession is several

metres thick and is discontinuous laterally (Figure 10E). In the Hekim Island, İncirli Island and Pirnalı Island unwelded trachytic ignimbrite facieses are located on the upper most part of the succession. It is maximum 8 m thick, is laterally continuous and is represented by a flow unit. Tafone (?) development on the whitish light gray coloured weathered surfaces is typical (Figure 9F). Homogenous lithics marked with centimetre size blint cornered trachyte fragments in general are either irregularly dispersed or form pebble clusters as seen in the İncirli Island. Three levels have been identified at the base of the same ignimbrite unit outcropping in the Pirnalı Island, lowest two of these levels are laterally discontinuous. I) on average 35 cm thick lowest part is marked



Figure 8- Some of epiclastic sedimentary facies observed within Pirnallı Island volcaniclastics. A) Proximal (?) turbidite facies with high-sediment concentration which coarse components are normally graded. Cut-and-fill deposits are observed in the lowermost part of the upper level (Pirnallı Island). B) a: Planar parallel bedded-laminated suspension deposits, b: High-density turbidite level, c: The weathering surface of unwelded ignimbrite level originated from trachytic volcanism has a tafoni form (Pirnallı Island), C) a: The suspension deposit succession is built from a planar parallel bedded-laminated claystone, siltstone and micritic limestone intercalation with turbiditic sandstone interbeds. Fine-medium grained volcanic sandstone levels comprise ‘rim-type’ accretionary lapillis, most of which are 1 cm in size (The scale is 10 cm in large photo), b: close-up view of the lahar level in B-b (Pirnallı Island). D) a: welded and thermally oxidized -first- ignimbrite unit in the lowermost part of Pirnallı Island volcaniclastic succession, b: The part of Pirnallı Island volcaniclastics represented by epiclastic distal turbidites, c: The lateral continuation of trachytic ignimbrite unit viewed in B-c (NW coasts of Hekim Island). E, F, G) Reverse graded volcanic sandstone beds in which white pumice fragments are particularly prominent (NW coasts of Hekim Island), H) Carbonized wood fragments within one of the turbiditic layers which indicate the hot origin of pyroclastic flow (NW coasts of Hekim Island).



Figure 9- Ignimbrite units within the epiclastic succession of Pınallı Island on Hekim Island. A) View of the second one from the bottom of four welded ignimbrite levels exposed on Hekim Island. Pumices are partly elongated and oriented. B) Third ignimbrite unit including black amorphous pumices (Hammer length is 33 cm). C) The fourth ignimbrite unit bearing white pumices in its lower part. a: Epiclastic turbidite level, b: The part in which partly oriented pumices increase (Reverse grading occurred at the bottom). D) Remains of a limb bone for a large mammal within the same horizon. E) Beach deposits (b) resting on fourth ignimbrite level (a). F) General view of unwelded trachytic ignimbrite level (Pınallı Island). a: lahar level shown in figure 8B-b, b1: Bottom of flow unit, b2: Pumice lapilli level, b3: Main ignimbrite body. G) The lower part of trachytic ignimbrite level. a: Upper massive part of the lahar level, b1: The planar/wavy parallel thin bedded lower part, b2: Reverse graded pumice lapilli level, b3: Main ignimbrite body in which cognate lithic clasts are reversely graded in its lower part.

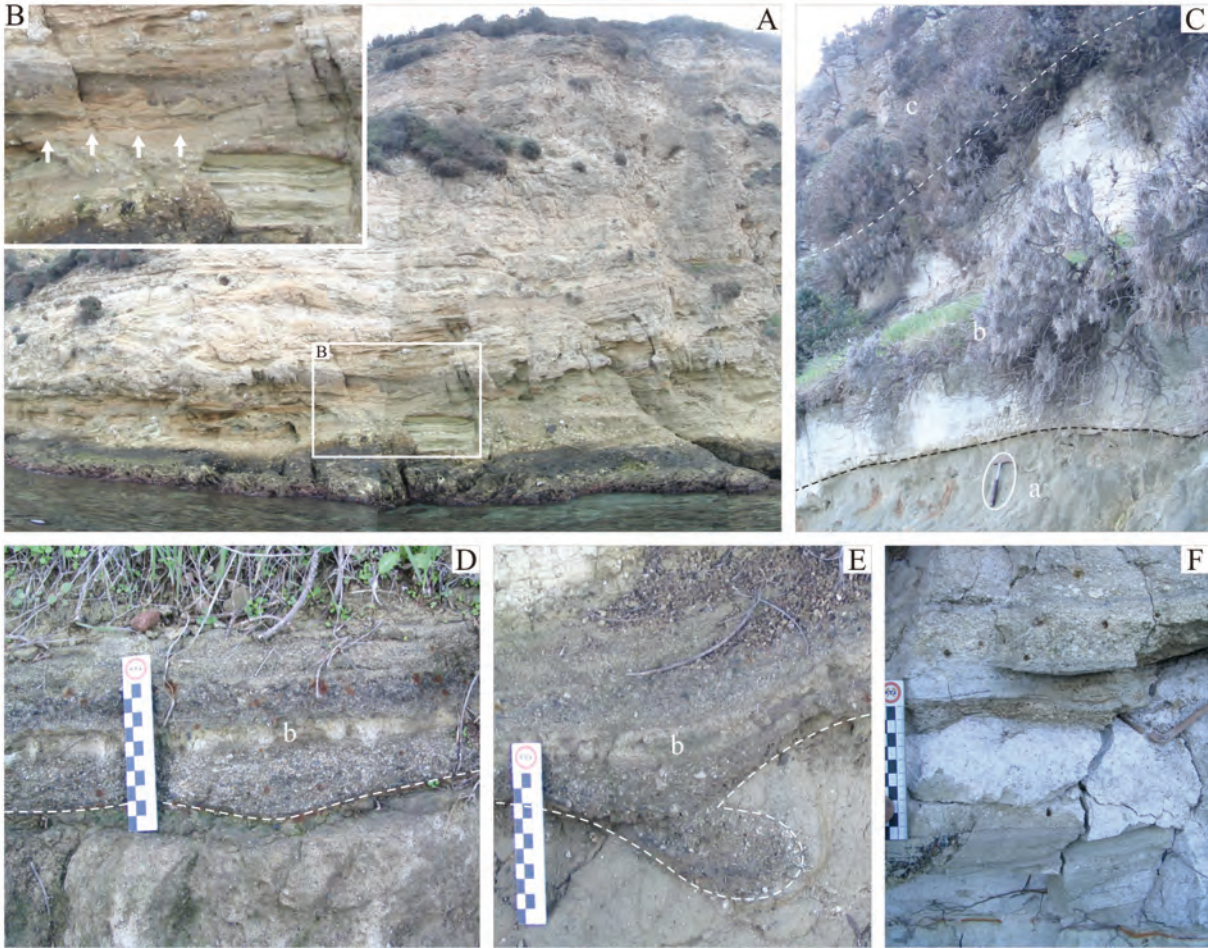


Figure 10- A) The base surge succession emplaced on a subaqueous environment in the beginning of Hekim Island basic volcanism. B) At the bottom, the base surge level changed into a debris flow because of undergoing to brittle deformation during lateral displacement. At the top, the flame structures, which reflect the moving of base surge in subaqueous environment (NW cliffs of Hekim Island). C) Basic pyroclastics emplaced on the sandy turbidites of Pınallı Island volcanoclastic succession (İncirli Island). a: Sandy turbidite level, b: Basic pyroclastics, c: Basalt lava (Hammer length is 33 cm). D) Basic pyroclastic succession initiates with scoria fall deposits (İncirli Island). E) A load cast at the bottom of scoria fall deposit over unconsolidated turbidite level. (İncirli Island). F) Planar parallel laminated base surge deposits observed together with scoria fall beds (İncirli Island).

with vertically grain size differentiation has planer/ undulated millimetre-centimetre scale beddings. In general coarse sand size volcanic elements are matrix supported and are well graded. Homogeneous granule size lava fragments are scarce (Figure 9G-b1). II) 40-60 cm thick white coloured pumice lapillies show thickness variations laterally and display reverse grading (Figure 9G-b2). III) Third part of the flow is the main part and is massive. At the lower 1 m part the homogeneous lava clasts have reverse grading (Figure 9G-b3). Locally small pebble size trachyte pebbles with blunt corners form clusters and pumice lapilli accumulations are encountered.

Outside of the ignimbrite parts of the Pınallı Island succession, lacustrine shoreface fillings of epiclastic flow sediments are dominant. From Pınallı

Island towards Hekim Island average grain size and thickness of the beds of the sediments reduce and along the same direction it shows changes from coarse trachyte clasts containing dense proximal turbidites to less dense distal turbidites. Fed by trachytic volcanisms (Menteş trachyte: Kaya, 1979; Menteş volcanics: Gökteş, 2011) in the Menteş peninsula, changes along lateral direction show the development of turbiditic processes northwards. Pınallı Island is located nearest to the volcanic centre. In the NE shore of the island (Pınallı Island), the unit with coarse trachytic lava clasts forming normal graded levels has been considered to be the high density paroxysmal turbidites. In the NW part of the island the pebble stone level, at the bottom is reversely and at the top normally graded and has a non erosive base is also a same type

turbidite. Reversely graded bottom part is at debris flow facieses, developed with laminar flow. In the normally graded top part, materials settled from the suspension of turbulent flow (Postma et al., 1988). Both of the pebble stone litho facieses consist of coarse trachytic lava fragments. Nearest source for these coarse materials is the block flows developed at the slopes of the Menteş volcanic centre.

In the Hekim Island low density distal turbidite facieses is dominant. Reversely graded sandstone beds with volcanic materials might be the distal extension of the material changed into grain flow as a result of basal underwater turbulent flow of sediments (Figure 8E, F, G). Charred woods remains (Figure 8H) in the beds with transported enlarged lapillies indicate that flow was hot and sub aerial. A big mammal bone fossil remains found in one of the welded ignimbrite level indicate that source area of the Menteş volcanics was above lake level. Lithic extent of same origin ignimbrites have same source and are marked by porphyritic trachytes. The lateral extent of the coarse grained sandstone level sedimented on top of the fourth welded ignimbrite level is limited with the extent of the ignimbrite flow. Based on the pebble bearing sandstone succession, development of teams of large scale-low angle cross beddings, fragment supported textures and litho stratigraphic position it was concluded that it was a beach face sedimentation. With the emplacement of ignimbrites lakes became locally shallow and following local shallowings, turbiditic sedimentations continued.

### 2.3.3. Hekim Island Basalt

The unit has basic pyroclastics at the bottom and less distinct alkali basic lavas on the top. It was for the first time defined in this study. Volcanics generated in the Hekim Island, their outcrops in the Çiçek Islands are 10-20 m thick. Basalt dyke cutting the Urla limestone in the Kaya Burnu, Southeast shore of Uzun Island is considered to have the same origin (Figure 4).

Volcanic activity started in lacustrine environment, first products were pyroclastics, they were mainly basal turbulent and scoria air-fall facieses. Pyroclastics developed in the marine environment are very thick (>50 m) and crop out in the Northern slopes of Hekim

Island (Figure 10A). Their bottom under the sea is not observable. The beds developed near to the outlet centre of the basal turbulent succession have mostly lost their original positions because of the volcanic tremors and they were subjected to gentle (soft) sedimentary deformations. Laterally displaced beds have been subjected to brittle deformation along the flow direction and were broken (Figure 10B). Some flame structures observable at the bottom of some beds are the products of advancing pyroclastic turbulent in water environment (Figure 10B). Pyroclastics outcropping in the İncirli Island are located in between sandy turbidites of Pınallı Island pyroclastics and basalt lavas (Figure 10C). The unit is most 4 m thick and starts with beds of slag falls and mainly consists of base turbulent sediments. Black coloured slag fall levels, marking the start of the volcanic activity developed in two explosion stages and are 10 cm thick. At the bottom soft deformation features like load mould. Millimetre size lithics (with vesicles-without vesicles) of same origin forming massive and weakly compacted face are fragment (grain) supported (Figure 10D, E). At the top overlying light gray basal turbulent succession has centimetre thick planer/undulated parallel bedded-laminated. Poorly developed cross beddings are rarely encountered (Figure 10F). Slag fall interlayer's containing lapillies with millimetres scale growth are commonly encountered in the basal turbulent succession.

Blackish dark gray coloured lavas are heavily fractured and display flow foliations In the Northern part of Yassica Island a lava block with a discontinuous spatter lava level may indicate at least two episodes of lava extraction (Figure 11A). About a10 m thick thick lava overlying the spatter level has decimetre scale flow foliations and alteration feature of exfoliations. Lavas came out from the secondary lava extraction channels in the northern part of the Hekim Island have polygonal joint patterns and entablature cooling columns commonly developed (Figure 11 B). Lava flow outcropping in the Çiçek Island has vesicles, peperites developed extensively on the surface of the in contact with water containing sediments (Figure 12).

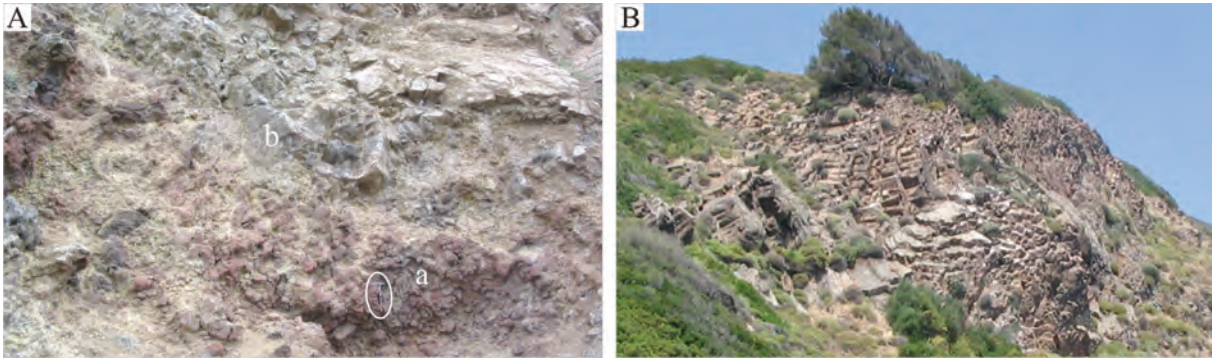


Figure 11- Hekim Island basalt. A) A Spatter level with no lateral continuity between two lava flows on Yassica Island. a: Spatter, b: Lava. (Hammer length is 33 cm). B) Entablature cooling columns observed in the north of Hekim Island.

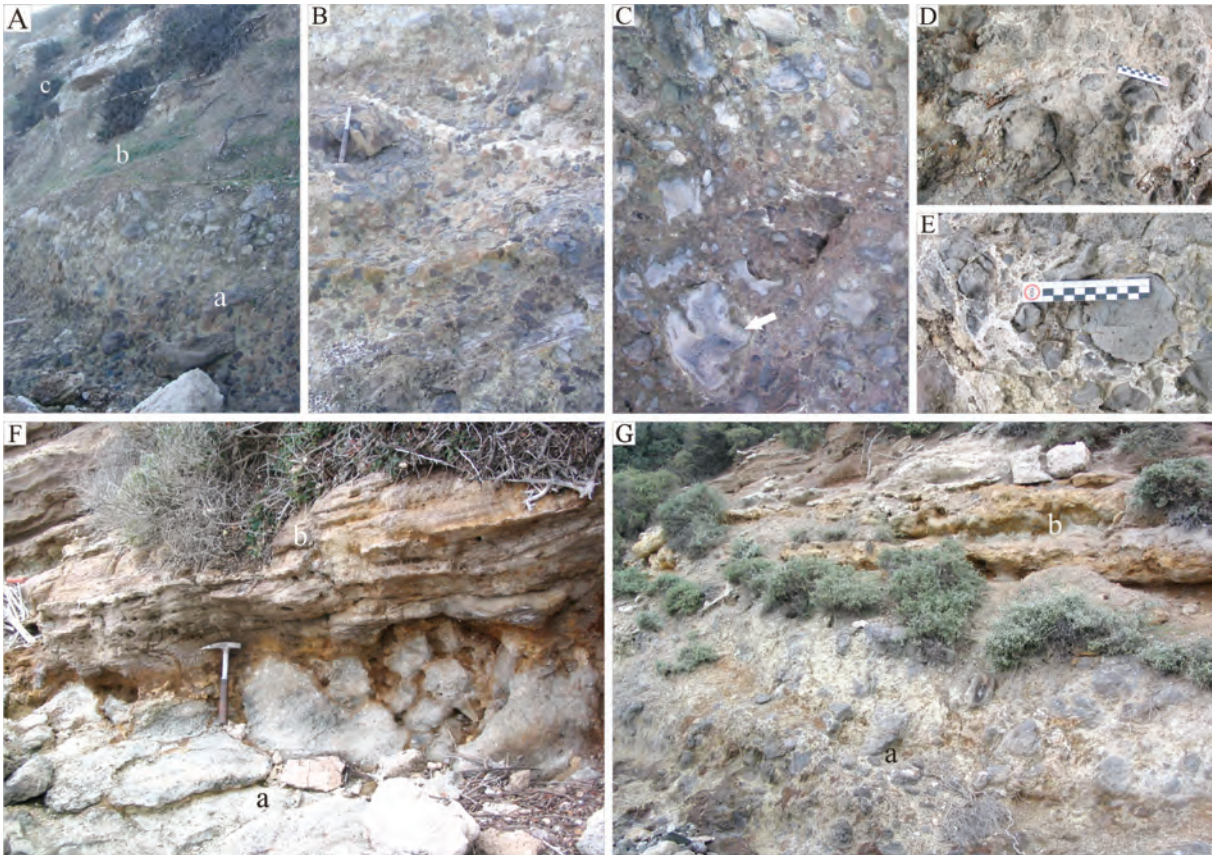


Figure 12- Peperites observed along the upper contact of Hekim Island basalt sill. A,B) Peperite zone with a thickness up to 3 meters on İncirli Island. a: Peperite zone, b: Backshore mudstones in the lowermost part of Urla limestone succession, c: Urla limestone. C) Hydrothermal alteration belts developed rapidly cooling walls of some fluid-shaping lava fragments by contact with unconsolidated sediment in the peperite zone on İncirli Island. D,E) Poorly developed jigsaw-fit texture is observed in some parts of the peperites on Pirnalli Island (Scale is 10 cm). F,G) Peperitization between the upper backshore mudstones and the lower intruding basalt sill on Yassica Island. a: Basalt, b: Backshore mudstones (Hammer length is 33 cm).

#### 2.3.4. Urla Limestone

Lacustrine limestones succession is the last unit of the Urla group. It was for the first time named by Kaya (1979) and has been defined at formation level. The unit crop out in the entire islands group and has thickest (>100m) succession is in the Uzun Island.

In the Çiçek Islands Urla limestones lie on top of the basalt lava. At the bottom of the limestone there is a scarlet-brown colour thinly bedded-laminated mudstone succession which is the dominant unit in this part (Figure 14A). The thickest succession (~10 m) is in Yassica Island (Figure 13 B, C, D).

The mudstone upwards with centimetre-desimeter scale thick intercalations goes into micritic limestone or like in the Pınallı Island overlain by limestone with a sharp contact (Figure 13 E). With maximum 70 cm, thickest limestones containing mudstone beds-laminas intercalations are in Yassica Island. Within the mudstone succession there are 1-3 cm

thick laterally discontinuous charcoal bands. The thickness of the thin bedded-laminated mudstone with charcoal bands is up to 30 cm in Yassica Island (Figure 13 D). In general and in the parts near to the overlying limestone, along the bedding planes development of laminated-nodular  $\text{CaCO}_3$  concentrations caliches could be seen (Figure 13 F).

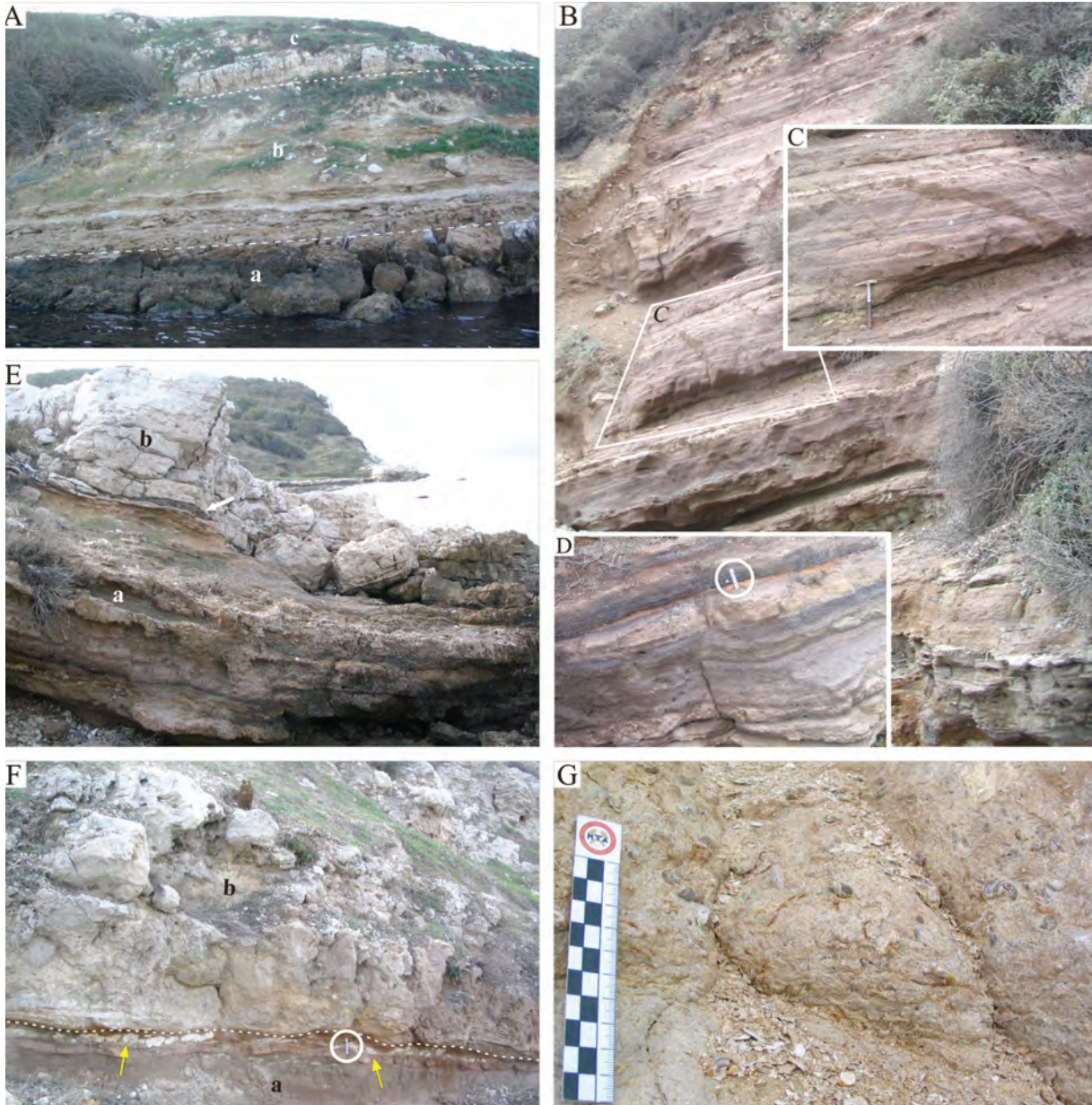


Figure 13- Mudstone-dominated backshore deposits exposed at the lowermost part of Urla limestone on Çiçek Islands. A) Basalt sill (a) overlain by backshore deposits (b) and algal limestones (c) on Akça Island. B,C) Planar parallel thin bedded-laminated mudstone succession observed on Yassica Island. D) Detailed view from the coal seams intercalated with the mudstones bearing gastropod shell fragments in the same succession (Scale is 10 cm). E) a: Mudstones bearing gastropod shell fragments and coal laminae, b: Limestones with chert lenses (white arrow) (Pınallı Island). F) a: Massive mudstone with caliche nodules (yellow arrows) and laminas, b: Algal limestones (Pınallı Island) (Scale is 10 cm). G) Carbonate-rich mudstone bearing relatively well-preserved (cm sized) gastropods (Pınallı Island).



Figure 14- Litho-facies observed in the beginning at the deposition of Urla limestone. A) Planar cross-bedded algal biosparite-biosparrudite facies with algal oncoids and bioclasts (Yassica Island). B) The low-angle planar cross-stratified biosparite-biosparrudite facies composed of algal bioclasts (Pırnallı Island). C) Close view of grain-supported biosparite-biosparrudite facies. D) Close-up view of bioturbated limestone with algal oncoids and hemispheroidal-ovoidal stromatolites included (Pırnallı Island). E) Poorly developed medium-thick bedded and cherty (white arrow) biogenic limestone (b), overlying red-brown massive mudstone succession with a sharp contact (a) (Pırnallı Island). F) Thick bedded micritic limestone with chert nodules and fenestral voids (Pırnallı Island). G) Planar cross-bedded, grain-supported and well-sorted coarse sandstone and fine conglomerate sequence, overlying sandy turbidites of Pırnallı Island unit (a) (Akça Island). H) Wave ripple cross-laminated thin-medium sandstone in the lower part, and planar cross-stratified coarse sandstone and granulestone at the top (Karantina Island).

White coloured shell fragments of gastropod remains are seen from top to bottom in all parts of the mudstone succession but parts with more organic materials are particularly rich. In Pırnallı Island centimeter scale thicker gastropod shells appear to have relatively better protected (Figure 13 G).

Apart from Uzun Island in entire islands group mudstone succession or transgressive limestone sedimentation overlying Pırnallı Island, sandy turbidites of the volcanoclastics start with algal bioclastics with low angle planer cross beddings. i) In Yassica Island and Pırnallı Island the allochemical composition lithofacies has been identified as Biosparrit-biosparrudit (Folk, 1962), columnar branched stromatolite fragments are the bioclasts and locally are algal oncolites (Figure 14 A, B). Less found coarse sand-granule size transported volcanoclasts in general have blunt corners. Algal oncolites (?) (onkoid) are mostly ovoid shape and their long axis rarely reach 10 cm. Main structural elements of biosparrit-biosparrudit with algal oncolite lithofacies are bioclasts which are in 0.5-15 mm dimensions and are well cemented with mostly well graded, fragment supported, packed and tightly cemented with spar calcite cement (Figure 14 C). Following these levels, the Lower levels of these limestones particularly are algal-biogenic. Allochem context is marked by blue-green algal (Cyanophyta) stromatolites. Beddings differ depending upon the growth geometry of stromatolites. In places where Hemispheroidal/Ovoidal stromatolites accumulated in different bioturbation rates with massive underdeveloped thick bedded bioclastic parts in most places this kind of accumulations reflects beginning of limestone sedimentation (Figure 14 D). In Pırnallı Island limestones formed by laminated stromatolites directly overlie mudstone succession. In places where medium-thick beddings become noticeable, on the bedding planes centimetre thick laterally discontinuous chert bands and concretions with fenestras (fenestral boşluk) become noticeable (Figure 14 E, F). ii) A low angle planer cross bedded sandstone-pebblestone accumulations is present at the bottom of the Algal limestone outcropping in Akça Island. About 2 m thick clastic succession has sedimented on to the Pırnallı Island turbidites. Light gray coloured succession with coarse grained sandstone and fine pebblestones is made of volcanic fragments transported from underlying sandy turbidites. Maximum 1 cm size

algal oncolites (onkolid) bearing sandstones are grain supported, well graded and is weakly compacted (Figure 14 G). In Karantina Island similar succession is also present outside the extension of Hekim Island basalts. Algal oncolite bearing bioclastic limestone sedimentation starts with planer cross bedded and ripple cross laminated sandstones, developed on the Pırnallı Island turbidites. In the planer cross bedded sets consisting coarse-very coarse sand and granule size volcanic components, small pebbles and algal bioclasts are present (Figure 14 H).

At the bottom of the limestone succession shore/beach sediments are located. The mudstones forming the bottom of the limestone succession around Çiçek Island have sedimented in the back shore mud plain which developed in a limited area as a result of emplacement of Hekim Island pyroclastics on to the Pırnallı Island volcanoclastics. Paleo oxidation associated scarlet-brown colour distribution, lateral discontinuous charcoal occurrences which points out temporary swamps, pedogenic caliche occurrences, gastropod shell fragments the food remains of the small mammals, all indicate that sedimentation developed behind the shore line. Like Karantina Island outside the extension of the Hekim Island pyroclastics where back shore sedimentation did not develop well, algal limestones, with the foreshore/beach face sediments directly covered Pırnallı Island volcanoclastics. Low angle planer cross bedded sets, with well developed textures, biosparites-biosparrudites and epiclastic sandstone lithofacies have been deposited in the fore shore/beach face environment. Allochthonous microbial (?) (mikrobial) oncolites with spheroidal stromatolites (wrapped products) mostly reflect wave related high energy environment conditions. Overlying limestones have developed by autochthon growing stromatolites under low energy conditions.

### 3. Petrography

In Uzun Island rhyolitic ignimbrites of the Foça tuffs have same type lithics. General characteristics of these lithics are the same with the rhyolites of the Foça volcanics studied by Akay ve Erdoğan (2001). Rock samples with aphyric, porphyritic textures mainly have phenocrysts of quartz and K-feldspath in glassy matrix.

In the Pınallı Island volcanoclastics succession, lava clasts in coarse grained turbidites have porphyritic texture and phenocrysts are plagioclase, biotite and sanidine. In the hand specimens' sanidins with Carlsbad twinings and zoned plagioclases are larger than 2 cm.

Lavas of the Hekim Island with porphyritic texture mainly have olivine, pyroxene and plagioclase phenocrysts. Black coloured filotaksitik (?) (phyllotaxy?) matrix, consist of plagioclase microlites, olivine and pyroxene microcrystals. Ksenoquartz phenocrysts, are encircled by clinopyroxene microlits-microcrystals representing magma mixing.

#### 4. Main Elements Oxide Geochemistry

Samples Fo-3, O8U-03 and O4 have been analysed in the ACME Analytical Laboratories LTD in Vancouver, Canada. The samples were first subjected to fusion with Lithium metaborate/tetraborate then dissolved in nitric acid. Following these the samples

were analysed by using ICP-emission spectrometer. Samples 07U-16, 18, 20, 22 have been analysed in the 'Mineral Analyses and Technology Department' laboratories of MTA. Samples were (crushed) powdered down to below 75 µ, then dried at 105°C. 3 gr powdered sample from each specimen have been taken and mixed with 0.9 gr cellulose binder and mixed and powdered again to achieve homogeneous mixing, then samples were pressed under 40 ton pressure. Following all these processes the samples were analysed by using Panalytical, Axios XRF instrument and results have been evaluated with IQ-program.

Coordinated and analyses are given in table 1. After subtracting the H<sub>2</sub>O values from the analyses, main elements oxide values of the samples have been normalized to 100% and Le Bas et al., (1986) total alkali (Na<sub>2</sub>O-K<sub>2</sub>O) and silica (SiO<sub>2</sub>) have been plotted on to the diagram (Figure 15 A, B).

Table 1- Major element oxide compositions of volcanic rock samples.

Sample	Coordinate	SiO <sub>2</sub>	Al <sub>2</sub> O <sub>3</sub>	Fe <sub>2</sub> O <sub>3</sub>	MgO	CaO	Na <sub>2</sub> O	K <sub>2</sub> O	TiO <sub>2</sub>	P <sub>2</sub> O <sub>5</sub>	MnO	SrO	BaO	LOI
Fo-3	79.845E-80.340N	79.14	12.15	0.34	0.04	0.22	1.91	4.22	0.08	0.03	<0.01	--	--	1.9
07U-18K	81.790E-49.940N	66.7	17.7	1.6	0.4	1.7	5.9	4.4	0.4	0.2	<0.1	0.03	<0.01	0.55
07U-20K	81.600E-50.350N	63.5	16.7	3.1	0.6	2.2	5.2	4.7	0.4	0.2	0.1	0.03	<0.01	1.95
07U-22K	79.100E-56.225N	53.3	16.2	4.6	1.7	1.1	5.0	5.5	0.2	0.1	0.2	<0.01	<0.01	8.25
08U-03K	79.115E-56.210N	60.13	17.72	2.71	0.36	1.86	5.08	6.76	0.22	0.08	0.07	--	--	4.90
07U-16K	81.775E-49.915N	48.40	17.20	10.10	4.40	9.20	3.80	1.70	1.60	0.50	0.20	<0.01	<0.01	2.70
08U-04K	80.210E-55.673N	48.47	16.84	9.84	3.58	8.30	3.76	2.40	1.59	0.44	0.16	--	--	4.30

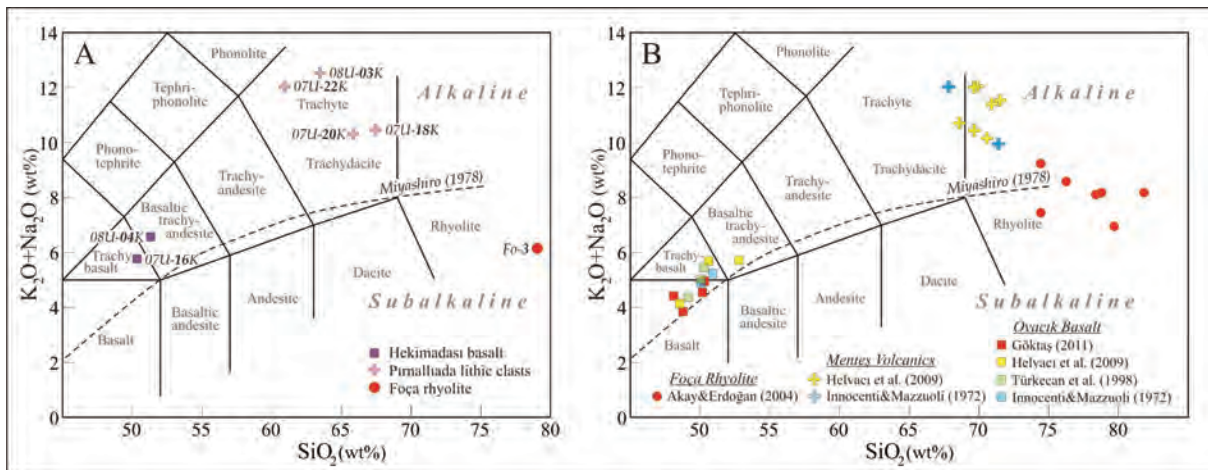


Figure 15- According to the major element oxide content of volcanic rock samples total alkali-silica (TAS) classification diagram suggested by Le Bas et al. (1986). A) This study. B) Previous studies (Innocenti and Mazzuoli, 1972; Türkecan et al., 1998; Helvacı et al., 2009; Göktaş, 2011).

Results of main oxide analyses of volcanic lithics of epiclastic and pyroclastics of Pırnallı Island volcanoclastics have been classified in the TAS diagram. Coarse lava components of the Pırnallı Island volcanoclastics (Figure 15 A: 07U-18K and 20K) and black coloured pumices of welded ignimbrite (Figure 15A: 07U-22K and 08U-03K) are in the trachyte field (Figure 15A). Menteş volcanic centre is considered to be the main source of the volcanoclastics. Lava samples collected from the Menteş Volcanic center by Mazzuoli (1972) and by Helvacı et al. (2009) have been evaluated together in figure 15B and genetic connection between the acidic products of volcanisms have been studied.

Results of main oxide element analyses of the two lava specimens collected from the Hekim Island basalts in this study together with the Ovacık basalt specimens collected from the Urla depression in the early work have been evaluated in the TAS diagrams. Hekim Island basalts plot (07U-16K and 08U-04K) in the ‘trachybasalt’, ‘basaltic trachandezit’ fields, on the other hand Ovacık basalts plot in the ‘basalt’, ‘trachybasalt’, ‘basaltic trachandezit’ fields and they are shown to be the products of the same volcanisms (Figure 15A, B).

### 5. K/Ar Geochronology

Radiometric K/Ar analysis of the Foça rhyolite has been carried out in the ACME Analytical Laboratories LTD in Vancouver, Canada. K concentration has been analysed by ICP, Argon analysis has been conducted by isotope dilution procedure on to the noble gases mass spectrometer.

Foça tuff is an important reference base as it is forming the base of the Urla group succession accumulated in the Foça depression province in general. Because of this age determination of the calc alkaline acidic volcanism considered to be essential, so during the field work in 2008 specimens were collected for K/Ar analysis from a rhyolite dome claimed to be laterally connected with the ignimbrites

by Akay and Erdoğan (2001). K/Ar analysis indicated  $16.0 \pm 0.6$  Ma age (Table 2). Specimens collected from similar lava domes in the area also gave 16.6 Ma and 16.1 Ma (Altunkaynak et al., 2010). Age data shows that in the Foça Peninsula pyroclastics of the same kind and laterally connected rhyolite domes were emplaced 16.6-16.0 Ma ago.

In Pırnallı Island a specimen (07U-16R) was collected from the extension of Hekim Island basalts. Location of the specimen is given in Figure 7B and K/Ar analysis is given in Table 2. Hekim Island basalt gave  $14.8 \pm 0.8$  Ma. whole rock age and  $14.5 \pm 0.5$  Ma. Age reported by Göktaş (2011) for the Ovacık basalts could chrono-stratigraphically be correlated.

### 6. Time-Rockstratigraphy Connections and Regional Correlation

Kocadağ volcanoclastics have been defined in the scope of Kocadağ volcanics are the oldest unit in the defined Neogene stratigraphy in the islands group. Correlated sediments around the study area mostly crop out in the Kocadağ volcanic complex and also locally in the NW of Menteş Peninsula (Figure 1B). Succession's bottom is not observable in Uzun Island, it is overlain with a sharp contact by ignimbrites of the Foça tuff. Felsic pyroclastic intercalations within the succession could be the early stage explosion products of the rhyolitic fiorite magmatism which produced The Foça Tuff. In the Kocadağ volcanic complex volcanoclastic sediment group has been cut by andesite-dacite lavas of 16.6-17.3 Ma (Borsi et al., 1972, 17.5 Ma (Helvacı et al., 2009) and 16.7 Ma (Karacık et al., 2015) age. Geochronological data indicate that in a general sense Kocadağ volcanoclastics are Early Miocene age.

Rhyolitic ignimbrites overlying the Kocadağ volcanoclastics in Uzun Island are the extension of the Foça tuffs defined in the Foça Peninsula. In the Foça volcanic centre the age of the rhyolites laterally related with the ignimbrites is 16.6-16.0 Ma. (Altunkaynak et al., 2010 and this study). Data may show that

Table 2- K/Ar analysis of volcanic rock samples.

Sample	Materyal	K (%)	$^{40}\text{Ar rad}$	$^{40}\text{Ar rad} (\%)$	Age (Ma)
Fo-3	K-spar	2.27	1.392 (nl/g)	87.5	$16.0 \pm 0.6$
07U-16R	whole rock	1.382	$7.985 \times 10^{-7}$ (ccSTP/gr)	31.5	$14.8 \pm 0.8$

ignimbrites, constituting Foça tuffs, emplaced in the Uzun Island area in Early Miocene. Foça tuffs in North of Çandarlı were first identified as dacitic tuffs by Öngür (1972). Demirtaş felsic pyroclastics defined by Ejima et al. (1987) and Aliğa pyroclastics around Menemen-Aliğa area Eşder et al. (1994) are also the equivalence of Foça tuffs. Akay (2000) and Akay ve Erdoğan (2001, 2004) studied rhyolitic pyroclastics in the Foça Peninsula within the scope of the Foça volcanics.

Değirmentepe member within the Foça tuff is the equivalent of 'Mordoğan lower unit' which was first defined as to be the same stratigraphic position in the southern part of Mordoğan by Kaya Kaya (1979). In the distribution area alluvial succession which separates the Foça tuffs into upper and lower parts represents the calm period of the fluorite magmatism which produced the rhyolitic ignimbrites and shows that ignimbrite flows emplaced to the area mainly in two explosion stages.

Urla groups sedimentation starts with an unconformity on the Foça tuffs outcropping in the Uzun Island. Göktaş (2014 *a,b*) defined the Hisarcık Formation. "Hisarcık Formation" is in the eastern side of the Karaburun peninsula which forms the western side of the Foça depression. Hisarcık formation is considered to be the stratigraphic equivalent of the Urla group.

Within the Urla group, alluvial Beşiktepe formation reflects beginning of Middle Miocene sedimentation. Foça tuffs form the base of the Middle Miocene basin in the Uzun Island and Beşiktepe formation sedimented on to the Foça tuffs with an unconformity. Urla limestone outcropping in Uzun Island with vertical and lateral transitions overlies Beşiktepe formation. Although relationships with the Pınallı Island volcanoclastics can not be observed but it is considered that Beşiktepe formation lies at the bottom (Figure 3). Time-rock stratigraphy correlations of the alluvial succession have been completed in the western side of the Foça depression and in Urla part. Hacıhüseyintepe member has been defined and around Karaburun town center (Göktaş, 2014*a,b*) and Alibey member (Göktaş 2011) in the west of Gülbahçe are known examples.

Bottom contact of the Pınallı Island volcanoclastic succession reflects lacustrine shore face sedimentation but at present as it is under the sea it can not be observed. In the synthesized stratigraphy,

it transitionally overlies Beşiktepe alluvial sediments and in Uzun Island direction, it was assumed that it missed the Urla limestone with lateral interfingering (Figure 3). Beyond Uzun Island, in the islands group the unit is overlain by pyroclastics of the Hekim Island basalts. Karantina Island is outside the extension of the Hekim Island volcanics. In the Karantina Island through sand face sediments it is overlain by the Urla limestone. Relative geological age of the unit sedimented before Hekim Island volcanisms (14.8 Ma) is Middle Miocene. In the Foca depression province correlation of the successions has been made defining Early Middle Miocene lacustrine shoreface sediments. Karaburun formation (Kaya, 1979) which has been defined in the Urla part and the fine fractions of the 'Güvenlik Member' (Göktaş, 2011) are in the same stratigraphic position with the Pınallı Island volcanoclastics. In the Foça part, possible equivalence of the fine grained lacustrine sediments are in the southern part of Maltepe (Dönmez et al., 1998). Lacustrine 'Karabağlar Member' (Göktaş 2014*b*) defined in the western edge of the Foça depression is the stratigraphic equivalence of the unit (Figure 2). Upper contacts of the Hekim Island basalts are observed outside Uzun Island and Karantina Island in the island group. Bottom contacts crop out in Hekim Island, İncirli Island and Pınallı Island. Pyroclastics defining beginning of explosive stage of the volcanic activity sedimented on to the sedimenting turbidites of the Pınallı Island volcanoclastics (Figure 16A). In the effusive stage lavas flowing on the its own pyroclastics, as it is recognizable in the Pınallı Island and part of İncirli Island developed a weak heat effected cooked zone. Turning south lava flow developed sills within the same origin pyroclastics as well as within the back shore mudstones settling on the pyroclastics (Figure 16B). Lavas getting in contact with watery sediments caused excessive vasculation and peperite development, typically seen in the İncirli Island, Pınallı Island and Yassıca Island. Hekim Island basalts outcropping in the islands group in the central part of the Foça depression could be correlated with the previously defined alkali mafic volcanics in Urla, Foça parts. In Urla and Foça parts Ovacık Basalts (14.5 Ma; Göktaş, 2011) described by Kaya (1979), Ilıpınar basalts (14.3 Ma; Ercan et al., 1997) and within the alkali volcanics context Akay ve Erdoğan (2004) described basic lava series in Foça Considering their time-rock stratigraphic position and volcanogenic character they could be correlated with the Hekim Island basalts.

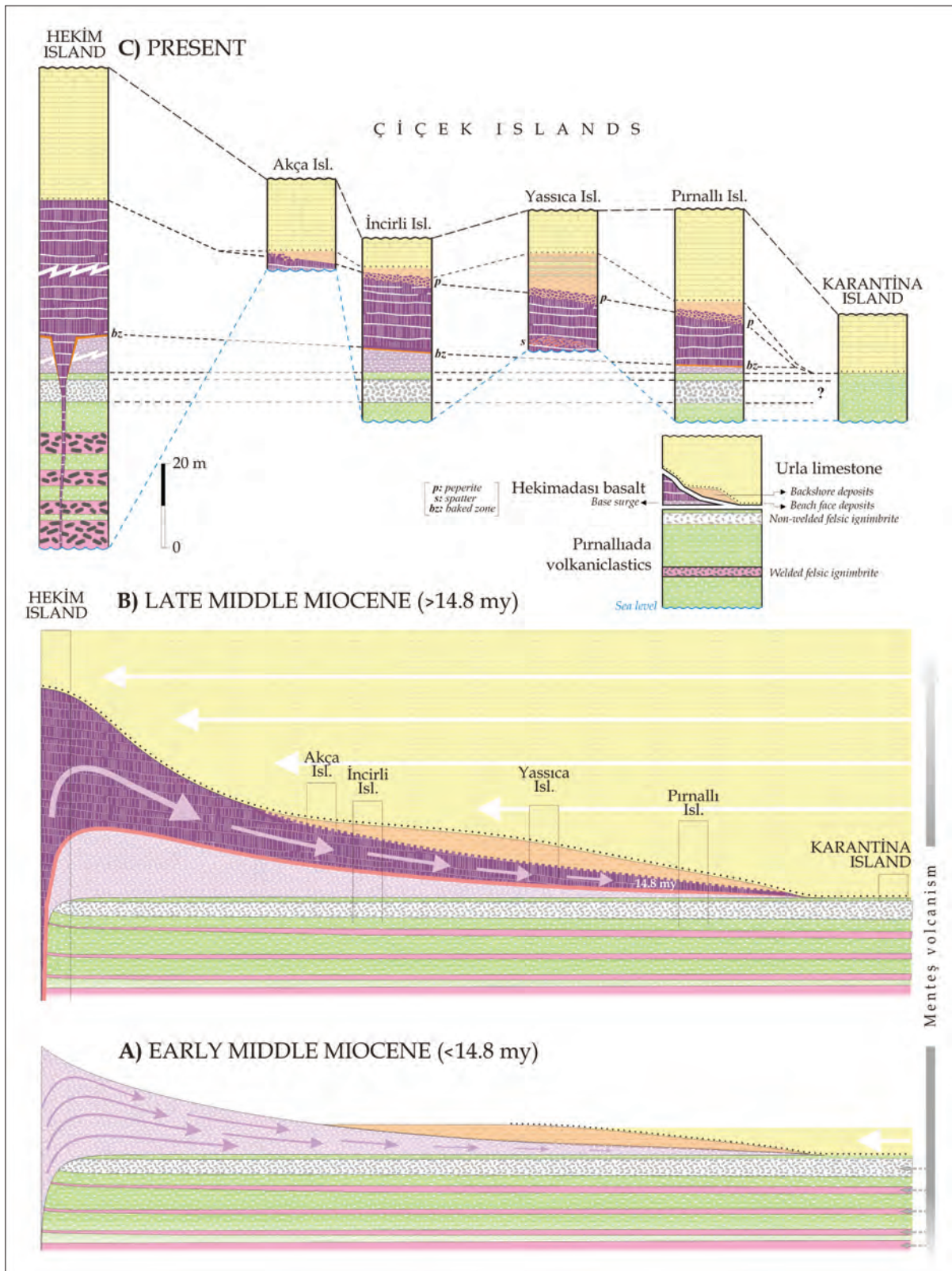


Figure 16- The palinspastic evolution of Middle Miocene sedimentation and volcanism represented by the Uurla group.

Urla limestone outcropping in Uzun Island with lateral-vertical transitions they overlay Alluvial sediments of the Beşiktepe formation (Figure 3). On the other hand in the Çiçek Islands they mostly sedimented following back shore mudstones (Figure 16 B). The lava-water reaction developed between Hekim Island basalts and mudstone succession. Sill intrusion took place 14.8 Ma ago, this shows that sill intrusion is at the same age with the sedimentation. Following intrusion of the sill transgression of the Urla limestone continued and Hekim Island basalt were covered in all of their extension areas (Figure 16 B). Like in the shore lane area between Menteş Peninsula and Karantina Island outside the extension area of the basic volcanics, Urla limestone overlay the Pırnallı Island volcanoclastics through shore face sediments. In the study Urla limestones top contact is marked with Quaternary erosion.

"Değirmentepe" limestone defined in the NE part of Karaburun Peninsula (Göktaş, 2014), 'Urla limestone' (Kaya, 1979; Göktaş, 2011) in Urla and 'Aliğa limestone' (Kaya, 1979, 1981; Akay and Erdoğan, 2004) in Foça Peninsula and 'Çamdağ limestone' (Eşder et al., 1994) are the defined equivalents of Urla limestones in the Foça Depression.

## 7. Conclusions

In this work Early Miocene volcanoclastics and Middle Miocene sediments and alkali volcanics outcropping in the outer bay islands group in İzmir have been studied. In the study area Late Early Miocene calc alkaline volcanisms have been represented by Kocadağ volcanoclastics and Foça tuffs. Dominant Middle Miocene lacustrine sediments and laterally connected alkali volcanics have been defined within the Urla group context.

Kocadağ volcanic complex produced mainly andesitic volcanoclastics and less dacitic pyroclastics and epiclastics constituting the Kocadağ volcanoclastics. They were generated from the N-NE slopes of the Kocadağ volcanic complex centre which was capable of producing these kinds of products and were emplaced in the area.

It was concluded that weakly welded ignimbrites overlaying the Kocadağ volcanoclastics with sharp contacts are the extension of the tuffs in the area, as defined Foça tuff in the Foça Peninsula .

In Foça Peninsula Akay (2000) described the lateral connection of the ignimbrites with an underwater rhyolite dome. In this study age determination of this underwater rhyolite dome has been carried out. The age is 16.0 Ma. According to this age it was suggested that ignimbrites of the Foça tuff emplaced to the area during towards the end of Early Miocene.

Alluvial Değirmentepe member is mainly consists of coarse materials derived from the Kocadağ volcanoclastics. It has been described as a discontinuous interface within the Foça tuff. Alluvium fan succession sedimented in the calm period of rhyolitic magmatism (?) shows that rhyolitic ignimbrites emplaced to the area mainly in two explosive period.

Sedimentation of the Urla group started with the alluvial Beşiktepe formation which was defined in the in the Uzun Island. Alluvial fan succession representing Middle Miocene basin edge sedimentation overlies Foça tuff with an unconformity and itself with vertical, lateral transitions is overlain by Urla limestones.

Pırnallı Island volcanoclastic succession is mainly consists of volcanic turbidites and is sedimented in lacustrine environment has weakly welded trachytic ignimbrite interfaces. Chemical and petrographic studies show that pyroclastic and epiclastic sediments consist of materials from trachytic origin. Pyroclastic and epiclastic sediments were generated from the volcanic centres in the Menteş Peninsula which produced alkali felsic products during Middle Miocene.

Extrusion centre of the Hekim Island basalts is in the Hekim Island, Hekim Island basalts have been distinguished for the first time in this study and volcanic facieses have been defined. Lavas main oxide elements compositions have been correlated and evaluated with the previous data of the basalts prior to the Ovacık basalts in the Urla Depression; the data show distribution in the basalt-trachybasalt-basaltic trachyandesit composition area. This distribution shows that these weakly alkali lavas all have same magmatic origin. In the lacustrine environment while Pırnallı Island volcanoclastics were sedimenting at the early stage of the explosive volcanic activity produced pyroclastics.

Pyroclastics lying on the sandy turbidites of the Pınallı Island volcanoclastics consist of basal turbulent sediments with some slag fall intercalations. Following the emplacement of pyroclastics, part of the lava flows coming out from Hekim Island take a south turn and intrude into the bottom of the back shore mud of the lake where Urla limestones were sedimenting, forming sills there. Along the contact peperites development indicate lava-water interaction and 14.8 Ma K/Ar age determination shows that intrusion was about the same age with the Early Middle Miocene sedimentation. Hekim Island basalt in Foça depression in general is included within the small volume lava of extrusions of the Early Middle Miocene alkali basic series.

In Çiçek Islands and Karantina Island back shore and shore face/sandy sediments outcropping at the bottom of the Urla limestone indicate that shore/sand sedimentations have developed. In the Karantina Island turbidites of the Pınallı Island volcanoclastics have been overlain by the limestone transgression through sand face sediments. Around the Çiçek Islands the limestone transgression covered back shore sediments and the outlet of the Hekim Island basalts and continued advancing towards, the end it totally covered the Foça Depression region. Sand facieses marked with Algal biosparit-biosparrudite or epiclastic coarse grained sandstone marking sand face facieses consist of detritus material with high textural maturity(?), have low angle planer cross beddings and have various amounts of algal oncolites (hemispheroidal-ovoid stromatolites). Particularly lower part of the limestone succession, sedimented on the sand facieses is biogenic and kinds of beddings show variations depending upon the growing type of the stromatolites. In the high energy parts of the lake, sedimented bioclastic limestones have less distinct beddings on the other hand micritic limestones developed by laminated stromatolites have middle-thick beds with ellipsoidal cherts and fenestrate voids.

## 8. Discussion

A connection has been drawn between rhyolitic pyroclastics present as interface in the Kocadağ volcanoclastics, under Foça tuffs and the plinian eruptions prior to the caldera sinking(?) which produced Foça tuffs, lateral connection has been

proposed between early stage of rhyolitic Foça volcanism and Kocadağ volcanism. In Foça Peninsula a similar lithostratigraphic correlation has been shown between Foça tuffs and andesites of the Yunt Mountain volcanics (Akyürek and Soysal, 1983) by Akay and Erdoğan (2004). Geochronology and lithostratigraphy data indicates that during Late, Early Miocene while Kocadağ volcanism continued developing along with it, rhyolitic fiorite (freat) magmatism producing Foça tuff became active.

The Foça tuff extends mainly in the Foça Peninsula. It is made of the materials from the product of fiorite (freto?) magmatizm which was active in the Late Early Miocene lake where Zetindağı group (Kaya et al., 2007) was sedimenting. In the area between Foça Peninsula and Yunt Mountain, ignimbrite lava flows generated from a possible underwater caldera development flowing westwards, past over the Kocadağ volcanoclastics and around Uzun Island leaned at the west side of the Foça Depression (East side of the Karaburun Peninsula).

Reflecting Middle Miocene basin development (Kaya, 1979, 1981; Göktaş, 2011, 2014a,b) in the Urla region defined Urla group sedimentation in the west side of Foça Depression, and in the islands group in İzmir bay, it starts with sediments of the alluvium fan deposits. Lacustrine part of the Urla group is likely to be correlated with the Aliğa limestone; previous work carried out in the depression's Foça region (Figure 1A) did not mention presence of alluvial sediments at the bottom of the Aliğa limestone, reflecting an unconformity. According to the stratigraphic observations Aliğa limestone lies concordantly and transitionally on the Foça tuff (Kaya, 1979, 1881; Eşder et al., 1994; Akay and Erdoğan, 2004). All these data may indicate that while Foça Depression was extending W-SW direction and forming the Urla basin at the beginning of Middle Miocene, in the Foça region, in the remaining Late Early Miocene basin lacustrine sedimentation continued following the emplacement of the Foça tuff.

The Urla group lies with an unconformity on the Foça tuffs, according to the geochronological data of the Foça tuff; lowest age boundary of the Urla group is considered to be the beginning of Middle Miocene. Intrusion of Hekim Island basalt into the lower

part of the Urla limestone 14.8 Ma ago, supports this suggestion. In the Foça depression in general, although there has not been any reliable data on the upper age limit of the Urla group, in the Urla basin, based on the 11.3 Ma. age of the Ovacık basalt (Borsi et al., 1972) intruding the Urla limestone it may be suggested that sedimentation process continued until the end of Middle Miocene.

Late Miocene unconformity is not observable in the study area but göktaş (2014 *a,b*) described it in the west side of the Foça depression. It was suggested that prior to the Late Miocene extension which effected Western Turkey, the Urla group sedimentation ended with short lasting compression phase (Yılmaz, 2000; Yılmaz et al., 2000).

### Acknowledgement

This study is a small part of an MTA project of ‘Stratigraphic and Paleogeographic evolution of the Neogene and Quaternary basins in the Çeşme, Urla, Cumaovası, Kemalpaşa-Torbali depression, coded as (2008-30-14-01.g)’ Geological Engineers Mr. Murat Yükcünç and Mr. Muharrem Göktaş took part in the field work in 2008. Assoc. Prof. Dr. Erhan Akay assisted in the introduction and sampling of the Foça rhyolite. Assoc. Prof. Dr. Fuat Erkül assisted in reorganizing the text. Geological Engineer Mr. Aytekin Çolak contributed in the evaluation of the geochemical data, Dr. H. Yavuz Hakyemez critically read the paper and made some valuable comments. Their contributions are greatly acknowledged.

### References

Agostini, S., Tokçaeer, M., Savaşçın, M.Y. 2010. Volcanic rocks from Foça-Karaburun and Ayvalık-Lesvos Grabens (Western Anatolia) and their petrogenic-geodynamic significance. *Turkish Journal of Earth Sciences* 19, 157-184.

Akay, E. 2000. Magmatic and tectonic evolution of the Yuntdağ volcanic complex (Western Anatolia). PhD thesis, Dokuz Eylül Üniversitesi, Fen Bilimleri Enstitüsü, 137 s. İzmir (unpublished)

Akay, E., Erdoğan, B. 2001. Formation of subaqueous felsic domes and accompanying pyroclastic deposits on the Foça Peninsula (İzmir, Turkey). *International Geology Review* 43, 661-674.

Akay, E., Erdoğan, B. 2004. Evolution of Neogene calc-alkaline to alkaline volcanism in the Aliağa-Foça region (western Anatolia, Turkey). *Journal of Asian Sciences* 24, 367-387.

Akyürek, B., Soysal, Y. 1983. Biga Yarımadası güneyinin (Savaştepe-Kırkağaç-Bergama-Ayvalık) temel jeolojisi özellikleri. *Maden Tetkik ve Arama Dergisi* 95/96, 1-12.

Altunkaynak, Ş., Yılmaz, Y. 2000. Foça yöresinin jeolojisi ve aktif tektoniği, Batı Anadolu. *Batı Anadolu'nun Depremselliği Sempozyumu (BADSEM 2000)*, 24-27 Mayıs 2000, İzmir, Bildiriler, 160-165.

Altunkaynak, Ş., Yılmaz, Y., Rogers, N., Kelley, S. 2006. Batı Anadolu'daki Çarpışma Sonrası Magmatizmanın Petrojenetik Evrimi; Foça Volkanikleri. *59. Türkiye Jeoloji Kurultayı*, 20-24 Mart 2006, Ankara, Bildiriler, 37-38.

Altunkaynak, Ş., Rogers, N.W., Kelley S.P. 2010. Causes and effects of geochemical variations in late Cenozoic volcanism of the Foça volcanic centre, NW Anatolia, Turkey. *International Geology Review* 52, 579-607.

Borsi, S., Ferrara, C., Innocenti, F., Mazzuoli, R. 1972. Geochronology and petrology of recent volcanics of Eastern Aegean Sea. *Bulletin of Volcanology*, 36, 473-496.

Brown, J.B., Bell, B.R. 2007. How do you grade peperites? *Journal of Volcanology and Geothermal Research* 159, 409-420.

Cas, R.A.F., Wright, J.V. 1987. Volcanic successions: modern and ancient. *Chapman & Hall, UK*, 528 s.

Çakmakoğlu, A., Bilgin, Z.R. 2006. Karaburun Yarımadası'nın Neojen öncesi stratigrafisi. *Maden Tetkik ve Arama Dergisi*, 132, 33-62.

Dönmez, M., Türkecan, A., Akçay, A.E., Hakyemez, H.Y., Sevin, D. 1998. İzmir ve kuzeyinin jeolojisi, Tersiyer volkanizmasının petrografik ve kimyasal özellikleri. *Maden Tetkik ve Arama Genel Müdürlüğü Rapor No: 10181* 123 s. Ankara (unpublished).

Ejima, Y., Fujina, T., Tagaki, H., Shimada, K., Iwagana, T., Yoneda, Y., Murakami, Y. 1987. The pre-feasibility study on the Dikili-Bergama geothermal development Project in the Republic of Turkey, Progress Report II: (unpublished).

Ercan, T., Satır, M., Sevin, D., Türkecan, A. 1997. Batı Anadolu'da Tersiyer ve Kuvaterner yaşlı volkanik kayalarda yeni yapılan radyometrik yaş ölçümlerinin yorumu. *Maden Tetkik ve Arama Dergisi* 119, 103-112.

- Eşder, T., Tunçay, İ., Yakabağ, A., Ölmez, E., Güner, A. 1994. Aliğa (İzmir) sahasının jeotermal enerji olanaklarının gradyan ve araştırma kuyuları ile jeoloji, jeofizik olarak incelenmesi. *Maden Tetkik ve Arama Genel Müdürlüğü Rapor No: 9467*, 213 s. Ankara (unpublished)
- Göktaş, F. 2010. Çeşme Yarımadası'ndaki Neojen tortullaşması ve volkanizmasının jeolojik etüdü. *Maden Tetkik ve Arama Genel Müdürlüğü Rapor No: 11389*, 64 s. Ankara (unpublished).
- Göktaş, F. 2011. Urla (İzmir) çöküntüsündeki Neojen tortullaşması ve volkanizmasının jeolojik etüdü. *Maden Tetkik ve Arama Genel Müdürlüğü Rapor No: 11568*, 112 s. Ankara (unpublished).
- Göktaş, F. 2014. Karaburun (İzmir) çevresinin Neojen stratigrafisi ve paleocoğrafik evrimi. *Maden Tetkik ve Arama Dergisi* 149, 71-94.
- Helvacı, C., Ersoy, Y., Sözbilir, H., Erkül, F., Sümer, Ö., Uzel, B. 2009. Geochemistry and <sup>40</sup>Ar/<sup>39</sup>Ar geochronology of Miocene volcanic rocks from the Karaburun Peninsula: Implications for amphibole-bearing lithospheric mantle source, Western Anatolia. *Journal of Volcanology and Geothermal Research*, 185, 181-202.
- Karacık, Z., Genç, Ş.C., Gülmez, F. 2013. Petrochemical features of Miocene volcanism around the Çubukludağ graben and Karaburun Peninsula, Western Turkey: Implications for crustal melting related silicic volcanism. *Journal of Asian Earth Science* 73, 199-217.
- Kaya, O. 1979. Ortadoğu Ege çöküntüsünün (Neojen) stratigrafisi ve tektoniği. *Türkiye Jeoloji Kurumu Bülteni* 22/1, 35-58.
- Kaya, O. 1981. Miocene reference section for the coastal parts of West Anatolia. *Newsletters on Stratigraphy* 10, 164-191.
- Kaya, O., Ünay, E., Göktaş, F., Saraç, G. 2007. Early Miocene stratigraphy of Central West Anatolia, Turkey: implications for the tectonic evolution of the Eastern Aegean area. *Geological Journal* 42, 85-109.
- Le Bas, M.J., Le Maitre, R.W., Streckeisen, A., Zanettin, B. 1986. A chemical classification of volcanic rocks based on total alkali-silica diagram. *Journal of Petrology* 27, 745-750.
- Miyashiro, A. 1978. Nature of alkaline volcanic series. *Contributions to Mineralogy and Petrology* 66, 91-104
- Öngür, T. 1972. Dikili-Bergama jeotermal araştırma sahasına ilişkin jeoloji raporu. *Maden Tetkik ve Arama Genel Müdürlüğü Rapor No:5444*, 70 s. Ankara (unpublished).
- Postma, G., Nemeç, W., Kleinspehn, K.L. 1988. Large floating clasts in turbidites: a mechanism for their emplacement. *Sedimentary Geology*, 58, 47-61.
- Sayın, E. 2003. Physical features of the İzmir Bay. *Continental Shelf Research* 23, 957-970.
- Seghedi, I., Helvacı, C., Pecskey, Z. 2015. Composite volcanoes in the South-eastern part of İzmir-Balıkesir Transfer Zone, Western Anatolia, Turkey. *Journal of Volcanology and Geothermal Research* 291, 72-85.
- Türkecan, A., Ercan, T., Sevin, D. 1998. Karaburun Yarımadası'nın Neojen volkanizması. *Maden Tetkik ve Arama Genel Müdürlüğü Rapor No:10185*, 35 s. Ankara (unpublished).
- Yılmaz, Y. 2000. Ege bölgesinin aktif tektoniği. *Batı Anadolu'nun depremselliği Sempozyumu (BADSEM-2000)*, 24-27 Mayıs 2000, İzmir, Bildiriler, 3-14.
- Yılmaz, Y., Genç, Ş.C., Gürer, O.F., Bozcu, M., Yılmaz, K., Karacık, Z., Altunkaynak, Ş., Elmas, A. 2000. When did the western Anatolian grabens begin to develop?, Bozkurt, E., Winchester, J.A., Piper, J.A.D. (eds), Tectonics and Magmatism in Turkey and the Surrounding Area. *Geological Society of London*, Special Publication 173, 353-384.



# BULLETIN OF THE MINERAL RESEARCH AND EXPLORATION

<http://bulletin.mta.gov.tr>

BULLETIN OF THE MINERAL RESEARCH AND EXPLORATION	
CONTENTS	
THE ILICA BRANCH OF THE SOUTHEASTERN ESKİŞEHİR FAULT ZONE: AN ACTIVE RIGHT-LATERAL STRIKE-SLIP STRUCTURE IN CENTRAL ANATOLIA, TURKEY	Korhan ESAT <sup>a*</sup> , Bülent KAYPAK <sup>b</sup> , Veysel İŞİK <sup>a</sup> , Berkan ECEVİTOĞLU <sup>c</sup> and Gürol SEYİTOĞLU <sup>a</sup>
Research Article	

## THE ILICA BRANCH OF THE SOUTHEASTERN ESKİŞEHİR FAULT ZONE: AN ACTIVE RIGHT-LATERAL STRIKE-SLIP STRUCTURE IN CENTRAL ANATOLIA, TURKEY

Korhan ESAT<sup>a\*</sup>, Bülent KAYPAK<sup>b</sup>, Veysel İŞİK<sup>a</sup>, Berkan ECEVİTOĞLU<sup>c</sup> and Gürol SEYİTOĞLU<sup>a</sup>

<sup>a</sup>Ankara Üniversitesi, Jeoloji Mühendisliği Bölümü, Tektonik Araştırma Grubu, 06100, Tandoğan, Ankara

<sup>b</sup>Ankara Üniversitesi, Jeofizik Mühendisliği Bölümü, 06100, Tandoğan, Ankara

<sup>c</sup>Anadolu Üniversitesi, Yer ve Uzay Bilimleri Enstitüsü, 26555, Eskişehir

Research Article

### ABSTRACT

Keywords:  
Ilica Branch,  
Eskişehir Fault Zone,  
Neotectonics, Strike-  
Slip, Central Anatolia

The Eskişehir Fault Zone is one of the prominent neotectonic structures of Turkey. It separates the west Anatolian extensional province and the strike-slip induced northwest central Anatolian contractional area in the Anatolian Block. Its southeastern part is generally divided into three branches, namely the Ilica, Yeniceoba, and Cihanbeyli from north to south, respectively. The right lateral strike-slip Ilica branch (IB) is an approximately 100-km-long fault and it is composed of several segments in a northwest-southeast direction. The slickensides, subsidiary fractures, cataclastic zone, fracture-controlled drainage pattern, right lateral stream deflections, deformation in the Quaternary unit observing in the seismic reflection sections, and seismicity of the region all indicate that the IB is an active right lateral strike-slip fault. The IB has also a regional tectonic importance as a boundary fault between the contractional and the extensional regions in central Anatolia considering that it is the southern limit of the contraction-related structures in the west-southwest of Ankara.

Received: 14.02.2015

Accepted: 30.07.2015

### 1. Introduction

The division of the neotectonic provinces of Turkey has been discussed by Şengör (1979, 1980), who proposed dividing them into the North Turkish Province, the East Anatolian Contractional Province, the Central Anatolian “Ova” Province and the West Anatolian Extensional Province (Şengör et al., 1985). The border between the Central Anatolian “Ova” Province and the West Anatolian Extensional Province is evaluated differently. While Şengör et al. (1985) suggest a transition zone, Barka and Reilinger (1997) propose a division according to the recumbent V-shaped borders created by the NW-SE trending Eskişehir and the NE-SW trending Fethiye-Burdur Fault Zones (Figure 1a). Barka and Reilinger (1997) attribute a major role only to the NW part of the Eskişehir Fault Zone (EFZ) because most studies have confirmed the Eskişehir Fault as a short structure around the Eskişehir settlement (Ketin, 1968; Şengör et al., 1985; Şaroğlu et al., 1987), with only one study showing the EFZ as a structure between İnegöl

and central Anatolia in its overall neotectonic map (Koçyiğit, 1991a). Another perspective concerning the EFZ is to extend it from Thrace to central Anatolia during the Early Miocene-Early Pliocene (Yaltrak, 2002). The thermochronological data from the Uludağ massif suggest that the initiation age of the EFZ dates back to Oligocene times (Okay et al., 2008). The regional importance of the EFZ as an eastern border of the West Anatolian Extensional Province has also been emphasized by Koçyiğit and Özacar (2003), especially in light of the normal fault-induced Sultandağ and Çay earthquakes (Taymaz and Tan, 2001; Başokur et al., 2002; Emre et al., 2003).

The northwestern sector of the EFZ is generally better documented than the southeastern sector, though there is no consensus about its structural characteristics. The views can be classified into two groups. One group of researchers suggests that the EFZ’s northwestern sector is composed of active normal faults that overprinted the earlier right lateral strike-slip faults (Yaltrak, 2002; Koçyiğit, 2005;

\*Corresponding author: Korhan ESAT, E-mail: [esat@ankara.edu.tr](mailto:esat@ankara.edu.tr)  
<http://dx.doi.org/10.19111/bmre.47900>

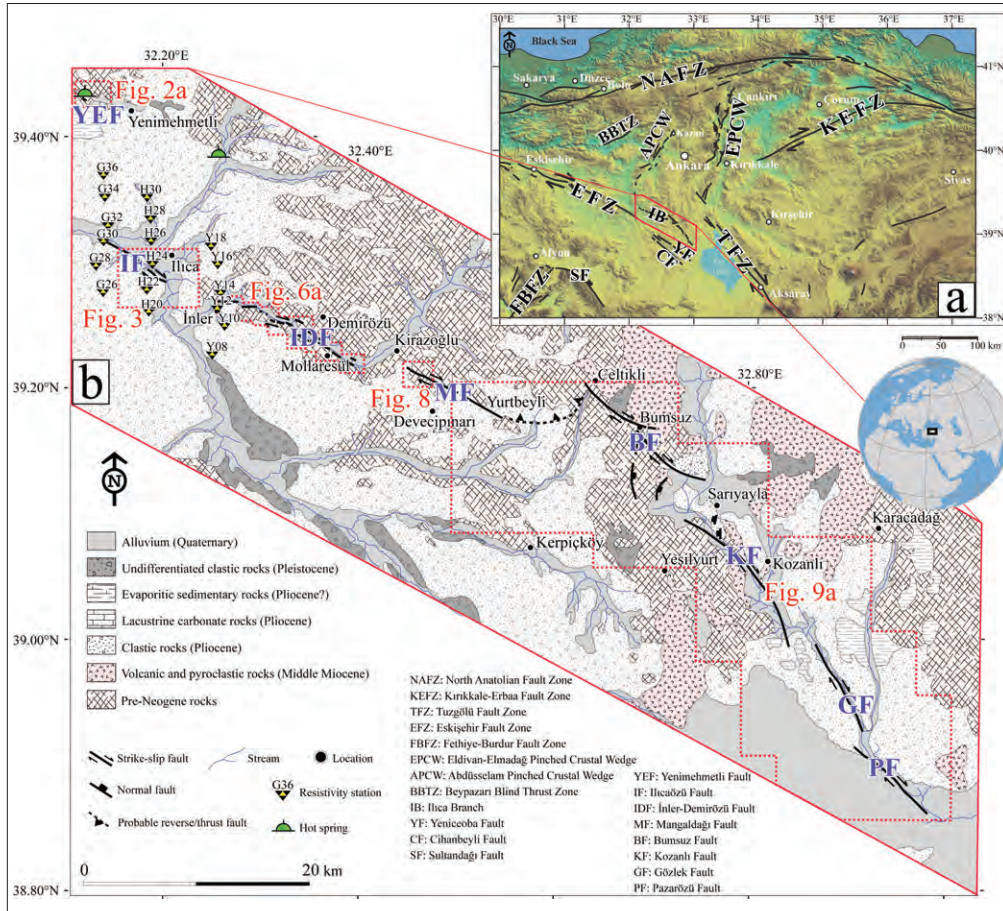


Figure 1- a) Main neotectonic elements of central Anatolia, b) Geological map of the study area (MTA, 2002). Faults were drawn in this study.

Ocakoğlu, 2007). The other group proposes that the strike-slip faults are active structures in the region that superimposed the earlier normal faults (Altunel and Barka, 1998; Seyitoğlu et al., 2010, 2015; Selçuk and Gökten, 2012).

The southeastern sector of the EFZ is composed of three branches: the Ilica, the Yeniceoba and the Çihanbeyli (Dirik and Erol, 2003). The Yeniceoba and Çihanbeyli branches (Çemen et al., 1999) have been investigated in detail by Özsayın and Dirik (2007), who concluded that the characteristics of the Yeniceoba branch vary from the right lateral strike-slip to the normal fault, while the Çihanbeyli branch has a normal fault character (Özsayın and Dirik, 2007, 2011). The northern Ilica branch appears on the maps (Koçyiğit, 1991b; Dirik and Erol, 2003) and has been drawn with the help of the right lateral displacements of the streams. However, its structural and geomorphological features have not been studied in detail.

This paper defines the morphotectonic characteristics of the Ilica branch (IB) by using remote sensing tools together with field data, seismological data and seismic reflection data. Our findings demonstrate that the IB has a right lateral strike-slip character. This result is very important when one considers the strike-slip character of the EFZ's northwestern sector (Seyitoğlu et al., 2015) indicating that the entire EFZ is undoubtedly a strike-slip structure.

## 2. Determination of the Faults Using Remote Sensing and Field Data

We used Google Earth images, SRTM, and ASTER-GDEM data to study the IB of the southeastern EFZ. High spatial resolution satellite images obtained from Google Earth software were mainly used to analyze the subsidiary faults and fractures, as well as morphotectonic features such as stream deflections. SRTM and ASTER-GDEM digital elevation

model (DEM) data were also used to determine the morphotectonic characteristics of the fault segments.

Together with the remote sensing studies, we performed field studies along the IB. We were thus able to observe and collect fault kinematic data from certain parts of the branch.

In this paper, we define the IB of the southeastern sector of the EFZ. It is composed of several faults, including, from northwest to southeast, the Yenimehmetli, Ilıcaözü, İner-Demirözü, Mangaldağı, Bumsuz, Kozanlı, Gözlek, and Pazarözü faults (Figure 1b).

### 2.1. The Yenimehmetli Fault

The best exposure of this fault is seen in the quarry located between the Yenimehmetli and the Karahamzalı villages, where a major right lateral strike-slip fault surface (N70°W, 86°SW) with horizontal slickenlines can be observed (Figure 2). Mesozoic limestone in this area is highly fractured;

these shear fractures are concurrent with the right lateral sense of shear that is apparent in the satellite images (Figure 2). The hot spring occurrences (Figure 1b) are one of the indicators of the fault activity in the area as also mentioned by Koçyiğit (1991b).

### 2.2. The Ilıcaözü Fault

A morphologically sharp contact of approximately 5 km in length is observed between the horizontal Neogene units and the Quaternary deposits near the Ilıca village (Figures 1b and 3). Although we did not obtain any fault kinematic data during the field studies, the fault is defined based on its morphological expression (Figure 3). The Ilıcaözü fault is also recognizable in the iso-resistivity sections (Figure 4a and b). These sections, which reflect electrical resistivity of the different soil and rock types near the Ilıcaözü Fault, have been produced from the unpublished data of the General Directorate of State Hydraulic Works of Turkey.

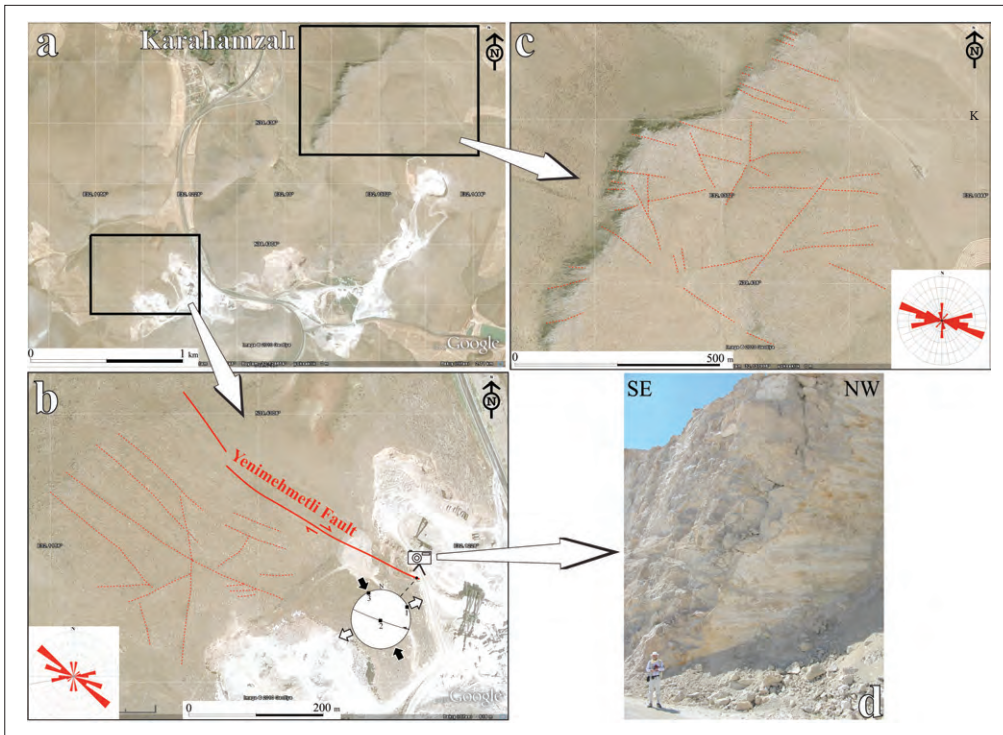


Figure 2- a) Satellite image of the Yenimehmetli fault area. See figure 1b for location, b) Position of the Yenimehmetli fault and the subsidiary fractures. Rose diagram of the fractures is displayed in the left bottom corner. The subsidiary fractures are compatible with the right lateral strike-slip Yenimehmetli fault. White circle is the lower hemisphere equal area stereographic projection of the fault plane. 1, 2, and 3 are the Linked Bingham (Kinematic) axes. Black and white arrows represent shortening and extension direction, respectively, c) Subsidiary fractures on the Mesozoic limestone. Rose diagram of the fractures is displayed in the right bottom corner. The fractures are compatible with the right lateral strike-slip Yenimehmetli fault, d) Strike-slip fault surface of the Yenimehmetli fault.

The Ilıca Branch of the Southeastern Eskişehir Fault Zone

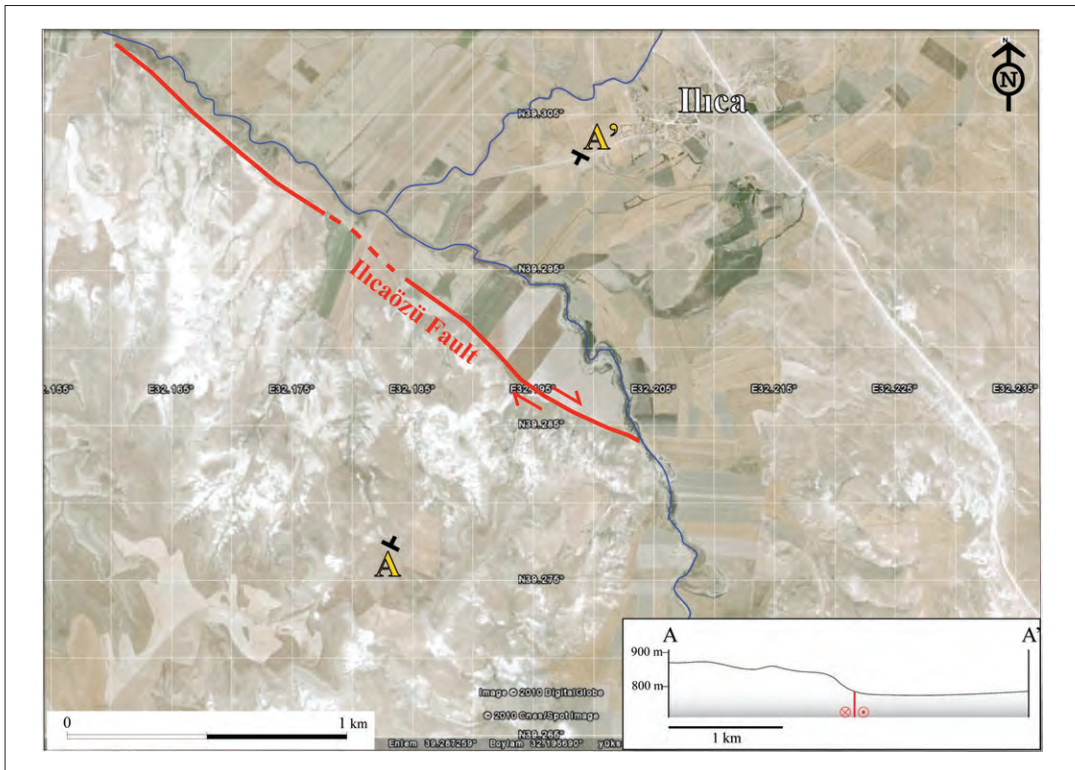


Figure 3- The Ilıcaözü fault is clearly seen on the satellite image with a morphologically sharp contact between the Neogene and the Quaternary units. See figure 1b for location. A-A' is the section line. The section is displayed in the right bottom corner.

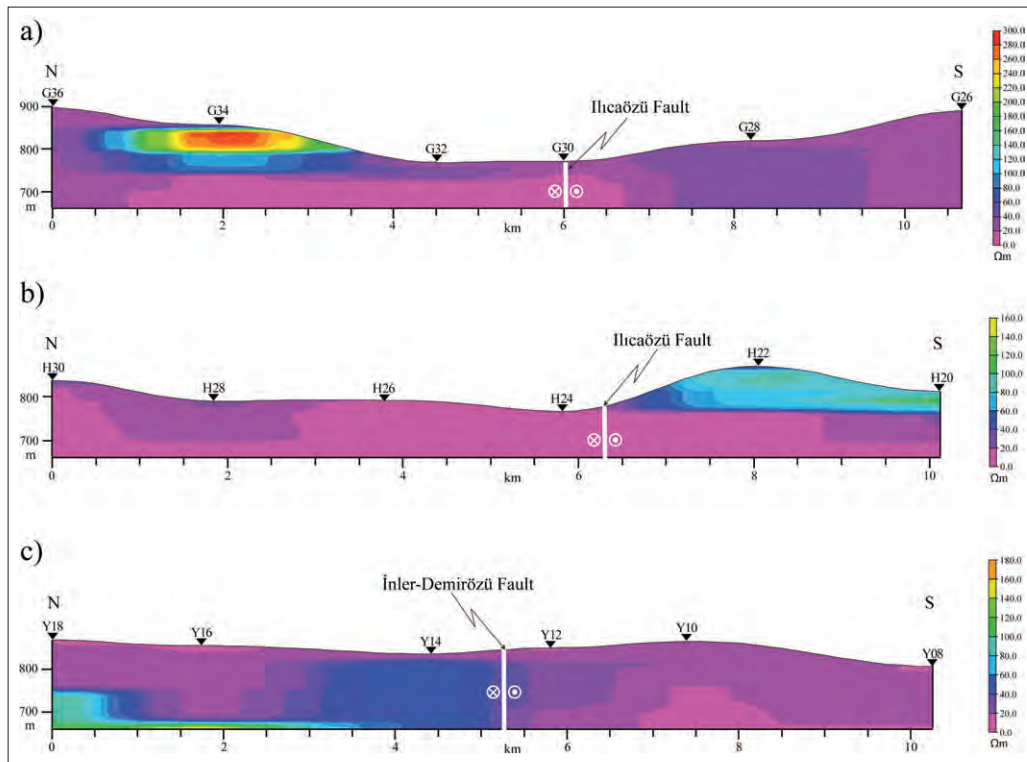


Figure 4- Iso-resistivity cross-sections. See figure 1b for locations of the sections. This unpublished resistivity data is obtained from the General Directorate of State Hydraulic Works of Turkey.

### 2.3. The İner-Demirözü Fault

Drainage pattern around the IB is dominantly fault/fracture-controlled rectangular type (Figure 5). As a typical example of this drainage style, the most important morphological expression of the İner-Demirözü fault is the cumulative 14 km right lateral diversion of the Katrancı River (Figures 1b, 5 and 6a). It is difficult to suggest that this diversion is created by the movement on the single fault segment, because the İner-Demirözü fault is composed of several en echelon segments (Figures 6a and b). The river might be emplaced and followed the trace of the fault segments. On the other hand, the structural data of the right lateral sense of shear obtained from the three locations, the small creeks are diverted right laterally in at least four locations in the range of 75 to 250 meters (Figures 6 and 7a, b, c, d). One of the typical structures along the İner-Demirözü fault is the cataclastic zone near the road between the Demirözü and Mollaresül villages. This zone can be traced along 100 m and has a width of 20 m (Figures 6 and 7c). It is characterized by crush breccia, which is a cohesive fault rock (Figure 6c). The host rock of the cataclastic zone is dark grey Mesozoic limestone that is highly fractured and crushed. The breccia consists of clasts

and matrix. The clasts are completely derived from the limestone and are a few centimetres in width, while the matrix consists of pulverised materials of the limestone which have attached to the clasts. The cataclastic zone displays fractures with calcite filling, which suggests not only a cataclasis deformation mechanism but also a diffusive mass transfer deformation mechanism. Our structural analysis of the conjugate shear fractures points out that the shortening axis direction is N10°W (Figure 6d). This direction can be correlated with right lateral sense of shearing. The İner-Demirözü fault can also be observed in the iso-resistivity section (Figure 4c).

### 2.4. The Mangaldağı Fault

This fault is separated from the İner-Demirözü fault with a 1.5-km stepover towards the NE (Figure 1b). The Mangaldağı fault is determined by using satellite images, where a 1.4-km displacement is clearly seen in the anticline of the upper Cretaceous-Paleocene (Türkönal, 1959; Yıldız et al., 2001) limestones (Figure 8a). In addition, many subsidiary fractures (R, R', P, and X) related to the fault are observed on the satellite images (Figure 8b). The orientation of these fractures is concordant with the right lateral strike-slip faulting.

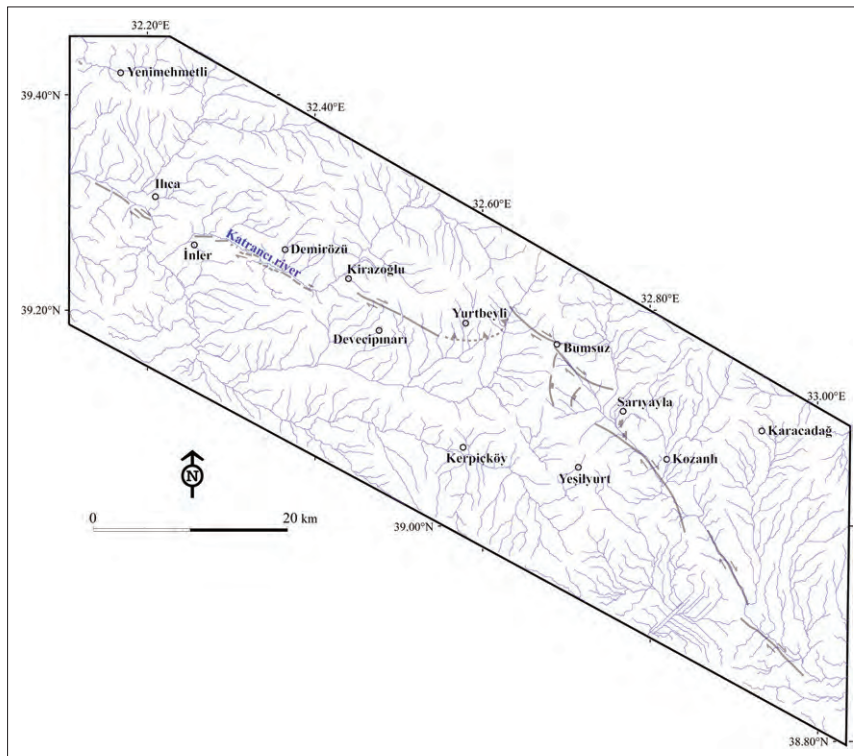


Figure 5- Dominantly fault/fracture-controlled rectangular drainage pattern of the study area.

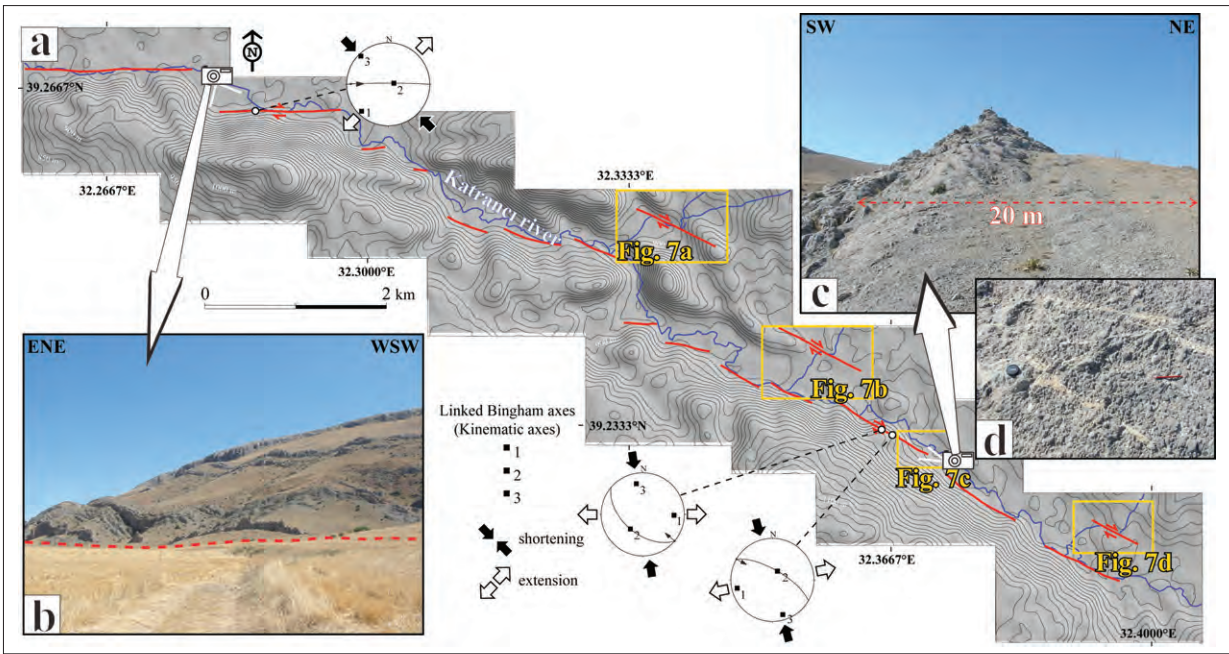


Figure 6- a) Segments of the İler-Demirözü fault on the ASTER-GDEM shaded relief image. See figure 1b for location. Circles are the lower hemisphere equal area stereographic projection of the fault planes. Black and white arrows represent shortening and extension direction, respectively. Elevation contours were derived from the ASTER-GDEM data. Yellow frames show locations of the stream offsets in figure 7, b) A view from the İler-Demirözü fault between the Paleocene clastic rocks and the Quaternary units, c) The cataclastic zone on the İler-Demirözü fault has a width of approximately 20 m, d) A close-up view from the cataclastic zone. Pencil shows the shortening axis direction of N10°W.

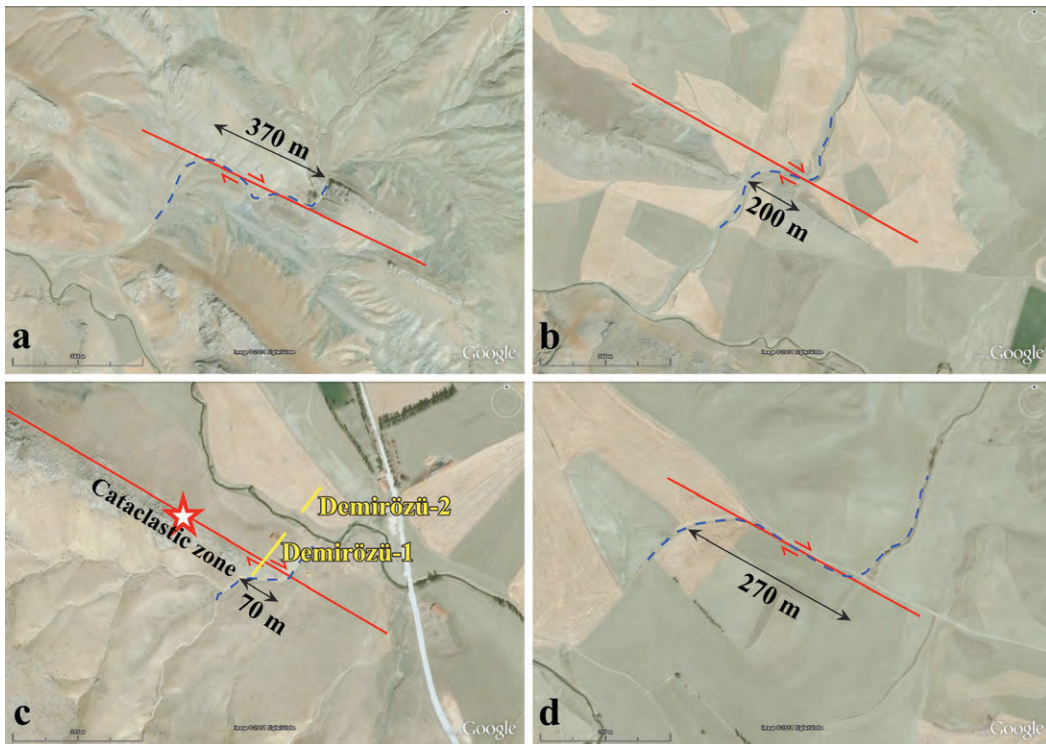


Figure 7- Satellite images related to the İler-Demirözü fault; a) 370 m stream-channel offset, b) 200 m stream-channel offset, c) 70 m stream-channel offset. The star shows the location of the cataclastic zone. Yellow lines indicate the Demirözü 1 and 2 seismic section lines, d) 270 m stream-channel offset. See figure 6 for locations.

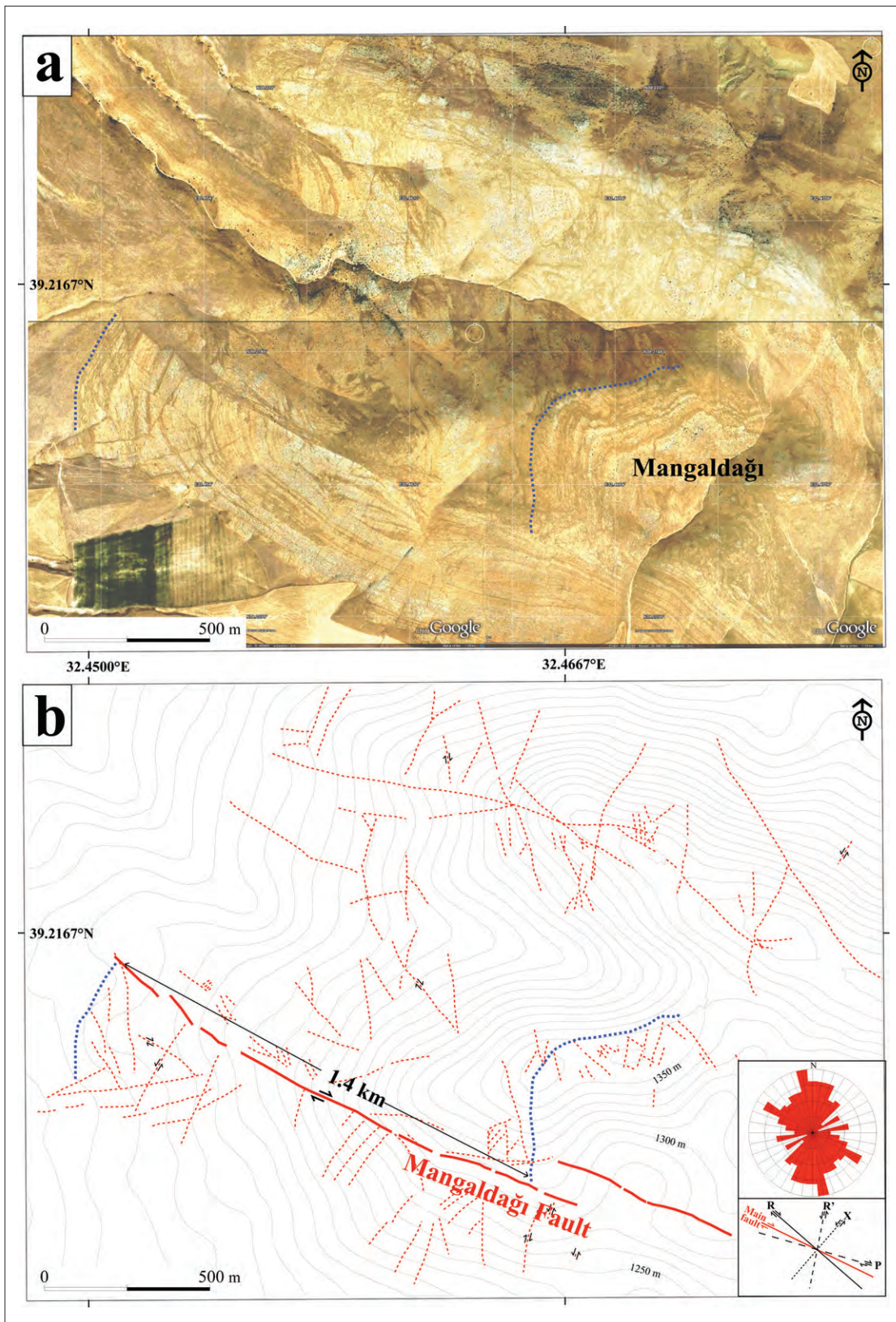


Figure 8- a) Satellite image related to the Mangaldağı fault. Brightness enhancement was applied to the image for better display of the structures, b) Position of the Mangaldağı fault and the subsidiary fractures derived from the satellite image above. 1.4 km displacement is clearly seen in the anticline of the upper Cretaceous-Paleocene limestones. Rose diagram of the fractures and theoretical position of subsidiary fractures (R, R', X, and P) are displayed in the left bottom corner for comparison. The subsidiary fractures are compatible with the right lateral strike-slip Mangaldağı fault.

## 2.5. The Bumsuz, Kozanlı, Gözlek and Pazarözü Faults

The Bumsuz fault is recognized by the sharp topographical differences between the Çeltikli and Bumsuz villages (Figures 1b and 9a) and also shown on the active fault map of Turkey (Emre et al., 2011). A shear zone and the strike-slip fault surfaces are observed on the Bumsuz fault (Figure 9b). The morphological features disappear at the north end of the Samsam Lake, but at the south of the lake, surface expressions are visible on the Kozanlı fault. Samsam Lake is located on the releasing stepover between the Bumsuz and the Kozanlı faults (Figure 9a). At the southeast end of the Kozanlı fault, a small lake called Gököl has formed due to the blocking of the stream drainage by the restraining stepover between the Kozanlı and the Gözlek faults (Figure 9a). The Gözlek stream continues along the Gözlek fault, and the fault creates a releasing offset with the Pazarözü

fault (Figure 9a). The IB, in the eastern sector of the EFZ, reaches the Tuzgölü plain following the Pazarözü fault.

## 3. Seismic Reflection Studies

The seismic reflection studies were performed on the İler-Demirözü fault, where a well-developed cataclastic zone was observed (Figure 7c).

### 3.1. Data Acquisition

We shot two seismic reflection profiles in the İler-Demirözü area (Figure 7c). The field-spread of Line Demirözü-1 was conducted using a regular ‘Walk-Away’ technique. Forty-eight vertical geophones (14 Hz) were planted with a 2-m group-interval (CDP interval was 2 m). The shot interval was 4 m. A total of 25 hammer-shots were performed with 3 vertical stacks. The first shot station was located 1 m ahead

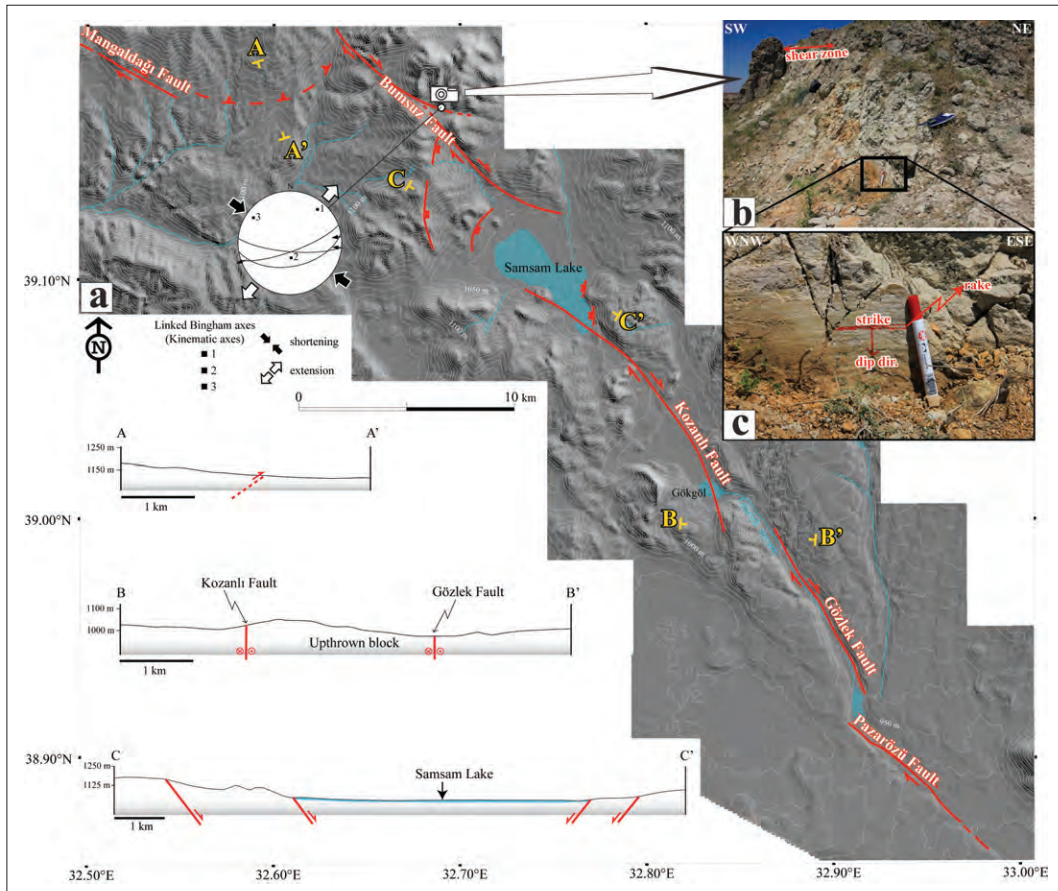


Figure 9- a) The Mangaldağı, Bumsuz, Kozanlı, Gözlek, and Pazarözü faults on the SRTM shaded relief image. A-A', B-B', and C-C' are the section lines. The sections are displayed in the left bottom side. The white circle is the lower hemisphere equal area stereographic projection of the fault planes. Black and white arrows represent shortening and extension direction, respectively. See figure 1b for location and text for explanation, b) The shear zone on the Bumsuz fault, c) A strike-slip fault surface from the shear zone.

of the first geophone station. The field-spread of Line Demirözü-2 was a special application of the ‘Walk-Away’ technique designed to cross the creek. Forty-eight vertical geophones (14 Hz) were planted at a 1-m group-interval (CDP interval was 0.5 m), with a shot interval of 2 m. A total of 25 hammer-shots were performed with 3 vertical stacks. The first shot station was located 70 m ahead of the first geophone station. For both profiles, the sampling interval was 0.5 ms, and the recording time was 2 s.

### 3.2. Data Processing

Data processing included many steps: (1) geometry definition; (2) band-pass trapezoidal filter: 1-5-90-100 Hertz; (3) time-powered gain application (power: 0.5 seconds); (4) trace editing; (5) ground-roll muting; (6) CDP-sort; (7) velocity analysis: CVS Interactive; (8) stack; (9) band-pass trapezoidal filter: 1-5-90-100 Hertz; (10) time-powered gain application (power: 0.5 seconds); (11) horizontal smoothing (weights: 0.25, 0.5, 1, 0.5, 0.25); and (12) time-to-depth conversion ( $t = 140$  ms,  $v = 1600$  m/s). While processing Line Demirözü-1, to consider the irregular topography, a static correction was applied.

### 3.3. Interpretation of the Seismic Sections

The southwest end of the Demirözü-1 seismic section corresponds to the cataclastic zone observed from the surface. This part of the seismic section is

highly deformed and fractured by the fault segments (Figure 10a). The main fault zone producing the apparent positive flower structures is located in the middle of the Demirözü-1 seismic section, which corresponds to the location between the cataclastic zone and the Katracı River in the field. All of the faults in this seismic section are clearly affected within the top 50 m from the surface, which confirms the recent activity of the İnlere-Demirözü fault (Figure 10a). The Demirözü-2 seismic section is the northeast continuation of the Demirözü-1 (Figure 10b) and is relatively less deformed. On both sides of the Katracı River, only small strike-slip fault segments buried under the recent alluvium can be observed (Figure 10b).

### 4. Seismicity of the Ilca Branch

On the basis of an earthquake catalogue prepared by KOERI for the instrumental period since 1900, the IB (shown in Figure 11) has a lesser seismic activity rate than its surroundings, such as the Bala region (Esat et al., 2014). However, the seismicity map clearly shows that the IB produced significant seismic activity ( $3 \leq M < 5$ ), especially in its northwestern and southeastern tips (Figure 11). Although the seismicity along the IB shows some clustering characteristics from place to place, it is generally distributed along the strike. In order to identify the fault geometry, a focal mechanism solution analysis was implemented using digital records of some recent earthquakes.

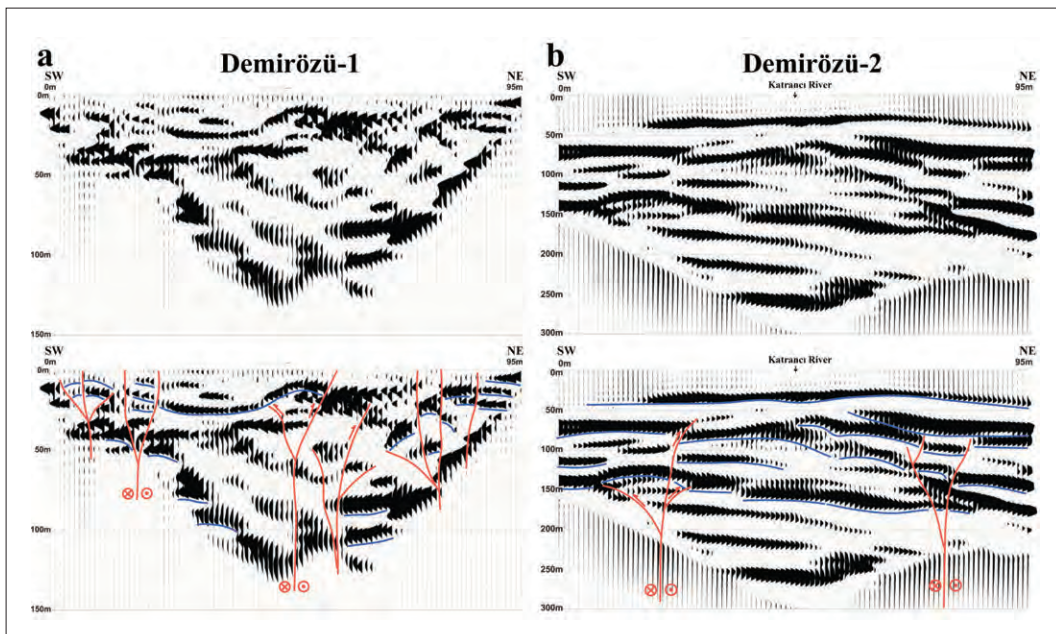


Figure 10- Seismic reflection sections from (a) Demirözü-1 and (b) Demirözü-2 section lines. Above, uninterpreted; below, interpreted. See text for explanation and figure 7c for location.

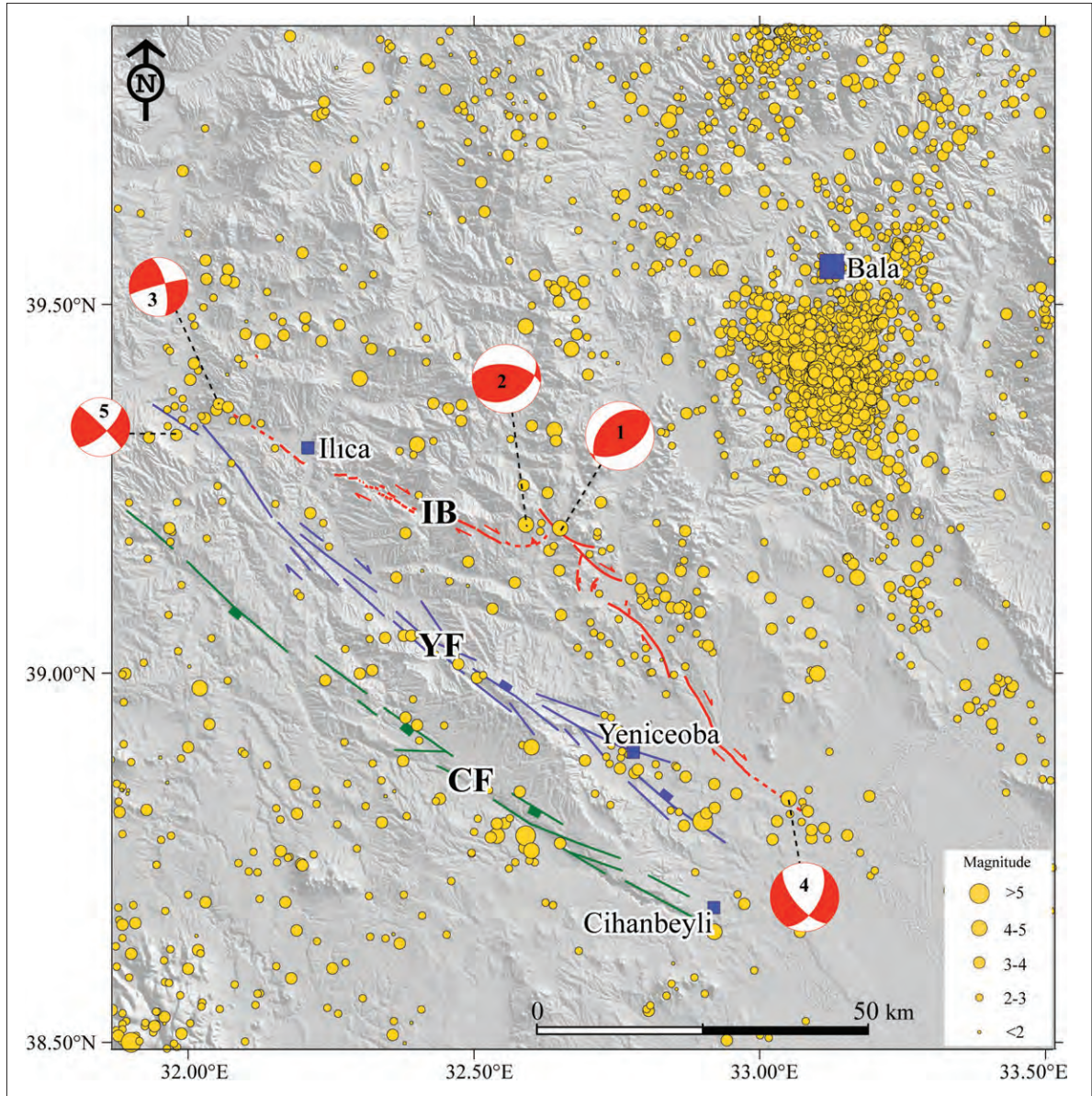


Figure 11- Earthquake distribution in the southeastern Eskişehir Fault Zone. Red line represents the Ilica branch (IB). Blue and green lines show Yeniceoba (YF) and Cihanbeyli (CF) faults, respectively (Özsayın and Dirik, 2007). Epicentral data were obtained from the Kandilli Observatory and Earthquake Research Institute (KOERI) of Turkey's catalogue for instrumental period. Parameters of the focal mechanism solutions are given in table 1.

To compute the focal mechanism solutions of the events, we used the FPFIT program (Reasenber and Oppenheimer, 1985), which computes double-couple fault plane solutions from P-wave first motion data using a grid search method. The focal mechanism solutions of the three earthquakes (06.03.2006,  $M = 3.1$ ; 13.12.2007,  $M = 4.9$  and 29.05.2010,  $M = 3.1$ ) located in both tips of the fault represent a typical strike-slip fault geometry, which is compatible with the IB (Figure 11 and table 1). Moreover, the focal mechanism solutions of the two sequential earthquakes (07.02.2004,  $M = 4.2$  and 08.02.2004,  $M = 4.4$ ) are in

the middle of the IB indicate thrust faulting (Figure 11 and table 1). This thrust faulting is expected in this area because these two earthquakes were located on the restraining stepover between the Mangaldağı and the Bumsuz faults, where the IB changes direction nearly  $30^\circ$  (Figures 9 and 11).

## 5. Discussion and Conclusions

In this study, the right lateral strike-slip IB was defined via remote sensing, field observations, seismology, and seismic reflection studies.

Table 1- Parameters of the focal mechanism solutions.

No	Date (dd/mm/yyyy)	Time (GMT)	Lat. N (°)	Lon. E (°)	Depth (km)	Mag.	Nodal Planes			P		T	
							Str.1(°) Str.2(°)	Dip1(°) Dip2(°)	Rake1(°) Rake2(°)	Azi. (°)	Plunge (°)	Azi. (°)	Plunge (°)
1	07/02/2004	19:26:19.20	39.1928	32.6547	2.0	4.2	60 225	50 41	100 78	143	5	23	81
2	08/02/2004	09:27:54.30	39.2037	32.5905	10.0	4.4	60 277	40 56	60 113	351	8	238	69
3	06/03/2006	20:18:35.85	39.3628	32.0570	17.2	3.1	255 347	85 70	-20 -175	209	18	303	10
4	13/12/2007	18:06:18.70	38.8267	33.0507	5.0	4.9	140 30	65 54	-140 -31	360	45	263	6
5	29/05/2010	13:47:12.07	39.3162	31.9940	7.2	3.1	315 47	85 70	160 5	3	10	269	18

The IB is considered as one of the three branches of the southeastern EFZ, and it is the southern limit of the contractional structures (i.e. folds, blind thrust faults, and pinched wedge structures) located between Kazan and Yenimehmetli (W and SW of Ankara) (Esat and Seyitoğlu, 2010; Esat, 2011). The IB is composed of several right lateral strike-slip faults and their corresponding segments. This is an important conclusion when we consider about the different views on the character of the EFZ. Some studies describe the EFZ as İnönü-Eskişehir Fault System (Özsayın and Dirik, 2007, 2011) which runs from Bursa to the west of Tuzgölü. In these studies, the Eskişehir, Ilıca, Yeniceoba, and Cihanbeyli branches constitute the İnönü-Eskişehir Fault System. Eskişehir and Ilıca branches have right lateral strike-slip character, but Yeniceoba and Cihanbeyli branches are determined as normal fault with right lateral strike-slip component and pure normal fault, respectively (Özsayın and Dirik, 2007, 2011). Apart from this, other researchers define the active faults in western part of the EFZ between İnönü and Eskişehir as normal faults (Yaltrak, 2002; Koçyiğit, 2005; Ocakoğlu, 2007). The recent study (Seyitoğlu et al., 2015), however, suggest that the active faults in this area have a N60W trending right lateral strike-slip character. Faults in the area between the east of Eskişehir and the IB are also mapped as right lateral strike-slip faults with normal components by Selçuk and Gökten (2012). These results together with our observations about the nature of IB are demonstrated that the EFZ is dominantly a right lateral strike-slip zone. Thus, the Yeniceoba and Cihanbeyli branches, which assumed to be the southeastern parts of the EFZ, could be considered as independent faults from the EFZ due to their normal fault nature, even if they appear to be morphologically related to the EFZ.

The triangle shaped area bounded with the NAFZ, KEFZ, and EFZ is under the influence of NW-SE contraction and it is defined as a neotectonic region called “NW central Anatolian contractional area”. The EFZ is a boundary structure between this contractional area and the west Anatolian extensional province (Esat and Seyitoğlu, 2010; Esat, 2011). The IB, eastern continuation of the EFZ, is the southern limit of the contractional structures which lie between immediately W and SW of Ankara, as also mentioned above. These structures are not observed south of the branch (Figure 1a; Esat, 2011). Consequently, the IB has an important meaning for the regional geology, considering its role as an eastern boundary between the contractional and the extensional regions in central Anatolia. Moreover, the seismic activity and the morphotectonic features also show that the IB is an active structure. Therefore, it should be taken into consideration for the earthquake risk assessment of the capital city Ankara and its surroundings together with the Yeniceoba and Cihanbeyli faults that described by earlier studies.

#### Acknowledgements

This work was supported by Ankara University (project no. 06B4343011) and the National Union of Geodesy and Geophysics of Turkey (TUJJB)-National Earthquake Programme (UDP) (project no. TUJJB-UDP-01-10). R.W. Allmendinger’s FaultKin software was used for the fault kinematic analysis. We are grateful to Timur Ustaömer and two anonymous reviewers for their valuable comments.

## References

- Altunel, E., Barka, A. 1998. Eskişehir fay zonunun İnönü-Sultandere arasında neotektonik aktivitesi. *Türkiye Jeoloji Bülteni* 41, 2, 41-52.
- Barka, A., Reilinger, R. 1997. Active tectonics of the Eastern Mediterranean region: deduced from GPS, neotectonic and seismicity data. *Annali Di Geofisica* 40, 3, 587-610.
- Başokur, A.T., Gökten, E., Seyitoğlu, G., Varol, B., Ulugergerli, E., Işık, V., Candansayar, E., Tokgöz, E. 2002. Jeoloji ve jeofizik çalışmalar ışığında 03.02.2002 Çay (Afyon) depremi'nin mekanizması, hasarın nedenleri ve bölgenin deprem etkinliği. *Ankara Üniversitesi Mühendislik Fakültesi Yayını*, 56 s.
- Çemen, I., Göncüoğlu, M.C., Dirik, K. 1999. Structural evolution of the Tuzgölü basin in Central Anatolia, Turkey. *Journal of Geology* 107, 693-706.
- Dirik, K., Erol, O. 2003. Tectonomorphologic evolution of Tuzgölü and surrounding area, central Anatolia, Turkey. *Türkiye Petrol Jeologları Derneği Özel Sayı* 5, 27-46.
- Emre, Ö., Duman, T.Y., Doğan, A., Özalp, S., Tokay, F., Kuşçu, İ. 2003. Surface faulting associated with the Sultandağı earthquake (Mw 6.5) of 3 February 2002, southwestern Turkey. *Seismological Research Letters* 74, 4, 382-392.
- Emre, Ö., Duman, T.Y., Özalp, S., Elmacı, H., Olgun, Ş. 2011. 1/250.000 Ölçekli Türkiye Diri Fay Haritası Serisi, Ankara (NJ 36-2) Paftası, Seri No: 20, *Maden Tetkik ve Arama Genel Müdürlüğü*, Ankara.
- Esat, K. 2011. Ankara çevresinde Orta Anadolu'nun neotektoniği ve depremselliği. Doktora Tezi, Ankara Üniversitesi, 144 s., Ankara (unpublished).
- Esat, K., Seyitoğlu, G. 2010. Neotectonics of north central Anatolia: a strike-slip induced compressional regime. *Tectonic Crossroads: Evolving Orogens of Eurasia-Africa-Arabia Conference*, 4-8 October 2010, Ankara, 38.
- Esat, K., Çıvgın, B., Kaypak, B., Işık, V., Ecevitoglu, B., Seyitoğlu, G. 2014. The 2005-2007 Bala (Ankara, central Turkey) earthquakes: a case study for strike-slip fault terminations. *Geologica Acta* 12, 1, 71-85.
- Ketin, İ. 1968. Relations between general tectonic features and the main earthquake regions of Turkey. *Maden Tetkik ve Arama Dergisi* 71, 63-67.
- Koçyiğit, A. 1991a. An example of an accretionary forearc basin from northern Central Anatolia and its implications for the history of subduction of Neo-Tethys in Turkey. *Geological Society of America Bulletin* 103, 22-36.
- Koçyiğit, A. 1991b. Changing stress orientation in progressive intracontinental deformation as indicated by the neotectonics of the Ankara region (NW central Anatolia). *Turkish Association of Petroleum Geologists Bulletin* 3, 43-55.
- Koçyiğit, A. 2005. The Denizli graben-horst system and the eastern limit of western Anatolian continental extension: basin fill, structure, deformational mode, throw amount and episodic evolutionary history, SW Turkey. *Geodinamica Acta* 18, 167-208.
- Koçyiğit, A., Özacar, A.A. 2003. Extensional neotectonic regime through the NE edge of the outer Isparta Angle, SW Turkey: new field and seismic data. *Turkish Journal of Earth Sciences* 12, 67-90.
- MTA. 2002. 1/500.000 ölçekli Türkiye Jeoloji Haritası, Ankara Paftası. *Maden Tetkik ve Arama Genel Müdürlüğü*, Ankara.
- Ocakoğlu, F. 2007. A re-evaluation of the Eskişehir Fault Zone as a recent extensional structure in NW Turkey. *Journal of Asian Earth Sciences* 31, 91-103.
- Okay, A.I., Satır, M., Zattin, M., Cavazza, W., Topuz, G. 2008. An Oligocene ductile strike-slip shear zone: the Uludağ Massif, northwest Turkey - Implications for the westward translation of Anatolia. *Geological Society of America Bulletin* 120, 893-911.
- Özsayın, E., Dirik, K. 2007. Quaternary activity of the Cihanbeyli and Yeniceoba Fault Zones: İnönü-Eskişehir Fault System, central Anatolia. *Turkish Journal of Earth Sciences* 16, 471-492.
- Özsayın, E., Dirik, K. 2011. The role of oroclinal bending in the structural evolution of the Central Anatolian Plateau: evidence of a regional changeover from shortening to extension. *Geologica Carpathica* 62, 4, 345-359.

- Reasenber, P., Oppenheimer, D. 1985. Fpfit, fpplot, and fppage: Fortran computer programs for calculating and displaying earthquake fault plane solutions. California, U.S. Geological Survey, Technical report.
- Selçuk, A.S., Gökten, E. 2012. Neotectonic characteristics of the İnönü-Eskişehir Fault System in the Kaymaz (Eskişehir) Region: influence on the development of the Mahmudiye-Çifteler-Emirdağ Basin. *Turkish Journal of Earth Sciences* 21, 521-545.
- Seyitoğlu, G., Esat, K., Temel, A., Telsiz, S. 2010. Determination of main strand of a strike-slip fault by using subsidiary structures: Eskişehir Fault Zone as a case study. *Tectonic Crossroads: Evolving Orogens of Eurasia-Africa-Arabia Conference*, 4-8 October 2010, Ankara, 32.
- Seyitoğlu, G., Ecevitöglu, B., Kaypak, B., Güney, Y., Tün, M., Esat, K., Avdan, U., Temel, A., Çabuk, A., Telsiz, S., Uyar Aldaş, G. 2015. Determining the main strand of the Eskişehir strike-slip fault zone using subsidiary structures and seismicity: a hypothesis tested by seismic reflection studies. *Turkish Journal of Earth Sciences* 24, 1, 1-20.
- Şaroğlu F., Emre, Ö., Boray, A. 1987. Türkiye'nin diri fayları ve depremsellikleri raporu. *Maden Tetkik ve Arama Genel Müdürlüğü Report No: 8174*, 394 s. Ankara (unpublished).
- Şengör, A.M.C. 1979. The North Anatolian transform fault: its age, offset and tectonic significance. *Journal of the Geological Society, London* 136, 269-282.
- Şengör, A.M.C. 1980. Türkiye'nin neotektoniğinin esasları. Türkiye Jeoloji Kurumu Konferans Serisi 2, 40 s.
- Şengör, A.M.C., Görür, N., Şaroğlu, F. 1985. Strike-slip faulting and related basin formation in zones of tectonic escape: Turkey as a case study. *The Society of Economic Paleontologists and Mineralogists, Special Publication* 37, 227-264.
- Taymaz, T., Tan, O. 2001. Source parameters of June 6, 2000 Orta-Çankırı and December 15, 2000 Sultandağ-Akşehir earthquakes (Mw = 6.0) obtained from inversion of teleseismic P- and SH-body-waveforms. *Symposia on Seismotectonics of the North-Western Anatolia-Aegean and Recent Turkish Earthquakes*, 8 May 2001, İstanbul, 96-107.
- Türkönal, M. 1959. Note on the Ammonite-bearing beds in the various localities of Turkey-Part one: Ankara region. *Maden Tetkik ve Arama Dergisi* 52, 68-75.
- Yaltırak, C. 2002. Tectonic evolution of the Marmara Sea and its surroundings. *Marine Geology* 190, 493-529.
- Yıldız, A., Ayyıldız, T., Sonel, N. 2001. Upper Maastrichtian-Paleocene biostratigraphy and palaeoecology in northwest Tuzgölü Basin (Karahoca-Mangaldağ-Yeşilyurt-Sarıhalit area). *Yerbilimleri* 23, 33-52.





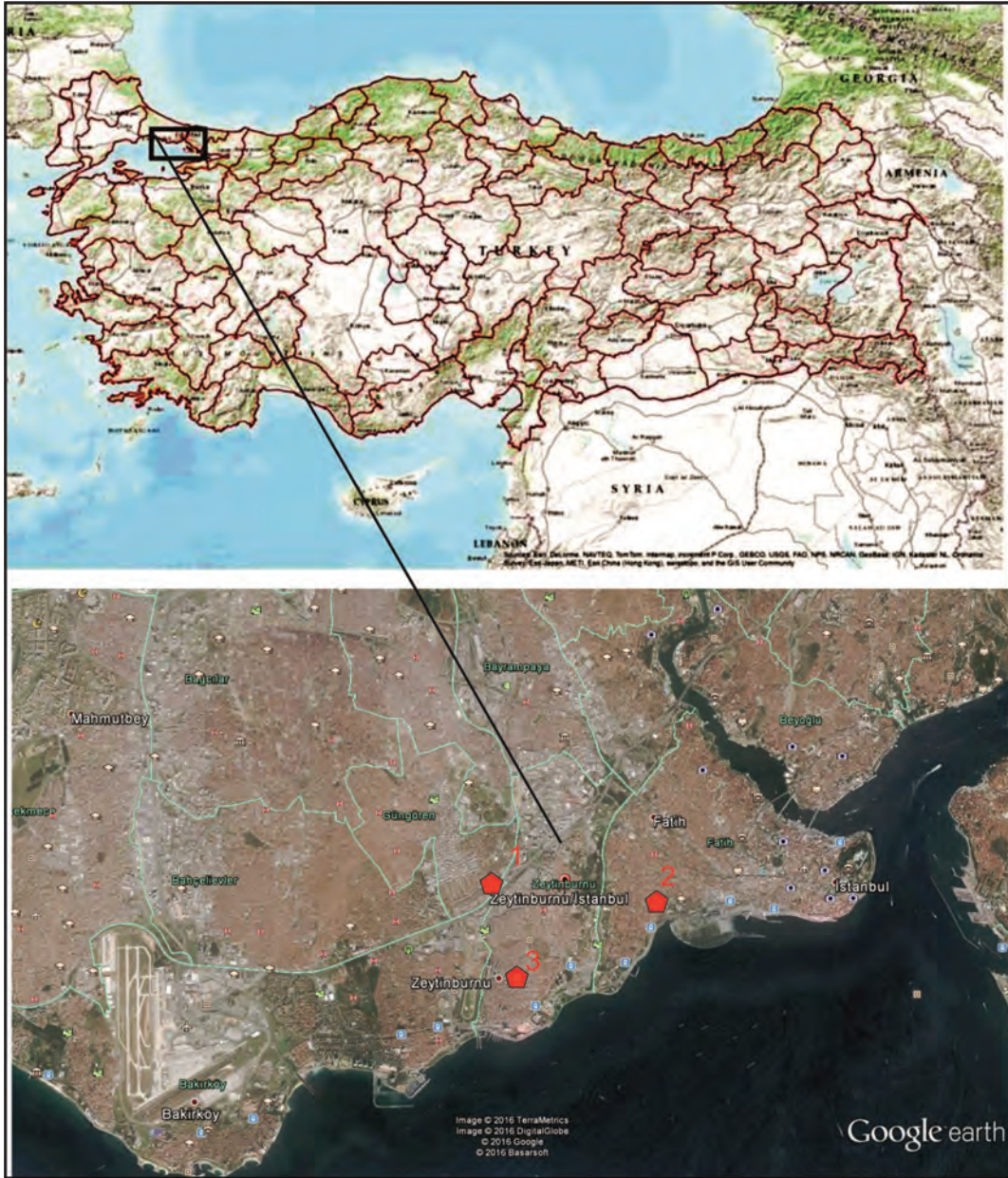


Figure 1- Location map of the study area.

especially the mollusk genera and species, which are compatible to limnic conditions, the studies of Wenz (1922), Bremer (1978), Taner (1980) and Sayar (1991) were used as basis.

SEM images of some ostracod genera and species described in this study were presented in plates 1-3.

## 2. Stratigraphy

In the study area, the Ceylan/Yenimuhacir formation is observed at the bottom and these units are conformably overlain by Danişmen formation.

The Bakırköy Formation and infilling material cover the Danişmen Formation (<http://www.ibb.gov.tr>). The units in drillings investigated in the study area from bottom to top are Danişmen and Bakırköy formations and the infilling material. These materials crop out in southwest of Istanbul and around Yedikule.

### 2.1. Danişmen Formation (Gürpınar Formation) (old)

The formation was defined by Ternek (1949) and Lebküchner (1974) as lignified sandstone; by Bear and Wright (1960) as one formation of Malkara clastic group; by Boer (1954), Gökçen (1967),

Kellog (1973), Sümengen and Terlemez(1991) as the Danişmen Formation; and as the Gürpınar formation by Sayar (1977) around Istanbul. The formation was also used under the same name in studies carried out by the Istanbul Municipality (<http://www.ibb.gov.tr>). It widely crops out in northern Thrace, on the slopes of Strandzha (Edirne), in vicinities of Süloğlu, Pınarhisar, Vize and Binkılıç and in open coal mines in southern Thrace.

The Danişmen Formation occasionally consists of varved shales, limestone, sandstone, pebble stone and coal, fish fossils in northern Thrace and silicified wooden fossils in southern Thrace (Siyako, 2002; MTA, 2006). Looking at the drillings in this study, the Danişmen Formation is formed by claystone, clayey limestone, siltstone, fossiliferous sandstone, blackish-green clay, organic clay, marl, sandy clay layers.

Ostracod genera and species such as; *Cytheromorpha zinndorfi* (Lienenklaus), *Cytheromorpha* sp., *Neocyprideis apostolescui* (Keij), *N. williamsoniana* (Bosquet), *Cytheridea pernota* (Oertli and Keij), *Cyamocytheridea punctatella* (Bosquet), *C. inflata* (Deltel), *Cyamocytheridea* sp., *Hemicyprideis montosa* (Jones and Sherborn), *H. elongata* (Keen), *H. helvetica* (Lienenklaus), *Cladarocythere apostolescui* (Margerie), *Loxococoncha delemontensis* (Oertli), *Xestoleberis subglobosa* (Bosquet), *Candona (Pseudocandona) fertilis* (Triebel), *Eucypris pechelbronnensis* (Stchepinsky), *Ilyocypris boehli* (Triebel), and micro mollusc genera such as; *Viviparussp.*, *Avimactra* sp. were described in Danişmen/Gürpınar formation (Figure 2). The age of the formation was determined as Early Oligocene due to this fossil content.

## 2.2. Bakırköy Formation (mib)

Bakırköy Formation was first described by Sayar (1977, 1989, 1992). The formation was defined as; limestone with *maetra* by Sayar (Arınç) (1955), *Melanopsis* and limestone bands with *maetra* by Ternek (1987) and as Bakırköy limestone by Sayar (1989). It outcrops in Beylikdüzü-Avcılar, Yeşilköy-Halkalı, Bağcılar-Bahçelievler, Bakırköy, Yenibosna-Mahmutbey, Merter-Esenler, Zeytinburnu-Topkapı-Kocamustafapaşa (MTA, 2006).

The formation is formed by white to dirty white, fine layered clay intercalated limestones

with *maetra* and its lower section consists of clay-limestone alternation. The Bakırköy Formation consists of limestone, fossiliferous clayey limestone, fossiliferous marl, clayey sand and clay layers in succession in this study.

The formation is gradually transitional with the underlying Güngören Formation, and it is overlain by Quaternary units. It is gradually transitional with Güngören formation, which underlies in sections discriminated and observed in Yedikule, Kazlıçeşme, Osmaniye, Rami, between Atışalanı-Esenler areas and in east of Güngören. The maximum thickness of the unit is 30 m in these regions (Arınç, 1955; <http://www.ibb.gov.tr>). The thickness of the unit was detected as 40 m by Sayar (1977, 1989, 1992). The average thickness of the unit was found as 24 m in this study. Ostracod and gastropod genera and species within Bakırköy formation such as; *Cyprideis seminulum* (Reuss), *C. torosa* (Jones), *C. anatolica* (Bassiouni), *C. pannonica* (Mehes), *C. sohni* (Bassiouni), *Miocyprideis sarmatica* (Zalanyi), *Darwinula cylindrica* (Straub), *Heterocypris salina* (Brady), *Ilyocypris bradyi* (Sars), *I. gibba* (Ramdohr), *Ilyocypris* sp., *Candona (Caspioypris) alta* (Zalanyi), *Candona (C) parallela pannonica* (Zalanyi), *Valvata* sp. were described in this study. Its age was found as Late Miocene based on vertebrate fossils and ostracods (Sayar-Arınç, 1955; Şafak, 1997; Nazik, 1998).

The environment of the unit is lake and lagoon according to its fossil content and lithology.

## 3. Drilling Findings

Lithological observations, fossil findings and environmental interpretations of drills 1-3 in Yedikule-Istanbul are as follows;

### 3.1. Yedikule-Istanbul Drill Log No 1

This drilling is located in coordinates of X: 28.74°, Y: 41.09° and Z: 113 m, in 1/25000 scaled İstanbul F23c3 sheet.

The drilling depth is 30 m. Below the infilling material at 1.90 m the carbonated clay; at 2.60 m the clay; at 3.00, 4.30 and 5.65 meters the contact between clay-disintegrated sand; at 7.00 m the yellowish-beige fossiliferous limestone; at 7.30 m the claystone and at 7.50, 9.00 and 9.00-10.50 meters limestones with *maetra*; between 10.50-11.00 meters and at 12.00 m the green clay (formation transition); at 12.80, 13.50, 14.00 meters the pale brown-dark yellow fossiliferous claystone layers take place.



very frequent; *C. seminulum*, *C. pannonica*, *C. anatolica*, *Heterocypris salina* frequent and very frequent; *Ilyocypris gibba* frequent; *Cyprideis torosa* widespread and frequent; *Darwinula cylindrica*, *Candona* sp. frequent; *C. sohni* as widespread.

The ostracod species belonging to the Danişmen/Gürpınar Formation, the following distribution was obtained; *Cytheromorpha zinndorfi*, *Neocyprideis williamsoniana*, *C. inflata*, *Hemicyprideis montosa*,

*H. helvetica*, *Xestoleberis subglobosa*, *Candona (Pseudocandona) fertilis*, *Eucypris pechelbronnensis* as generally widespread and frequent; *Cytheridea pernota*, *Cyamocytheridea punctatella*, *Hemicyprideis montosa* as frequent and *Neocyprideis apostolescui*, *Cyamocytheridea inflata*, *Hemicyprideis elongata* as rare.

Ostracod species described in this drill characterizes the neritic environment (Figure 3).

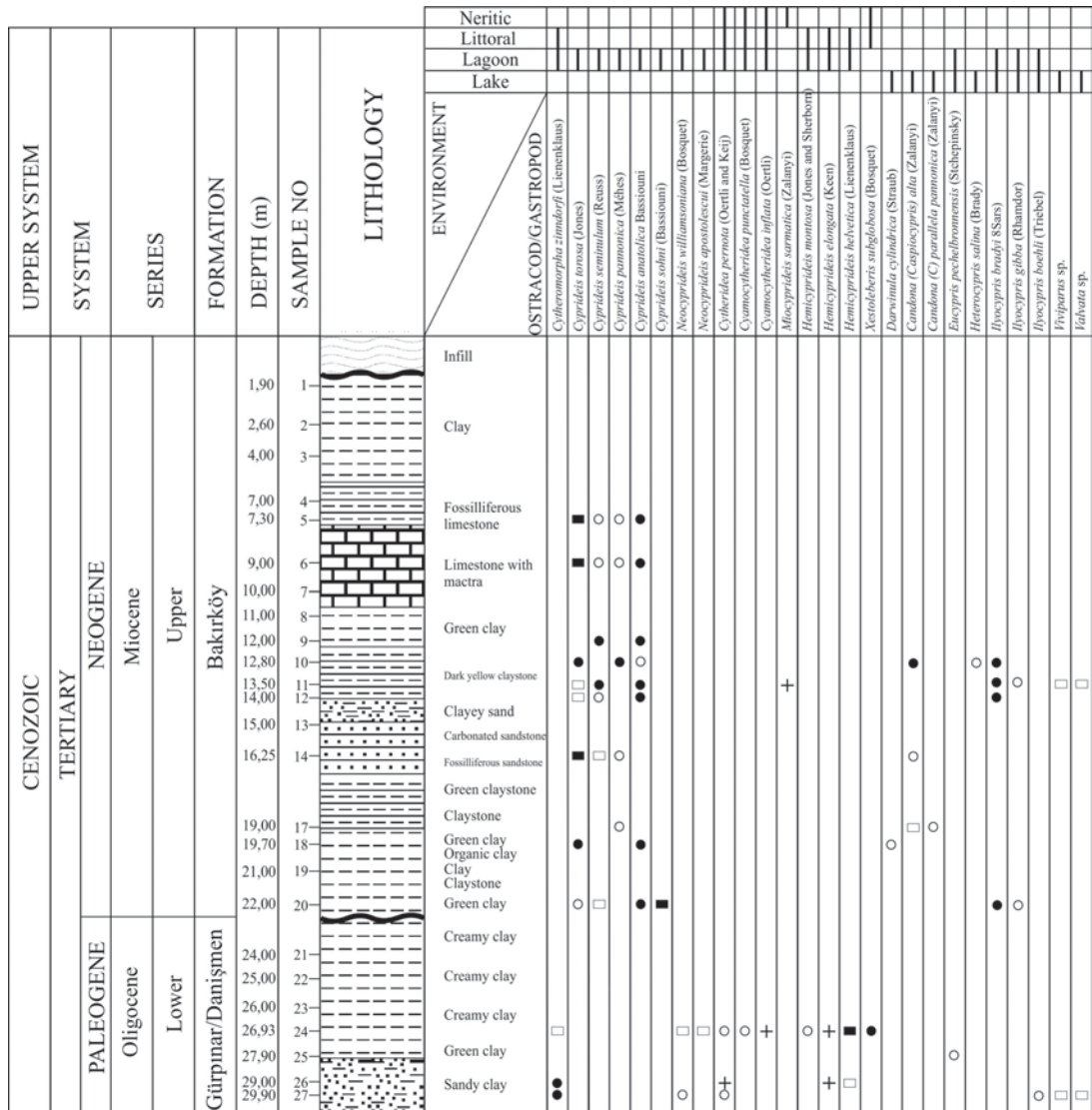


Figure 3- The ostracod distribution in core samples of the drill well no 1. Legend explanation for Figure 3-5; quantitative abundances of ostracods (+) 1-2 very rare, (□) 3-5 rare, (■) widespread 6-15, (○) frequent 16-25, (●) very frequent >25, from Sissingh (1972).

### 3.2. Yedikule-Istanbul Drill Log No 2

This drilling is located in coordinates of X: 28.91°, Y: 41.01° and Z: 49 m, in 1/25.000 scaled Istanbul F23c3 sheet.

The depth of the drill is 30 meters and the following lithologies were cut below the infilling material; at 3.50–4.50–5.90–6.00 meters cream colored, altered marl; between 6.00–7.50 meters the limestone; at 10.50 m the marl; at 11.00 m the clay; at 11.20 m the petroleum green clay; at 11.50 the limestone with *avimactra*; at 12.70–13.50 m the petroleum green clay; at 13.55 m limy pebble; at 14.70 fossiliferous silty clay; at 14.85 m green-cream colored silt-limestone transition; at 15.10 m the limestone; at 16.50 m limestone transition; at 17.80, 19.50–21.00 and 22.10 m the limestone with *mactra*; at 23.10 limestone with *mactra*; at 26.00 m the transition between limestone-green marl; at 28.20 m green claystone and sandstone; at 30.00 m cream colored siltstone were cut. Total of 28 wash samples were collected in this drilling and rich ostracod assemblages were observed in samples 7, 11, 13, 14, 15, 16, 20 and 25 in Bakırköy Formation and in wash sample 28 of the Danişmen/Gürpınar Formation.

Among the ostracod species distinguished in this drill in the Bakırköy Formation the following distribution was obtained; *Ilyocypris bradyi* as very frequent; *C. seminulum*, *C. anatolica*, *Cyprideis torosa* as widespread, frequent and very frequent; *Miocyprideis sarmatica* as widespread and rare; *C. pannonica* as widespread; *Cyprideis sublittoralis*, *Cyprideis sohni* as rare.

The following genera and environments were detected in this drilling; micro pelecypod genus *Avimactra* and ostracod genus *Ilyocypris* lake-lagoon; *Cyprideis*, *Neocyprideis* lagoon, *Cytheromorpha*, *Cytheridea*, *Cyamocytheridea*, *Hemicyprideis*, *Loxiconcha*, *Xestoleberis* lagoon-littoral, *Miocyprideis* neritic environments (Figure 4).

### 3.3. Yedikule-Istanbul Drill Log No 3

This drilling is located in coordinates of X: 28.82°, Y: 41.07° and Z: 102 m, in 1/25.000 scaled Istanbul F23c3 sheet.

The depth of the drilling is 30 meters and the following lithologies were cut; at 1.50–4.50 m infilling material; at 5.00 m pebbly-sandy fossiliferous

claystone; at 7.00 m the fossiliferous claystone-limestone; at 11.50 m the limestone with *mactra*; at 13.50–16.00–19.00 hard, fossiliferous limestone; at 21.80 m sandy clay and clay; at 22.10 m fossiliferous, cream colored clay; at 22.50 m fossiliferous, cream-dark green clay transition; at 23.50 m fossiliferous, dark green clayey sand; at 23.80 m the fossiliferous, foliated clay; at 24.50 m the limestone with *mactra*; at 25.50 m dark green claystone-marl transition; at 26.80 m the green marl; at 28.00 m the limestone with *mactra*; at 29.80 m the sandstone; at 30.60 m the claystone. Total of 30 wash samples were taken in this drill and very well preserved, several ostracod assemblages were observed in wash samples numbered 4, 19, 20 and 21 belonging to the Bakırköy formation, and wash samples numbered as; 29 and 30 belonging to Danişmen/Gürpınar Formation.

From ostracod species distinguished in this drilling *Cyprideis torosa*, *C. anatolica*, *C. pannonica*, *C. sohni* are generally frequent and very frequent; *Cyprideis seminulum* are rare and widespread; and *Cladarocythere apostolescui*, *Neocyprideis williamsoniana*, *N. apostolescui*, *Cytheridea pernota*, *Hemicyprideis elongata*, *Eucypris pechelbronnensis*, *Ilyocypris boehli* the number of valves are frequent and widespread, *Hemicyprideis montosa* the number of valves are very frequent; *Cyamocytheridea punctatella*, *Cyamocytheridea* sp. have rare valves among ostracod species belonging to Danişmen/Gürpınar Formation.

From the ostracod species described in this drilling the following environments were characterized; *Candona*, *Eucypris*, *Ilyocypris* lake-lagoon, *Cyprideis*, *Neocyprideis*, *Cladarocythere* lagoon, *Cytheridea*, *Cyamocytheridea*, *Hemicyprideis* lagoon-littoral (Figure 5).

## 4. Distribution of Ostracod Types in Time

In this study, the findings of ostracod types defined within Bakırköy and Danişmen formations through geological time are significant in dating. Therefore; the distributions of important ostracod types defined in different locations on the world through time can be summarized as below.

*Cyprideis seminulum*; Upper Pontian in Yugoslavia (Republic of Monte Negro) (Krstic; 1963, 1970); and Upper Miocene and Pliocene in Austria, Bulgaria, and Turkey (Kollmann, 1960; Bassiouni, 1979; Şafak, 1997; Nazik, 1998; Şafak et al., 1999 a,b).

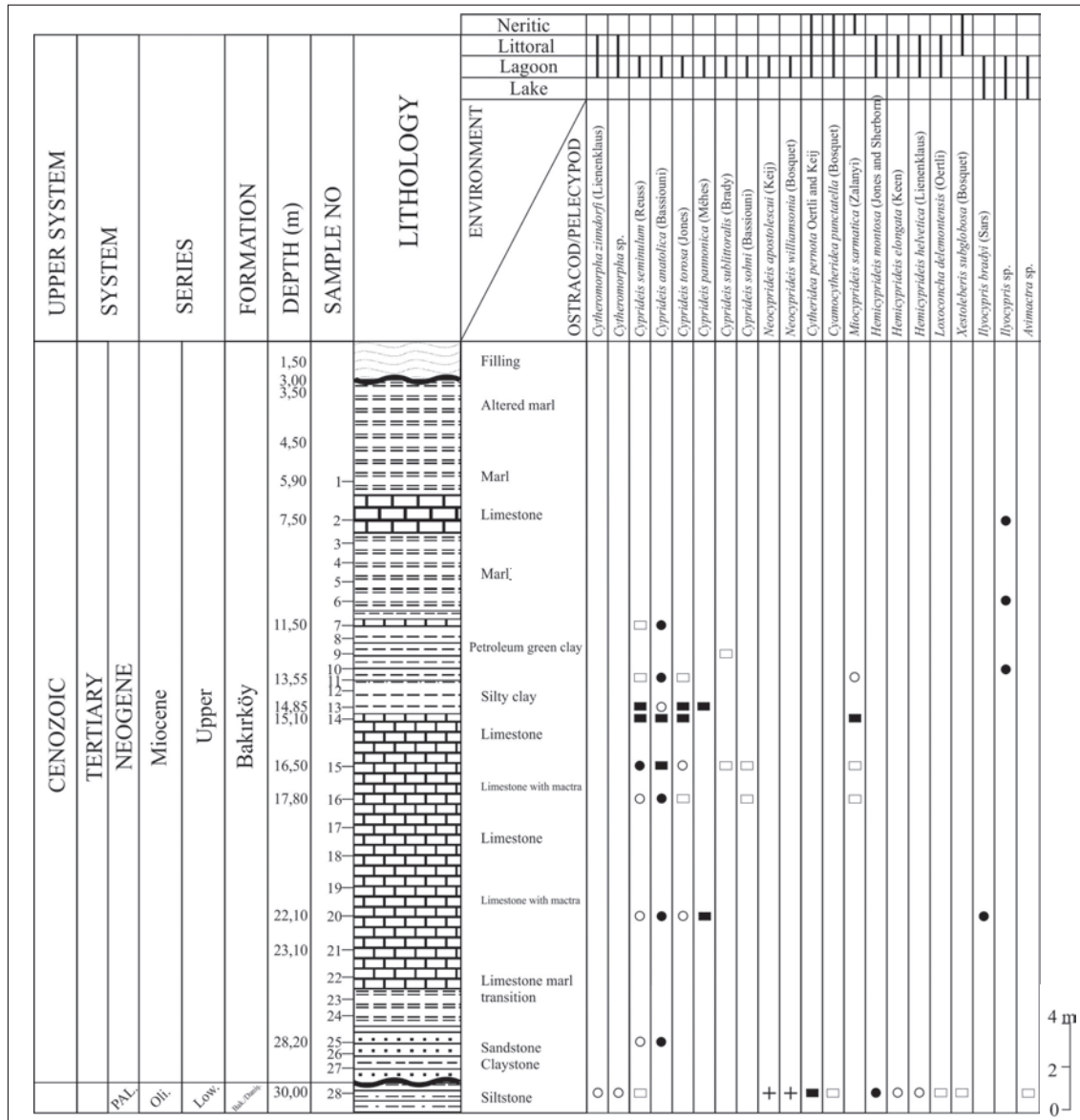


Figure 4- Ostracod distribution in core samples of the drill well no 2.

*Cyprideis torosa*; Messinian in Italy (Decima, 1962), Late Miocene in France (Carbonnel, 1969) and Pannonian-Pontian in Turkey (Ünal and Tunoğlu, 1996; Ünal, 1996; Nazik et al., 2008), Plio-Pleistocene (Bassiouni, 1979); Pliocene (Nazik and Gökçen, 1995; Tunoğlu et al., 1995). Species is observed also as actual.

*Cyprideis pannonica*; Lower Pannonian in Austria, Hungary, Czech Republic and Yugoslavia (Kollmann, 1960; Mehes, 1908; Pokorny, 1944; Krstic, 1970), Upper Miocene in Italy (Decima, 1964); Upper Miocene in Bursa, Denizli, Ankara, Kayseri, Erzurum

(Bassiouni, 1979) and Upper Miocene-Pliocene in İstanbul (Turkey) (Şafak, 1997; Nazik, 1998; Şafak et al., 1999 a,b; Nazik et al., 2008).

*Cyprideis anatolica*; Late Pliocene in Hatay, Late Pliocene in North of Eastern Mediterranean (Bassiouni, 1979); Late Miocene and Pliocene in Bakırköy basin, western İstanbul and in west Bakırköy (Şafak, 1993, 1997; Şafak et al., 1999a, Şafak et al., 1999b; Nazik et al., 2008);

*Cyprideis sublittoralis*; Pannonian in Italy, Austria and Yugoslavia (Decima, 1962; Krstic, 1971; Jiricek, 1983;



*Ilyocypris gibba*; Pleistocene in North America (Delorme, 1971), Pleistocene in England (Siddiqui, 1971; Whatley et al., 1971); Helvetian-Tortonian in Germany (Straub, 1952), Pleistocene (Triebel, 1941; Lüttig, 1955); Pliocene in France (Carbonnel, 1969); Holocene in Netherlands, Turkey (Wagner, 1957, Nazik et al., 1999); Pleistocene in Italy (Devoto, 1965); Upper Oligocene-Quaternary in Yugoslavia (Malez and Sokac, 1968), Pleistocene (Gagic and Sokac, 1970); Pliocene in Former Soviet Union (Agalarova, 1956); Pontian in Turkey (Gökçen, 1979; Nazik, 1988), Pliocene (Şafak, 1993b, Şafak et al., 1992; Nazik et al., 1992); Messinian (Şafak, 1993b; Şafak et al., 2009); Late Miocene (Nazik et al., 2008; Şafak, 2010a);

*Heterocypris salina*; Upper Miocene in Konya, Elbistan, İstanbul, Malatya (Turkey) (Freels, 1980; Şafak, 1997; Nazik, 1998; Nazik et al., 2008; Şafak, 2010a); Pliocene in Tufanbeyli, Burdur, İstanbul (Nazik et al., 1992; Tunoğlu and Bayhan, 1996; Şafak et al., 1999a,b); Plio-Pleistocene in Yalova, Konya-Karapınar, Elbistan (Witt, 2003; Beker et al., 2008; Tunoğlu et al., 2012), Holocene (Nazik et al., 1999); Late Miocene-Recent in North and Baltic Sea (Meisch, 2000); Middle Miocene in Serbia (Krstic, 1972); Upper Miocene in Slovakia (Pipik, 2001); Quaternary-Neogene in Middle East, North Africa and Europe (Meisch and Broodbakker, 1993; Gliozzi and Mazzini, 1998; Matzke-Karazs and Witt, 2005), Miocene-Recent in Europe, North Africa, Middle East, Central Asia and South America (Meisch, 2000);

*Candona (Caspicypris) alta*; Sarmatian in Caspian Basin (Zalanyi, 1929); Romania (Hanganu, 1974); Mio-Pliocene in South Carpathians (Vasiliev et al., 2005); Upper Miocene in Sivas and Şebinkarahisar (Turkey) (Freels, 1980), Pliocene in Sarız and Tufanbeyli (Turkey) (Şafak et al., 1992; Nazik et al., 1992); Pliocene-Pleistocene in Erzurum (Şafak, 2013);

*Cladarocythere apostolescui*; Early Oligocene and Late Eocene in England and Turkey (Keen, 1972; Şafak, 2008; Şafak et al., 2013; Şafak and Güldürek, 2014, Şafak et al., 2015);

*Cytheromorpha zinndorfi*; Early Oligocene in France and Turkey (Estéouille et al., 1986; Sönmez-Gökçen, 1973; Şafak, 1997; Şafak, 2010a; Şafak et al., 2013; Şafak and Güldürek, 2014; Şafak et al., 2015);

*Neocyprideis apostolescui*; Middle-Late Eocene and Early Oligocene in studies made in England, France and Turkey (Haskins, 1969; Oertli, 1985; Şafak, 1990; Şafak, 2008, 2010a,b; Şafak et al., 2013; Şafak and Güldürek, 2014; Şafak et al., 2015);

*Neocyprideis williamsoniana*; Early Oligocene in England and France (Haskins, 1969; Keen, 1972; Oertli, 1985); Late Eocene and Early Oligocene in Turkey (Şafak, 2008, 2010a,b; Şafak et al., 2013; Şafak and Güldürek, 2014; Şafak et al., 2015);

*Hemicyprideis montosa, Hemicyprideis elongata*; Lower Oligocene in England and France (Keen, 1972; Oertli, 1985); Lower Oligocene and Late Eocene in Turkey (Tanar and Gökçen, 1990; Şafak, 2008, 2010a,b; Şafak et al., 2005, 2013; Şafak and Güldürek, 2014; Şafak et al., 2015)

*Hemicyprideis helvetica*; Lower Oligocene in England, Paris and Turkey (Keen, 1972; Oertli, 1985, Şafak, 2008; 2010a; Şafak and Güldürek, 2014 Şafak et al., 2015); Upper Oligocene in Romania (Jiricek, 1983);

*Cytheridea pernota*; Upper Eocene and Lower Oligocene in England, France, Hungary, Romania and Turkey (Keen, 1972; Oertli, 1985; Monostori, 1983; Jiricek, 1983, Şafak, 2008; Şafak and Güldürek, 2014; Şafak et al., 2015);

*Cyamocytheridea punctatella*; Upper Eocene in Hungary and Romania and Lower Oligocene in NW Europe and Turkey (Monostori, 1983; Jiricek, 1983; Keen, 1972; Şafak, 2008; Şafak and Güldürek, 2014);

*Cyamocytheridea inflata*; Late Eocene- Early Oligocene (Deltel, 1963), Lower Oligocene (Oertli, 1985) in France- Akiten Basin.

*Loxoconcha delemontensis*; Oligocene in Germany (Lienenklaus, 1894); Lutetian-Rupelian in France-Akiten Basin (Deltel, 1961); Rupelian in Switzerland (Oertli, 1956); Sannoisian in NW Europe (Keen, 1972); Early Oligocene in Turkey (Sönmez-Gökçen, 1973);

*Xestoleberis subglobosa*; Lutetian-Bartonian in France-Paris Basin (Apostolescu, 1964; Bosquet, 1852); Late Eocene in Akiten Basin (Ducasse, 1959); Lutetian-Bartonian in Netherlands (Keij, 1957); Middle-Late Eocene – Oligocene in Turkey (Şafak, 1999; Şafak et al., 1999a,b; Şafak and Güldürek, 2014);

*Candona (Pseudocandona) fertilis*; Oligocene in Europe (Triebel, 1963), Early-Late Oligocen in Germany (Carbonel and Ritzkovski, 1969), Early-Late Oligocene in Switzerland and France (Carbonel, Weidmann and Berger; 1985, Keen, 1972) and Karsanti Basin/Adana (Ünlügenç et al., 1991; Şafak, 1993b; Şafak, 2010a,b, Şafak and Güldürek, 2014; Şafak et al., 2015);

*Eucypris pechelbronnensis*; Sannoisian in France (Pechelbronn) (Keen, 1972);

*Ilyocypris boehl*; Lower Oligocene in England (Keen, 1972); Lower and Upper Oligocene in Turkey (Sönmez-Gökçen, 1973; Tanar and Gökçen, 1990; Şafak, 1993a; Şafak et al., 2015).

## 5. Results

This study was carried out to micropaleontologically assess the successions in cores excavated around Yedikule during micro zonation study performed by the Istanbul Municipality in the southern part of European side in Istanbul province. For this reason, total of 85 core samples were collected from 3 drills excavated and classified wells. In succession, where limestone, marl, silty sandstone, sandstone, organic clay, claystone, clayey limestone and fossiliferous limestones are dense, 16 genera and 25 species of ostracods and 3 micro mollusc genera were described from samples belonging to Bakırköy and Danişmen/Gürpınar Formation.

Ostracod and gastropod genera and species such as; *Cyprideis seminulum* (Reuss), *C. torosa* (Jones), *C. anatolica* (Bassiouni), *C. pannonica* (Mehes), *C. sohni* Bassiouni, *Miocyprideis sarmatica* (Zalanyi), *Darwinula cylindrica* Straub, *Heterocypris salina* (Brady), *Ilyocypris bradyi* Sars, *I. gibba* (Ramdohr), *Ilyocypris* sp., *Candona (Caspiocypris) alta* (Zalanyi), *Candona (C) parallela pannonica* (Zalanyi), *Valvata* sp. were determined in Bakırköy Formation.

Ostracod genera and species such as; *Cytheromorpha zinndorfi* (Lienenklaus), *Cytheromorpha* sp., *Neocyprideis apostolescui* (Keij), *N. williamsoniana* (Bosquet), *Cytheridea pernota* (Oertli and Keij), *Cyamocytheridea punctatella* (Bosquet), *C. inflata* (Deltel), *Cyamocytheridea* sp., *Hemicyprideis montosa* (Jones and Sherborn),

*H. elongata* (Keen), *H. helvetica* (Lienenklaus), *Cladarocythere apostolescui* (Margerie), *Loxococoncha delemontensis* (Oertli), *Xestoleberis subglobosa* (Bosquet), *Candona (Pseudocandona) fertilis* (Triebel), *Eucypris pechelbronnensis* (Stchepinsky), *Ilyocypris boehli* (Triebel), and micro molluscs genera such as; *Viviparus* sp., *Avimactra* sp. were described in Danişmen/Gürpınar Formation.

Described ostracod species were correlated with studies carried out in Central Europe (Keen, 1972; Oertli, 1985; Monostori, 1983), Italy, France, Monte Negro, Romania, Austria, Hungary, Czech Republic (Mehes, 1908; Decima, 1964; Stancheva, 1965; Krstic, 1973) and in Turkey (Nazik, 1993; Tanar and Gökçen, 1990; Sönmez-Gökçen, 1973; Şafak, 2008, 2010; Şafak and Güldürek, 2014), and Bakırköy and Danişmen/Gürpınar formations were dated as Late Miocene and Early Oligocene, respectively.

*Candona*, *Candona (Pseudocandona)*, *Candona (Caspiocypris)*, *Eucypris*, *Heterocypris*, *Darwinula* from ostracoda genera described in drill cores and *Viviparus*, *Valvata* from micro gastropods present lake environment, micro pelecypod genera *Avimactra* and *Ilyocypris* lake-lagoon, *Cyprideis*, *Neocyprideis* lagoon, *Cytheromorpha*, *Cytheridea*, *Cyamocytheridea*, *Hemicyprideis*, *Xestoleberis* lagoon-littoral and *Miocyprideis* characterizes neritic environment.

Considering data of this and previous studies, the marl, silty sandstone, claystone, clayey limestones and fossiliferous limestones deposited especially in lower and upper layers of organic clay and claystone indicate that they contain generally lagoonal ostracods in both formations.

## Acknowledgements

The author would like to thank to engineers and the team of the micro zonation project of the Istanbul Municipality in providing and classifying drill core samples after 2006, to the Head of Geological Engineering of Çukurova University, to Aynur Gürbüz for SEM studies, the expert in Advanced Technological Education at the Research and Application Center in Mersin University and to Prof. Kemal Taşlı (Mersin University).

## References

- Agalarova, D.A. 1956. Microfauna from Productive Beds in Azerbaijan and Red Deposits in Turkmenistan, Turkmen SSR., *Yymlar Akademiasy, Geol. Inst.*, 190p., Ashgabat.
- Akartuna, M. 1953. Çatalca-Karacaköy bölgesinin jeolojisi, İstanbul Üniversitesi Fen Fakültesi Monografileri, 13, 88s.
- Apostolescu, V. 1964. Répartition stratigraphique générale des ostracodes du Paléogène des Bassins de Paris et Bruxelles, *Colloque Paléogène*, Mémoires. B.R.G.M., no. 28.
- Arınç, C. 1955. <http://www.ibb.gov.tr>
- Aslaner, M. 1966. Tozakkı-Poyralı linyitleri ve Pınarhisar civarının jeolojisi: *Maden Tetkik ve Arama Dergisi* 66, 126-142, Ankara.
- Athersuch, J. Horne, D.J., Whittaker, J.E. 1989. Marine and Brackish Ostracods, *Synopses of the British Fauna* (N.S.), 43.
- Bassiouni, M.A. 1979. Brackische und marine Ostrocoden (Cytherideinae, Hemicytherinae, Trachyleberidinae) aus dem Oligozoen und Neogen der Türkei, *Geol. Jb. Reihe B*, Heft 31, Hannover, 1-200.
- Bear, H., Wright J.A. 1960. Stratigraphy of the Ganosdağ, Korudağ and Keşan Hills District I, (Thrace), *TPAO Arşiv* no: 736, Ankara (unpublished).
- Beker, K., Tunoğlu, C., Ertekin, I, K. 2008. Pliocene—Lower Pleistocene Ostracoda fauna from Insuyu Limestone (Karapınar-Konya/Central Turkey) and its paleoenvironmental implications, *Geol. Bull. Turkey* 51, 1—31
- Boer, N.P. de 1954. Report on geological reconnaissance in Turkish Thrace. G.A. Report no: Ç 25373, Petrol Dairesi, The Hague, February, 1954.
- Bosquet, J. 1852. Description des Entomostracés fossiles des terrains tertiaires de la France et de la Belgique: Mémoires Couronnes et Mémoires des Savants Etrangers publiés par l'Académie Royale des Sciences des lettres et des Beaux-Arts de Belgique., 24 81850-1852): 1-142.
- Bremer, H. 1978. Paleontoloji, *Ege Üniversitesi Fen Fakültesi Kitapları Serisi*, No. 46, Bornova-İzmir.
- Carbonnel, G., Ritzkovski, S., 1969. Ostrocodes Lacustres de l'Oligocene (Melanienon) de la Hesse (Allemagne). *Arch. Sc.*, Geneve, 22:1, 55-82.
- Carbonnel, G., 1969. Les Ostracodes du Miocène Rhodanien, Docum. Lab. *Géol. Fac. Sci. Lyon*, 32, I: 228 s., 11Abb., 16 Taf., 4 Tab., Lyon.
- Carbonnel, G., Weidmann, M., Berger, J.P. 1985. Les Ostracodes lacustres et saumâtres de la molasse de suisse occidentale. *Revue de Paleobiologie*, 4:2, 215-251.
- Decima, A. 1964. Ostracodi del genus Cyprideis Jones del Neogene e del Quaternario Italiani, *Paleontographia Ital.*, V:62, 81-133, 9 Abb., Taf. 24-38, Pisa.
- Delorme, L.D., 1971. Paleocological determinations using Pleistocene freshwater ostracodes: *Bulletin Centre rech.*, 5, 341-347, Pau-SNPA.
- Deltel, B. 1961. Les Ostracodes du Paléogène moyen et supérieur d'Aquitaine méridionale, Univ. de Bordeaux, 30 Cycle, no. D'ordre 95, Bordeaux.
- Deltel, B. 1963. Nouveaux ostracodes de l'Eocène et de l'Oligocene de l'Aquitaine méridionale: *Actes Societe Linn. V.* 100, Bordeaux.
- Devoto, G. 1965. Lacustrine Pleistocene in the Lower Liri Valley.-*Geol. Romana*, 4:291-368, 61 Figure; Roma.
- Ducasse, O. 1959. Les Ostracodes del'Eocène du sous-sol Bordelais: répartition, intérêt stratigraphique et paléogéographique. Université de Bordeaux, Thèse 3 Cycle, Bordeaux.
- Erentöz, C. 1953. Etudes géologiques dans la région de Çatalca (İstanbul), Publ. Maden Tetkik ve Arama Genel Müdürlüğü Ser. B., No: 17, Ankara.
- Estéoule-Choux, J., Margerel, J-P., Guernet, C., Rivoalland, H. 1986. Données sur le bassin stampien de Quessos (massif armoricain), Etude sédimentologique et micropaléontologique du gisement du moulin de Boguet. *Revue de Micropaléontologie* V. 28, N. 4, p. 243-254, Paris.
- Freels, D. 1980. Limnische Ostrakoden aus jungtertiär und Quartär Turkey. *Geol. Jahr.Reihe B*, Heft 39, 172 s., Hannover.
- Gagic, N., Sokac, A. 1970. Fauna Ostracoda Paludirskih naslaga vukomedickin gorica: VII. Kongres geologa str. Jugoslavie-Zagreb, 28, 9, 1979, s. 1311-1148.

- Gliozzi E., Mazzini I. 1998. Palaeoenvironmental analysis of the 250,000 years Quaternary sediment core of vale di Castiglione (Latium, Italy) using Ostracods. In: Crasquin-Soleau, Braccini, and Lethiers (Eds.): What about Ostracoda. Elf., 69—81.
- Gökçen, N. 1979. Denizli-Muğla Çevresi Neojen istifinin Stratigrafisi ve Paleontolojisi Doçentlik Tezi, Hacettepe Üniversitesi, Ankara.
- Gökçen, S.L. 1967. Eocene-Oligocene Sedimentation in the Keşan Area, SW Turkish Thrace, *Maden Tetkik ve Arama Dergisi* Institute of Turkey, No. 69, Ankara.
- Guernet, C., Sauvage, J., Soulie Marsche, I. 1977. Le Levantin De Joanina (Epire, Grece): Observations stratigraphiques et paleontologiques, *Geobios*, no: 10, fasc: 2, 297-309, Lyon.
- Hanganu, E. 1974. Observations sur l'ostracofaune pontienne de la région entre la vallée du Danube et la vallée du Motru, *Revista Espanola Micropaleontologia*, 6, 3, 335-345, 3 Taf., Madrid.
- Hartmann, G., Puri, H. 1974. Summary of neontological and paleontological classification of Ostracoda, Mitteilungen aus dem hamburgischen Zoologischen Museum und Institut, 70, 7-73.
- Haskins, C.W. 1969. Tertiary Ostracoda from the Isle of Wight and Barton, Hampshire, England, *Revue de Micropaléontologie*, Part IV, N. 3, Paris.
- Jiříček, R. 1974. Biostratigraphische Bedeutung der Ostracoden des Sarmats s. str. In: E. Brestenská (ed.), *Chronostratigraphie und Neostratotypen*, M5, Sarmatien, 434-457. VEDA, Bratislava.
- Jiricek, R. 1983. Redefinition of the Oligocene and Neogene Ostracod Zonation of the Paratethys, *Knihovnicka Zemniho plynu a nafyt (Nr.4)* pp. 195-236/6, Hodonin.
- Jiříček, R., Řiha J. 1990. Correlation of Ostracod Zones in the Paratethys and Tethys. In: Proceedings of the *International Symposium on Shallow Tethys* 3, Sendai, Japan, September 1990. Saito Hoon Kai Spec. Publ. 3, 435—457.
- Keen, M.C. 1972. The Sannoisian and some other Upper Palaeogene Ostracoda from North-west Europe, *Palaeontology*, V. 15, Part 2, London.
- Keij, A. 1957. Eocene and Oligocene Ostracoda of Belgium, Institut Royale Science Naturelles Belgique, Brussels, Mémoires No. 136:1-210.
- Kellog, H.E. 1973. Geology and petroleum prospect gulf of Saros and vicinity Southwestern Thrace, Turkey, *TPAO Arşiv* no: 902 Ankara (unpublished).
- Kemper, E., 1966. Beobachtungen an obereozänen Riffen am Nordrand des Ergene Beckens (Türkei-Thrazien), *Neues Jahrbuch Geologische Palaeontologische Abhandlungen*, 125, 540-554.
- Keskin, C. 1974. Kuzey Ergene Havzasının Stratigrafisi, Türkiye II. Petrol Kongresi Tebliğleri
- Kollmann, K. 1960. Cytherideinae und Schulerideinae n. subfam. (Ostracoda) aus dem Neogen des östlichen Österreich, *Mitt. Geol. Ges. Wien*, 51: 89-195, 5 Abb., 4 Tab., 21 Taf., 1 Kt., Wien.
- Krstic, N. 1963. Pontian ostracodes at some localities in Serbiawith regards to the family Cytheridae, *Vesnik*, A21: 103-110, Abb.1-12, 2 Tab., Beograd.
- Krstic, N. 1970. Ostracodes des couches congériennes: 1. Cyprideis II.-*Bull. Mus. Hist. Nat.*, A23: 153-183, 8 Taf., Beograd.
- Krstic, N. 1971. Neogene Ostracoden aus Serbien revision des Originalmaterials zu Zalanyi (1929), Földtani Közlöny, *Bulletin Hungarian Geol. Soc.*, 101: 373-379, 3 Taf., Budapest.
- Krstic, N. 1972. Neue Ostracoden aus der Obermiozän von Donja mutnica (Paracin, Serbien), *Bulletin Scientifique* A17, 153-155.
- Krstic N. 1973. Pliocene Ostracodes from Metohija. 1. Pontian of the Krusevo locality. *Bull. Mus. Hist. Nat.*, Ser. A, Livre 28,151-173.
- Lebküchner, R.F., 1974. Orta Trakya Oligoseninin jeolojisi Hakkında, *Maden Tetkik ve Arama Genel Müdürlüğü Raporu*, No. 2983, Ankara (unpublished),
- Lienenklaus, E. 1894. Monographie der Ostrakoden des Nordwestdeutschen Tertiaers, *Zeitschrift der Deutschen Geologischen Gesellschaft* 46.
- Lüttig, G. 1955. Die Ostrakoden des Interglazials von Elze, *Paläontologische Zeitschrift*, 29, 3/4: 146-169, 3 Taf., Stuttgart.
- Maden Tetkik ve Arama Genel Müdürlüğü Trakya Bölgesi Litostratigrafi Birimleri, Stratigrafi Komitesi, Litostratigrafi Birimleri Serisi-2, 2006.

- Malez, M., Sokac, A. 1968. New conception on the age of the freshwater deposits of Ervenik and Zegar fields in Dalmatia: *Bull. Scientifique, A.*, 13 811-12), 371.
- Matzke-Karasz R., Witt W. 2005. Ostracods of the Paratethyan Neogene Kılıç and Yalakdere Formations near of Yalova (Izmit Province, Turkey). *Zitteliana A* 45, 115—133.
- Mehes, G. 1908. Beiträge zur Kenntnis der pliozänen Ostrakoden Ungarns. II. Die Darwinulidäen und Cytheridäen der unterpannonischen Stufe, Földtani Közlöny, (Suppl.),38 (7-10): 601-635, 3 Abb., Taf. 8-11, Budapest.
- Meisch, C. 2000. Freshwater Ostracoda of Western and Central Europe, Süßwasserfauna von Mitteleuropa 8/3, *Akademischer Verlag*, Heidelberg.
- Meisch, C., Broodbakker, N.W. 1993. Freshwater Ostracoda (Crustacea) collected by Prof. J.H. Stock on the Canary and Cape Verde Islands. With an annotated checklist of the freshwater Ostracoda of the Azores, Madeira, the Canary, the Selvagens and Cape Verde Islands, *rav. Sci. Nat. Hist. Nat. Luxembourg* 19 (Ostracoda),1—75.
- Monostori, M. 1983. Ostracodes of Eocene/Oligocene Boundary profiles in Hungary, *Annales Universitatis Scientiarum Budapestinensis de roland, Eötvös Nominatae Sectio Geologica tomus XXV*.
- Nazik, A. 1988. Ulukışla Tersiyer İstifinin stratigrafik ve mikropaleontolojik ostrakod ve foraminifer) incelemesi, *Ç.Ü. Fen Bilimleri Enstitüsü Yüksek Lisans Tezi*, 128 s., Adana.
- Nazik, A. 1998. Bakırköy formasyonunun (Küçükçekmece-İstanbul) ostrakod faunasına göre yaşı ve oluşum ortamı hakkında yeni görüşler, *İstanbul Üniversitesi Mühendislik Fakültesi Yerbilimleri Dergisi*, Cilt:11, 87-101.
- Nazik, A., Şafak, Ü., Şenol, M. 1992. Micro-paleontological Investigation (Ostracoda) of the Pliocene sequence of the Tufanbeyli (Adana) Area, *Yerbilimleri*, 1992 1st International Symposium on Eastern Mediterranean Geology, proceedings and abstracts, 281-304, Adana.
- Nazik, A., Gökçen, N. 1995. Ostracods of the uppermost Tertiary srquence of the North Adana Basin and Misis area, in *Ostracoda and Biostratigraphy*, J. Riha, ed: A. A. Balkema, Rotterdam, p. 251-260, Balkema-Rotterdam.
- Nazik, A., Evans, G., Gürbüz, K. 1999. Sedimentology and palaeontology with special reference to the ostracoda fauna of Akyatan Lagoon (Adana-SE Turkey ). *Geosound* 35, 127-147.
- Nazik, A., Türkmen, İ., Koç, C., Aksoy, E., Avşar, N., Yayık, H. 2008. Fresh and Brackish Water Ostracods of Upper Miocene Deposits, Arguvan/Malatya (Eastern Anatolia), *Turkish Journal of Earth Sciences*, Vol. 17, pp. 481-495.
- Oertli, H.J. 1956. Ostrakoden aus der oligozänen und miozänen Molasse der Schweiz. *Abhandlungen der Schweizerischen paläontologischen Gesellschaft*, 74: 1-119, Basel.
- Oertli, H.J. 1985. Atlas des Ostracodes de France. *Bull. centres rech. explor.-prod. Elf-Aquitaine, Mem. 9. Pau 1985. Mémoires Elf-Aquitaine*,9, p.17-311 Paléogène.
- Ozansoy, F. 1962. Doğu Trakya Alt Oligosen Antrakoterienleri, *Maden Tetkik Arama Enstitüsü Dergisi*, 58, 85-96, Ankara.
- Ozansoy, F. 1964. Le niveau du Sannoisien et sa faune mamalienne de la Thrace Orientale (Turquie) dans le Systeme de l'Oligocene d'Europe. *Mem. Bureau Rech. Geol. et Min. Colloque sur le Paleogene*. Sept. 1962, II, Bordeaux
- Pamir, H.N., 1954. Recherces géologiques au Bassin d'Ergene, *Rev. Fac. Sci. Univ. d'İstanbul, série b*, t. 19, fasc.1.
- Pamir, H. N. Sayar, A. M. 1933. Vertebres fossiles de Küçükçekmece. *Extrait du Bull. Fac. Sci. İstanbul* (No. 3 et 4), *Publ. Inst. Geol. Univ. İstanbul*, No. 8.
- Pipik, R. 2001. Les ostracodes d'un lac ancien et ses paléobiotopes au-Mioène supérieur: Le Bassin de Turiec (Slovaquie), *Thèse Université Claude Bernard Lyon*, 337.
- Pokorny, V. 1944. La microstratigraphie du Pannonien entre Hodonin et Mikulcice, *Bull. İnt. Acad. Tcheque Sci.*, 23, 1-25.
- Remane, A. 1958. Die Biologie des Brackwassers. In: THIENEMANN, A: Die Binenge wasser, Einzeldarstellungen aus der Limnologie und ihren Nachbargebieten, 22: 1-348.

- Rückert-Ülkümen, N. 1964. Tertiäre Fische aus Thrakien und den Dardanellen, *İstanbul Üniversitesi Fen Fakültesi Monografileri*, no. 16.
- Rückert-Ülkümen, N. 1965. Fossile Fische aus dem Sarmat von Pınarhisar (Türkisch-Thrakien), *Senckenbergiana*, Bd. 46a, Frankfurt.
- Rückert-Ülkümen, N., Özkar-Öngen, İ., Çevik-Öner, B. 2009. Doğu Paratetis'in Ergene Havzası'ndaki paleobiyocoğrafik özellikleri, *İstanbul Yer bilimleri Dergisi*, C. 22, s.2, 119-140.
- Sayar (Arınç) C. 1955. Haliç-Küçükçekmece bölgesinin jeolojisi, Doktora tezi, İTÜ Maden Fakültesi Yayını.
- Sayar, C. 1977. İstanbul yeni iskan yöreleri geoteknik ve sismik etüdü, B.Ü. *Deprem Araştırma Enstitüsü* rapor no: 77-14T. (unpublished).
- Sayar, C. 1989. İstanbul ve çevresi Neojen çökelleri ve Paratetis içindeki konumu, İTÜ Maden Fakültesi. *35. Yıl Sempozyumu Kitabı*, s. 250-266.
- Sayar, C. 1991. Paleontoloji Omurgasız Fosiller, İstanbul Teknik Üniversitesi Kütüphanesi Sayı: 1435, İstanbul.
- Sayar, C. 1992. Biyostratigrafi, İstanbul Teknik Üniversitesi Yayınları, 1484, 336 s.
- Sıddıqui, Q. 1971. Early Tertiary Ostracoda of the family Trachyleberididae from West Pakistan: British Museum (Natural History), *Geol. Supp.* 9, 1-195.
- Sissingh, W. 1972. Late Cenozoic Ostracoda of the South Aegean Island Arc, *Utrecht Micropaleontological Bulletins*, 6: 1-187.
- Siyako, M. 2002. Trakya Havzası Tersiyer Kaya Birimleri, Trakya Bölgesi Litostratigrafi Birimleri, *Maden Tetkik ve Arama Genel Müdürlüğü Stratigrafi Komitesi Litostratigrafi Birimleri Serisi-2*, 2006, 43-77, Ankara.
- Sönmez, N. 1963. Deux nouveaux genres d'Ostracodes du Paléogène de Thrace (Turquie). *Revue de Micropaléontologie*, V. 6, no. 2, Paris.
- Sönmez-Gökçen, N. 1964. Notice sur le nouvel age determine par les Ostracodes de la serie a Congeria du Neogene des environs de Çatalca (Thrace). *Maden Tetkik ve Arama Dergisi*, No. 63, Ankara.
- Sönmez-Gökçen, N. 1973. Etude paléontologique (ostracodes) et stratigraphique de niveaux du Paléogène du Sud-Est de la Thrace, *Maden Tetkik ve Arama Dergisi*, No.147, Ankara.
- Stancheva, M. 1965. Ostracoda from the Neogene in North-Western Bulgaria, IV. Pontian Ostracoda; V. Development and stratigraphical importance, *trav. Géol. Bulgarie, ser. Paléont.*, 7: 15-69, 8 Tab., 4 Taf., Sofia.
- Stancheva, M. 1966. Notes on the stratigraphy and the ostracoda fauna from the Pliocene and post Pliocene in the district of Silistra. Bult.“S. Dimitrov” Inst. *Géol., Série Paleont.* 15, 205—209.
- Straub, E.W. 1952. Mikropaläontologische Untersuchungen im Tertiär zwischen Ehingen und Ulm an der Donau. *Geologisches Jahrbuch* 66, 433—524.
- Sümengen, M., Terlemez, İ. 1991. Güneybatı Trakya Yöresi Eosen Çökellerinin stratigrafisi, *Maden Tetkik Arama Dergisi*, 113, 17-30, Ankara.
- Şafak, Ü. 1990. Malatya Kuzeybatısının (Medik-Ebreme yöresi) Üst Lütisiyen Ostrakod Faunası, *Ç.Ü. Müh-Mim Fak. Dergisi*, Cilt 5, Sayı 1, 135-149, Adana.
- Şafak, Ü. 1993a. Karsanti yöresinde (KKD Adana) yüzeyleyen Tersiyer istifinin Ostrakod dağılımı ve ortamsal özellikleri, *Türkiye Jeoloji Bülteni*, c.36 s. 1.
- Şafak, Ü. 1993b. Antakya Havzası ostrakod biyostratigrafisi, *Türkiye Jeoloji Bülteni*, c.36, s.2, 115-137, Ankara.
- Şafak, Ü. 1997. Bakırköy Havzası (İstanbul) Tersiyer Çökellerinin Ostrakod Faunası, *Yerbilimleri*, 30, 255-285.
- Şafak, Ü. 1999. Karaman civarında yüzeyleyen Eosen istifinin mikropaleontolojik Planktonik foraminifer-ostrakod) İncelenmesi, *Maden Tetkik Arama Dergisi*, 121, 1-17, Ankara.
- Şafak, Ü. 2003. Yumurtalık Koyu (Adana) Ostrakod Topluluğu, *Maden Tetkik Arama Dergisi*, 126, 1-10, Ankara.
- Şafak, Ü. 2008. Malkara (Tekirdağ) yöresi Erken/Alt Oligosen çökellerinin ostrakod faunası ve ortamsal özellikleri, *Ç.Ü. Yerbilimleri Dergisi*, Sayı:52, s 263-282, Adana.
- Şafak, Ü. 2010a. Güney-Buldan-Babadağ-Yenicekent-Kale (Denizli, GB Anadolu) Çevresi Tersiyer Çökellerinin Ostrakod Topluluğu ve Ortamsal Özellikleri, *KSÜ Mühendislik Bilimleri Dergisi*, 13 (2), 44-62.

- Şafak, Ü. 2010b. Pınarhisar-Vize/Kırklareli (KB Anadolu) Yöresi Oligosen Yaşlı Linyitli Çökellerin Ostrakod Faunası ve Ortamsal Özellikleri, *TPJD Bülteni*, Cilt:22, Sayı:2, s. 11-29, Ankara.
- Şafak, Ü. 2013. Hınıs (Erzurum, Doğu Anadolu) yöresindeki volkano-sedimanter Yolüstü Formasyonu ostrakod faunası ve ortamsal özellikleri, *Maden Tetkik Arama Dergisi*, 146, 55-81, Ankara.
- Şafak, Ü. 2014. Yedikule-İstanbul Bölgesi Erken Oligosen Çökellerinin ostrakod faunası ve ortamsal özellikleri, 15. Paleontoloji-Stratigrafi Çalıştayı Bildiri Özleri Kitabı, s. 55-56, Side, Antalya.
- Şafak, Ü. Nazik, A. Şenol, M. 1992. Kayseri Güneydoğusu (Sarız) Pliyosen Ostrakod ve Gastropod Faunası, *Ç. Ü. Müh. Mim. Fak. Dergisi*, Cilt 7, Sayı 1, s. 171-195, Adana.
- Şafak, Ü. Taner, G. 1998. Kılbasan Yöresinde (Karaman Kuzeyi) Bulunana Kuvterner Tatlısu Faunası, *Maden Tetkik Arama Dergisi*, 120, 35-45, Ankara.
- Şafak, Ü., Avşar, N., Meriç, E. 1999a. Ostracoda and benthic foraminifera of tertiary sequence of western part of İstanbul, *Yerbilimleri Dergisi*, 4 th *European Ostracodologists Meeting*, No:35, p. 173-201, Adana.
- Şafak, Ü., Avşar, N., Meriç, E. 1999b. Batı Bakırköy (İstanbul) Tersiyer Çökellerinin ostrakod ve foraminifer topluluğu, *Maden Tetkik Arama Dergisi*, No. 121, s. 17-33, Ankara.
- Şafak, Ü., Kelling, G., Gökçen, N.S., Gürbüz, K. 2005. The mid-Cenozoic succession and evolution of the Mut Basin, southern Turkey, and its regional significance. *Sedimentary Geology*, 173, p. 121-150.
- Şafak, Ü., Kapucuoğlu, U., Heybeli-Donat, D. 2009. Besni-Kahta (Adıyaman) Civarında Yer Alan Tersiyer İstifinin Ostrakod faunası ve Ortamsal Yorumu. *Ç.Ü. Müh. Mim. Fak. Dergisi*, Cilt 24, Sayı 1-2, 193-208, Adana.
- Şafak, Ü., Ocakoğlu, F., Açıkalın, S. 2013. Ostracod associations and depositional environments of Eocene sections in the Central Sakarya Region (NW Anatolia). 17 th International Symposium on Ostracoda, *IL Naturalista Siciliano* Vol. XXXVII, N.1, pp.333-334, Roma, Italy.
- Şafak, Ü., Güldürek, M. 2014. KB Trakya Eosen-Oligosen geçişinin ostrakod topluluğu: Kırklareli Edirne yöresi 7KB Türkiye, 67th Türkiye Jeoloji Kurultayı Bildiri Özleri Kitabı, 726-727, Ankara.
- Şafak, Ü., Özseri, F., Yıldız, C.E. 2015. Tekirdağ yöresi Oligosen çökellerinin (Hacısungurlu Sondajı) ostrakod faunası ve ortamsal özellikleri, 68th Türkiye Jeoloji Kurultayı Bildiri Özleri Kitabı, 552-553, Ankara.
- Şenol, M., 1980. Keşan (Edirne) ve Marmara Ereğlisi (Tekirdağ) Yörelerinde Oligosen Yaşlı Birimlerin Çökel Ortamları ve Linyit Oluşumları, *TJK Bülteni*, C. 23, 133-140, Ankara.
- Tanar, Ü., Gökçen, N. 1990. Mut-Ermenek Tersiyer İstifinin Stratigrafisi ve Mikropaleontolojisi, *Maden Tetkik Arama Enstitüsü Dergisi*, 110, 175-181, Ankara.
- Taner, G. 1980. Das Neogen der Umgebung Yalova, *Communications de la Faculté des Sciences de l'Université d'Ankara, Série C1, Géologie, Tome 23*, Ankara.
- Ternek, Z. 1949. Geological study of the region of Keşan-Korudağ, *Maden Tetkik ve Arama Enstitüsü Neşriyatı*, D12, 78 s.
- Ternek, Z. 1987. Türkiye Jeoloji Haritası: 1/500.000 Ölçekli, İstanbul. *Maden Tetkik ve Arama Genel Müdürlüğü*, Ankara.
- Töth, E. 2008. Budapest Sarmatian (Middle Miocene) ostracod fauna from the Zsámbék Basin, Hungary, *Geologica Pannonica* 36, 101—151
- Triebel, E. 1941. Zur Morphologie und Ökologie des fossilen Ostracoden, Mit Beschreibung einiger neuer Gattungen und Arten, *Senckenbergiana Lethaea*, 23 (4-6): 294-400.
- Triebel, E. 1963. Ostrakoden aus dem Sannois und Jungeren Schichten des Mainzer Beckens: 1. Cypritidae, *Senckenbergiana*, Bd. 44, Frankfurt.
- Tunoğlu, C., Çelik, M., Temel, A. 1995. Doğanbey-Seydişehir (GB Konya yöresi) Neojen istifinin ostrakod topluluğu ve ortamsal yorumu, *KTÜ 30. Yıl Sempozyum Bildirileri*, Trabzon.
- Tunoğlu, C., Bayhan, E. 1996. Burdur Havzası Pliyosen istifinin mikropaleontolojik incelenmesi ve ortamsal yorumu, *Maden Tetkik Arama Enstitüsü Dergisi*, 118, 9-16, Ankara.

- Tunođlu, C., Besbelli, B., Ertekin, I.M.K. 2012. Ostracoda (Crustacea) association and a new species (*Dolerocypris anatolia* nov.sp.) from the Pliocene-Pleistocene Afşin-Elbistan (Kahramanmaraş) Coal Basin of Turkey, *Geologica Carpathica*, 63, 2, 165-174.
- Ünal, A. 1996. Gelibolu Yarımadası Neojen İstifinin ostrakod biyostratigrafisi, Yüksek Müh. Tezi, Hacettepe Üniv., 160 s., Ankara.
- Ünal, A., Tunođlu, C. 1996. The upper Miocene Ostracoda fauna of Gelibolu Peninsula (NW Turkey), 30 European Ostracodologists Meeting, Abstracts, Bierville, Paris, p. 23.
- Ünlügenç, U.C., Demirkol, C., Şafak, Ü. 1991. Adana Baseni K-KD'nda yer alan Karsanti Baseni Çökellerinin Stratigrafik-Sedimentolojik Ni-telikleri, A. Suat Erk Jeoloji Simpozyumu (2-5 Eylül 1991), Bildirileri, 1993, s. 215-227, Ankara.
- Van Morkhoven, F.P.C.M. 1963. Post-Palaeozoic Ostracoda, V.II, 478 p., Newyork.
- Vasiliev, J., Krigsman, W., Stoica, M., Langereis, Cor G. 2005. Mio-Pliocene magnetostratigraphy in the southern Carpathian foredeep and Mediterranean-Paratethys correlations, *Terra Nova*, 17, 376-384.
- Wagner, C. W. 1957. Sur les ostracodes du Quaternaire Récent des Pays-Bas et leur Utilisation dans l'étude géologique des Dépôts Holoènes, Dissertation Univ. De Paris, 259 pp.
- Wenz, W. 1922. Zur Nomenklatur tertiärer Land und Süßwassergastropoden, *Senckenbergiana*, Bd. IV, Heft 5, 2, 75-86, Frankfurt.
- Whatley, R.C., Kaye, P. 1971. The palaeoecology of Eemian (last interglacial) Ostracoda from selsey: Sussex. *Bull. Centre Rech.*, 5: 311-330, Pau-SNPA.
- Witt, W. 2003. Freshwater ostracods from Neogene deposits of Develiköy (Manisa Turkey), *Zittelina*, A 43, 93—108.
- Witt, W. 2011. Mixed ostracod faunas, co-occurrence of marine Oligocene and non-marine Miocene taxa at Pınarhisar, Thrace, Turkey, *Zitteliana*, A51, 237-254.
- Zalanyi, B. 1929. Morpho-systematische Studien über fossil: Muschelkrebse, *Geological of Hungary Services Paleontology*, 5:1-153.

## **PLATE**

**PLATE I**

Figure 1. *Cladarocythere apostolescui* (Margerie)

1. Carapace, right lateral view, drill log no 3, sample no 29

Figure 2-3. *Cytheromorpha zinndorfi* (Lienenklaus)

2. Right valve, external view, drill log no 2, sample no 28

3. Carapace, right lateral view, drill log no 1, sample no 26

Figure 4-5. *Cytheridea pernota* (Oertli and Keij)

4. Carapace, left lateral view, drill log no 1, sample no 24

5. Carapace, right lateral view drill log no 1, sample no 24

Figure 6-7. *Neocyprideis williamsoniana* (Bosquet)

6. Left valve, external view, drill log no 1, sample no 25

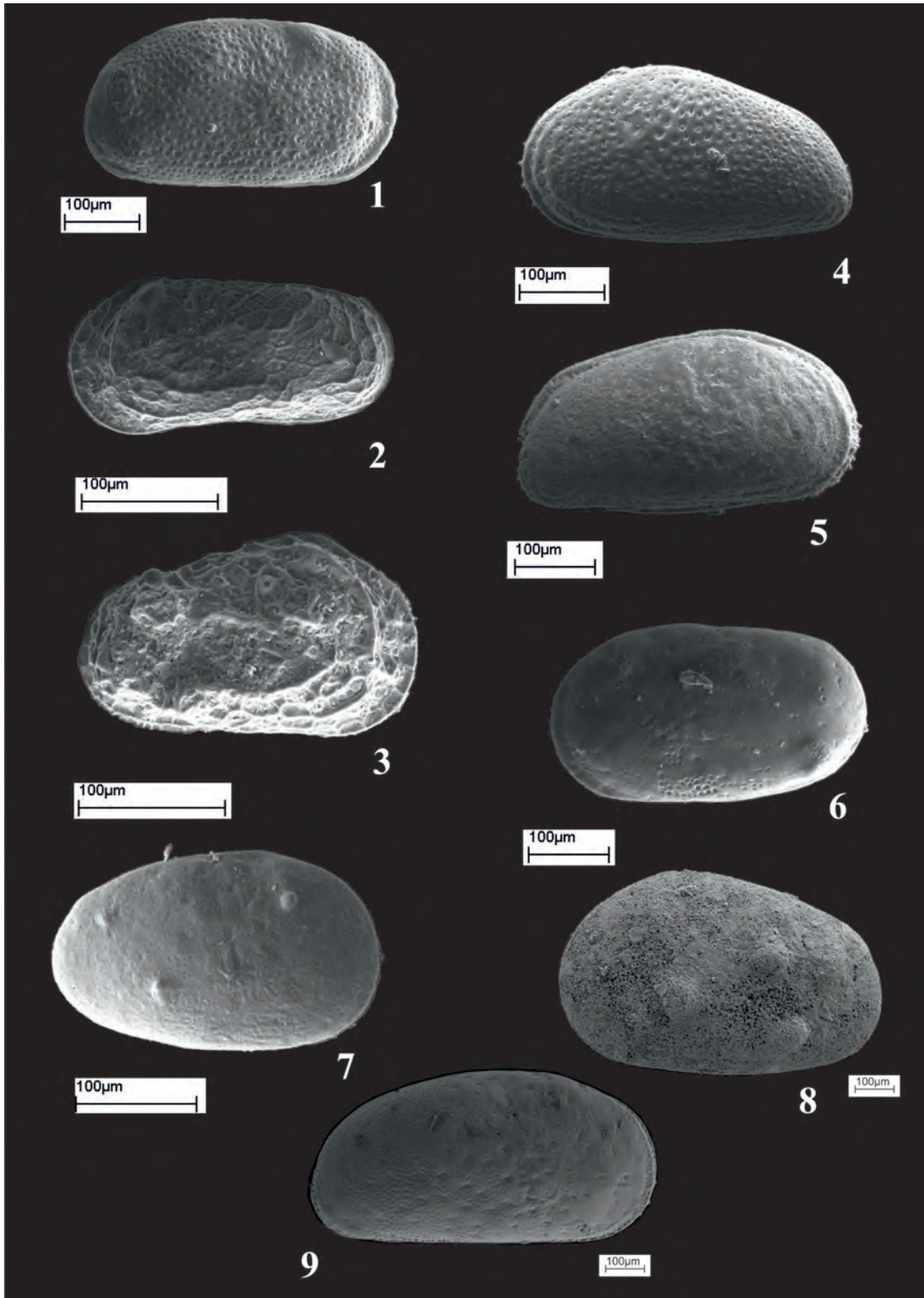
7. Carapace, right lateral view, drill log no 3, sample no 30

Figure 8. *Cyprideis anatolica* Bassiouni

8. Left valve, external view, drill log no 1, sample no 9

Figure 9. *Cyprideis torosa* (Jones)

9. Right valve, external view, drill log no 3, sample no 19



**PLATE II**

Figure 1-2. *Cyprideis torosa* (Jones)

1. Carapace, right lateral view, drill log no 1, sample no 10
2. Carapace, left lateral view, drill log no 3, sample no 2

Figure 3-5. *Cyprideis pannonica* (Mehes)

3. Left valve, external view, drill log no 3, sample no 21
4. Left valve, external view, drill log no 1, sample no 10
5. Carapace, left lateral view, drill log no 2, sample no 13

6. *Miocyprideis sarmatica* (Zalanyi)

6. Carapace, left lateral view, drill log no 2, sample no 11

Figure 7-8. *Cyprideis seminulum* (Reuss)

7. Carapace, left lateral view, drill log no 3, sample no 20
8. Left valve, external view, drill log no 2, sample no 11

Figure 9-10. *Cyprideis sublittoralis* Pokorny

9. Carapace, right lateral view, drill log no 2, sample no 15
10. Carapace, left lateral view, drill log no 2, sample no 15

PLATE II

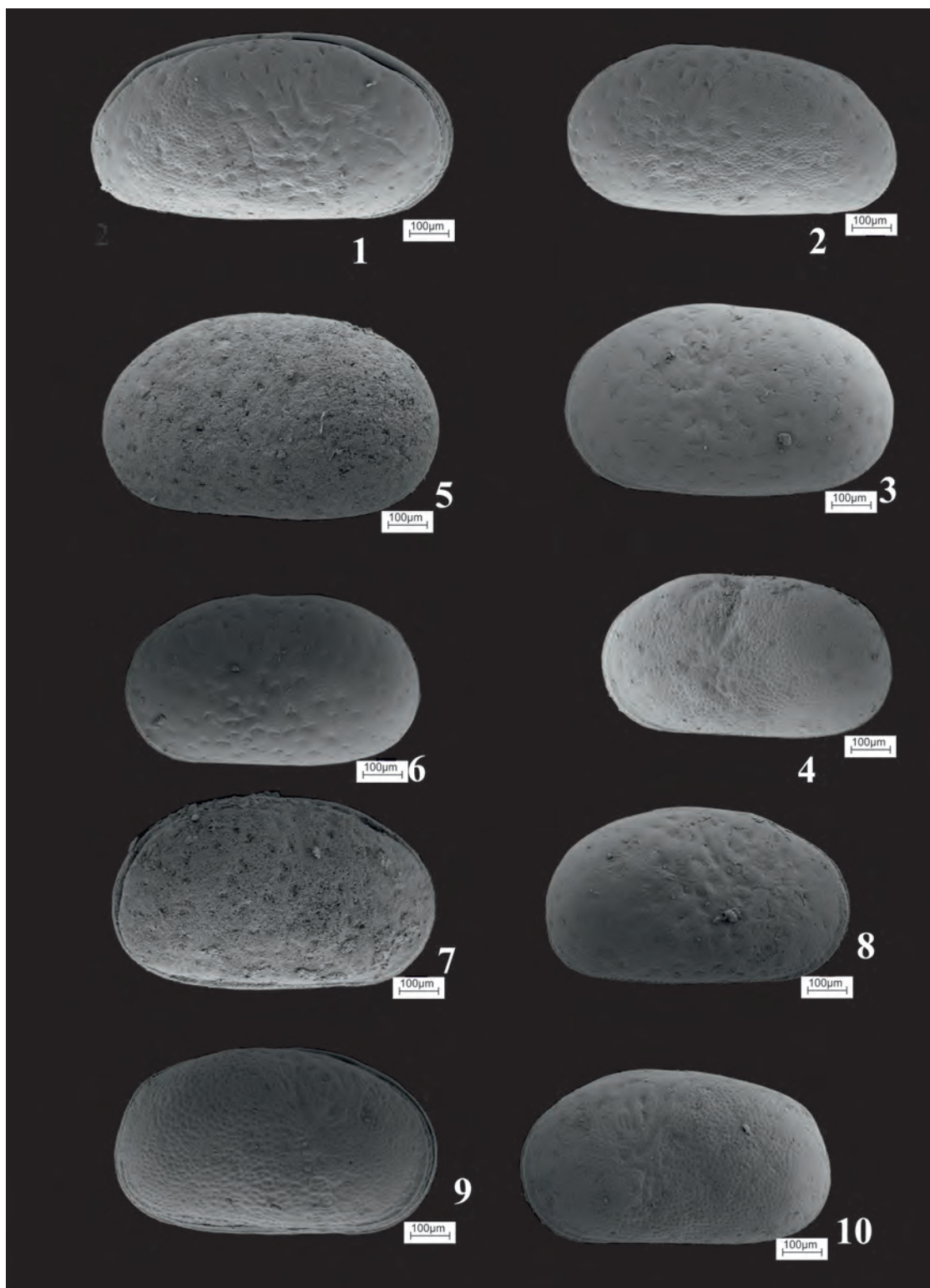


**PLATE III**

Figure 1-2. *Heterocypris salina* (Brady)

1. Carapace, left lateral view, drill log no 3, sample no 25
2. Carapace, right lateral view, drill log no 3, sample no 1

Figure 3. *Xestoleberis ventricosa* Mueller

3. Carapace, left lateral view, drill log no 3, sample no 21

Figure 4. *Xestoleberis subglobosa* (Bosquet)

4. Carapace, left lateral view, drill log no 1, sample no 24

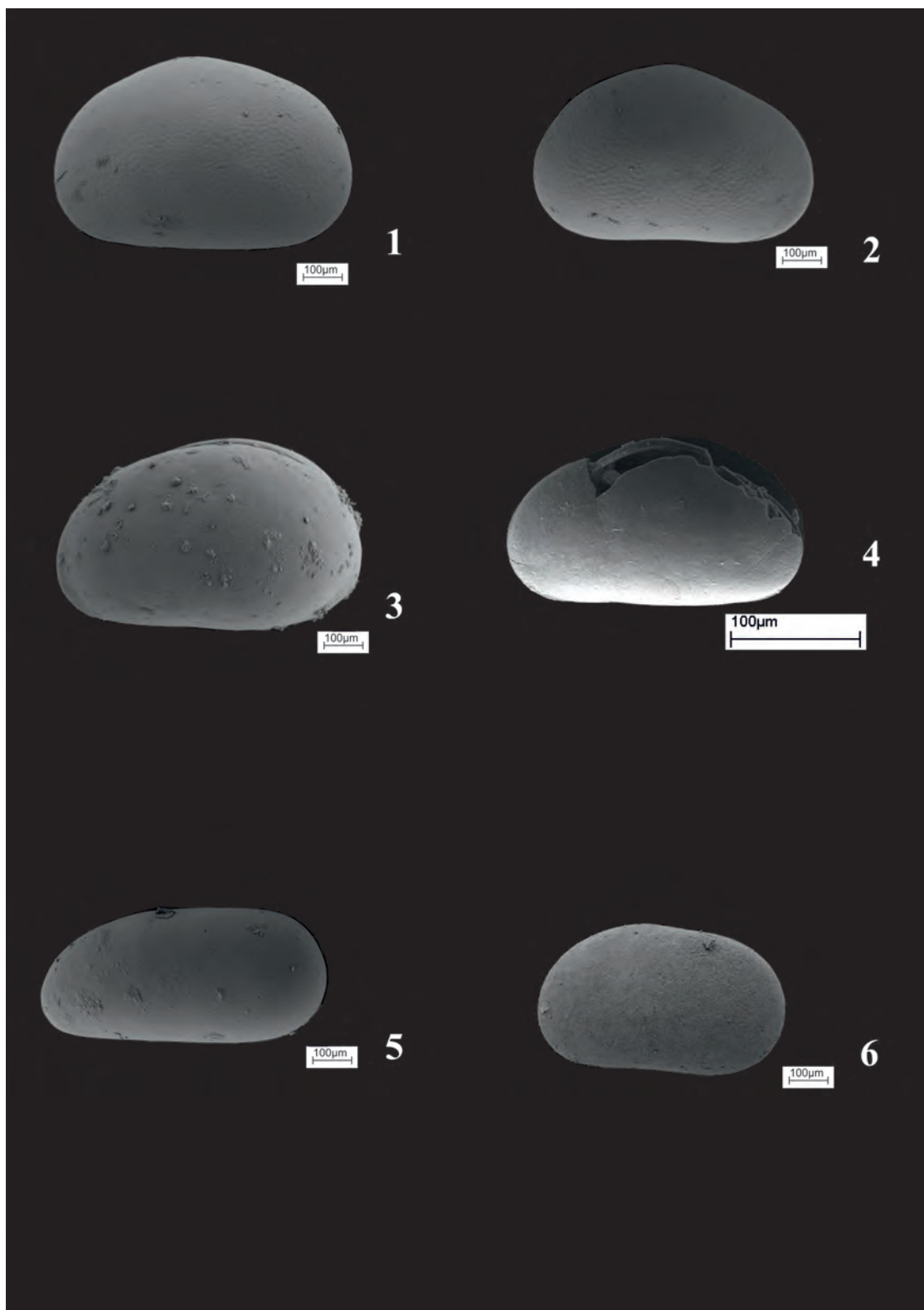
Figure 5. *Darwinula cylindrica* Straub

5. Carapace, left lateral view, drill log no 1, sample no 18

Figure 6. *Candona (Caspiocypris) alta* (Zalanyi)

6. Right valve, external view, drill log no 1, sample no 10

PLATE III







# BULLETIN OF THE MINERAL RESEARCH AND EXPLORATION

<http://bulletin.mta.gov.tr>

BULLETIN OF THE MINERAL RESEARCH AND EXPLORATION	
CONTENTS	
OSTRACODS OF THE MEDITERRANEAN (THE GULF OF ANTALYA) AND THE AEGEAN SEA (AYVALIK AND KUŞADASI) AND THEIR BIOGEOGRAPHICAL DISTRIBUTIONS	Derya PARLAK <sup>a</sup> and Atike NAZİK <sup>b*</sup>
RESEARCH ARTICLE	

## OSTRACODS OF THE MEDITERRANEAN (THE GULF OF ANTALYA) AND THE AEGEAN SEA (AYVALIK AND KUŞADASI) AND THEIR BIOGEOGRAPHICAL DISTRIBUTIONS

Derya PARLAK<sup>a</sup> and Atike NAZİK<sup>b\*</sup>

<sup>a</sup>Çukurova Univ., Fac. of Sci., Dept. of Geol. Eng., 01330, Sarıçam, Adana, TURKEY

<sup>b</sup>Çukurova Univ., Fac. of Eng. and Arch., Dept. of Geol. Eng., 01330, Sarıçam, Adana, TURKEY

Research Article

### Keywords:

Ostracod, Geological Time, Biogeography, Mediterranean, Aegean Sea.

### ABSTRACT

The aim of this study is taxonomic investigation and environmental distribution of ostracoda association from the bottom sediments of the Mediterranean (The Gulf of Antalya) and Aegean Sea (Alibey and Maden islands/Ayvalık and Kuşadası) and identification of species surviving up to present. Twenty genera and 26 species are determined by examining the ostracoda contents of the 197 samples from the bottom sediments from 5 to 30 m depth in the Antalya Bay (Mediterranean). 24 genera and 34 species in 84 samples belonging to 4 cores around Alibey and Maden islands to the north of Ayvalık in Aegean Sea have been determined. Also, 23 genera and 29 species from the 45 samples at the depth of 8,5-22.3 m around Kuşadası have been determined. According to carapace morphology and depth of water, shallow marine group genera are belonging to subfamilies Trachyleberidae and Hemicytheridae which have well-developed hinge, branching marginal-pore canals, clear eye-spots and more ornamentation, are relatively abundant specimens. The ostracoda association defined in this study is correlated with previous studies in Mediterranean, Aegean islands, Adriatic Sea, Algeria, Aegean and Marmara Sea of Turkey. The well-known ostracoda species such as *Aurila convexa*, *Jugosocythereis prava*, *Carinocythereis antiquata*, *Carinocythereis carinata*, *Costa batei*, *Semicytherura inversa*, *Loxococoncha rhomboidea*, *Sahnia fasciata*, *Cushmanidea elongata* from Atlantic and Mediterranean and *Neonesidea formosa*, *Trieblina raripila*, *Cytherella (Cytherelloidea) beckmanni*, *Cytherelloidea sordida*, *Aurila arborescens*, *Carinocythereis rhombica*, *Hiltermannicythere rubra*, *Hiltermannicythere turbida*, *Cytheretta adriatica*, *Cytheretta judaea*, *Callistocythere intricatoides*, *Urocythereis crenulosa*, *Acanthocythereis hystrix*, *Paracytheridea depressa*, *Xestoleberis communis*, *Xestoleberis dispar* and *Pontocypris acuminata* from in Mediterranean are wide-spread.

Received: 09.12.2015

Accepted: 18.01.2016

## 1. Introduction

The study area covers The Gulf of Antalya (Mediterranean) and Ayvalık-Kuşadası (Aegean Sea) regions (Figure 1). In various regions of the Aegean Sea and the Mediterranean, the ostracod and foraminiferal distributions and their systematical studies close to the subject of this research were carried out (Altınsaçlı and Kubanç, 1990; Kubanç and Altınsaçlı, 1990; Nazik, 1994; Şafak, 1999, 2008; Tunoğlu, 2001; Kubanç, 1995; 2005; 2006; Çulha and Tunoğlu, 2008, 2009; Ertekin and Tunoğlu, 2008; Meriç et al., 2002; Meriç et al., 2008a, b, c, d, e; Meriç et al., 2009a,b; Perçin-Paçal, 2011; Meriç et al., 2012a, b, c; Meriç et al., 2014; Parlak and Nazik, 2014).

The bottom sediments collected from different stations in The Gulf of Antalya, which they have

different environmental conditions, the core studies carried out within sea bottom sediments around Ayvalık (Alibey and Maden islands) in the Aegean Sea, and samples possessing different characteristics taken from the vicinity of mineral water springs in the Gulf of Kuşadası were investigated. The purpose of the study is; a) to examine taxonomically, b) to observe the effects of the environmental conditions, c) to determine living species through geological time to present, and d) to compare species determined in this study with previous studies carried out in the Atlantic and Mediterranean and to establish their biogeographical distributions benefiting from the similarities and differences of genera and species of the ostracod assemblage found in bottom sediments of Mediterranean and Aegean Sea.

\*Corresponding author: Atike Nazik, [anazik@cu.edu.tr](mailto:anazik@cu.edu.tr)

<http://dx.doi.org/10.19111/bmre.45467>



Figure 1- Location map of study areas (Parlak and Nazik, 2014).

## 2. Material and Method

The main material of the study is formed by 106 samples taken from bottom sediments at depths of 5-30 meters in the Gulf of Antalya, 84 samples belonging to 4 cores taken from the vicinities of Alibey and Maden islands located in northwestern Ayvalık and 45 samples collected from Kuşadası region at depths of 8.5-22.3 meters in the Aegean Sea.

Samples from the Gulf of Antalya (Mediterranean) were taken by the member of Bosphorus University Diving Club within scope of "Ecological Regional Scale Protection and Responsible Tourism on Lycian Coasts Project, Marine Biodiversity Research, 2002" by the World Wildlife Fund (WWF-Turkey).

Samples belonging to 11 cores in the Aegean Sea were taken by Meriç et al. (2009c) in 4 areas (3 locations in northern part of the Alibey Island and 1 location in east of the Maden Island). The material of this research consist of total 84 samples of each core selected in 4 localities and their ostracod content was studies. The depths at which the samples were taken vary between 0.80-8.00 meters. The coordinates of the points, where the cores were taken, and the length of cores are given in table 1.

The samples taken from Pamucak Bay at northwest of Kuşadası in Aydın province covers samples collected from the vicinity of a mineral water spring which is 200 meters away from the shore at 12.40 m depth, at 19.6 °C temperature. 45 actual sediment samples were collected in 2007 autumn by free diving

Table 1- Lengths, coordinates and water depths of cores taken from Ayvalık region (Meriç et al., 2009c)

Core name	Latitude	Longitude	Water Depth (m)	Core Length (cm)
1 c	39°22.548'	26°38.552'	-1,5	45
2 c	39°23.427'	26°36.029'	-8	42
3 a	39°22.394'	26°36.929'	-2,7	45
4 b	39°22.220'	26°37.499'	-0,8	52

method; one of them being at the center, and the others being at 5-100 m in east, 5-45 m in west, 5-50 m in north and 5-50 m south directions horizontally, with depths varying between 8.5-20.2 meters (Meriç et al., 2009b). The horizontal distance, direction, water depth and water temperature estimations of these samples with respect to source area are given in table 2.

All samples used in this study were supplied by Prof. Engin Meriç as a research material.

The identification of genera and species of ostracods were examined under binocular microscope. Both the external and internal views of carapace and valves of ostracods were studied. In determining genera and species, Van Morkhoven (1963), Hartmann and Puri (1974), Bonaduce et al. (1975), Breman (1975), Yassinsi (1979), Guillaume et al. (1985), Athersuch et al. (1989), Zangger and Malz, (1989), Mostafawi and Matzke-Karasch (2006), Joachim and Langer (2008) and “MarBEF Data System” (<http://www.marbef.org/data/>) were used.

Ostracod images of the Antalya samples were taken in Scanning Electron Microscope (SEM) of Şişecam Group, Turkey and as for the images of Ayvalık and Kuşadası samples SEM images were taken in the laboratory of the Advanced Technology Education, Research and Application Center (METIAM), Mersin University. SEM images of ostracod species are given in plates 1-3.

### 3. Research Findings

The study was conducted with the ostracod investigation of samples taken from the Gulf of Antalya and Ayvalık-Kuşadası (Aegean Sea). 26 species in Mediterranean, 34 species in Ayvalık region) and 29 species in Kuşadası region in the Aegean Sea were identified. The graphic of family percentage distribution for ostracods in the study was prepared (Figure 2). When the ostracod assemblage is numerically assessed, and the carapace morphology and depth are taken into consideration, it is observed

that genera of Trachyleberidae and Hemicytheridae families, which have very ornamentation with distinctive shallow marine characteristics, with developed hinge, distinct eye spots and branched margin-pore canals, are relatively more than the number of individuals.

As a result of this study, the information about the ostracod assemblage of both regions was given below in detail.

Table 2-Direction, distance, depth and water temperature of samples taken from the vicinity of Kuşadası Spring.

Sample Number		Horizontal distance	Direction	Depth	Water
CB 001	A	From Spring	From Spring	12,4 m	19,6
CB 002	A	5 m	South	11,1 m	17,5
CB 003	A	10 m	South	9,7 m	17,5
CB 004	A	15 m	South	9,2 m	17,5
CB 005	A	20 m	South	9,5 m	17,5
CB 006	A	25 m	South	10,5 m	17,5
CB 007	A	30 m	South	11,3 m	17,5
CB 008	A	35 m	South	12,3 m	17,5
CB 009	A	40 m	South	12,5 m	17,5
CB 010	A	45 m	South	13,7 m	17,5
CB 011	A	50 m	South	14,9 m	17,5
CB 012	A	5 m	North	8,9 m	17,5
CB 013	A	10 m	North	8,5 m	17,5
CB 014	A	15 m	North	8,7 m	17,5
CB 015	A	20 m	North	9,0 m	17,5
CB 016	A	25 m	North	10,1 m	17,5
CB 017	A	30 m	North	10,9 m	17,5
CB 018	A	35 m	North	12 m	17,5
CB 019	A	40 m	North	13,1 m	17,5
CB 020	A	45 m	North	14,2 m	17,5
CB 021	A	50 m	North	20,1 m	17,5
CB 022	A	5 m	West	9,1 m	17,5
CB 023	A	10 m	West	9,3 m	17,5
CB 024	A	15 m	West	11,3 m	17,5
CB 025	A	20 m	West	12,8 m	17,5
CB 026	A	25 m	West	14,7 m	17,5
CB 027	A	30 m	West	17,3 m	17,5
CB 028	A	35 m	West	17,9 m	17,5
CB 029	A	40 m	West	18,2 m	17,5
CB 030	A	45 m	West	22,3 m	17,5
CB 031	A	5 m	East	12,8 m	17,5
CB 032	A	10 m	East	11,9 m	17,5
CB 033	A	15 m	East	12,1 m	17,5
CB 034	A	20 m	East	11,5 m	17,5
CB 035	A	25 m	East	14,4 m	17,5
CB 036	A	30 m	East	15,3 m	17,5
CB 037	A	35 m	East	15,9 m	17,5
CB 038	A	40 m	East	18,1 m	17,5
CB 039	A	45 m	East	19,1 m	17,5
CB 040	A	50 m	East	19,5 m	17,5
CB 041	A	60 m	East	19,4 m	17,5
CB 042	A	70 m	East	19,1 m	17,5
CB 043	A	80 m	East	20,2 m	17,5
CB 044	A	90 m	East	20,1 m	17,5
CB 045	A	100 m	East	20,2 m	17,5

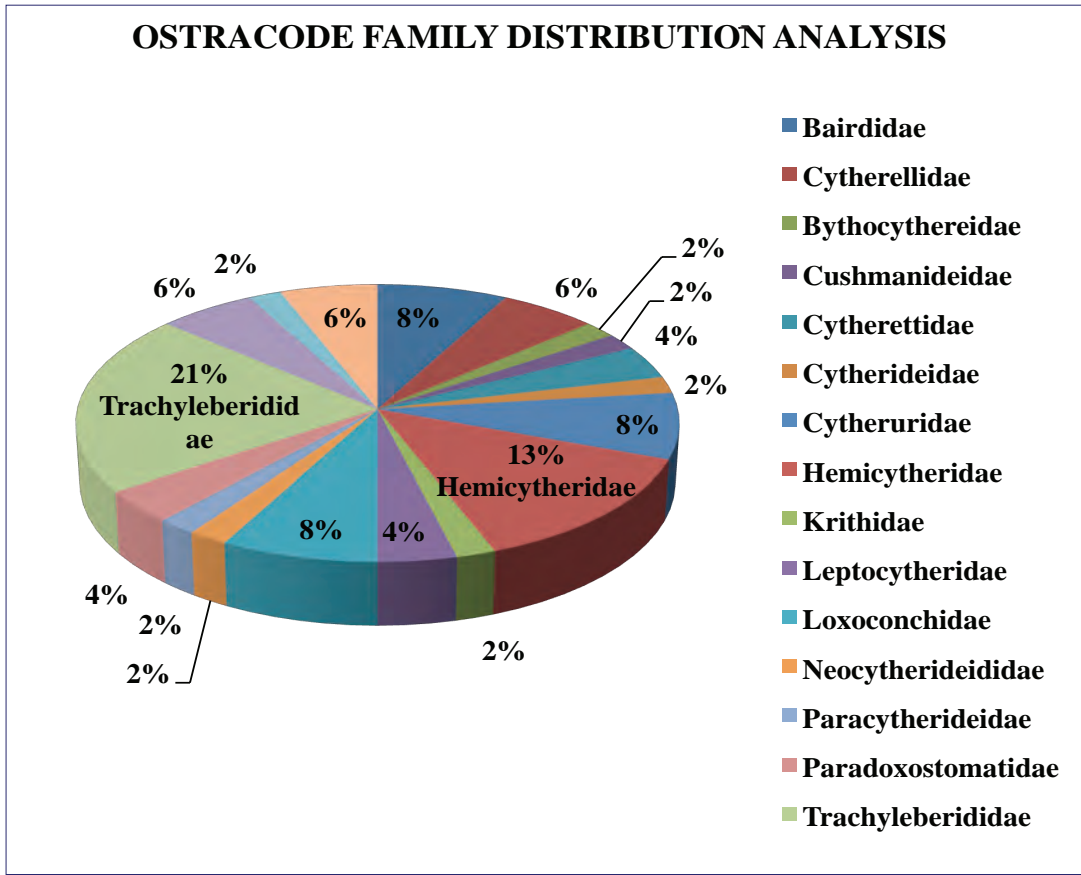


Figure 2- The percentage distribution of ostracod families in the study.

### 3.1. The Gulf of Antalya Ostracod Assemblage

The ostracod content of 197 samples taken from bottom sediments at depths of 5-30 meters in Antalya Bay was investigated, and 20 genera and 26 species were identified (Table 3a, b).

Genera of *Xestoleberis*, *Loxoconcha*, *Neonesidea*, *Urocythereis*, *Aurila*, *Jugosocythereis* from the the Gulf of Antalya ostracod assemblage were widely observed. According to recent ostracod studies carried out among widespread genera, it is known that *Neonesidea* lives at depths of 5-40 m, in sandy silty layers; *Jugosocythereis* at depths of 12-120 m in layers with *Posidonia*, calcereous algae and in sands with *Amphioxus*; *Loxoconcha* generally at depths below 30-40 m; *Urocythereis* at depths of 0-30 m in sandy layers and *Aurila* lives at depths of 0-128 m in sandy layers (Van Morkhoven, 1963; Breman, 1975; Bonaduce et al., 1975; Yassini, 1979). The genera of *Pterygocythereis*, *Henryhowella* and *Propontocypris*, which generally live in bathyal environment but rarely observed in littoral environment, were identified in a couple of stations. Besides; the ostracod assemblage

with genera less than 2 were encountered in stations 8/12m, 10/8m, 25/A1 S10, 35/14-15m, 51/14m, 69/12-24m, 86/15m, 100/12-24m, 106/12m, 107/24m, 112/12m, 114/24m, 115/24m, 116/20m, 135/10 m.

The Gulf of Antalya ostracod assemblage was compared with ostracod assemblages found in studies carried out in Aegean Islands (Sissing, 1972; Adriatic Sea (Bonaduce et al., 1975; Breman, 1975), Algeria (Yassini, 1979), Gökçeada-Bozcaada-Çanakkale (Şafak, 1999; Meriç et al., 2002; Meriç et al., 2009a; Öner et al., 2013), Sea of Marmara (Tunoğlu, 1999; Nazik, 2001; Kubanç, C. 2002; Kubanç, N. 2005; Kırıcı-Elmas et al., 2007), western Black Sea (Kılıç, 2001; Ongan et al., 2009;), Izmir (Meriç et al., 2011; 2012b), Edremit Bay (Meriç, 2012c), and in Mediterranean (Nazik, 1994; Şafak, 2003, 2008; Ertekin and Tunoğlu, 2008); so big similarities in genera and species were identified. It was also determined that *Aurila convexa*, *Loxoconcha rhomboidea*, *Cytheridea neapolitana*, *Xestoleberis communis*, *Xestoleberis dispar*, *Jugosocythereis prava*, *Neonesidea corpulenta* and *Urocythereis margaritifera* species were also widespread.





### 3.2. Ostracod Assemblage

Alibey and Maden islands, Ayvalık and Kuşadası regions were studied in the Aegean Sea. Detailed information related to the ostracod assemblage of these two regions is given below.

#### 3.2.1. Ayvalık (Alibey and Maden Islands) Ostracod Assemblage

For each 4 cores performed in the vicinity of Alibey and Maden islands in northwest Ayvalık, 21 samples were collected from core 4b at a water depth of 0.80 m, from core 1c at 1.5 m, from core 3a at 2.70 m and from core 2c at 8.00 m. The distribution of ostracod species according to cores is given in table 4. As a result of studies carried out in these samples, 3 species from Bairdiidae family, 2 species from Cytherellidae family, 5 species from Hemicytheridae family, 8 species from Trachyleberidae family, 2 species from Cytherettidae family, 2 species from Leptocytheridae family, 1 species from Cytheruridae family, 1 species from Paracytheridae family, 3 species from Loxoconchidae family, 1 species from Cytherideidae family, 1 species from Neocytherideidae family, 1 species from Cushmanidae family, 1 species from Pontocytheridae family and 1 species from Cyprididae family were determined.

Ostracods were compared with studies carried out by Yassini (1979); Guillaume et al. (1985), Nazik (1994), Gülen et al. (1995), Oertli (1985), Szczechura (1998), Tunoğlu (1999), Şafak (1999), Meriç et al. (2005), Schneider et al. (2005). Among these species, *Carinocythereis*, *Xestoleberis*, *Loxoconcha*, *Urocythereis*, *Cytheretta*, *Aurila* and *Cytherelloidea* genera were identified also in 4 cores taken in the study area. It was observed that the number of ostracod genera and species increased based on water depth. These genera generally constitute epineritic (0-100 m) assemblage. Considering the carapace morphology and depth, it was observed that genera of Trachyleberidae and Hemicytheridae families, which have very ornamentation with distinctive shallow marine characteristics, with developed hinge, distinct eye spots and branched margin-pore canals, were relatively more than the number of individuals.

In the study, ostracod species known in the Atlantic and the Mediterranean such as; *Neonesidea corpulenta*, *Aurila convexa*, *Jugosocythereis prava*,

*Carinocythereis antiquata*, *Carinocythereis carinata*, *Costa batei*, *Semicytherura inversa*, *Loxoconcha rhomboidea*, *Sahnia fasciata*, *Cushmanidea elongata*, *Urocythereis oblonga* and ostracod species known in the Mediterranean such as; *Neonesidea formosa*, *Triebelina raripila*, *Cytherella (Cytherelloidea) beckmanni*, *Cytherelloidea sordida*, *Aurila arborescens*, *Carinocythereis rhombica*, *Hiltermannicythere rubra*, *Hiltermannicythere turbida*, *Cytheretta adriatica*, *Cytheretta judaea*, *Callistocythere intricatoides*, *Urocythereis crenulosa*, *Acanthocythereis hystrix*, *Paracytheridea depressa*, *Loxoconcha stellifera*, *Xestoleberis communis*, *Xestoleberis dispar*, *Pontocypris mytiloides*, *Caudites calceolatus* were determined.

Table 4- Ostracod species in cores of the Ayvalık region.

OSTRACODA	Ayvalık 1c	Ayvalık 2c	Ayvalık 3a	Ayvalık 4b
<i>Neonesidea corpulenta</i>	*	*	*	
<i>Neonesidea formosa</i>	*	*		
<i>Triebelina raripila</i>		*		
<i>Cytherella (Cytherelloidea) beckmanni</i>	*	*		*
<i>Cytherelloidea sordida</i>	*	*	*	*
<i>Aurila arborescens</i>	*	*	*	*
<i>Aurila convexa</i>	*	*	*	*
<i>Caudites calceolatus</i>		*		
<i>Jugosocythereis prava</i>	*	*	*	
<i>Carinocythereis antiquata</i>		*	*	
<i>Carinocythereis carinata</i>	*	*	*	
<i>Carinocythereis rhombica</i>		*	*	
<i>Hiltermannicythere rubra</i>	*	*	*	
<i>Hiltermannicythere turbida</i>	*	*	*	
<i>Cytheretta adriatica</i>	*	*	*	*
<i>Cytheretta judaea</i>		*		
<i>Costa batei</i>	*	*	*	
<i>Callistocythere intricatoides</i>	*	*	*	
<i>Leptocythere sp.</i>	*			
<i>Urocythereis crenulosa</i>		*	*	
<i>Urocythereis oblonga</i>	*	*	*	*
<i>Acanthocythereis hystrix</i>		*	*	
<i>Semicytherura inversa</i>	*	*	*	
<i>Paracytheridea depressa</i>	*	*	*	
<i>Loxoconcha rhomboidea</i>	*	*	*	*
<i>Loxoconcha stellifera</i>		*	*	
<i>Cyprideis torosa</i>		*		
<i>Sahnia fasciata</i>		*		
<i>Cushmanidea elongata</i>	*	*		
<i>Xestoleberis communis</i>	*	*	*	
<i>Xestoleberis depressa</i>	*	*	*	
<i>Xestoleberis dispar</i>	*	*	*	*
<i>Pontocypris mytiloides</i>		*	*	
<i>Heterocypris salina</i>		*		

### 3.2.2. Kuşadası Region Ostracod Assemblage

In the Pamucak Bay, NW Kuşadası of Aydın Province, total of 23 genera and 29 species were identified in 45 samples collected at depths of 8.5-22.3 meters at a distance of 200 meters from the coast (Table 5).

When the ostracod distribution is studied in Kuşadası samples, *Neonesidea corpulenta*, *Neonesidea formosa* from Bairdiidae family; *Aurila convexa*, *Jugosocythereis prava* from Hemicytheridae family; *Loxoconcha bairdi*, *Loxoconcha gibberosa* from Loxoconchidae family; *Xestoleberis communis*, *Xestoleberis dispar* from Xestoleberididae family and *Macropyxis adriatica* from Macrocyprididae family were widely observed. Whereas; genera such as; *Carinocythereis*, *Callistocythereis*, *Acanthocythereis*, *Bosquetina*, *Hiltermannicythere*, which are generally known in the Mediterranean, were found in very few samples. Genera of *Cytheretta*, *Carinocythereis*, *Cytherella* and *Hiltermannicythere* were observed in east of the sampling station in samples taken from deeper parts.

In sampling, it was also investigated whether hot water springs have effects on the life of organisms. When ostracod individuals were examined, there was not observed any physical and chemical differences such as; the shape failure on carapace, color change. Accordingly; there is not any negative effect of hot waters on the ostracods.

Besides; *Urocythereis* and *Pterygocythereis* genera have never been observed in Kuşadası samples.

### 4. Stratigraphical and Biogeographical Distribution of Ostracods

The stratigraphical and biogeographical distribution of samples, which are the main subject of this study, were studied through geological time to present (Table 6). Besides; the original distribution of identified ostracods was given in table 7, as well. In this study, Van Morkhoven (1963), Sissing (1972), Bonaduce et al. (1975), Breman (1975), Yassinski (1979), Athersuch et al. (1989), Meisch (2000), Schneider et al. (2005) and <http://www.marinespecies.org/ostracoda/> site were mainly used.

*Bosquetina carinella* and *Pterygocythereis ceratoptera* from Eocene to Recent were first identified on European coast and is recently known in the Mediterranean.

*Acanthocythereis hystrix*, *Aurila convexa*, *Callistocythere intricatoides*, *Carinocythereis carinata*, *Cushmanidea elongata*, *Cyprideis torosa*, *Cytheretta adriatica*, *Heterocypris salina*, *Hiltermannicythere rubra*, *Hiltermannicythere turbida*, *Semicytherura inversa*, *Triebelina raripila*, *Xestoleberis communis*, *Caudites calceolatus* are genera from Miocene to Recent.

*Costa batei*, *Jugosocythereis prava*, *Loxoconcha gibberosa*, *Loxoconcha stellifera*, *Macropyxis adriatica*, *Neonesidea corpulenta*, *Neonesidea formosa*, *Pseudopsammocythere reniformis*, *Semicytherura acuticostata*, *Urocythereis crenulosa*, *Urocythereis margaritifera*, *Xestoleberis dispar* are living genera from Pliocene to Recent.

*Carinocythereis rhombica*, *Cytherella (Cytherelloidea) beckmanni*, *Loxoconcha bairdi*, *Sahnia fasciata* are genera from Pleistocene to Recent.

*Cytherella alvearium*, *Cytherelloidea sordida*, *Ekpontocypris pirifera*, *Microcytherura fulva*, *Neonesidea formosa*, *Paracytheridea depressa*, *Paradoxostoma tenuissimum*, *Pontocypris acuminata*, *Urocythereis oblonga*, *Xestoleberis depressa* are genera described as Recent.

### 5. Results

The study was conducted by the ostracod examination of samples collected from the the Gulf of Antalya, Ayvalık-Kuşadası (Aegean Sea), and results obtained were given below.

The number of species identified in this study and their locations are as follows; 26 species in the Mediterranean, 34 species Ayvalık region and 29 species in Kuşadası in the Aegean Sea. 2 species from Eocene, 14 species from Miocene, 15 species from Pliocene and 6 species from Pleistocene have continued till Recent. Nine species are known in the Recent.

When the ostracod assemblage was numerically assessed, and the shell morphology and depth were taken into consideration, it was observed that genera of Trachyleberidae and Hemicytheridae families, which have very ornamented with distinctive shallow marine characteristics, with developed hinge, distinct eye spots and branched marginal pore canals, were relatively more than the number of individuals.



Table 6-The stratigraphical and biogeographical distributions of ostracod species in the study.

OSTRACODA	Eocene/Oligocene	Miocene	Pliocene	Pleistocene	Holocene
<i>Bosquetina carinella</i>	Ec	Ec, Ew, Mt	Ec, Ew, Mt	Mt	Mt
<i>Pterygocythereis ceratoptera</i>	Ecw	Ecw, Mt	Mt	Mt	Mt, Ew
<i>Acanthocythereis hystrix</i>		Ec, Mt	Mt	Mt	Mt
<i>Aurila convexa</i>		Ew	Mt, Ew	Mt, Ew	Mt, Ew
<i>Callistocythere intricatoides</i>		Mg	Mt	Mt	Mt, B
<i>Carinocythereis carinata</i>		Mt	Mt	Mt	Mt, B
<i>Caudites calceolatus</i>		Mg	Mg	Mg	Mt
<i>Cushmanidea elongata</i>		Mt	Mt	Mt, Ew	Mt, Ew, A
<i>Cyprideis torosa</i>		W	W	W	W
<i>Cytheretta adriatica</i>		Mt	Mt	Mt	Mt
<i>Heterocypris salina</i>		W	W	W	W
<i>Hiltermannicythere rubra</i>		Mt	Mt	Mt	Mt, B
<i>Hiltermannicythere turbida</i>		Mt	Mt	Mt	Mt, B
<i>Semicatherura inversa</i>		Ew	Ew, Mt	Ew, Mt	Mt
<i>Triebelina raripila</i>		Mt	Mt	Mt	Mt
<i>Xestoleberis communis</i>		Mg	Mt	Mt	Mt
<i>Aurila arborescens</i>			Mt	Mt	Mt
<i>Carinocythereis antiquata</i>			Mt	Mt	Mt, Ew
<i>Costa batei</i>			Mi	Mi	Mi
<i>Jugosocythereis prava</i>			Mt	Mt	Mt, B
<i>Loxoconcha gibberosa</i>			Mg	Mg	Mg, Ag
<i>Loxoconcha stellifera</i>			Mg	Mt	Mt
<i>Macropyxis adriatica</i>			Mi	Ew	Ew
<i>Neonesidea corpulenta</i>			Mg	Mt	Mt, Ew
<i>Neonesidea formosa</i>			Mt	Mt	Mt
<i>Pseudopsammocythere reniformis</i>			Mi	Mi	Mt
<i>Semicatherura acuticostata</i>			Mt	Mt	Mt
<i>Semicatherura paradoxa</i>			Mt	Mt	Mt
<i>Urocythereis crenulosa</i>			Mt	Mt	Mt
<i>Urocythereis margaritifera</i>			Mg	Mt	Mt, Ew
<i>Xestoleberis dispar</i>			Mg	Mt	Mt
<i>Carinocythereis rhombica</i>				Mg	Mg, Ag
<i>Cytherella (Cytherelloidea) beckmanni</i>				Mt	Mt
<i>Cytheretta judaea</i>				Mi	Mt
<i>Loxoconcha bairdi</i>				Mi	Mt
<i>Sahnia fasciata</i>				Mi	Mt, Ew
<i>Sclerochilus contortus</i>				Mt, Ew	Mt, Ew
<i>Cytherella alvearium</i>					Mt
<i>Cytherelloidea sordida</i>					Mt
<i>Ekpontocypris pirifera</i>					Mt, Ew
<i>Loxoconcha rhomboidea</i>					Mt
<i>Microcytherura fulva</i>					Ma
<i>Paracytheridea depressa</i>					Mt, Ew
<i>Paradoxostoma acuminatum</i>					Ew
<i>Pontocypris acuminata</i>					Mt, Ew
<i>Pontocypris mytiloides</i>					Mt, Ew
Mt= Whole Mediterranean		Ec= Central Europe			
Mi= Italian coasts		Ew=Atlantic coast of Europe			
Ma=Adriatic		A=Atlantic coasts of Central America			
Mg= Greek coasts		W= Worldwide			
B= Black Sea		Ag= Aegean Sea			

Table 7- The correlation of ostracod species in the study based on their regions and origins.

OSTRACODA	ANTALYA	AYVALIK	KUŞADASI	MEDITERRANEAN ORIGIN	MEDITERRANEAN-ATLANTIC ORIGIN
<i>Acanthocythereis hystrix</i>		*	*	●	
<i>Aurila arborescens</i>	*	*		●	
<i>Aurila convexa</i>	*	*	*		▲
<i>Bosquetina carinella</i>			*		▲
<i>Callistocythere intricatoides</i>	*	*	*	●	
<i>Carinocythereis antiquata</i>		*			▲
<i>Carinocythereis carinata</i>	*	*	*		▲
<i>Carinocythereis rhombica</i>		*		●	
<i>Caudites calceolatus</i>		*	*	●	
<i>Costa batei</i>	*	*			▲
<i>Cushmanidea elongata</i>	*	*			▲
<i>Cyprideis torosa</i>		*			▲
<i>Cytherella (Cytherelloidea) beckmanni</i>	*	*		●	
<i>Cytherella alvearium</i>			*	●	
<i>Cytherelloidea sordida</i>	*	*		●	
<i>Cytheretta adriatica</i>		*		●	
<i>Cytheretta judaea</i>		*	*	●	
<i>Cytherois sp.</i>	*		*		
<i>Ekpontocypris pirifera</i>	*		*		▲
<i>Henryhowella sp.</i>	*				
<i>Heterocypris salina</i>		*			▲
<i>Hiltermannicythere rubra</i>	*	*	*	●	
<i>Hiltermannicythere turbida</i>	*	*	*	●	
<i>Jugosocythereis prava</i>	*	*	*	●	
<i>Leptocythere sp.</i>		*			
<i>Loxoconcha bairdi</i>			*	●	
<i>Loxoconcha gibberosa</i>			*	●	
<i>Loxoconcha rhomboidea</i>	*	*		●	
<i>Loxoconcha stellifera</i>		*		●	
<i>Macropyxis adriatica</i>			*		▲
<i>Microcytherura fulva</i>	*			●	
<i>Neonesidea corpulenta</i>	*	*	*		▲
<i>Neonesidea formosa</i>	*	*	*	●	
<i>Paracytheridea depressa</i>		*	*		▲
<i>Paradoxostoma acuminatum</i>			*		▲
<i>Pontocypris acuminata</i>			*		▲
<i>Pontocypris mytiloides</i>		*	*		▲
<i>Pseudopsammocythere reniformis</i>			*	●	
<i>Pterygocythereis ceratoptera</i>	*				▲
<i>Sahnia fasciata</i>	*	*			▲
<i>Sclerochilus contortus</i>			*		▲
<i>Semicytherura acuticostata</i>			*	●	
<i>Semicytherura inversa</i>		*	*		▲
<i>Semicytherura paradoxa</i>			*	●	
<i>Triebelina raripila</i>	*	*	*	●	
<i>Urocythereis crenulosa</i>		*		●	
<i>Urocythereis margaritifera</i>	*				▲
<i>Urocythereis oblonga</i>	*	*			▲
<i>Xestoleberis communis</i>	*	*	*	●	
<i>Xestoleberis depressa</i>	*	*			▲
<i>Xestoleberis dispar</i>	*	*	*	●	

(● Endemik Akdeniz).

(▲ Akdeniz- Atlantik)

The ostracod assemblage found in this study were compared with previous studies carried out in the Mediterranean, the Aegean islands, the Adriatic Sea, Algeria, the Sea of Marmara and the Aegean Sea (Turkey). As a result; prevailing ostracod species such as; *Neonesidea corpulenta*, *Aurila convexa*, *Jugosocythereis prava*, *Carinocythereis antiquata*, *Carinocythereis carinata*, *Costa batei*, *Semicytherura inversa*, *Loxococoncha rhomboidea*, *Sahnia fasciata*, *Cushmanidea elongata* known in Atlantic and the Mediterranean, and species such as; *Neonesidea formosa*, *Triebelina raripila*, *Cytherella (Cytherelloidea) beckmanni*, *Cytherelloidea sordida*, *Aurila arborescens*, *Carinocythereis rhombica*, *Hiltermannicythere rubra*, *Hiltermannicythere turbida*, *Cytheretta adriatica*, *Cytheretta judaea*, *Callistocythere intricatoides*, *Urocythereis crenulosa*, *Acanthocythereis hystrix*, *Paracytheridea depressa*, *Xestoleberis communis*, *Xestoleberis dispar* and *Pontocypris acuminata* known in the Mediterranean were determined.

Besides; *Callistocythereis intricatoides*, *Carinocythereis carinata*, *Hiltermannicythere rubra*, *Hiltermannicythere turbida* and *Jugosocythereis prava* species, which are Mediterranean in origin, were found in studies carried out in Black Sea.

### Acknowledgements

Authors thank to the Geological Dept. of the Çukurova University for research facilities given during the preparation of this article, to the retired academician of the Istanbul University, Prof. Engin Meriç, who gave support and provided actual samples collected from Antalya, Ayvalık and Kuşadası regions. Besides; the authors present their appreciation to Advanced Technology Education, Research and Application Center (MEİTAM), Mersin University and to the executives of Şişecam Group.

### References

- Altınsaçlı, S., Kubanç, C. 1990. Ayvalık Yöresi Ostrakod (Crustacea) Faunası Dağılımı. *10. Ulusal Biyoloji Kongresi*, 18-20 Temmuz, Erzurum, 47-55.
- Athersuch, J., Horne, D.J., Whittaker, J.E. 1989. Marine and brackish water ostracods. Synopses of the British Fauna (New Series), *E.J.Brill.*, 43, 1-343.
- Bonaduce, G., Ciampo, G., Masoli, M. 1975. Distribution of ostracoda in the Adriatic Sea. *Pubblicazioni della Stazione Zoologica di Napoli* 40 (Suppl.), 1-304.

- Breman, E. 1975. The Distribution of Ostracodes in the Bottom Sediments Of The Adriatic Sea. Vrije Universiteit te Amsterdam, *Krips Repto, Meppel*, 1-165.
- Çulha G., Tunoğlu C. 2008. Gökçeada ve Marmaris arasında yer alan Ege Körfezleri'nin (Batı Türkiye) Güncel ostrakod topluluğu (Recent Ostracoda associations along the Aegean Gulfs between Gökçeada and Marmaris-West of Turkey), *61. Türkiye Jeoloji Kurultayı, Bildiri Özleri*, 24-28 Mart 2008, Ankara, 329-330.
- Çulha, G., Tunoğlu, C. 2009. Türkiye'nin Ege Körfezlerinde Polyclope cinsinin (Ostracoda) dağılımı ve sistematigi. *IPETGAS 2009, 17. Int. Petroleum and Natural Gas, Congress and Exhibition of Turkey* 31-32, Ankara.
- Ertekin, İ. K., Tunoğlu C. 2008. Pleistocene-Holocene Marine Ostracods From Mersin Offshore Sediments, Turkey, Eastern Mediterranean, 51, 4, Part II, P. Frenzel, I. Boomer, U. Schudack, J.-P. Colin (Ed.). *Revue de Micropaléontologie* 309-326.
- Guillaume, M.C., Peypouquet, J.P, Tetart, J. 1985. Quaternaire et actuel. Atlas des Ostracodes de France. H.J. Oertli (Ed.). *Bulletin Centres Recherche Exploration Proceeding Elf-Aquitaine. Mémoire* 9, 337-377.
- Gülen, D., Kubanç, C., Altınsaçlı, S. 1995. Ostracoda fauna of the Quaternary sequence in the Gulf of İzmit. Quaternary sequence in the Gulf of İzmit. E. Meriç (Ed.), *Kocaeli Valiliği Çevre Koruma Vakfı* 153-171.
- Hartmann, G., Puri, S.H. 1974. Summary of neontological and paleontological classification of ostracoda, *Mitteilungen aus dem Zoologischen Staatsinstitut und Zoologischem Museum in Hamburg, Band, 70*, 7-73.
- Joachim, C., Langer, M.R. 2008. The 80 most common Ostracods from the Bay of Fetovaia Elba Island (Mediterranean Sea). *Universität Bonn*, 29p.
- Kılıç, M. 2001. Recent Ostracoda (Crustacea) Fauna of the Black Sea Coasts of Turkey. *Turkish Journal Zoology* 25, 375-388.
- Kırcı-Elmas, E., Algan, O., Özkar Öngen, İ., Struck, U., Altenbach, A. V., Sagular, E. K., Nazik, A. 2007. Palaeoenvironmental Investigation of Sapropelic Sediments from the Marmara Sea: A Biostratigraphic Approach to Palaeoceanographic History During the Last Glacial-Holocene. *Turkish Journal Earth Sciences* 17, 129-168.

- Kubanç, C. 1995. Ege Denizi Ostrakod (Crustacea) faunası. Doktora tezi, İstanbul Üniversitesi, 117s, İstanbul (unpublished).
- Kubanç, C. 2002. Preliminary study on the ostracoda (Crustacea) fauna of Marmara Sea. İstanbul Üniversitesi, *Journal of Fisheries and Aquatic Sciences* 13, 65-80.
- Kubanç C., Altınsoçlu S. 1990. Ayvalık-Bergama Lagün Ostrakod (Crustacea) Faunası, 10. *Ulusal Biyoloji Kongresi*, Erzurum, 18-20 Temmuz 1990, 37-46.
- Kubanç, S.N. 2005. Diversity and Comparison of Ostracoda of South Marmara Sea. *Journal of Black Sea/Mediterranean Environment* 11, 257-275.
- Kubanç, S.N. 2006. Saros Körfezi Ostracod (Crustacea) Faunası. *İstanbul Üniversitesi Su Ürünleri Dergisi* 20, 27-43.
- Meisch, C. 2000. Freshwater Ostracoda of Western and Central Europe. 522p. *Spektrum Akademischer*, Heidelberg, Berlin.
- Meriç, E., Avşar, N., Nazik, A. 2002. Benthic Foraminifera and Ostracoda fauna of the Bozcaada (Northern Aegean Sea) and local variations in these assemblages. *Yerbilimleri Geosound* 40-41, 97-119.
- Meriç, E., Avşar, N., Nazik, A., Alpar, B., Yokeş, B., Barut, İ.F., Ünlü, S. 2005. Gemlik Körfezi yüzey çökellerinin foraminifer, ostrakod ve mollusk faunası, foraminifer kavkılarında gözlenen morfolojik anomaliler ile bölgenin sedimentolojik, hidrojeokimyasal ve biyokimyasal özellikleri. *Maden Tetkik ve Arama Dergisi* 131, 21-48.
- Meriç, E., Avşar, N., Yokeş, B., Dinçer, F. 2008a. Alibey ve Maden Adaları (Ayvalık-Balıkesir) yakın çevresi bentik foraminiferlerinin taksonomik dağılımı. *Maden Tetkik ve Arama Dergisi* 137, 49-65.
- Meriç, E., Avşar, N., Nazik, A., Yokeş, B., Dinçer, F. 2008b. A review of benthic foraminifers and ostracodes of the Antalya coast. *Micropaleontology* 54, 199-240.
- Meriç, E., Avşar, N., Nazik, A., Yokeş, B., Tuğrul, A.B., Bayarı, S., Özyurt, N., Barut, İ.F., Balkis, N., Uysal, K., Kam, E. 2008c. Morphological abnormalities in benthic foraminifers of the Antalya coast. *Micropaleontology* 54, 241-276.
- Meriç, E., Avşar, N., Yokeş, B. 2008d. *Amphisorus hemprii* Ehrenberg (Rhizopoda, foraminifera) along the Antalya coast. *Micropaleontology* 54, 307-349.
- Meriç, E., Avşar, N., Yokeş, B. 2008e. Some alien foraminifers along the Aegean and southwestern coasts of Turkey. E. Meriç, M. B. Yokeş (Ed.). Recent benthic foraminifera along the southwest coasts of Antalya (SW Turkey) and the impact of alien species on autochthonous fauna. *Micropaleontology* 54, 307-349.
- Meriç, E., Avşar, N., Nazik, A., Yokeş, B., Ergin, M., Eryılmaz, M., Yücesoy-Eryılmaz, F., Gökaşan, E., Suner, F., Tur, H., Aydın, Ş., Dinçer, F. 2009a. Çanak-kale Boğazı'nın Güncel Bentik Foraminifer, Ostrakod, Mollusk Topluluğunu Denetleyen Faktörler ile Çökel Dağılımının Jeokimyası. *Türkiye Jeoloji Bülteni* 52, 155-216.
- Meriç, E., Avşar, N., Barut, İ.F., Yokeş, B., Taş, S., Eryılmaz, M., Dinçer, F., Bircan, C. 2009b. Kuşadası (Aydın) Deniz Dibi Mineralli Su Kaynağı Çevresi Bentik Foraminifer Topluluğu Hakkında Görüş ve Yorumlar. Önlü, H. (Ed.). 13. *Sualtı Bilim ve Teknolojileri Toplantısı Bildiri Kitabı*, 7-8 Kasım 2009, 80-92.
- Meriç, E., Avşar, N., Mekik, F., Yokeş, B., Barut, İ.F., Dora, Ö., Suner, F., Yücesoy-Eryılmaz F., Eryılmaz, M., Dinçer F., Kam, E. 2009c. Alibey ve Maden Adaları (Ayvalık-Balıkesir) Çevresi Genç Çökellerinde Gözlenen Bentik Foraminifer Kavkılarındaki Anormal Oluşumlar ve Nedenleri. *Türkiye Jeoloji Bülteni* 52, 31-84.
- Meriç, E., Avşar, Nazik, A., Yokeş, M.B., Barut, F.İ., Eryılmaz, M., Kam, E., Taşkın, H., Başsarı, A., Dinçer, F., Bircan, C., Kaygun, A. 2011. Ilıca Koyu (Çeşme-İzmir) bentik foraminifer-ostrakod toplulukları ile Pasifik Okyanusu ve Kızıl Deniz kökenli göçmen foraminiferler ve anormal bireyler. 64. *Türkiye Jeoloji Kurultayı Bildiri Özleri Kitabı* 272-273, Ankara.
- Meriç, E., Avşar, N., Nazik, A., Yokeş, B., Dora, Ö., Barut, İ.F., Eryılmaz, M., Dinçer, F., Kam, E., Aksu, A., Taşkın, H., Başsarı, A., Bircan, C., Kaygun, A. 2012a. Karaburun Yarımadası Kuzey Kıyılarındaki Oşinografik Özelliklerinin Bentik Foraminifer ve Ostrakod Toplulukları Üzerindeki Etkileri. *Maden Tetkik ve Arama Dergisi* 145, 22-47.
- Meriç, E., Avşar, N., Nazik, A., Yokeş, B., Barut, İ.F., Eryılmaz, M., Kam, E., Taşkın, H., Başsarı, A., Dinçer, F., Bircan, C., Kaygun, A. 2012b. Ilıca koyu (Çeşme-İzmir) Bentik Foraminifer, Ostrakod Toplulukları ile Pasifik Okyanusu ve Kızıldeniz Kökenli Göçmen Foraminifer ve Anormal Bireyler, *Maden Tetkik ve Arama Dergisi* 145, 62-78.
- Meriç, E., Avşar, N., Nazik, A., Koçak, F., Yücesoy-Eryılmaz, F., Eryılmaz, M., Barut, İ.F., Yokeş, B., Dinçer, F., Efendi, F., Esenli, V., Özdemir, Z., Türker, A., Aydın, Ş., Dinçer, F. 2012c. Edremit Körfezi (Balıkesir) kıyı alanlarında oşinografik özelliklerin bentik foraminifer, ostrakod ve bryozoon toplulukları üzerindeki etkileri ile ilgili yeni veriler. *Türkiye Petrol Jeologları Bülteni* 24, 7-29.

- Meriç, E., Avşar, N., Yokeş, M.B., Barut, İ., Taş, S., Eryılmaz, M., Dinçer, F., Bircan, C. 2014. Opinions and comments on the benthic foraminiferal assemblage observed around the mineral submarine spring in Kuşadası (Aydın, Turkey). *Marine Biodiversity Records, Marine Biological Association of the United Kingdom*, 7, 1 – 17, e103; *Published online*, doi:10.1017/S1755267214000840.
- Mostafawi, N., Matzke-Karasz, R. 2006. Pliocene Ostracoda of Cephalonia, Greece. The Unrevised species of Uliczny (1969). *Revista Española de Micropaleontología* 38, 11-48.
- Nazik, A. 1994. İskenderun Körfezi Holosen ostrakodları. *Maden Teknik Arama Dergisi* 116, 15-20.
- Nazik, A. 2001. Ostracode faunas of bottom sediments from the continental shelf, south Marmara Sea, NW Turkey and their comparison with other shelf environments in the Mediterranean and Aegean regions. *Geological Journal* 36, 111-123.
- Oerthli, H.J. 1985. Atlas des Ostracodes de France. *Bulletin Centres Recherche Exploration Proceeding Elf-Aquitaine, Mémoire* 9, 257-335.
- Ongan, D., Algan, O., Kapan-Yeşilyurt, S., Nazik, A., Ergin, M., Eastoe, C. 2009. Benthic Faunal Assemblages of the Holocene Sediments from the Southwest Black Sea Shelf. *Turkish Journal of Earth Sciences* 18, 239-297.
- Öner, E., Meriç, E., Nazik, A., Avşar, N. 2013. Yeni Bademli Höyüğü Çevresinde Alüvyal Jeomorfoloji ve Paleontoloji Araştırmaları (Gökçeada-Çanakkale). Öner, E. (Ed.). *Prof.Dr. İlhan Kayan'a Armağan, Ege Üniversitesi Yayınları Edebiyat Fakültesi Yayını* 181, 839-871
- Parlak, D., Nazik, A. 2014. Akdeniz (Antalya Körfezi) ve Ege Denizi (Ayvalık ve Kuşadası) Dip Sedimentlerinin Ostrakod dağılımı: Benzerlikler ve Farklılıklar. 15. *Paleontoloji-Stratigrafi Çalıştayı, Bildiri Özleri Kitabı* 209-210.
- Perçin-Paçal, F. 2011. The ecology of the Ostracoda (Crustacea) species obtained from the coasts of İskenderun Bay (Eastern Mediterranean Sea). *Journal Black Sea/Mediterranean Environment* 17, 127-144.
- Schneider, S., Witt, W., Yiğitbaş, E. 2005. Ostracods and bivalves from an Upper Pleistocene (Tyrrenian) Marine Terrace Near Altınova (İzmit Province, Turkey). *Zitteliana* A45, 87-114.
- Sissingh, W. 1972. Late Cenozoic Ostracoda of the South Aegean Island Arc. *Utrecht Micropaleontological Bulletins* 6, 1-187.
- Szcechura, J. 1998. The distribution of *Triebelina raripila* and *Carinocythereis carinata* (Ostracoda) from the Middle Miocene of the Central Paratethys and Their Palaeogeographic Implications. *Journal of Micropalaeontology* 17, 125-130.
- Şafak, Ü. 1999. Recent Ostracoda Assemblage of the Gökçeada-Bozcaada-Dardanelles Region. *Yerbilimleri (Geosound)* 35, 149-172.
- Şafak, Ü. 2003. Recent ostracodes of the Yumurtalık Gulf. *Bulletin of the Mineral Research and Exploration Contents* 126, 1-10.
- Şafak, Ü. 2008. Recent Ostracoda fauna of the Mersin Gulf; Southern Turkey, and their correlation with other gulf and shelf environments in the Mediterranean and Aegean regions. *Yerbilimleri (Geosound)* 52, 1-20.
- Tunoğlu, C. 1999. Recent ostracoda association in the Sea of Marmara, NW Turkey. *Hacettepe Üniversitesi Yerbilimleri Dergisi* 21, 63-89.
- Tunoğlu, C. 2001. Recent Ostracoda assemblage and distribution in Saros Gulf (NE Aegean Sea), NW Turkey. *14th International Symposium on Ostracoda*, July 27-August 8, 2001, Shizuoka, Japan, 90.
- Van Morkhoven, F.P.C.M. 1963. Post-palaeozoic Ostracoda. Their Morphology, Taxonomy, and Economic Use. – Vol. II, Generic Descriptions, Amsterdam – London – New York, *Elsevier Publishing Company*, 1-478.
- Yassini, I. 1979. The littoral system ostracodes from the bay of Bou-İsmail, Algiers, Algeria, National Iranian Oil Company. *Revista Espanola de Micropaleontologia* XI, 353-416.
- Zangger, E., Malz, H. 1989. Late Pleistocene, Holocene, and Recent ostracods from the Gulf of Argos, Greece. *Courier Forschungsinstitut Senckenberg* 113, 159-175

**PLATE**

**PLATE I**

Figure 1. *Cytherella alvearium*, left valve side view, core Ayvalık 2c 0-2cm.

Figure 2. *Cytherella (Cytherelloidea) beckmanni*, left valve side view, core Ayvalık 2c 2-4cm.

Figure 3. *Cytherelloidea sordida*, left valve side view, ×63, Kekova-Antalya, Station 84/3m.

Figure 4. *Neonesidea corpulenta*, right valve side view, Kuşadası, Station 20.

Figure 5. *Neonesidea formosa*, left valve side view, Kuşadası, Station 24.

Figure 6. *Triebelina raripila*, right valve side view, Kuşadası, Station 23.

Figure 7. *Sclerochilus contortus*, left valve side view, Kuşadası, Station 38.

Figure 8. *Cushmanidea elongata*, right valve side view, core Ayvalık 2c 4-6 cm.

Figure 9. *Cytheretta adriatica*, left valve side view, core Ayvalık 4b 24-26 cm.

Figure 10. *Cytheretta judaea*, a. Left valve interior view, Kuşadası, Station 45, b. Right valve side view, Kuşadası, Station 38

Figure 11. *Cyprideis torosa*, left valve side view, core Ayvalık 2c 8-10 cm.

Figure 12. *Microcytherura fulva*, right valve side view, ×62, Kaş-Antalya, Station 43/21 m.

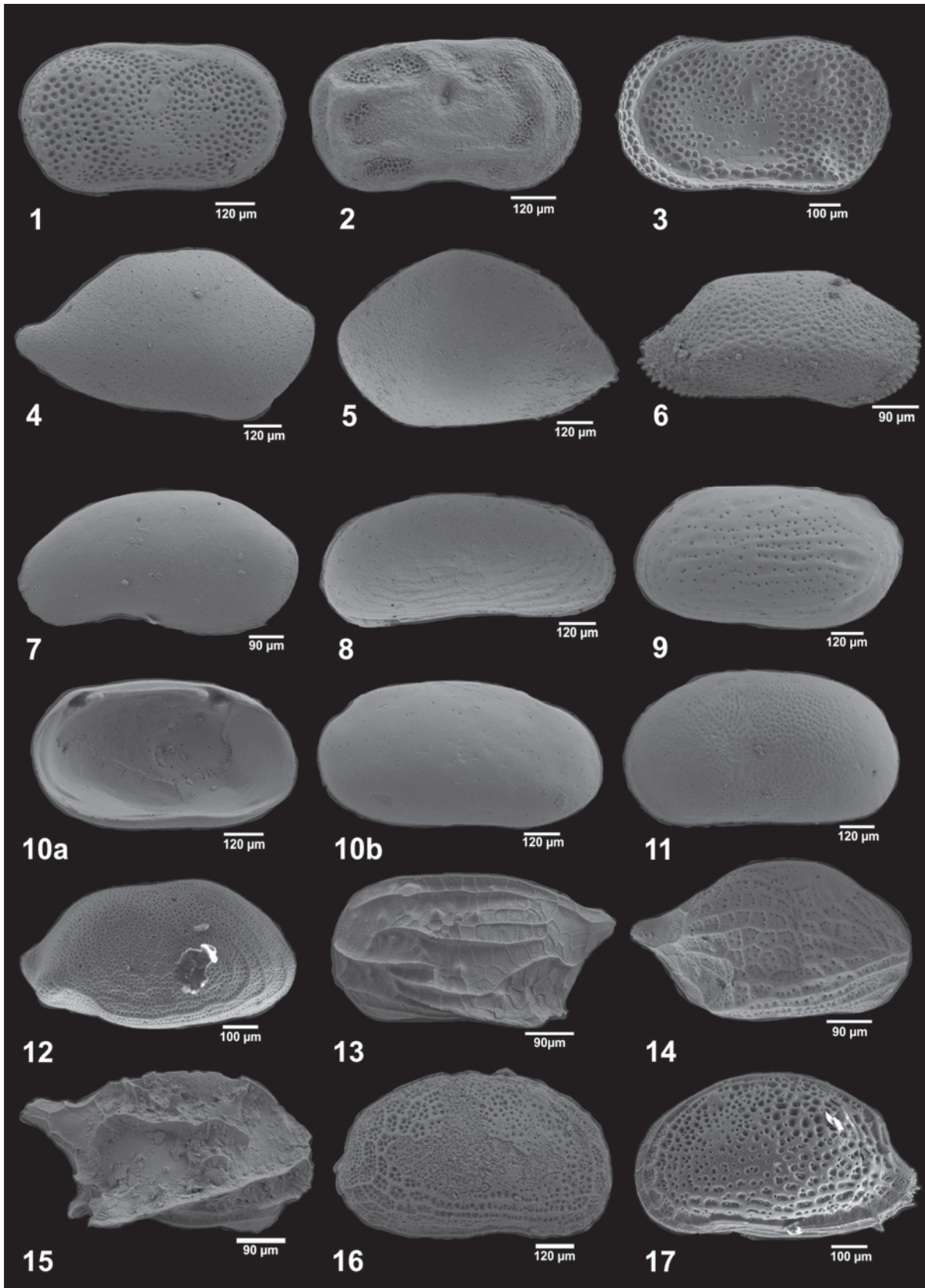
Figure 13. *Semicytherura acuticostata*, left valve side view, Kuşadası, Station 8.

Figure 14. *Semicytherura inversa*, right valve side view, Kuşadası, Station 42.

Figure 15. *Semicytherura paradoxa*, right valve side view, Kuşadası, Station 17.

Figure 16. *Aurila arborescens*, right valve side view, core Ayvalık 3a 40-42 cm.

Figure 17. *Aurila convexa*, left valve side view, ×64, Kekova-Antalya, Station 71/15m.



**PLATE II**

Figure 1. *Caudites calceolatus*, left valve side view, Kuşadası, Station 3.

Figure 2. *Jugosocythereis prava*, right valve side view, Kaş-Antalya, Station 42/9 m.

Figure 3. *Urocythereis crenulosa*, right valve side view, core Ayvalık 2c 2-4 cm.

Figure 4. *Urocythereis margaritifera*, left valve side view, Üçadalar-Antalya, Station 128/20 m.

Figure 5. *Urocythereis oblonga*, right valve side view, Kalkan-Antalya, Station 5/5 m.

Figure 6. *Pseudosammocythere reniformis*, a. Shell right external view, Kuşadası, Station 24; b. Right valve external view, Kuşadası, Station 29.

Figure 7. *Callistocythere intricatoides*, left valve external view, Kalkan-Antalya, Station 14/12 m.

Figure 8. *Loxoconcha bairdi*, left valve side view, Kuşadası, Station 34.

Figure 9. *Loxoconcha gibberosa*, left valve side view, Kuşadası, Station 18.

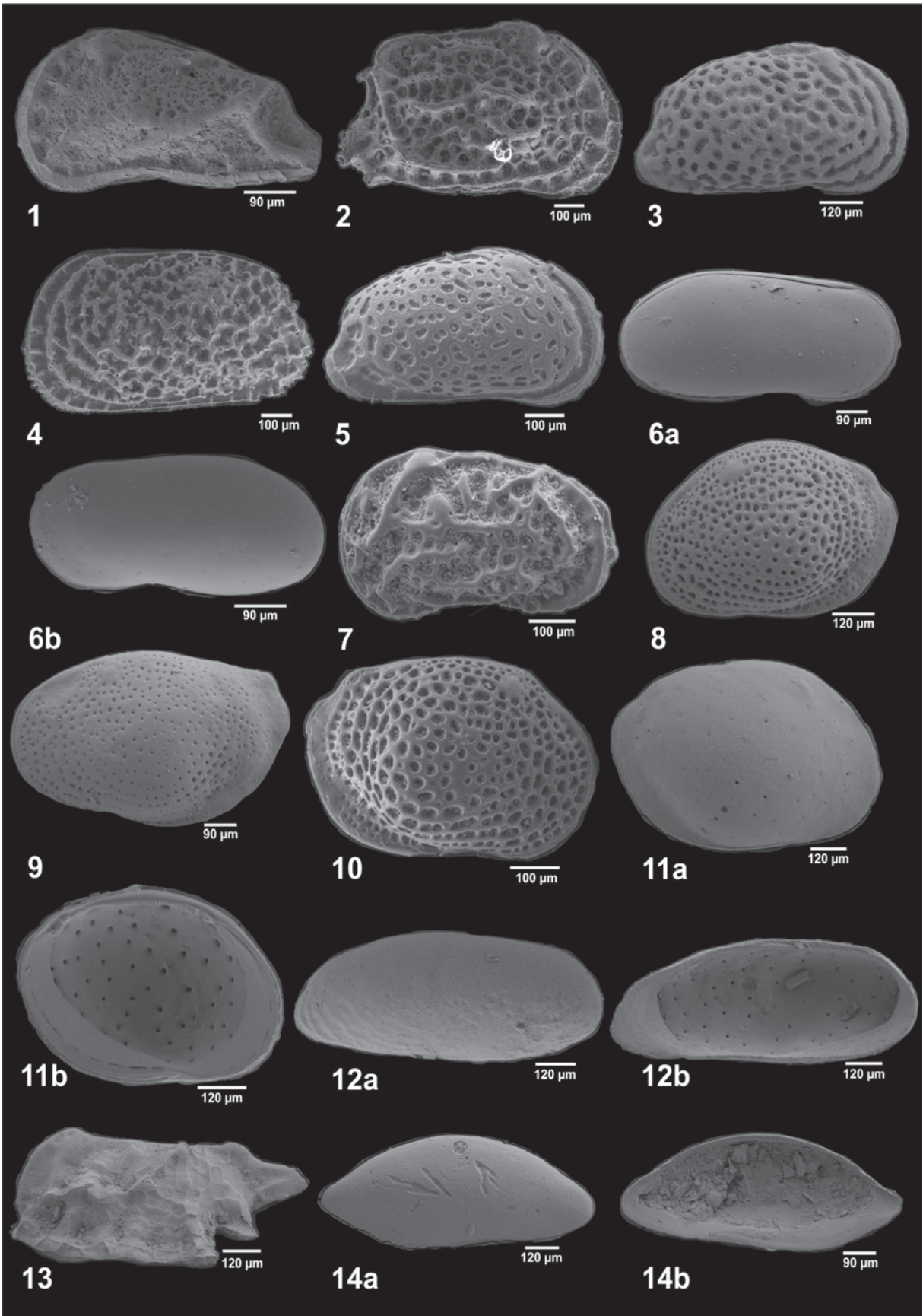
Figure 10. *Loxoconcha rhomboidea*, right valve side view  $\times 86$ , Kekova-Antalya, Station 74/23m.

Figure 11. *Loxoconcha stellifera*, a. right valve side view, b. Left valve internal view, core Ayvalık 2c 14-16 cm.

Figure 12. *Sahnia fasciata*, a. left valve side view, core Ayvalık 2c 14-16 cm; b. Left valve internal view, core Ayvalık 2c 24-26 cm.

Figure 13. *Paracytheridea depressa*, left valve side view, Kuşadası, Station 38.

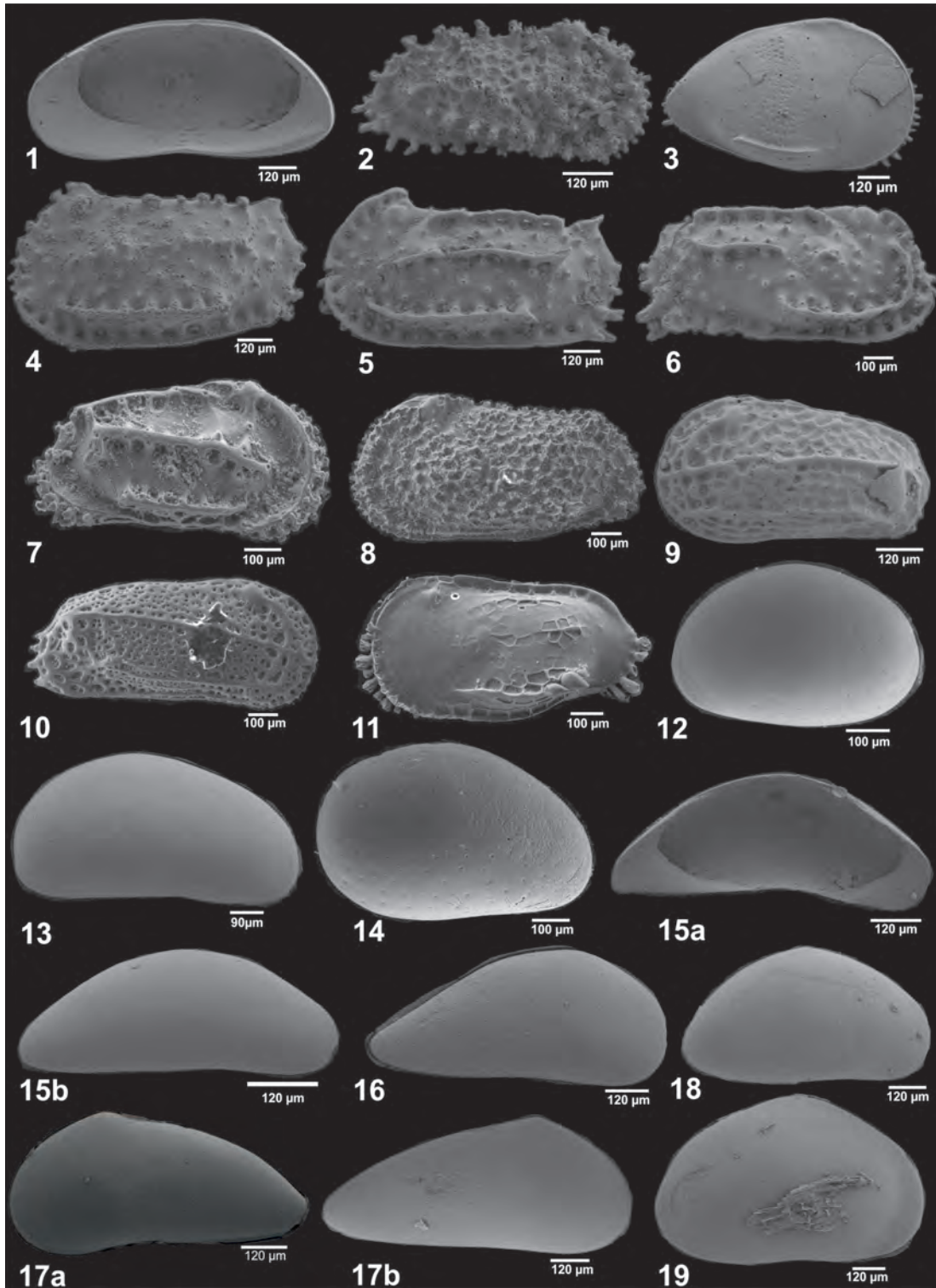
Figure 14. *Paradoxostoma acuminatum*, a. right valve side view, Kuşadası, Station 19; b. Right valve internal view, Kuşadası, Station 24.



**PLATE III**

- Figure 1. *Cytherois* sp., right valve internal view, Kuşadası, Station 20.
- Figure 2. *Acanthocythereis hystrix*, right valve external view, Kuşadası, Station, 30.
- Figure 3. *Bosquetina carinella*, right valve external view, Kuşadası, Station, 45.
- Figure 4. *Carinocythereis antiquata*, left valve external view, core Ayvalık 3a 34-36 cm.
- Figure 5. *Carinocythereis carinata*, left valve external view, core Ayvalık 2c 40-42 cm.
- Figure 6. *Carinocythereis rhombica*, right valve external view, core Ayvalık 2c 24, 26 cm
- Figure 7. *Costa batei*, right valve external view, ×61, Kekova-Antalya, Station 99/24 m.
- Figure 8. *Henryhowella* sp., left valve external view, ×53, Üçadalar-Antalya, Station 122/30 m.
- Figure 9. *Hiltermannicythere rubra*, left valve external view, Ayvalık 2c karotu 40-42 cm.
- Figure 10. *Hiltermannicythere turbida*, right valve external view, ×57, Kekova/Antalya, Station 102/24 m.
- Figure 11. *Pterygocythereis ceratoptera*, left valve external view, ×62, Kekova-Antalya, Station 99/12 m.
- Figure 12. *Xestoleberis communis*, left valve external view, ×83, Kaş-Antalya, Station 52/14 m.
- Figure 13. *Xestoleberis depressa*, right valve external view, Kuşadası, Station 24.
- Figure 14. *Xestoleberis dispar*, right valve external view, ×61, Kekova-Antalya, Station 94/24 m.
- Figure 15. *Macropyxis adriatica*, a. left valve internal view, Kuşadası, Station 19; b. Right valve external view Kuşadası, Station 6.
- Figure 16. *Pontocypris acuminata*, right valve external view, Kuşadası, Station 19.
- Figure 17. *Pontocypris mytiloides*, a. left valve external view, core Ayvalık 2c 2-4 cm;  
b. Right valve external view, core Ayvalık 2c 24-26
- Figure 18. *Ekpontocypris pirifera*, right valve external view, core Ayvalık 2c 40-42 cm.
- Figure 19. *Heterocypris salina*, right valve external view, core Ayvalık 2c 30-32 cm.

PLATE III







# BULLETIN OF THE MINERAL RESEARCH AND EXPLORATION

<http://bulletin.mta.gov.tr>

BULLETIN OF THE MINERAL RESEARCH AND EXPLORATION	
CONTENTS	
CRICETODONTINI FROM THE EARLY MIOCENE OF ANATOLIA	Nihal ÇINAR DURGUT* and Engin ÜNAY <sup>a</sup>
RESEARCH ARTICLE	
ABSTRACT	
KEYWORDS	
RECEIVED	
ACCEPTED	

## CRICETODONTINI FROM THE EARLY MIOCENE OF ANATOLIA

Nihal ÇINAR DURGUT<sup>a\*</sup> and Engin ÜNAY<sup>a</sup>

<sup>a</sup>Maden Tetkik ve Arama Genel Müdürlüğü Jeoloji Etütleri Dairesi, 06520 Ankara, Turkey.

Research Article

### Keywords:

Anatolia, Early Miocene,  
Rodentia, *Cricetodon*,  
*Deperetomys*, Taxonomy,  
Phylogeny

Received:06.03.2015

Accepted:04.05.2015

### ABSTRACT

*Cricetodon* and *Deperetomys* from the early Miocene localities Söke, Dededağ (Aydın), Kınık, Harta (Manisa) Western Anatolia and Yapıntı (İçel) Southern Anatolia are studied. Seven species, four of which are new, are described: *Cricetodon trallesensis* n. sp., *Cricetodon fikreti* n. sp., *Cricetodon magnesiensis* n. sp., *Cricetodon yapintiensis* n. sp., *Cricetodon versteegi*, *Cricetodon kasapligili* and *Cricetodon* cf. *kasapligili*, *Deperetomys* cf. *intermedius*. In order to establish phylogenetic relations of the *Cricetodon* species, a cladistic analysis are performed.

## 1. Introduction

The Miocene is a significant period of the mammals due to their greatest evolutionary stage. In the early Miocene, Anatolia plays an important role as a bridge for species dispersal between Asia, Europe and North Africa. In this paper, the *Cricetodontini* which is the first record from Anatolia in early Miocene is studied. The geographical range of the *Cricetodontini* is quite large, covering Eurasia from Kazakhstan to Portugal and North Africa and China. Its representatives remained in Anatolia during the early Miocene and they occurred in Europe during the latest early Miocene. The tribe was widely extended in Europe in the middle Miocene. Their decline starts in the late Miocene and their extinction is at the beginning of the Pliocene.

The early Miocene *Cricetodon* and *Deperetomys* collected from Söke, Dededağ (Aydın), Kınık, Harta (Manisa) and Yapıntı (İçel) (Figure 1) by Fikret Göktaş, Engin Ünay, Gerçek Saraç (General Directorate of Mineral Research and Exploration (MTA), Turkey) and Hans de Bruijn (Utrecht University, The Netherlands)

during the MTA geology projects carried out between the years of 1992-2001 are studied. Most of the rodent faunas from these localities have so far only been mentioned in preliminary lists in some internal reports of MTA (Ünay and Göktaş, 1999; 2000; Göktaş and Ünay, 2000) and in an international report (Ünay et al., 2001).

## 2. Material and Methods

The measurements of the teeth were taken with a Leica S8AP0 ocular micrometer (20 micron units). All values are given in 1 mm units. For easy comparison all the teeth are presented as if they were from the left side. If the original is from the right side the number on the plates has been underlined. The terminology of the parts of cheek teeth follows Mein and Freudenthal (1971, b) and Reig (1977) (Figure 2).

The photographs were taken with an environmental scanning electron microscope FEI Quanta 400 MK2 at MTA. The images processing was made using Adobe Photoshop software. All the material is stored in the collections of MTA.

\*Corresponding author: [nihalcinardurgut@gmail.com](mailto:nihalcinardurgut@gmail.com)  
<http://dx.doi.org/10.19111/bmre.35767>



Figure 1- Sketch map of Western and Southern Turkey showing the geographical position of the localities. For the geological setting of the localities the reader is referred to Ünay and Göktaş, 1999; 2000; Göktaş and Ünay, 2000; Ünay et al., 2001

### 3. Systematic Paleontology

**Order:** Rodentia Bowdich, 1821

**Family:** Muridae Illiger, 1811

**Tribe:** Cricetodontini Simpson, 1945

**Genus:** *Cricetodon* Lartet, 1851

**Type species:** *Cricetodon sansaniensis* Lartet, 1851

**Other species recognized:** *C. caucaticus* Argyropulo, 1938, *C. meini* Freudenthal, 1963, *C. albanensis* Mein and Freudenthal, 1971, *C. aureus* Mein and Freudenthal, 1971, *C. jotae* Mein and Freudenthal, 1971, *C. pasalarensis* (Tobien, 1978), *C. candirensis* (Tobien, 1978), *C. cariensis* (Şen and Ünay, 1979), *C. hungaricus* (Kordos, 1986), *C. aliveriensis* Klein Hofmeijer and de Bruijn, 1988, *C. versteegi* de Bruijn et al., 1993, *C. kasapligili* de Bruijn et al., 1993, *C. tobieni* de Bruijn et al., 1993, *C. bolligeri* Rummel, 1995, *C. jumanensis* Rummel, 2001, *C. engesseri* Rummel and Kálin, 2003, *C. orientalis* Bi, 2005, *C. soriae* Fernandez et al., 2006, *C. klariankae* Hir, 2007, *C. volkeri* Wu, 2009, “*C. fandli* Prieto et al., 2010, *C. wanhei* Qiu, 2010, *C. nievei* López-Guerrero et al., 2014

***Cricetodon trallesensis* n. sp.**

**(Plate 1)**

**Type locality:** Söke

**Age:** Early Miocene, MN4 (Ünay and Göktaş, 1999)

**Holotype:** M1 dext. Nr: SO, 102

**Derivatio nominis:** The species is named after Tralles, the ancient name of Aydın.

Material and measurements of the *Cricetodon trallesensis* n. sp.

	LENGTH		N	WIDTH	
	Min-Max	Mean		Min-Max	Mean
M1	2.43-3.00	2.70	52	1.65-2.05	1.89
M2	1.88-2.25	2.05	82	1.53-2.00	1.80
M3	1.33-1.85	1.54	56	1.45-1.70	1.56
m1	2.03-2.40	2.20	51	1.45-1.73	1.57
m2	1.90-2.35	2.12	73	1.60-1.93	1.74
m3	1.95-2.43	2.10	38	1.50-1.85	1.63

**Diagnosis:** The species *C. trallesensis* n. sp. is a medium sized *Cricetodon* with plump cusps. The rather small anterocone of the M1 is indistinctly divided into two cusps. The labial anterolophule is parallel to the longitudinal ridge. The protolophule and metalophule

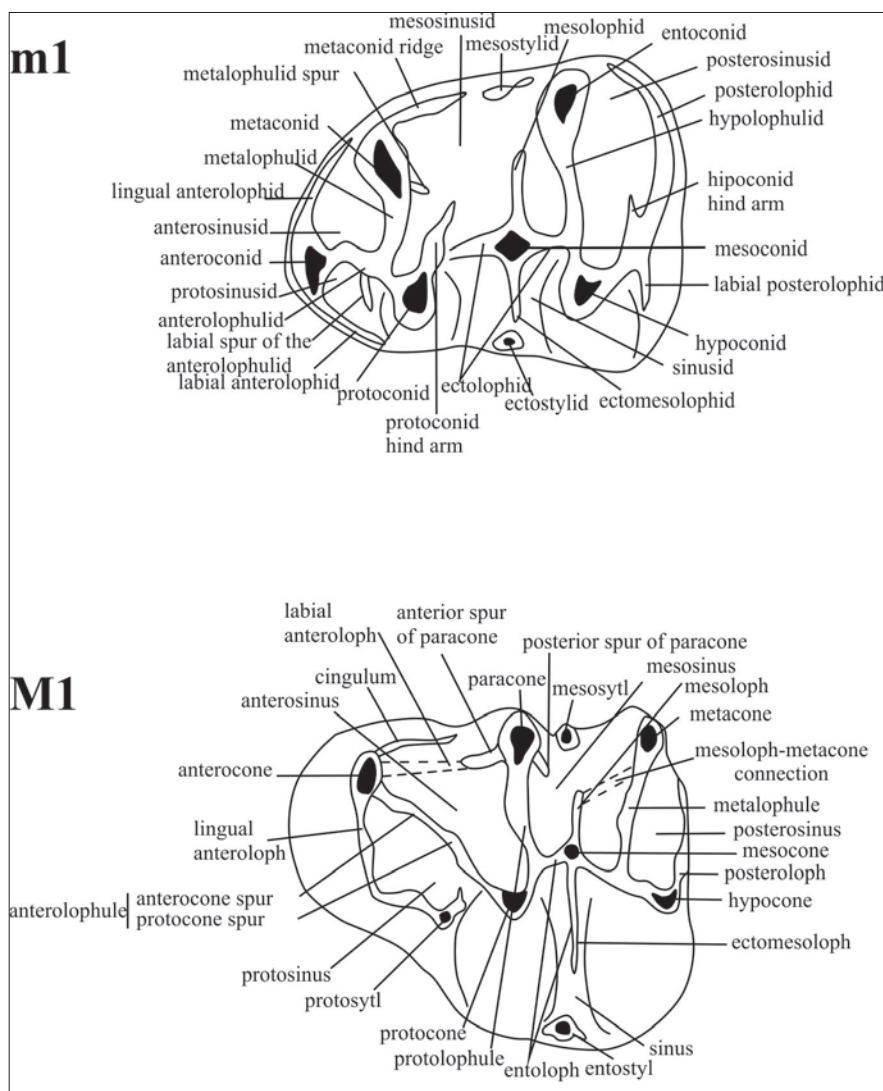


Figure 2- Terminology of the cheek teeth (Mein and Freudenthal (1971b) and Reig (1977))

of the M1 and M2 are parallel and directed posteriorly. The posteroloph does not continue beyond the point where it meets the metalophule. The m1 has one or two metalophulids. The shape of the M3 maybe rounded or elongated. The M1 and M2 have three or four roots.

**Differential Diagnosis:** Among the early Miocene cricetodons *C. trallesensis* n. sp. differs from *C. tobieni* from Horlak 1a in having comparatively higher crowned molars, plumber cusps, more elongated M3. Moreover the labial anterolophule in general is parallel to longitudinal ridge in *C. trallesensis* n. sp. whereas it is inclined to the labial edge in *C. tobieni*. *C. trallesensis* n. sp. differs from *C. kasapligili* in having more developed labial anterolophule and posterior

spur of the paracone in upper molars. The posteroloph connects to the metacone suggesting a more advanced stage of evolution than in *C. kasapligili*. The molars of *C. trallesensis* n. sp. are larger and rather higher crowned than in *C. aliveriensis* and *C. versteegi*.

**Description**

**M1:** The labial outline of the M1 is oblique, not parallel to the lingual border. The anterocone is situated mesio-labially in thirty-three of the fifty-nine specimens and mesially in the others. This tubercle is divided into two equal cusps by an anterior valley that does not extend to the base of the crown so it is single in worn specimens. The labial anterolophule is strong and reaches the base of the paracone in forty two out

of the fifty five specimens, it is short in nine and absent in four. The lingual anterolophule is absent. There is a transverse spur in the protosinus in twenty-four specimens. The protolophule is directed backwards and connected to the mure behind the protocone. There may be a crest (protolophule I?) on the anterolophule which may connect to the paracone in one specimen. The posterior spur of paracone shows a good deal of variation. It is long reaching to the metalophule in thirty three out of fifty six, short in twenty two and absent in two specimens. The mesoloph is short in fifty specimens and absent in five. The metalophule is directed posteriorly joining the posteroloph at the postero-medial corner of the metacone where the posteroloph also ends. The sinus is inclined anteriorly. The M1 has four roots in six, three in thirty four out of the forty specimens.

**M2:** The labial and lingual anterolophs are about equally well developed and connect to the paracone and protocone respectively. A weak protolophule I is present in two out of eighty tree specimens only. The protolophule II is transverse or posteriorly directed. The posterior spur of paracone is long reaching the metalophule in twenty three, long but free in forty two, short in sixteen and absent in the two other specimens. A short mesoloph is present in only eight specimens out of sixty eight. The posteriorly directed metalophule is almost parallel to the longitudinal axis. The posteroloph ends where it meets the metalophule. The sinus is transverse or directed anteriorly. The M2 has three roots in forty one and four in five specimens.

**M3:** The M3 shows a wide variation in outline ranging from the long to short morph types with intermediate. The labial and the lingual branches of the anteroloph are about equally well developed and connect to the paracone and protocone respectively. The protolophule is double in twenty five out of fifty five specimens. The posterior spur of paracone is short or absent. The homology of the mesoloph is not easy to detect in every specimen. It is long and posteriorly directed in the clearly elongated specimens whereas in the median valley of some shorter specimens there is a short labially free, anteriorly directed crest which may join to form a longer crest enclosing an island with protocone. The metalophule is directed posteriorly. The posteroloph reaches the base of the metacone. The sinus is directed anteriorly in elongated specimens and posteriorly in the rounded specimens. The M3 has three roots.

**m1:** The anteroconid is situated on the longitudinal axis of the occlusal surface. The labial anterolophid reaches the base of the protoconid. The lingual anterolophid is weak or absent. The metaconid and the entoconid have a posterior spur. The metalophulid is double in ten out of fifty two specimens. The metalophulid II is directed posteriorly connecting to the posterior part of the protoconid. The mesolophid is short or absent. The hypolophulid is transverse or directed anteriorly connecting to the longitudinal ridge in front of the hypoconid. Most specimens have an ectomesolophid. The hypoconulid is distinct. The wide sinusid is transverse. The m1 has two strong roots.

**m2:** The labial anterolophid is quite strong reaching the base of the protoconid. The lingual anterolophid connects to the base of the metaconid in five specimens, short in fourteen and absent in fifty. The metalophulid and hypolophulid are directed anteriorly. The short mesolophid is inclined posteriorly. The posterolophid reaches the base of the entoconid. The wide sinusid is transverse. The m2 has two strong roots.

**m3:** The labial anterolophid is rather strong reaching the base of the protoconid. The lingual anterolophid is short or absent. The metalophulid is directed anteriorly. The mesolophid is short in thirteen specimens and absent in twenty two specimens. The hypolophulid is transverse or directed anteriorly connecting to the longitudinal ridge in front of the hypoconid. The posterolophid reaches the base of the entoconid. The sinusid is transverse. The m3 has two strong roots.

**Remarks:** *Cricetodon trallesensis* n. sp. from Söke shows both plesiomorphic characters such as three rooted molars in M1 and M2 and long mesoloph in the M2 and M3 and apomorphic characters such as strongly divided anterocone, plump cusps, well developed labial anteroloph and posterior spur of paracone and the posteroloph-metalophule connection. In apomorphic characters *C. trallesensis* n. sp. is more evolved than *C. tobieni*, *C. kasapligili*, *C. versteegi* and *C. aliveriensis*.

***Cricetodon fikreti* n. sp.**

**(Plate 2)**

**Type locality:** Dededağ

**Age:** Early Miocene, MN4 (Ünay and Göktaş, 1999)

**Holotype:** M1 dext, Nr: DD, 1

**Derivatio nominis:** The species is named after the geologist Fikret Göktaş who collected most of the material from Dededağ.

Material and measurements of the *Cricetodon fikreti* n. sp.

	LENGTH		N	WIDTH	
	Min-Max	Mean		Min-Max	Mean
M1	2.58-2.79	2.69	2	1.95-2.05	2.00
M2	2.05-2.28	2.20	6	1.63-1.98	1.78
M3	1.55-1.80	1.68	3	1.55-1.63	1.58
m1	2.40-2.53	2.50	5	1.55-1.60	1.58
m2	2.15-2.30	2.22	7	1.83-1.93	1.86
m3	2.10-2.34	2.22	2	1.61-1.75	1.68

**Diagnosis:** The species *C. fikreti* n. sp. is a large and rather high crowned *Cricetodon*. The posteroloph of the M1 and M2 continue beyond the point where the metalophule joins the posteroloph. The posterior spur of the M2 is long reaching the metacone. The labial and lingual anterolophids of the m1 are well developed. The metalophulid is single or double. The M1 has three roots.

**Differential diagnosis:** *C. fikreti* n. sp. differs from *C. tobieni* in having plumper cusps, higher crowned cheek teeth and larger size. Additionally, the labial anteroloph is less developed in the M1, the spur of the paracone is longer, the mesoloph is shorter and the posteroloph has a more advance condition not continuing beyond the point where the metalophule meets in the M1 and M2. *C. fikreti* n. sp. is much larger in size than *C. kasapligili* and its M1 shows distinctly divided anterocone and the posterolophs of its M1 and M2 continue beyond the point where the metalophule joins the posteroloph. *C. fikreti* n. sp. differs from *C. versteegi* in having much larger and higher crowned cheek teeth. Furthermore the labial anteroloph and the posterior spur of the paracone are well developed, the metalophule is directed posteriorly, the anterocone is asymmetrical and metalophulid is double in the m1 in *C. fikreti* n. sp. *C. fikreti* n. sp. has also much larger and rather higher crowned molars than those of *C. aliveriensis*. Moreover in *C. aliveriensis* the spur of the paracone is weak or absent and the mesoloph is longer in the M1 and M2. *C. fikreti* n. sp. differs from *C. trallesensis* n. sp. from Söke in having much larger and higher crowned cheek teeth. Moreover, the labial

anteroloph of the M1 is longer and usually parallel to longitudinal ridge, the posterior spur of the paracone is longer and the mesoloph is shorter in *C. trallesensis* n. sp.

## Description

**M1:** The anterocone of the M1 has a mesio-labial position with the labial cusp slightly larger than the lingual one. The anterior valley is short, shallow and narrow so the anterocone is single in worn specimens. The labial and lingual anterolophs are absent. There is a transverse spur in the protosinus in three specimens. A weak protolophule I is present in one specimen out of three. The protolophule II directs posteriorly and connects to the longitudinal ridge behind the protocone. The posterior spur of the paracone and mesoloph are short. The short metalophule is strongly directed backwards being almost parallel to the longitudinal axis. The lingual sinus is transverse.

**M2:** The labial and lingual anterolophs are about equally well developed and connected to the paracone and the protocone respectively. The protolophule is directed posteriorly. The posterior spur of the paracone shows wide variation. It is long reaching the metacone in three out of ten M2, short in six and absent in one. The mesoloph is short or absent. The metalophule, as in the M1 is directed backwards being almost parallel to the longitudinal axis. The posteroloph reaches to the base of the metacone. The lingual sinus is directed anteriorly.

**M3:** The outline of the occlusal surface is elongated. The labial and lingual anterolophs are about equally well developed and connect to the paracone and the protocone respectively. The single protolophule is transverse. The posterior spur of the paracone is long or absent. The metalophule is directed posteriorly. The long posteriorly inclined mesoloph is almost parallel to the metalophule. The deep lingual sinus is directed anteriorly.

**m1:** The anteroconid is situated on the longitudinal axis of the occlusal surface. The labial anterolophid reaches the base of the protoconid. The lingual one is weak or absent. The metaconid and the entoconid have a posterior spur. The metalophulid is double in four out of five m1. The metalophulid I is directed anteriorly and connected to the anteroconid while the metalophulid II is directed posteriorly and connected to the longitudinal ridge behind the protoconid. The

mesolophid is short. The hypolophulid is inclined anteriorly and connected to the longitudinal ridge in front of the hypoconid. The posterolophid reaches to the base of the entoconid. Most specimens have an ectomesolophid. The hypoconulid is distinct. The wide sinusid is transverse. The m1 has two roots.

**m2:** The labial anterolophid is quite strong reaching the base of the protoconid. The lingual anterolophulid is absent. The short metalophulid and hypolophulid are directed anteriorly. The former joins the middle of the anterior edge of the tooth whereas the latter joins the longitudinal ridge behind the hypoconid. The short mesolophid is directed anteriorly. The posterolophid reaches the base of the entoconid. The hypoconulid is distinct in four out of the eight specimens. The wide sinusid is transverse or directed anteriorly. The m2 has two roots.

**m3:** The labial anterolophid is rather strong reaching the base of the protoconid, the lingual one is short. The metalophulid is directed anteriorly. The mesolophid is of medium length. The transverse hypolophulid reaches the longitudinal ridge in front of the hypoconid. The sinusid is transverse.

**Remarks:** *C. fikreti* n. sp. differs from all the Eastern Mediterranean *Cricetodon* species in having larger and higher crowned molars. Among the early Miocene *Cricetodon* species, *C. fikreti* n. sp. resembles *C. trallesensis* n. sp. morphologically most. The smaller and lower crowned molars, longer labial anteroloph of the M1 and shorter mesoloph of the M1 and M2 of *C. trallesensis* n. sp., however, suggests a more primitive stage of evolution for this species. The localities, Söke and Dededağ, where these two species come from, are in superposition. So we consider these two taxa as chrono-species belonging to the same lineage.

### *Cricetodon yapintiensis* n. sp.

(Plate 3)

**Type locality:** Yapıntı

**Age:** Early Miocene, MN3-4 (Ünay et al., 2001)

**Holotype:** M1 dext., Nr: YP, 121

**Derivatio nominis:** The species is named after its type locality.

Material and measurements of the *Cricetodon yapintiensis* n. sp.

	LENGTH			WIDTH	
	Min-Max	Mean	N	Min-Max	Mean
M1	2.18-2.33	2.26	4	1.50-1.63	1.55
M2	1.75-1.88	1.83	4	1.43-1.55	1.50
M3	1.63	1.63	1	1.35	1.35
m1	2.00-2.10	2.05	3	1.30-1.33	1.31

**Diagnosis:** *C. yapintiensis* n. sp. is a rather small *Cricetodon*. The anterocone of the M1 is divided into two cusps. The M1 has three roots. The mesoloph of the M1 and M2 is long. The posteroloph of the M1 and M2 continues beyond the point where the metalophule joins the posteroloph. The M3 is elongated. The m1 has a labially free weak metalophulid I.

**Differential diagnosis:** *Cricetodon yapintiensis* n. sp. is smaller than *C. tobieni* and *C. kasapligili*, but larger than *C. versteegi* and *C. aliveriensis*. *C. yapintiensis* n. sp. differ from any other early Miocene *Cricetodon* species in having rectangular M2. Furthermore, *C. yapintiensis* n. sp. differs from *C. tobieni* in having plumper cusps and less developed labial anteroloph in the M1 and elongated M3. *C. yapintiensis* n. sp. differs from *C. kasapligili* in having a more centrally placed and rather larger anterocone and a longer mesoloph. *C. yapintiensis* n. sp. differs from *Cricetodon versteegi* in having a more centrally situated anterocone, a shorter spur of paracone and an elongated M3. *C. yapintiensis* n. sp. differs from *C. aliveriensis* in having higher crowned cheek teeth, more centrally situated anterocone, stronger posterior spur of the paracone, shorter mesoloph in the M1 and M2 and three-rooted M1. *C. yapintiensis* n. sp. differs from *C. trallesensis* n. sp. and *C. fikreti* n. sp. In having smaller and rather lower crowned cheek teeth and less developed ectolophs.

### Description

**M1:** The anterocone is situated mesio-labially and divided into two cusps in three out of the four M1. Its position is central in the remaining one specimen. The anterior valley is short, shallow and narrow. The labial anteroloph reaches the base of the paracone. The lingual anteroloph is absent. There is a transverse crest in the protosinus. One specimen shows a lingually free incipient (protolophule I?). The protolophule is

directed posteriorly and connected to the longitudinal ridge. The posterior spur of the paracone is weak or absent. The mesoloph is of medium length. The metalophule is directed posteriorly and isolated from the posteroloph in one specimen. The posteroloph extends beyond the point where the metalophule reaches the posteroloph in three of the four M1. The lingual sinus is directed anteriorly. The M1 has three roots.

**M2:** M2 has a rectangular shape. The labial and lingual anterolophs are about equally well developed and connected to the paracone and the protocone respectively. The protolophule and the metalophule are directed posteriorly. The posterior spur of the paracone is either of medium length, short or absent. The mesoloph is long and directed posteriorly in one specimen but of medium length and transverse in the other three. The posteroloph reaches the base of the metacone. The lingual sinus is inclined anteriorly.

**M3:** The outline of the occlusal surface in the only available M3 is elongated. The labial and lingual anterolophs are about equally well developed and connected to the paracone and the protocone respectively. The single protolophule is directed anteriorly connecting the paracone to the protocone. The posterior spur of the paracone is long. The mesoloph is short. The lingual sinus is inclined anteriorly.

**m1:** The anteroconid is situated at the longitudinal axis of the occlusal surface in the only available m1. The labial anterolophid reaches the base of the protoconid. The lingual anterolophid is absent. The metalophulid I is weak, the metalophulid II is directed posteriorly and connected to the longitudinal ridge behind the protoconid. The metaconid and the entoconid have a posterior spur descending from their tips. The mesolophid is absent. The hypolophulid is anteriorly directed connecting to the longitudinal ridge just in front of the hypolophid. The posterolophid reaches the base of the entoconid. The transverse sinusid is with an ectomesolophid. The m1 has two roots.

**Remarks:** With its three-rooted M1, that has a weak posterior spur of the paracone, a long mesoloph and the posteroloph continuing beyond the point where the metalophule joins the posteroloph in the upper molars *C. yapintiensis* n. sp. is more primitive than the other early Miocene *Cricetodon* species except

*C. versteegi*. *C. yapintiensis* n. sp. is more evolved than *C. versteegi* in having a posteriorly directed protolophule and metalophule.

### *Cricetodon kasapligili* de Bruijn et al., 1993

#### (Plate 4)

**Locality:** Yapıntı

**Age:** Early Miocene, MN 3/4 (Ünay et al., 2001)

Other localities with *C. kasapligili*: Keseköy, Harta Material and measurements of the *Cricetodon kasapligili* from Yapıntı

	LENGTH		N	WIDTH	
	Min-Max	Mean		Min-Max	Mean
M1	2.50-2.63	2.55	10	1.60-1.90	1.76
M2	1.83-2.05	1.94	22	1.70-1.93	1.82
M3	1.55-1.88	1.72	18	1.45-1.93	1.63
m1	2.00-2.40	2.19	14	1.30-1.63	1.47
m2	1.88-2.10	1.98	17	1.53-1.80	1.66
m3	1.88-2.23	2.08	19	1.48-1.73	1.62

#### Description

**M1:** The anterocone is mesio-labially situated and has two cusps divided by a short, shallow and narrow anterior valley, the lingual one of these is often larger than the labial one. The labial anteroloph reaches the base of the paracone while the lingual one is absent. There is a transverse crest in the protosinus in four of the eleven M1. The anterolophule connects the protocone to the lingual part of the anterocone. The protolophule is directed posteriorly connecting to the longitudinal ridge behind the protocone. The posterior spur of the paracone is short in four specimens and absent in the remaining seven. The mesoloph is of medium length in eight specimens and short in four. The metalophule is directed posteriorly connecting to the posteroloph that extends beyond the point where the metalophule reaches the posteroloph. The lingual sinus is either transverse or directed anteriorly. The M1 has three roots.

**M2:** The labial and the lingual anterolophs are equally well developed and connected to the paracone and the protocone respectively. The protolophule and the metalophule are directed posteriorly. The posterior spur of the paracone is short in eighteen out of the twenty two specimens and absent in the others. The mesoloph is short and transverse in five, of medium

length in four and long and directed posteriorly in thirteen specimens. The posteroloph extends beyond the point where the metalophule reaches the posteroloph. The lingual sinus is directed anteriorly. The M2 has four roots.

**M3:** The outline of the occlusal surface of the M3 is elongated. The labial and the lingual anteroloph connecting to the paracone and the protocone respectively are about the same length, but the labial one is higher than the lingual one. The single protolophule is directed anteriorly. The posterior spur of the paracone is short in eight out of eighteen and absent in the other specimens. The mesoloph is short and directed posteriorly in five, transverse and long reaching the labial cingulum in seven other specimens. A short, longitudinal, anteriorly free loph originating from the lingual part of the mesoloph is present in six specimens. The metalophule is directed anteriorly and connected to the longitudinal ridge. The posteroloph reaches the base of the metacone. The lingual sinus is directed anteriorly. The M3 has three roots.

**m1:** The anteroconid is small and situated at the longitudinal axis of the occlusal surface. The labial anterolophid reaches the base of the protoconid while the lingual one is weak or absent. The metalophulid is double in nine out of fourteen specimens. The metalophulid I is directed anteriorly and connected to the anteroconid, the metalophulid II is directed posteriorly and connected to the longitudinal ridge behind the protoconid. The metaconid and the entoconid have a posterior spur. The mesolophid is usually of medium length. The hypolophulid is short and connected to the longitudinal ridge in front of the hypoconid. The hypoconulid is distinct. The sinusid is transverse. The m1 has two strong roots.

**m2:** The labial anterolophid is quite strong, reaching the base of the protoconid. The lingual anterolophid reaches the base of the metaconid in three, is short in four, and absent in ten specimens. The short metalophulid is directed anteriorly. The short mesolophid is transverse or directed posteriorly. The hypolophulid is inclined anteriorly and connected to the longitudinal ridge just in front of the hypoconid. An ectomesolophid is present in two out of seventeen specimens. The posterolophid which may bear a hypoconulid is strong reaching the base of the entoconid. The sinusid is transverse or directed anteriorly. The m2 has two roots.

**m3:** The labial anterolophid is strong, reaching the base of the protoconid. The lingual one is also strong, connecting to the base of the metaconid in thirteen, but is absent in the other five specimens. The short metalophulid is directed anteriorly. The mesolophid is of medium length. The hypolophulid is transverse and connected to the longitudinal ridge in front of the hypoconid. The posterolophid reaches the base of the entoconid. The sinusid is transverse. The m3 has two roots.

**Remarks:** The *Yapıntı Cricetodon* and *C. kasapligili* from Keseköy have many common characters: size, height of crown, inflated cusps, indistinctly divided anterocone, weak posterior spur and posteroloph which continue beyond the point where the metalophule joins the posteroloph in the M1 and M2. And there are no major character differences that contradict our assignment of this material to *C. kasapligili*.

#### *Cricetodon cf. kasapligili* de Bruijn et al. 1993

#### (Plate 5)

**Locality:** Harta

**Age:** Early Miocene, MN3 (Göktaş and Ünay, 2000)

**Other localities with *C. kasapligili*:** Keseköy, Yapıntı

Material and measurements of the *Cricetodon cf. kasapligili* from Harta

	LENGTH		N	WIDTH	
	Min-Max	Mean		Min-Max	Mean
M1	2.40-2.45	2.43	2	1.70-1.75	1.73
M2	2.10	2.10	1	1.80	1.80
M3	1.75	1.75	1	1.60	1.60
m1	2.33	2.33	1	1.50	1.50
m2	2.05-2.23	2.14	2	1.75-1.88	1.82
m3	2.15-2.33	2.24	2	1.70-1.73	1.72

#### Description

**M1:** The mesio-labially or centrally situated rather narrow anterocone is divided into two cusps. The valley separating these cusps is short, shallow and narrow. The anterolophule connects the protocone to the lingual part of the anterocone. The long labial anteroloph connects to the base of the paracone in one specimen, but it absent in the other. The lingual

anteroloph is absent. There is a transverse crest in the protosinus. The short protolophule is directed posteriorly connecting to the longitudinal ridge behind the protocone. The mesoloph is short. The metalophule is directed posteriorly. The posteroloph extends beyond the point where the metalophule reaches the posteroloph. The lingual sinus is directed anteriorly. The M1 has three roots.

**M2:** The labial and the lingual anterolophs are well developed and connected to the paracone and the protocone respectively. The protolophule is directed posteriorly and connected to the longitudinal ridge behind the protocone. The posterior spur of the paracone and mesoloph are short. The metalophule has a twist in the middle and is connected to the hypocone. The posteroloph reaches the base of the metacone. The sinus is directed anteriorly.

**M3:** The posterior part of the M3 is not much reduced. The labial and the lingual anterolophs are about equally well developed and connected to the paracone and the protocone respectively. The single, short protolophule is directed anteriorly connecting to the protocone. The posterior spur of the paracone is short. The long mesoloph is inclined posteriorly. The sinus is directed anteriorly.

**m1:** The posterior part of the only available m1 is worn. The anteroconid is situated on the longitudinal axis of the occlusal surface. The labial anterolophid reaches the base of the protoconid while the lingual one is absent. The metalophulid I is directed anteriorly and connected to the anteroconid whereas the metalophulid II is directed posteriorly connecting to the longitudinal ridge behind the protoconid. The sinusid is inclined anteriorly. The m1 has two roots.

**m2:** The labial anterolophid is rather strong reaching the base of the protoconid. The lingual anterolophid is absent. The short mesolophid is directed anteriorly. The short hypolophulid is transverse connecting to the longitudinal ridge just in front of the hypoconid. The strong posterolophid reaches the entoconid. The hypoconulid is distinct. The sinusid is transverse. The m2 has two roots.

**m3:** The labial and the lingual anterolophids are rather strong, reaching the base of the protoconid and the metaconid respectively. The short metalophulid is directed anteriorly. The mesolophid is short or absent. The strong posterolophid connects to the base of the entoconid. The sinusid is transverse.

**Remarks:** The *Cricetodon* from Harta and *C. kasapligili* from Keseköy have many characters in common: size, crown height, inflated cusps, indistinctly divided and narrow anterocone, weak posterior spur of paracone, short mesoloph and the posteroloph continuing beyond the point where the metalophule joins the posteroloph in the M1 and M2. Unfortunately, the Harta material as well as the type material are rather poor. The only available m1 from Harta is worn and M3 is not represented in the type material preventing further comparison. Hence, the Harta material is identified as *C. cf. kasapligili*.

***Cricetodon magnesiensis* n. sp.**

**(Plate 6)**

**Type Locality:** Kınık

**Age:** Early Miocene, MN3 (Ünay and Göktaş, 2000)

**Holotype:** M1 sin, Nr: KN, 101

**Derivatio nominis:** The species is named after Magnesia which was the ancient name of Manisa city.

Material and measurements of the *Cricetodon magnesiensis* n. sp.

	LENGTH		WIDTH		
	Min-Max	Mean	N	Min-Max	Mean
M1	2.33	2.33	1	1.58	1.58
M2	1.98-2.00	1.99	2	1.73-1.80	1.77
M3	1.73-1.80	1.77	2	1.63-1.75	1.69
m2	2.10-2.13	2.12	2	1.55-1.80	1.74
m3	1.90-2.15	2.06	3	1.60-1.63	1.59

**Diagnosis:** *Cricetodon magnesiensis* n. sp. is a medium-sized and high crowned *Cricetodon*. The rather wide anterocone is divided into two unequal cusps. The posterior spur of the paracones of the M1 and M2 are long. The M3 is elongated. The M2 has three roots.

**Differential Diagnosis:** *Cricetodon magnesiensis* n. sp. differs from all the Eastern Mediterranean *Cricetodon* species in having rather higher crowned cheek teeth and unequal cusps of the anterocone. *C. magnesiensis* n. sp. differs from *C. tobieni* in having plumper cusps, longer posterior spur of the paracone, double protolophule in the M1, three-rooted M2 and elongated M3. *C. magnesiensis* n. sp. differs from *C. kasapligili* in having more labially placed and distinctly divided anterocone and strong posterior spur

of the paracone of the M1. *C. magnesiensis* n. sp. have much larger and higher crowned cheek teeth than *C. versteegi*, *C. aliveriensis* and *C. yapintiensis* n. sp. *C. magnesiensis* n. sp. differs from *C. trallesensis* n. sp. in having unequally developed cusps of the anterocone and weaker posterior inclination of the mesoloph of the M1 and better developed posterior spur of the paracone in the M2. *C. magnesiensis* n. sp. differs from *C. fikreti* n. sp. in having labial anterolophule in the M1, less developed posterior spur of the paracone and mesoloph in the M2.

### Description

**M1:** The anterocone is divided into two cusps in the only available M1, the labial one being larger than the lingual cusp. The anterior valley is long, deep and wide. The labial anterolophule reaches the base of the paracone while the lingual anteroloph is absent. The protolophule is directed posteriorly and connected to the longitudinal ridge. The protolophule II (?) is short. The burgee-shaped posterior spur of the paracone reaches the base of the metacone. The mesoloph is short. The weak posteroloph connects to the metacone. The wide and deep lingual sinus is transverse.

**M2:** The labial and lingual anterolophs connect to the paracone and the protocone respectively. The protolophule is directed posteriorly. The posterior spur of the paracone is short. The mesoloph is absent. The short metalophule is almost parallel to the longitudinal ridge. The weak posteroloph reaches the metacone. The lingual sinus is directed anteriorly.

**M3:** The posterior part of the M3 is reduced. The labial and lingual anterolophs are connected to the paracone and the protocone respectively. The single protolophule and the metalophule are directed anteriorly. The short mesoloph is inclined anteriorly in one specimen and posteriorly in the other. The posteroloph reaches the base of the metacone. The lingual sinus is directed posteriorly.

**m2:** The m2 is worn, so the morphological characteristics cannot be observed.

**m3:** The labial anterolophid is rather strong reaching the base of the protoconid while the lingual one is short. The single metalophulid is directed anteriorly. The mesolophid is absent. The hypolophulid is transverse in one specimen, directed anteriorly in the other two connecting to the longitudinal ridge in front

of the hypoconid. The strong posterolophid reaches the base of the entoconid. The sinusid is transverse or directed posteriorly.

**Remarks:** *Cricetodon magnesiensis* n. sp. shows plesiomorphic features such as the elongated M3 and the posteroloph-metacone connection in upper molars as well as apomorphic characters such as strongly divided anterocone, plump cusps, well developed posterior spur of the paracone and short mesoloph in the M1. In the apomorphic characters *C. magnesiensis* n. sp. is more evolved than *C. tobieni*, *C. kasapligili*, *C. versteegi* and *C. aliveriensis*.

### *Cricetodon versteegi* de Bruijn et al. 1993

#### (Plate 7)

**Locality:** Kınık

**Age:** Early Miocene, MN3 (Ünay and Göktaş, 2000)

**Other localities with *C. versteegi*:** Kılçak 0", Kılçak 3a

Material and measurements of the *Cricetodon versteegi* from Kınık

	LENGTH		N	WIDTH	
	Min-Max	Mean		Min-Max	Mean
M1	1.98-2.23	2.12	3	1.48-1.58	1.53
M2	1.53-1.68	1.62	13	1.40-1.65	1.53
M3	1.20-1.40	1.31	11	1.25-1.43	1.35
m1	1.83-2.03	1.92	9	1.20-1.35	1.27
m2	1.65-1.85	1.75	8	1.35-1.48	1.43
m3	1.55-1.75	1.67	9	1.30-1.43	1.35

### Description

**M1:** The rather wide anterocone of the M1 has a labial position and is divided into two equal cusps. The valley between these cusps is long, deep and wide. The labial anteroloph reaches the base of the paracone while the lingual one is absent. A weak protolophule I is present in all the three specimens. The protolophule is directed posteriorly and connected to the longitudinal ridge behind the protocone. The posterior spur of the paracone is long reaching the metacone. The mesoloph is short. The metalophule is directed posteriorly. The posteroloph extends beyond the point where the metalophule reaches the posteroloph. The wide and deep lingual sinus is transverse or directed posteriorly. The M1 has three roots.

**M2:** The labial and lingual anterolophs are long connecting to the paracone and the protocone respectively. The protolophule I is present, but protolophule II is absent in four out of twelve specimens, the protolophule II is present and while the protolophule I is absent in three specimens and the both protolophules are absent in the other specimens. The posterior spur of the paracone is short. The mesoloph is short in two specimens, absent in the others. The posteroloph reaches to the base of the metacone. The lingual sinus is transverse or directed posteriorly. The M2 has three roots.

**M3:** The outline of the occlusal surface of the M3 is rounded. Both the labial and the lingual anterolophs are about equally long reaching the base of the paracone and the protocone respectively. The single protolophule is directed anteriorly. The mesoloph shows considerable variation in length: It is being long in one out of nine M1, short in four and absent in the other four. The metalophule is directed anteriorly. The posteroloph reaches the base of the metacone. The lingual sinus is directed anteriorly.

**m1:** The anteroconid is situated labially. The labial anterolophid reaches the base of the protoconid. The lingual one is absent. The metalophulid I is directed anteriorly and connected to the anteroconid while the metalophulid II is directed posteriorly and connected to the protoconid. The mesolophid is absent. The wide hypolophulid is anteriorly directed, connecting to the longitudinal ridge in front of the hypoconid. The posterolophid reaches the base of the entoconid. The sinusid is inclined anteriorly. The m1 has two roots.

**m2:** The labial anterolophid is rather strong reaching the base of the protoconid while the lingual one is weak. The short metalophulid is directed anteriorly. The mesolophid is short. The hypolophulid is directed anteriorly and connected to the longitudinal ridge in front of the hypoconid. The posterolophid which may bear a hypoconulid is strong reaching the base of the entoconid. The sinusid is directed anteriorly. The m2 has two roots.

**m3:** The strong labial anterolophid is connected to the base of the protoconid while the lingual one is absent. The anteriorly directed metalophulid is short. Mesolophid is also short and inclined posteriorly. The hypolophulid is transverse or directed anteriorly connecting to the longitudinal ridge in front of the hypoconid. The strong posterolophid reaches the base

of the entoconid. The sinusid is transverse or directed anteriorly. The m3 has two roots.

**Remarks:** Although, the *Cricetodon* material from Kınık is somewhat larger than *C. versteegi* from the type locality Kılçak 3a, it shares many characters with the type association: three-rooted M1 and M2, wide, centrally placed, clearly bi-cuspid anterocone, well developed labial anterolophule, spur of the paracone and protolophule I in the M1, anteriorly directed metalophule in the M2, rounded M3 with single protolophule and assymmetric anteroconid complex and double metalophulid in the m1. Therefore the second *Cricetodon* assemblages from Kınık have been included in the species *Cricetodon versteegi*.

### ***Deperetomys* Mein and Freudenthal, 1971**

#### ***Deperetomys* cf. *intermedius***

#### **(Plate 8)**

**Locality:** Kınık

**Age:** Early Miocene, MN3 (Ünay and Göktaş, 2000)

**Other localities with *D. intermedius*:** Harami 1, Harami 3

#### **Material and measurements of the *Deperetomys* cf. *intermedius* from the Kınık**

One M1 (2.98x2.15), two M2 (2.13x2.30-2.03x2.05)

#### **Description**

**M1:** The rather wide anterocone of the M1 has a mesio-labial position and two completely separated cusps. The posterior spur of the labial cusp of the anterocone is burgee-shaped and tends to close the antero-labial sinus. The posterior spur of the lingual cusp of the anterocone reaches the base of the protocone. The weak protolophule I and the protolophule II connect the paracone to the protocone anteriorly and posteriorly. The burgee-shaped posterior spur of the paracone reaches the labial edge. The mesoloph is long. The burgee-shaped anterior spur of the metacone reaches the mesoloph. The strong posteriorly directed metalophule is connected to the posteroloph. There is low endomesoloph in the transverse lingual sinus. The M1 has four roots.

**M2:** The labial and the lingual anterolophs are strong; lingual one being lower than the labial one.

They connect to the paracone and the protocone respectively. The protolophule is connected to the postero-labial part of the protocone. The long and burgee-shaped posterior spur of the paracone reaches the labial edge. The mesoloph is long and connected to the anterior spur of the metacone. The metalophule is directed posteriorly meeting the posteroloph. The endomesoloph is indistinct. The lingual sinus is transverse. The M2 has four roots.

**Remarks:** The Kınık *Deperetomys* and *D. intermedius* from Harami 1 have many characters in common: size, crown height, completely separated anterocone, well developed posterior spur of the labial cusp and weak protolophule I in the M1, long mesoloph in the M1 and M2. Unfortunately, the Kınık material is poor, only one M1 and two M2 are available. Hence the Kınık material is identified as *D. cf. intermedius*. The stratigraphical range of the genus *Deperetomys* is from MN 1 to 7/8 with a long gap between MN2-MN7/8. The Kınık finding fills the MN3 part of this gap.

#### 4. Paleogeography and Paleocology

According to de Bruijn and Ünay (1996) Cricetodontini members appeared as immigrants into Asia Minor around the Oligo-Miocene boundary, because there are no potential ancestors known from the area from older levels than MN1. Biogeographical distribution of Cricetodontini follows a symmetrical model, in which the first occurrence of the tribe is in a small area during the early Miocene (Alvarez-Sierra et al., 2013). The diversity of the tribe starting in MN4 was accompanied by migration westward, first into southeastern Europe and later (MN5) into southwestern Europe. During the MN 6, the genus reached its maximum geographic range. Since the late middle Miocene, the distribution area of the representatives of the tribe starts to show fragmentation and contraction that precede the extinction at the end of the Pliocene (Alvarez-Sierra et al., 2013). The new discoveries of Chinese *Cricetodon* species suggests that the diversification of the *Cricetodon* was accompanied not only by migration westward, but also migration eastward into Central Asia and China (Bi, 2005).

The diversity and geographical expansion of the tribe (MN4) coincides with the drop in diversity of the insectivore faunas in Anatolia. This suggestion has been interpreted as indicating that the climate become drier and the Cricetodontini preferred drier biotopes (de Bruijn and Ünay, 1996).

The genus *Deperetomys* occurs in Anatolia and in central and south western Europe. The oldest record of genus is from Anatolia where it appears in MN1-2-3. The first appearance of *Deperetomys* in Central and South Western Europe however is in MN 6-8. This indicates a westward migration of the genus. The stability of the dental structure of *Deperetomys* over a long period—as in having forwards directed lophs in the lower molars, backwards directed lophs in upper molars and four roots in M1 and M2—suggests that the species of *Deperetomys* occupied a very special ecological niche. The combination of gracile cheek teeth and very strong roots make it unlikely herbivores (de Bruijn et al., 1993).

The distribution of the various species of Cricetodontini in time of the different localities is shown in figure 3. (modified from de Bruijn et al., 1993).

#### 5. Phylogeny of the Genus *Cricetodon*

The phylogenetic analysis of the tribe Cricetodontini and the genus *Cricetodon* have been largely discussed in some previous studies (Bi, 2005; Sen and Erbajeva, 2011; Maridet and Sen, 2012; Lopez Guerro, 2014; Prieto et al., 2014). Bi's (2005) phylogenetic analysis forms a basis for our attempt of phylogenetic analysis of *Cricetodon* in this study. *Euricetodon collatus* considered as a primitive cricetid (Bi, 2005) which has been selected as out-group. Out of the known twenty eight *Cricetodon* species twenty five were selected for this analysis (see Table 1). Since the species *Cricetodon jumanensis* (Rummel, 2001) is represented by two teeth and *Cricetodon volkeri* (Wu, 2009) is represented with three teeth only, these species have not been included. “*Cricetodon*” *fandli* (Prieto et al., 2010) has been excluded because its allocation to *Cricetodon* is uncertain. The species *C. bolligeri*, *C. klariankae*, *C. soriae*, *C. engesseri*, *C. nievei* and *C. wanhei* which were not included in Bi's (2005) analysis were added in this study.

The software of phylogenetic reconstruction used was PAST 2.08 (Hammer et al., 2001). A total of thirty phylogenetically informative characters of the upper and lower molars and their characteristic states have been adopted from Bi (2005). Eighteen characters are binary whereas twenty are multistate. Characters are listed in Table 1. Missing data or not represented character states in some species are coded with a question mark (?).

Thirty phylogenetically informative characters and their character states are shown in Appendix 1.

MN Zones	Anatolia	SE Europe	Central Europe	SW Europe	China
15				<i>R. europeus</i> <sup>+</sup>	
14	-			<i>R. europeus</i>	
13	<i>B. uenayae</i>	<i>R. hellenicus</i>		<i>R. lasallei</i>	
12	<i>B. uenayae</i> <i>B. dardanellensis</i> <i>B. pikermiensis</i> <i>Byzantinia</i> sp.	<i>B. pikermiensis</i> <sup>+</sup> <i>B. hellenicus</i>	?	<i>R. schaubi</i>	
11	?	?	?	<i>R. freudenthali</i>	
10	<i>B. uenayae</i> <i>B. dardanellensis</i> <i>B. nikosi</i> <i>B. pikermiensis</i>	→ <i>B. nikosi</i>	?	<i>H. mediterraneus</i> <i>H. peralensis</i>	
9	<i>B. dardanellensis</i> <i>B. cf. nikosi</i> <i>B. debruijini</i> <i>B. bayraktépensis</i> <i>B. menderesensis</i>	?	<i>C. bolligeri</i>	<i>H. aragoniensis</i> <i>H. nombrevillae</i> <i>H. thaleri</i> <i>H. lavocati</i>	
8 7	<i>B. ozansoyi</i> <i>B. bayraktépensis</i> <i>B. eskihisarensis</i> <i>C. cariensis</i>	<i>Cricetodon/Byzantinia</i> transitional population	<i>D. hagni</i> <i>C. klariankae</i> <i>C. cf. sansaniensis</i> <i>C. fandli</i> <i>C. engesseeri</i> <i>C. jumanensis</i>	<i>H. lavocati</i> <i>H. aguirrei</i> <i>H. dispectus</i> <i>H. decedens</i> <i>H. daamsi</i> <i>H. bijugatus</i> <i>C. nievei</i> <i>C. albanensis</i>	
6	<i>C. caucaticus</i> <i>C. candirensis</i> <i>C. pasalarensis</i>	<i>Cricetodon</i> sp.	<i>C. jumanensis</i> <i>C. hungaricus</i> <i>C. aff. meini</i>	<i>C. jotae</i> <i>C. sansaniensis</i>	<i>C. orientalis</i> <i>C. volkeri</i>
5	<i>Cricetodon</i> sp.			<i>Cricetodon</i> sp.3 <i>C. soridae</i> <i>C. aureus</i>	
		<i>C. meini</i> ←		→ <i>C. meini</i>	
4	<i>C. trallesiensis</i> <i>C. fikreti</i> <i>Cricetodon</i> sp.2 <i>C. tobieni</i>				<i>C. wanhei</i>
3	<i>C. yapintiensis</i> <i>C. kasapligili</i> <i>C. magnesiensis</i> <i>D. cf. intermedius</i>	→ <i>C. aliveriensis</i>			
2	<i>D. intermedius</i>				
1	<i>D. anatolicus</i> <i>Cricetodon</i> sp.1 <i>C. aff. versteegi</i> <i>C. versteegi</i> <i>Cricetodon</i> sp.				

Figure 3- The distribution of the various species of *Cricetodontini* in time of the different localities (modified from de Bruijn et al., 1993)

### 5.1. Results

According to the outcome shown in figure 4 *Cricetodon versteegi* is the most primitive lineage and the early Miocene species of the Eastern Mediterranean area are more primitive and more closely related to each other than to the *Cricetodon* species from in the other regions.

Within the early Miocene *Cricetodon* species from Anatolia *C. yapintiensis* n. sp., *C. trallesiensis* n. sp. and *C. magnesiensis* n. sp. constitute a clade and *C. fikreti* n. sp. appears as a sister group of this clade.

*C. orientalis* is located between the Anatolian *Cricetodon* species and European species. *C. meini* and *C. aureus* are more primitive species and they

Cricetodontini From the Early Miocene of Anatolia

Table 1- Matrix of character coding used in the analysts of relationships of species of *Cricetodon*. Question mark indicate missing data, A indicate polymorphisms; A= 0/1.

Species/Characters	1	2	3	4	5	6	7	8	9	10	11	12	13	14	15	16	17	18	19	20	21	22	23	24	25	26	27	28	29	30	
<i>E. collatus</i>	0	0	0	0	0	?	0	0	0	0	0	0	0	0	?	0	0	0	0	0	0	0	0	0	0	0	0	0	0	0	
<i>C. versteegi</i>	2	1	0	A	1	?	A	1	0	0	0	1	0	0	?	1	0	1	0	1	1	0	2	0	0	1	0	0	0	0	
<i>C. kasapligili</i>	A	1	0	A	0	?	1	1	0	1	1	1	0	0	?	1	1	?	?	?	0	0	2	0	?	?	?	0	0	1	
<i>C. tobieni</i>	2	0	0	A	1	?	1	1	0	1	1	1	0	1	?	1	1	1	0	1	A	0	1	0	0	1	0	0	0	1	
<i>C. yapintiensis</i>	2	1	2	1	0	?	1	1	0	1	1	1	1	1	?	1	?	0	1	?	0	0	2	0	?	?	?	?	?	?	
<i>C. aliverienseis</i>	2	0	0	0	0	?	1	2	1	1	1	1	0	1	?	2	1	0	0	1	1	0	1	0	0	1	0	0	0	1	
<i>C. trallesenis</i>	2	1	2	A	2	A	1	2	0	1	1	2	A	1	?	2	0	A	1	0	A	0	2	0	0	1	0	0	1	1	
<i>C. fikreti</i>	2	1	0	A	1	?	1	2	?	1	1	1	1	1	?	2	?	0	0	1	1	0	2	0	1	1	0	0	1	1	
<i>C. magnesienseis</i>	2	1	2	1	2	1	1	1	?	1	1	2	1	1	?	2	?	0	1	0	?	?	?	?	?	?	?	?	0	1	2
<i>C. orientalis</i>	1	1	0	1	1	?	2	2	1	1	1	1	0	1	?	2	1	1	0	1	1	0	2	0	0	1	0	0	0	0	
<i>C. meini</i>	A	1	0	1	0	?	2	2	1	1	1	2	0	0	?	2	1	1	0	1	A	0	2	0	0	1	0	1	0	1	
<i>C. aureus</i>	A	1	0	1	0	?	2	2	1	1	1	2	0	0	?	2	1	1	0	1	0	0	2	0	0	1	0	1	0	1	
<i>C. sansanienseis</i>	2	1	0	1	0	?	2	2	1	1	1	2	0	1	?	2	1	1	0	1	A	0	2	0	0	1	0	1	0	1	
<i>C. jotae</i>	2	1	0	1	0	?	2	2	1	1	1	2	0	1	?	2	1	1	0	1	1	1	2	0	0	1	0	1	0	1	
<i>C. albanenseis</i>	2	1	1	1	0	?	1	2	1	1	1	2	0	1	?	2	1	1	1	1	1	1	2	0	0	1	0	1	1	1	
<i>C. pasalarensis</i>	2	1	1	1	2	0	2	2	1	1	1	2	0	2	0	2	1	1	0	1	A	0	2	1	1	1	1	0	0	1	
<i>C. caucaticus</i>	2	1	1	1	2	0	2	2	1	1	1	1	2	0	?	2	1	1	0	0	0	0	2	1	1	2	2	0	0	1	
<i>C. hungaricus</i>	2	1	1	1	2	1	1	2	1	1	1	1	1	2	1	2	1	0	0	0	1	0	1	1	1	1	1	0	0	1	
<i>C. candirensis</i>	2	1	2	1	2	1	1	2	1	1	1	1	1	2	1	2	1	0	0	0	0	0	2	1	1	1	0	1	1	1	
<i>C. carienseis</i>	2	0	1	1	2	1	1	2	1	1	1	1	1	2	1	2	0	0	0	0	0	0	2	1	1	1	1	0	1	1	
<i>C. klariankae</i>	2	1	1	0	2	0	2	2	1	1	1	2	1	2	0	2	1	0	1	0	0	0	2	1	1	2	1	1	1	2	
<i>C. bolligeri</i>	1	1	1	0	1	?	2	2	1	1	1	2	1	1	?	2	1	1	2	1	0	0	2	1	1	2	1	1	1	2	
<i>C. soriae</i>	2	1	0	1	1	?	2	1	1	1	1	2	0	1	?	2	1	0	A	0	1	1	2	0	1	1	0	0	1	1	
<i>C. nievei</i>	2	1	1	0	1	?	2	1	1	2	1	2	A	1	?	2	?	1	2	1	1	1	2	0	1	2	0	0	1	2	
<i>C. engesseri</i>	1	1	2	0	1	?	2	1	?	1	1	2	0	1	0	2	?	0	0	1	1	1	1	0	1	1	0	?	?	0	
<i>C. wanhei</i>	A	1	1	0	1	?	2	1	1	0	1	2	0	1	?	1	1	0	2	1	1	1	2	0	1	2	0	0	0	1	

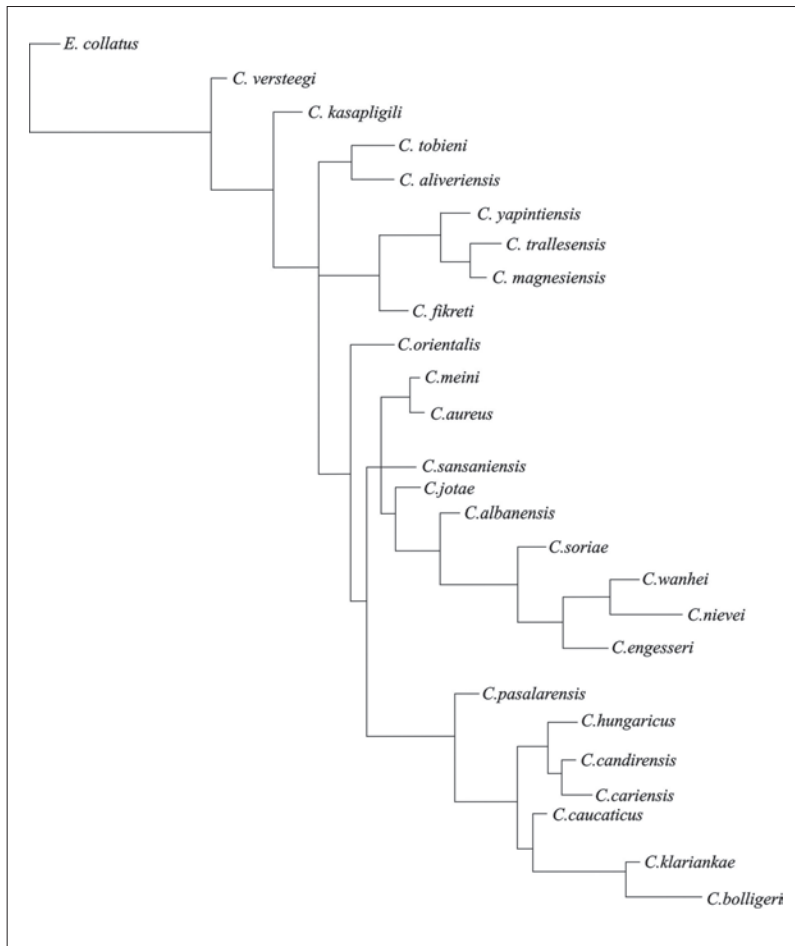


Figure 4- Cladogram illustrating the relationships among the species of the *Cricetodon*. Tree statistics: Length= 120, Consistency Index=0,359, Retention Index = 0,72

are known as being earlier cricetodonts of Europe. As is seen in this analysis, *C. sansaniensis* is usually considered as derived from *C. aureus* and compared to the Anatolian species, these species are an independent lineage.

The other clade is mainly included advanced Anatolian and European species. *C. pasalarensis* is the basal position of this group. This analysis is shown that *C. hungaricus*, *C. klariankae* and *C. bolligeri* migrated from Anatolia.

This analysis also supports that the *Cricetodon* species do not form a monophyletic group.

### Acknowledgments

We thank to the Fikret Göktaş, Gerçek Saraç and Eşref Atabey for supporting the fieldwork during the MTA geology projects which are carried out between the years of 1992-2001 are studied. We are grateful to the Hans de Bruijn (Utrecht University, The Netherlands) for useful comments and suggestions. We thank to Okan Zimitoğlu and Tolga Görmüş for taking SEM photographs.

### References

- Alvarez-Sierra, M. A., I. Garcia-Paredes, V., Hernandez-Ballarín, L.W., Van den Hoek Ostende, K., Hordijk, P. Lopez-Guerrero, A. J., Van der Meulen, A., Oliver, and Pelaez-Campomanes, P. 2013. Models of historical biogeography and continental biochronology. *Spanish Journal of Palaeontology*, 28, 129–138.
- Argyropulo, A. I. 1938. On the fauna of Tertiary Cricetidae of the USSR. *Comptes Rendus (Doklady) de l'Académie des Sciences de l'URSS*, 20, 223–226.
- Bi, S.D. 2005. Evolution, systematics and functional anatomy of a new species of Cricetodontini (Cricetidae, Rodentia, Mammalia) from the northern Junggar Basin, northwestern China. Ph. D. Thesis. Howard University, 183 p. Washington DC (unpublished).
- de Bruijn, H., Fahlbusch, V., Saraç, G., Ünay E. 1993. Early Miocene rodent faunas from the Eastern Mediterranean area. Part III. The genera *Deperetomys* and *Cricetodon*, with a discussion of the evolutionary history of the Cricetodontini. *Proceedings van de Koninklijke Nederlandse Akademie van Wetenschappen Series*, 96, 2, 151-216.
- de Bruijn, H., Ünay, E. 1996. On the evolutionary History of the Cricetodontini from Europe and Asia Minor and Its Bearing on the Reconstruction of Migrations and the Continental Biotope During the Neogene. In Bernor, R.L., Fahlbusch, V. and Mittmann, H.W. (Ed.). *The Evolution of Western Eurasian Later Neogene Faunas*, 227-234. New York: Columbia University Press.
- Fernández, M. H., Cárdena J. A., Cuevas-González, J., Fesharaki O., Salesa M. J., Corrales, B., Domingo, L., Elez J., López Guerrero P., Sala-Burgos N., Morales J., López Martínez N. 2006. Los yacimientos de vertebrados del Mioceno medio de Somosaguas (Pozuelo de Alarcón, Madrid): implicaciones paleoambientales y paleoclimáticas. *Estudios Geológicos*, 62, 1, 263-294.
- Freudenthal, M. 1963. Entwicklungsstufen der Cricetodontinae (Mam. Rod.), Mittelspaniens und ihre stratigraphische Bedeutung. *Beaufortia*, 10, 51–157.
- Göktaş, F., Ünay, E. 2000. The stratigraphy of the NW parts of the Akhisar (Manisa) Neogene basin. *International Earth Science Congress on Aegean Region*, Abstracts, p. 72.
- Hammer, Ø., Harper, D.A.T., Ryan P.D. 2001. Paleontological statistics software package for education and data analysis. *Paleontologica Electronica*, 41, p. 9.
- Hír, J. 2007. *Cricetodon klariankae* n. sp. (Cricetodontini, Rodentia) from Felsőtárkány-Felnémet (Northern Hungary). *Fragmenta Paleontologica Hungarica*, 24–25, 16–24.
- Jarvis, A., Reuter, H.I., Nelson, A., Guevara, E. 2008. Hole-filled SRTM for the Globe, Version 4. CGIAR-CSI SRTM 90m Database, <http://srtm.csi.cgiar.org>.
- Klein Hofmeijer, G., de Bruijn, H. 1988. The mammals from the lower Miocene of Aliveri (Island of Evia, Greece) part 8: the Cricetidae. *Proceedings of the Koninklijke Nederlandse Akademie van Wetenschappen Series B*, 91, 185–204.

- Kordos, L. 1986. Upper Miocene hamsters (Cricetidae, Mammalia) of Hasznos and Szentendre. *Magyar Allami Földtani Intézet Jelentése Az*, 1984, 523–553.
- Lartet, E. 1851. Notice sur la colline de Sansan, suivie d'unerécapitulation des diverses espèces d'animaux vertébrés fossiles trouvés soit à Sansan, soit dans d'autres gisements du terrain tertiaire miocène dans le Bassin Sous-Pyrénéen. *J. A. Portes, Auch*, 41 pp.
- López-Guerrero, P. 2014. Cricetodontini (Rodentia, Mammalia) del Mioceno medio y superior del área de Daroca (Aragón, España): sistemática y filogenia. Ph. D. Thesis. Universidad Complutense De Madrid, 388 p. Madrid (unpublished).
- López-Guerrero, P., García-Paredes, I., Álvarez-Sierra, M.A. 2013. Revision of *Cricetodon soriae* (Rodentia Mammalia), new data from the middle Aragonian (Middle Miocene) of the Calatayud-Daroca Basin (Zaragoza, Spain). *Journal of Vertebrate Paleontology*, 33, 169–184.
- López-Guerrero, P., Álvarez-Sierra, M.A., García-Paredes, I., Peláez-Campomanes, P. 2014. New Cricetodontini from the middle Miocene of Europe: an example of mosaic evolution. *Bulletin of Geosciences*, 89. Czech Geological Survey, Prague. ISSN 1214-1119.
- Maridet, O., Sen, S. 2012. Les Cricetidae du gisement de Sansan. Peigné, S., Sen, S. (Ed.). Mammifères de Sansan. *Mémoires du Muséum d'Histoire Naturelle de Paris*, 203, 29-65.
- Mein P, Freudenthal M. 1971a. Les Cricetidae (Mammalia, Rodentia) du Néogène Moyen de vieux-Collonges Partie 1: Le genre *Cricetodon* Lartet, 1851. *Scripta Geologica*, 5, 1–49.
- Mein, P., Freudenthal, M. 1971b. Les Cricetidae (Mammalia, Rodentia) du Neogene Moyen de Vieux-Collonges. Partie 1: Le genre *Cricetodon* Lartet, 1851. *Scripta Geologica*, 5, 1-51.
- Prieto J., Böhme M., Gross, M. 2010. The cricetid rodents from Gratkorn (Austria, Styria): a benchmark locality for the continental Sarmatian sensu stricto (late Middle Miocene) in the Central Paratethys. *Geologica Carpathica*, 61, 5, 419-436.
- Prieto, J., Angelone, C., Casanovas-Vilar, I., Gross, M., Hír, J., Hoek Ostende L.W. van den, Maul, L., Vasylian, D. 2014. The small mammals from Gratkorn: an overview. *Palaeobiodiversity and Palaeoenvironments*, 94, 1, 135-162.
- Qiu, Z. D. 2010. Cricetids rodents from the early Miocene Xiacaowan formation, Sihong, Jiangsu. *Vertebrata Palasiatica*, 48, 27–47.
- Reig, O. A. 1977. A proposed unified nomenclature for the enameled components of the molar teeth of the Cricetidae (Rodentia). *Journal of Zoology (London)*, 181, 227-241.
- Rummel, M. 1995. *Cricetodon bolligeri* n. sp. ein neuer Cricetide aus dem Obermiozän von Petersbuch bei Eichstätt. *Mitteilungen der Bayerischen Staatssammlung für Paläontologie und Historische Geologie*, 35, 109–123.
- Rummel, M. 2001. Ein neuer *Cricetodon* aus dem Miozän von Petersbuch bei Eichstätt. *Stuttgarter Beiträge zur Naturkunde B*, 311, 1–6.
- Rummel, M., D. Kälin. 2003. Die Gattung *Cricetodon* (Mammalia, Rodentia) aus den Mittelmiozän der Schweizer Molasse. *Zitteliana*, 43, 123–141.
- Simpson, G.G. 1945. The principles of classification and a classification of mammals. *Bulletin of the American Museum of Natural History*, 85, 1-350.
- Şen, S., Ünay, E. 1979. Sur quelques Cricetodontini (Rod.) du Miocène moyen d'Anatolie. *Proceedings of the Koninklijke Nederlandse Akademie van Wetenschappen*, 82, 293–301.
- Şen, S., Erbajeva, M. A. 2011. A new species of *Gobicricetodon* Qiu, 1996 (Mammalia, Rodentia, Cricetidae) from the Middle Miocene of Aya Cave, Lake Baikal. *Vertebrata Palasiatica*, 49, 257–274.
- Tobien, H. 1978. New species of Cricetodontini (Rod. Mam.) from the Miocene of Turkey. *Mainzer Geowissenschaftliche Mitteilungen Geologisches Landesamt Rheinland-Pfalz*, 6, 209-219.
- Ünay, E., Göktaş, F. 1999. Söke çevresi (Aydın) Geç Erken Miyosen ve Kuvaterner yaşlı küçük memelileri: ön sonuçlar. *Türkiye Jeoloji Bülteni*, 42, 2, 99-115.
- Ünay, E., Göktaş, F. 2000. Kınık (Gördes) çevresindeki Erken Miyosen yaşlı linyitli çökellerin küçük memeli biyokronolojisi: ön sonuçlar. *Türkiye Jeoloji Bülteni*, 43, 1, 1-5.

Ünay, E., Atabey, E., Saraç, G. 2001. Small mammals and foraminifera from the Anatolian (Central Taurus) Early Miocene. *Annals of Carnegie Museum*, 70, 4, 247-256.

Wu, W., Meng, J., Ye, J. Ni, X. J., Bi, S.D., Wei, Y. P. 2009. The Miocene mammals from Dingshanyanchi formation of North Junggar Basin, Xinjiang. *Vertebrata Palasiatica*, 47, 3, 208-233.

### Appendix 1:

#### 1. Bifurcation of anterocone on M1:

(0) single, undivided cusp; (1) slight incision in the wall of the anterocone; separation of antero-lingual and antero-labial conules into distinct cusps at the top; (2) deep incision in the wall of the anterocone; separation of antero-lingual and antero-labial conules into distinct cusps at the base

#### 2. Inflation of cusps:

(0) slender; (1) plump

#### 3. Labial anteroloph of M1:

(0) absent, or weakly developed; (1) a short spur; (2) complete

#### 4. Protolophule I of M1:

(0) absent; (1) a labial spur on the anterolophule pointing to the paracone

#### 5. Posterior spur of the paracone of M1:

(0) absent; (1) a posterior spur on the paracone; (2) a complete crest between paracone and metacone

#### 6. Shape of posterior spur of the paracone:

(0) straight; (1) concave

#### 7. Mesoloph on M1:

(0) long, extending from median mure to labial cingulum; (1) of medium length, about half the distance between median mure and labial cingulum; (2) absent, or minimally suggested in unworn molars as an enamel deflection of the median mure

#### 8. Posteroloph of M1:

(0) a transverse elongate ridge, surrounding a basined protosinus posteriorly with a metalophule; (1) continues beyond the point where it meets the metalophule; (2) not continuing beyond the point where it meets the metalophule

#### 9. M1 roots:

(0) three roots; (1) four roots

#### 10. Protolophule of M2:

(0) connected to the anterior branch of the protocone, or to its anterior corner; (1) connected to the posterior corner of the protocone or to the entoloph

#### 11. Metalophule of M2:

(0) connected to the anterior tip of the hypocone, or to the entoloph; (1) connected to the posterior tip or posterior branch of the hypocone

#### 12. Mesoloph of M2:

(0) long, extending from median mure to labial cingulum; (1) of medium length, about half the distance between median mure and labial cingulum; (2) absent, or minimally suggested in unworn molars as an enamel deflection of the median mure

#### 13. Sinus of M2:

(0) relatively wide and almost transverse; (1) relatively narrow and directed forwards

#### 14. Posterior spur of the paracone of M2:

(0) absent; (1) a posterior spur on the paracone; (2) a complete crest between paracone and metacone

#### 15. Shape of posterior spur of the paracone:

(0) straight; (1) concave

#### 16. Posteroloph of M2:

(0) a transverse elongate ridge, surrounding a basined protosinus posteriorly with a metalophule; (1) continuing beyond the point where it meets the metalophule; (2) not continuing beyond the point where it meets the metalophule

#### 17. M2 roots:

(0) three roots; (1) four roots

#### 18. Shape of reduced M3:

(0) elongate; (1) rounded

#### 19. Mesoloph of M3:

(0) long, extending from median mure to labial cingulum; (1) of medium length, about half the distance between median mure and labial cingulum; (2) absent, or minimally suggested in unworn molars as an enamel deflection of the median mure

20. Metacone of M3:

(0) distinct; (1) ridge-like

21. Metalophulid I of m1:

(0) absent; (1) present

22. Metalophulid II of m1:

(0) present; (1) absent

23. Mesolophid of m1:

(0) long, reaching the border of the molar; (1) of medium length, about half the distance between the longitudinal ridge and lingual border; (2) short, or absent

24. Sinusid of m1:

(0) relatively wide and almost transverse; (1) relatively narrow and directed forwards

25. Lingual anterolophid of m2:

(0) developed; (1) undeveloped

26. Mesolophid of m2:

(0) long, reaching the border of the molar; (1) of medium length, about half the distance between the longitudinal ridge and lingual border ; (2) short, or absent

27. Sinusid of m2:

(0) relatively wide and almost transverse; (1) relatively narrow and directed forwards

28. Shape of reduced m3:

(0) elongate; (1) round

29. Protosinusid of m3:

(0) circular; (1) retracted and directed forwards

30. Mesolophid of m3:

(0) long, reaching the border of the molar; (1) of medium length, about half the distance between the longitudinal ridge and lingual border; (2) short, or absent

**PLATE**

**PLATE I**

*C. fikreti* n. sp. from Dededağ:

a: M1 (holotype), DD-1;

b: M2, DD-11;

c: M3, DD-21;

d: m1, DD-31;

e: m2, DD-41;

f: m3, DD-51

PLATE I

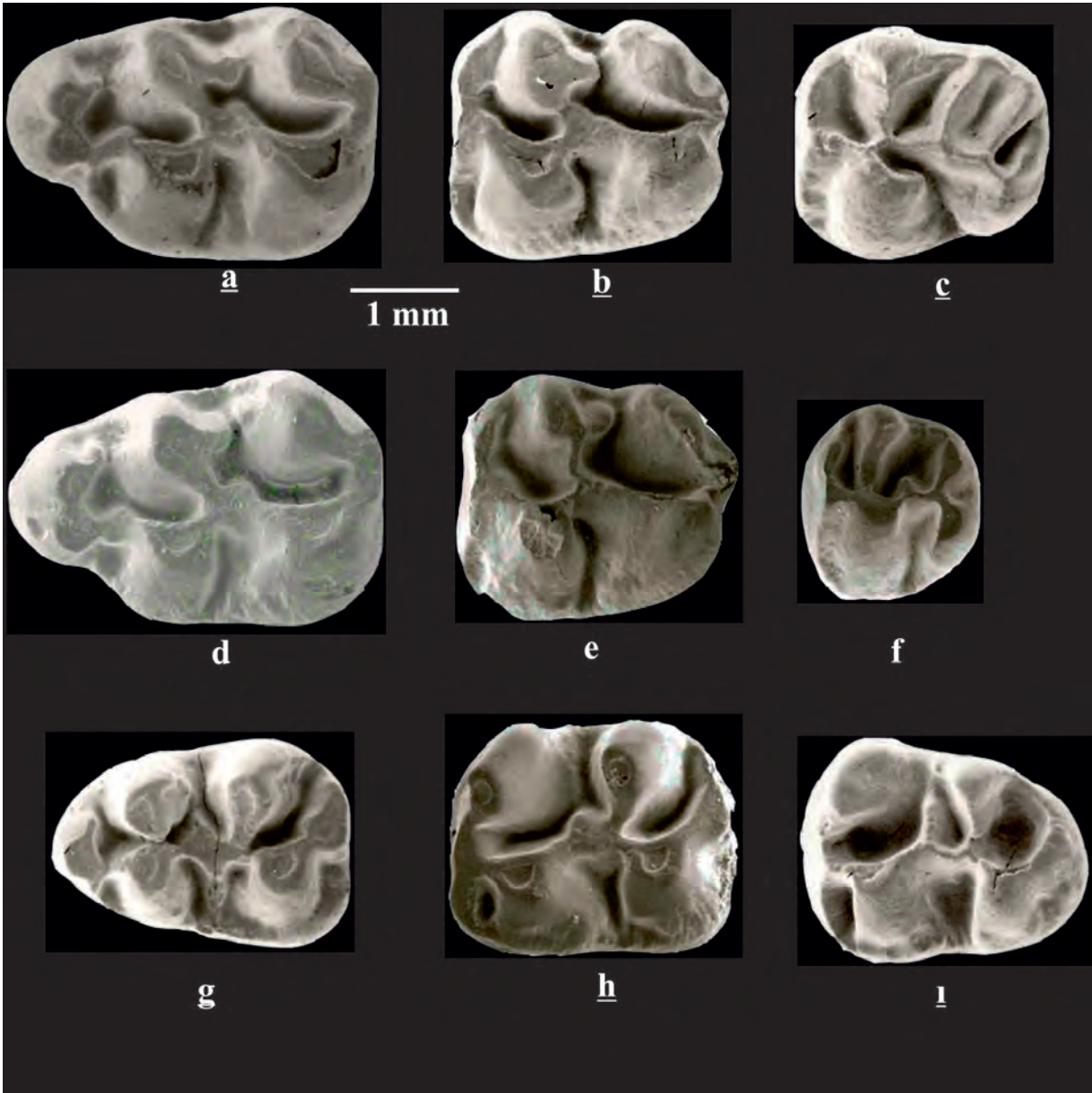


**PLATE II**

*C. fikreti* n. sp. from Dededağ:

a: M1 (holotype), DD-1;

b: M2, DD-11;

c: M3, DD-21;

d: m1, DD-31;

e: m2, DD-41;

f: m3, DD-51

PLATE II

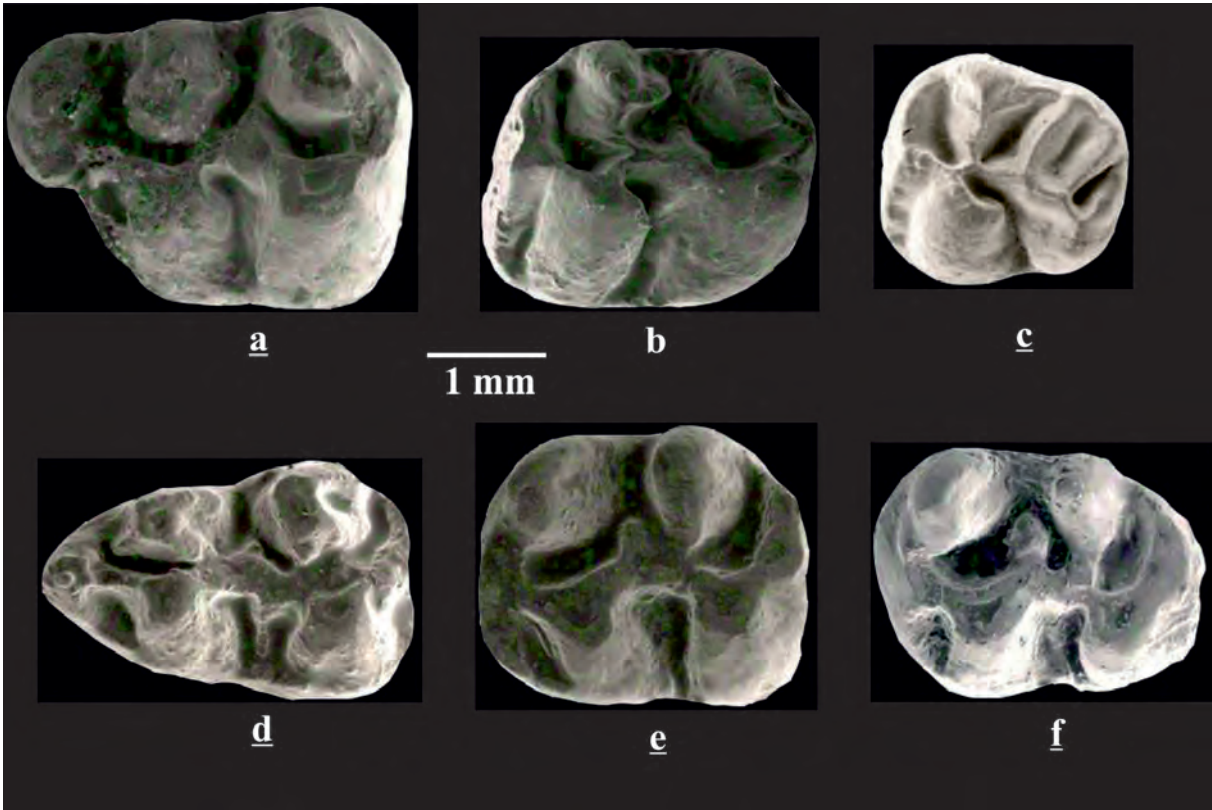


**PLATE III**

*C. yapintiensis* n. sp. from Yapıntı:

a: M1 (holotype), YP-121;

b: M2, YP-133;

c: M3, YP-141;

d: M2, YP-131;

e: m1, YP-151

PLATE III

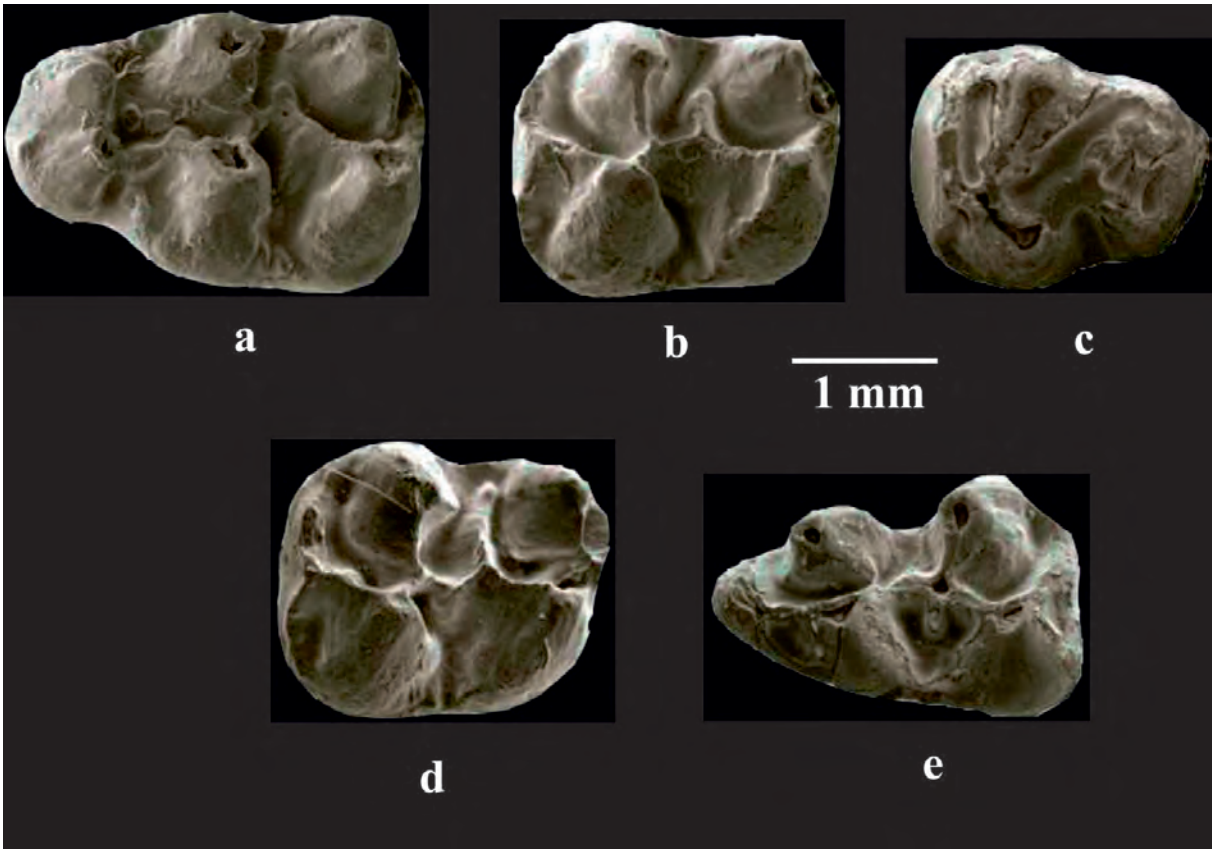


**PLATE IV**

*C. kasapligili* from Yapıntı:

a: M1, YP-9;

b: M2, YP-33;

c: M3, YP-47;

d: m1, YP-74;

e: m2, YP-89;

f: m3, YP-104

PLATE IV

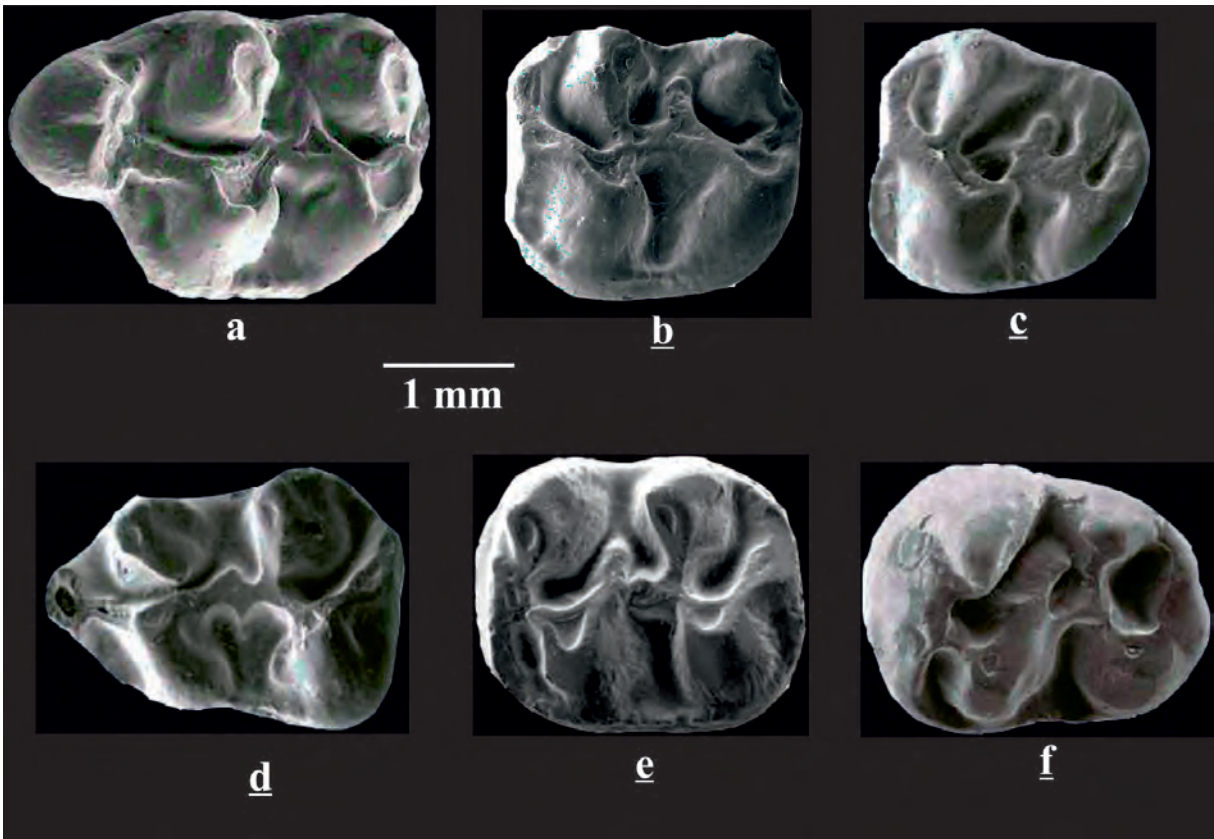


**PLATE V**

*C. cf. kasapligili* from Harta:

a: M1, HT-82;

b: M2, HT-86;

c: M3, HT-89;

d: m1, HT-91;

e: m2, HT-95;

f: m3, HT-100

PLATE V

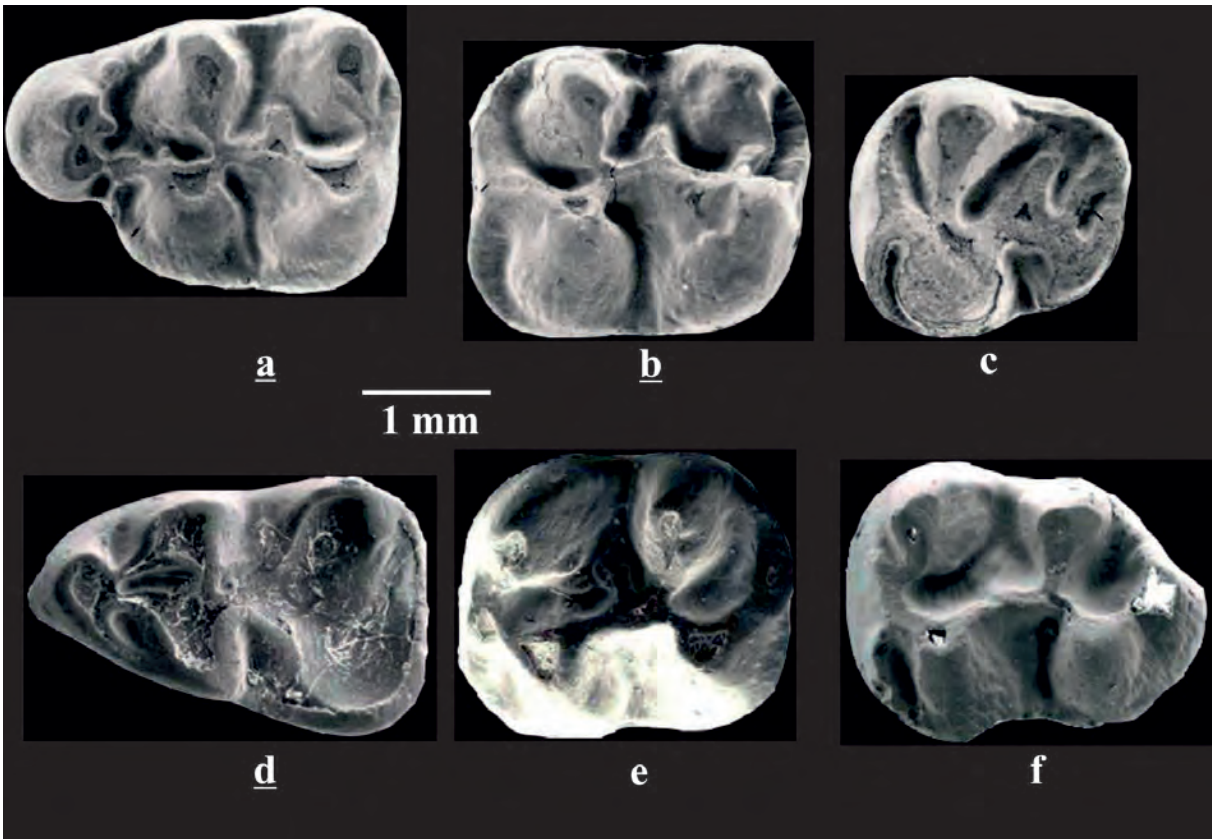


**PLATE VI**

*C. magnesiensis* n. sp. from Kınık:

a: M1 (holotype), KN-101;

b: M2, KN-111;

c: M3, KN-142;

d: m2, KN-171;

e: m3, KN-201

PLATE VI

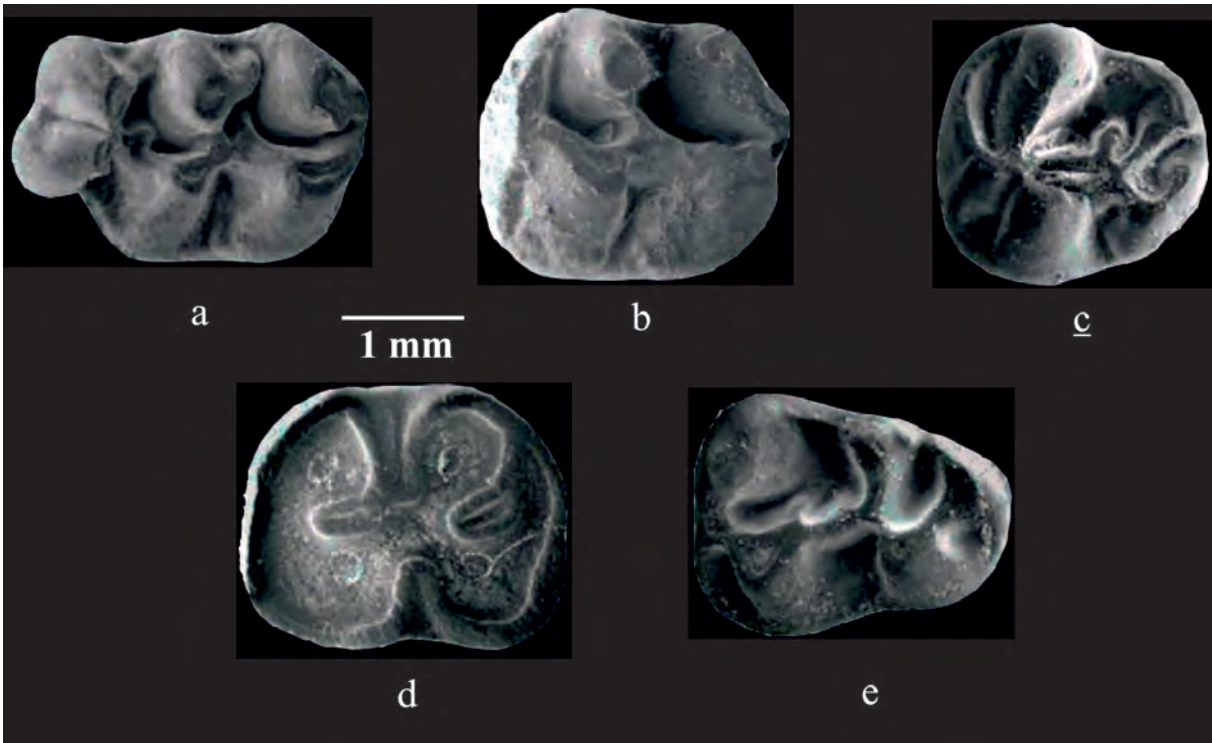


**PLATE VII**

*C. versteegi* from Kınık:

a: M1, KN-105;

b: M2, KN-123;

c: M3, KN-144;

d: m1, KN-163;

e: m2, KN-173;

f: m3, KN-191

PLATE VII

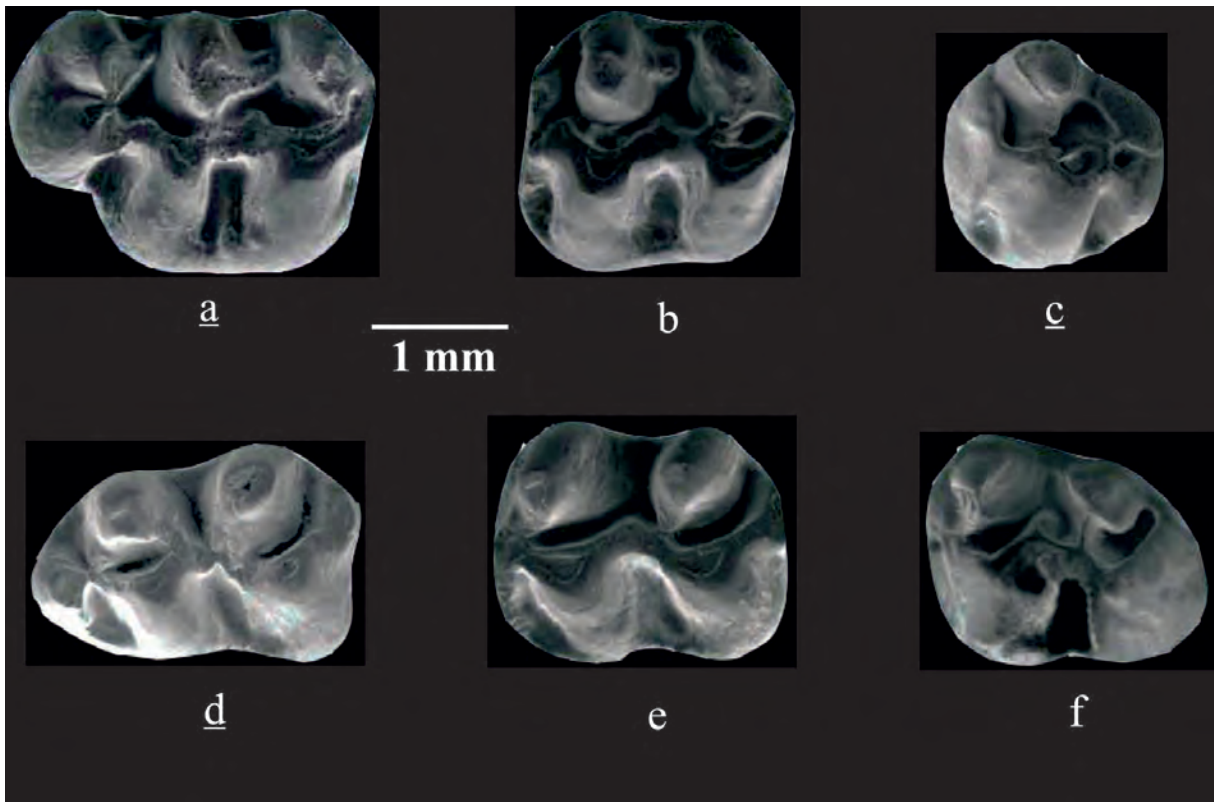


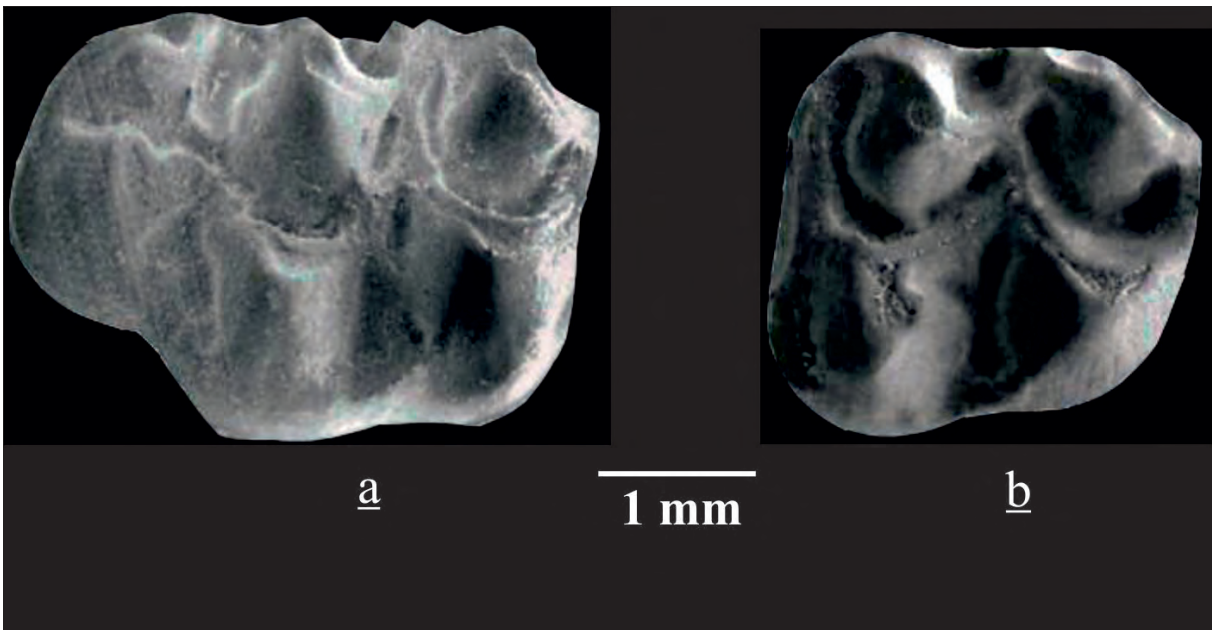
**PLATE VIII**

*Deperetomys* cf. *intermedius* from Kınık:

a: M1, KN-1;

b: M2, KN-11

PLATE VIII







# BULLETIN OF THE MINERAL RESEARCH AND EXPLORATION

<http://bulletin.mta.gov.tr>

BULLETIN OF THE MINERAL RESEARCH AND EXPLORATION	
CONTENTS	
AN APPROACH TO THE ORIGIN OF THE EARLY CAMBRIAN KARAÇAT IRON DEPOSIT (MANSURLU BASIN, ADANA) AND IRON DEPOSITS OUTCROPS AT ITS EASTERN PARTS	Deniz TİRİNGA <sup>a*</sup> , Taner ÜNLÜ <sup>b</sup> and Semih GÜRSU <sup>c</sup>
Research Article	

## AN APPROACH TO THE ORIGIN OF THE EARLY CAMBRIAN KARAÇAT IRON DEPOSIT (MANSURLU BASIN, ADANA) AND IRON DEPOSITS OUTCROPS AT ITS EASTERN PARTS

Deniz TİRİNGA<sup>a\*</sup>, Taner ÜNLÜ<sup>b</sup> and Semih GÜRSU<sup>c</sup>

<sup>a</sup>General Directorate of Mineral Research and Exploration (MTA), Department of Mineral Research and Exploration, Ankara, Turkey

<sup>b</sup>Ankara University, Department of Geological Engineering, Ankara, Turkey

<sup>c</sup>Muğla Sıtkı Koçman University, Department of Geological Engineering, Muğla, Turkey

Research Article

### Keywords:

Iron Mineralization,  
Karaçat Iron Deposit,  
Mansurlu, Exhalative  
Syn-Sedimentary.

### ABSTRACT

The Neoproterozoic basement and the Early Cambrian units are widely exposed around the Karaçat Iron Deposit and its surrounding, which are located at the eastern part of Tauride-Anatolide platform. The main mineralization was detected as hematite in all deposits in the study area. The ore microscopy, SEM and EDX studies show that carbonate pseudomorphs in hematite have developed and their chemical compositions are enriched in Ca, Mg, Fe, C and O elements. The geochemical analyses of hematite and siderite minerals reveal that both ore mineral types have similar patterns of Rare Earth Element (REE). These data and field observations reveal that hematite is the replacement product after sedimentary siderite mineralization. The genesis of the hematite mineralization that is effective over large areas and widely observed on the basement and overlying units, was formed during Late Neoproterozoic- Early Cambrian volcanism in the region defined as Peri-Gondwana. They are genetically described as volcano syn-sedimentary and/or exhalative syn-sedimentary type mineralization.

Received: 09.11.2015

Accepted: 27.11.2015

## 1. Introduction

Different types of economic ore mineralizations have been developed in our country located along a belt that was actively affected by Pan-African, Cadomian, Variscan and Alpine orogeneses. Iron deposits formed one of these mineralizations has been observed in the different basins indicating different genesis, ages and lithologies (Cihnioğlu et al., 1994).

Mansurlu Basin iron deposits are observed within the siliciclastic rocks of the Late Proterozoic-Early Cambrian. Similar formations in the Precambrian shields in North and South America, Africa, Australia and Russia are shortly defined as Banded Iron formations (BIF). The BIFs form significant portion of iron ore deposits in the whole world. The Mansurlu basin is the second biggest iron deposit in terms of reserve in our country. Iron deposits and occurrences, located at the eastern part of Mansurlu Basin, host

good quality direct reduced iron ores in their bodies for blast furnaces. They contain 65 % Fe content as tenure and do not include any harmful compound.

Among deposits in the basin, several studies were carried out to reveal the formation of iron deposits in Attepe and its close vicinity (Lucius, 1927; Brennich, 1961; Arıkan, 1966, 1968; Henden et al., 1978; Önder and Şahin, 1979; Henden and Önder, 1980; Ünlü et al., 1984; Ünlü, 2003; Küpeli, 1986; 1991 and 1998; Ünlü and Stendal, 1986, 1989; Dağlıoğlu and Bahçeci, 1992; Dağlıoğlu et al., 1998; Çolakoğlu and Kuru, 2002; Küpeli et al., 2006; Dayan, 2007; Arda et al., 2008; Dayan et al., 2008; Tiringa, 2009; Tiringa et al., 2009, 2011).

The genesis of the iron deposits in the studied area is not well known though some researchers proposed hydrothermal-type genesis (related to the granitic intrusions) as their possible provenance

\*Corresponding author: Deniz TİRİNGA, [deniz.tiringa@mta.gov.tr](mailto:deniz.tiringa@mta.gov.tr)

<http://dx.doi.org/10.19111/bmre.16543>

(Henden and Önder, 1980; Küpeli, 1991; Küpeli et al., 2006). However; the other researchers mentioned that primary iron mineralizations were formed from siderites in the graphitic schists of the Precambrian Emirgazi formation and from sedimentary hematite observed in their upper parts and from sedimentary pyrites showing disseminated and conformal bedding relationships within the graphitic schists (Küpeli, 1991; Dağlıoğlu et al., 1998; Arda et al., 2008; Dayan, 2007; Dayan et al., 2008; Tiringa, 2009; Tiringa et al., 2009). Some of the researches (Dayan et al., 2008; Tiringa et al., 2009, 2011) provided evidence for volcano syn-sedimentary and/or exhalative syn-sedimentary type genesis models for their occurrences.

The aim of the study is to determine the origin of the iron deposits observed in the Mansurlu basin by field studies, tectonic evolution modelling and petrogenetic studies.

## 2. Geology of the Study Area

The study area represents characteristic features of the Eastern Taurides in the Tauride-Anatolide platform (Özgül, 1976; 1983; Göncüoğlu, 2010). It is located in the southeastern part of the central Anatolia region between Karaköy village of Yahyalı Town in Kayseri and Bahçecik and Bekirhacılı villages of Feke town in Adana. The geological map of this area is given in figure 1a.

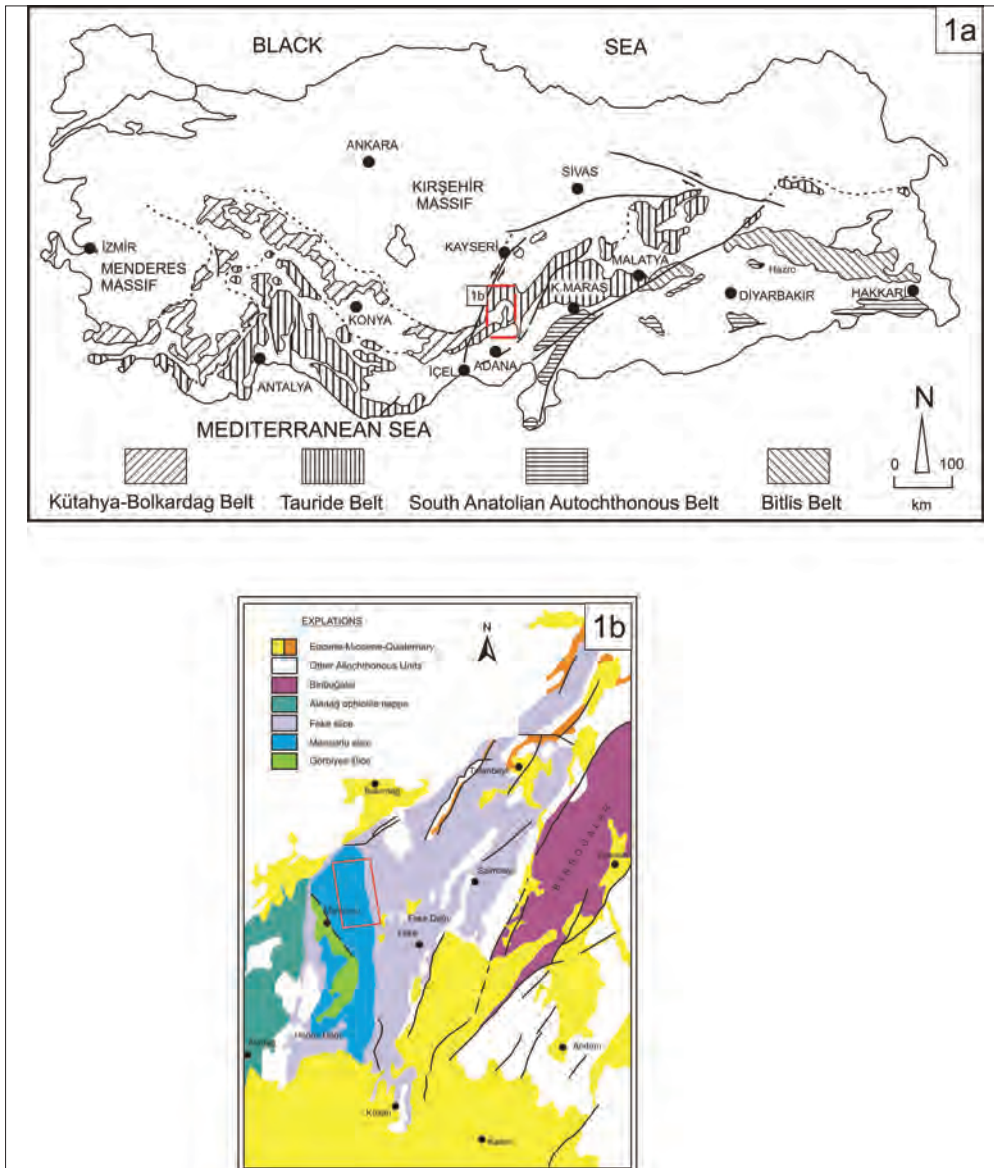


Figure 1- (a) Tectonic terranes of the Southern Anatolites (Göncüoğlu et al., 1997), (b) Studied area and tectonic slices of the Geyikdağı Unit (adapted from Şenel et al., 2004).

In the study area, diverse tectonic slices were described as Görbiyes, Mansurlu and Feke indicating different stratigraphic and tectonic settings assessed within the Geyikdağı unit (Özgül and Kozlu, 2002; Şenel et al., 2004) (Figure 1b). The allochthonous Görbiyes tectonic slice located at the basement in the region is tectonically overlain by Mansurlu slice. Feke slice, which is formed from different rock groups between the Late Proterozoic-Late Cretaceous, tectonically overlies Mansurlu slice in the studied area. The studied area is located within the Mansurlu tectonic slice (Özgül and Kozlu, 2002) and partly interpolates with the rocks of the Feke slice (Figure 1b).

The Late Neoproterozoic-Early Ordovician rock units in the Mansurlu tectonic slices are cropped out in the studied area (Figure 2). The base unit of the Mansurlu slice is composed of the Emirgazi formation representing the oldest lithostratigraphic unit of the

region and is made up of shallow siliciclastics as meta-siltstone and meta-mudstone with meta-volcanic and meta-carbonate interlayers associated with meta-clastics.

The Early Cambrian Koçyazı formation is composed of graphite schist and meta-siltstones/meta-sandstones with meta-mudstones/meta-siltstones inlayers. Mafic volcanic rocks and dykes are observed at lower parts of the formation (Özgül and Kozlu, 2002).

The Zabuk formation, which is intercalated with sandstones and slates in the lower layers, is mainly composed of quartzite (quartz arenites).

The Middle Cambrian Değirmentaş formation is mainly composed of neritic carbonates (Özgül and Kozlu, 2002).

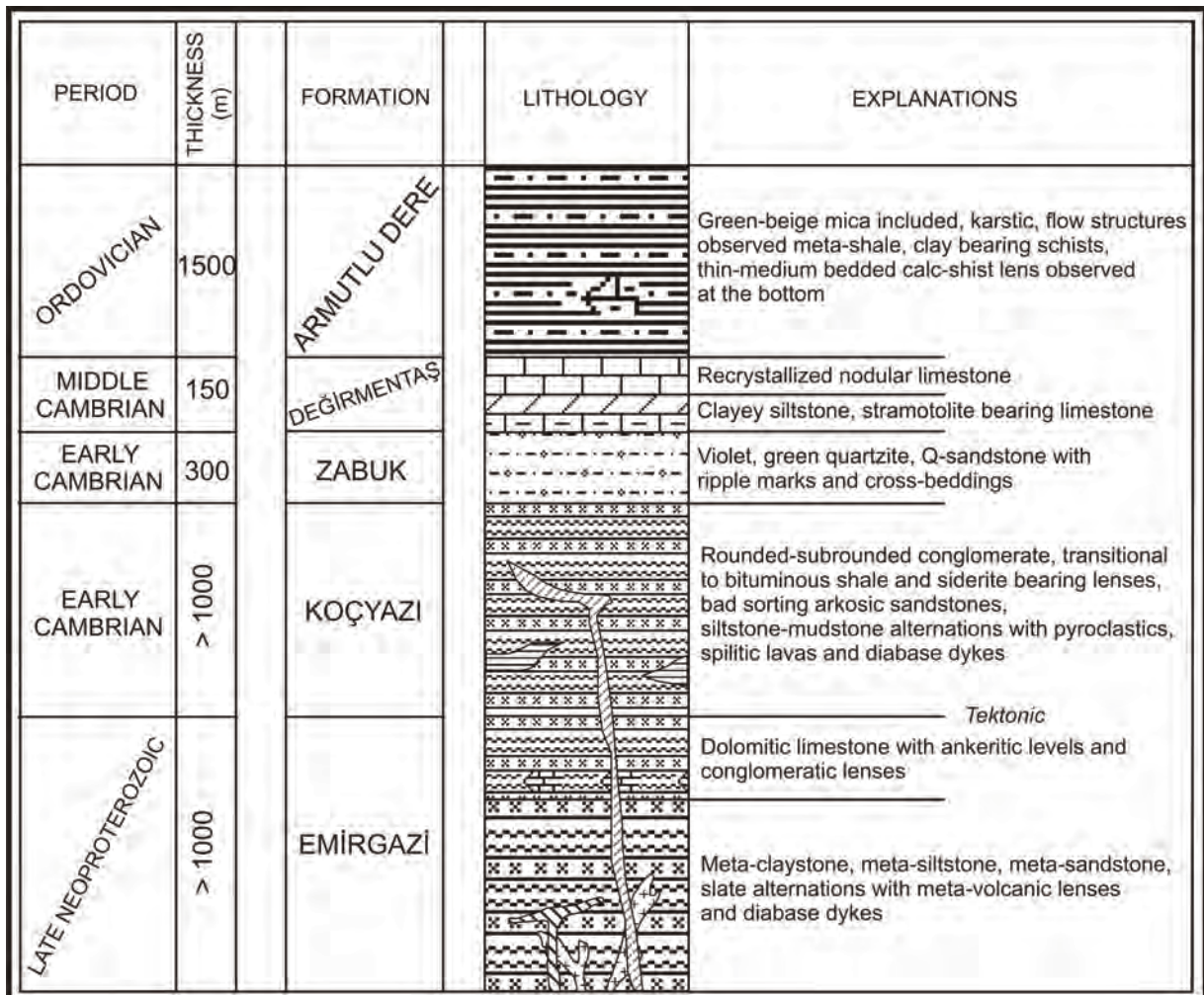


Figure 2- Generalized columnar section of the Mansurlu slice in the studied area (modified from Özgül and Kozlu, 2002).

The Armutludere formation (Demirtaşlı, 1967) is composed of Late Cambrian-Early Ordovician siliciclastic rocks. The folded nodular limestone layers and rare quartz arenite intercalations are observed in the lower part of the succession.

Iron deposits and mineralizations in the Mansurlu basin are stratigraphically observed in the successions from the Late Neoproterozoic Emirgazi formation to Ordovician Armutludere formation. However, no mineralization is observed in the younger successions in the studied area (Figure 3).

### 2.1. Emirgazi Formation (Late Proterozoic)

Outcrops of the Late Neoproterozoic Emirgazi formation in the basement are located in Üçtepel within the eastern part of Bahçecik creek, Gökbelen Hill near Hıdıruşağı village, Yüksün Hill, Bekirhacılı village and southern part of Hıdıruşağı village (Figure 3).

The main lithology of the Emirgazi formation consists of alternation of meta-sandstone, meta-siltstone with meta-tuff, meta-volcanite, ankerite and meta-carbonate inlayers. The acidic and intermediate felsic volcanic rocks are rarely observed in the succession. The quartzitic rocks are dominant in the upper part of the formation and continue with the recrystallized limestones, dolomitic limestones, dolomites and meta-clastic rocks. Limestones in the upper part of the formation are generally pale to dark ash, yellowish-gray, fine to medium bedded and fine to medium crystallized.

Randomly specularite bearing reddish-brown color carbonate layers that turn into ankerite, lens shaped dolomite and dolomitic limestone layers having 1-10 m thickness are frequently observed in the Emirgazi formation (Özgül and Kozlu, 2002) (Figure 4).

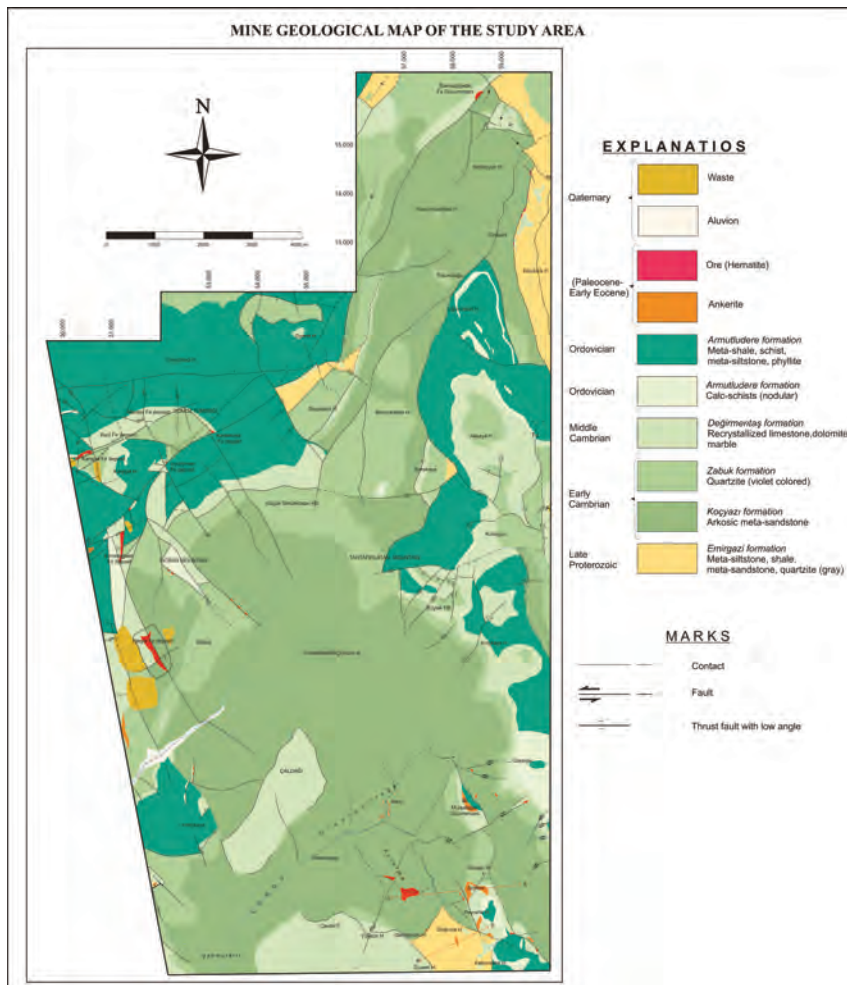


Figure 3- The map of the ore geology in the studied area (adapted from Tiringa et al., 2011).

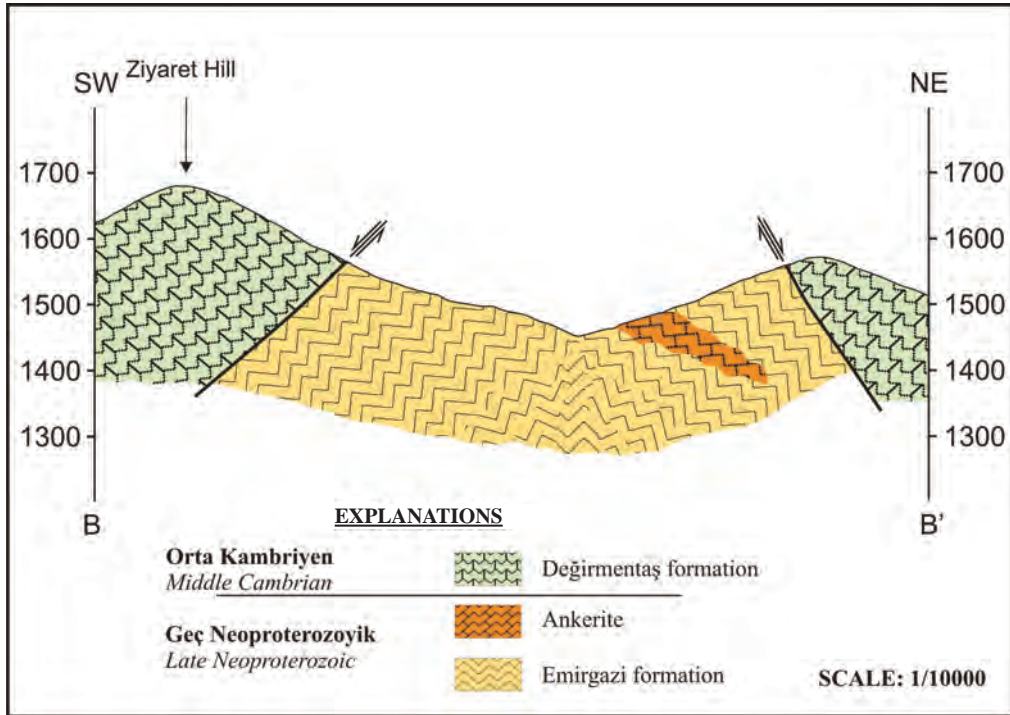


Figure 4- Cross section of the Emirgazi formation showing the ankeritic levels at the Ziyaret hill.

In petrographical studies, the ankerites were mainly formed from the different grain sized carbonate minerals that display pressure twinning due to active tectonic deformations. Secondary iron oxide developments are observed along the fractures and cleavage planes of the carbonate minerals. The secondary carbonate minerals are hosted in the pores and fracture zones (Figure 5).

Additionally, limonites formed by the alteration product of ankerite and anhedral disseminate along the outer boundaries with grain size of the 14-240 microns

displaying parallel to bedding planes of the host rocks are observed in the samples. It is considered that these iron rich minerals observed in the hand specimens and thin sections were products of the iron deposits in the basin studied as main ore sources.

The formation is adversely affected by the Late Alpine deformation phase having a thickness higher than 1000 meters. The Emirgazi formation is tectonically overlain by the Early Cambrian Koçyazi formation (Özgül and Kozlu, 2002).

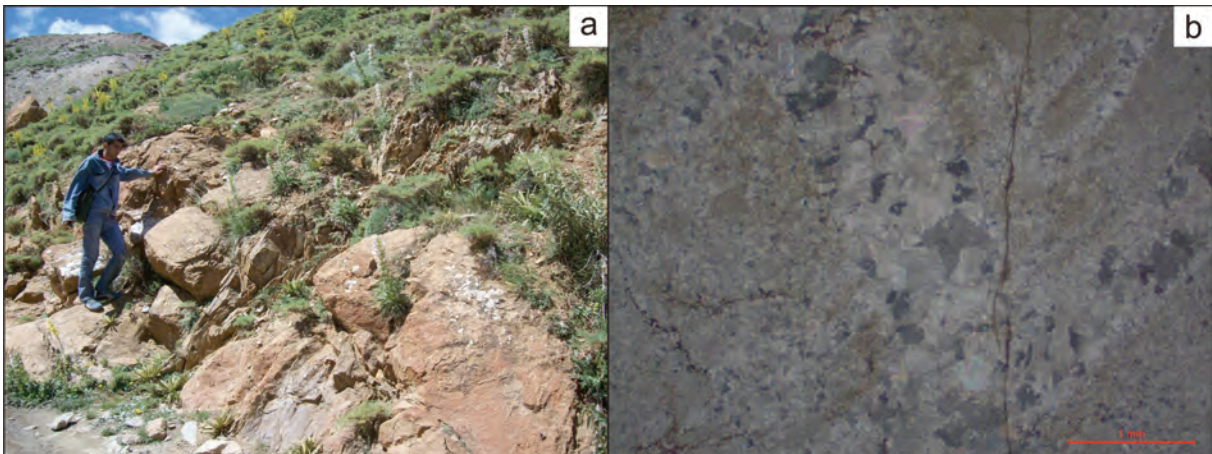


Figure 5- (a) Field photograph of the Ankerite (Menteş dere), (b) photographs of the iron oxides stained ankerite (XPL)

## 2.2. Koçyazı Formation (Early Cambrian)

The type locality of the formation in the study area is located between Avuç District and Çaldağ. The other outcrops are observed in Küçüktahtafırlatan Hill near the eastern part of Attepe, Şahmuratlı and Kerimuşağı areas of Oruçlu village near the southern part of Yüksün Hill and Kavurmaderesi Hill in the north near the southern part of the Banazlıgedik Hill (Figure 3).

The succession is predominated by meta-sandstone/meta-siltstone. Greyish-black pyrite bearing bituminous shale and sideritic bands are observed in the lower part of the formation (Figure 6a). The type locality of the sideritic bands is placed in NE part of Attepe Iron Deposit at the western part of the study area (Dayan, 2007) (Figure 6b). The basic volcanic rocks are only observed in Karaçam creek

in the study area and mark the active basic volcanism at the lower parts of the succession. The upper parts of the succession are composed of fluvial siliciclastic rocks characterized by red-vivid-pink mudstone/siltstone alternations.

The Koçyazı formation is conformably overlain by sandstone-dominated Early Cambrian Zabuk formation that has a continuous succession throughout TAP (Figure 7).

## 2.3. Zabuk Formation (Early Cambrian)

The outcrops of the formation are placed in Domuztümseği Hill in the northeastern Karaçat Iron Deposit, Tahtafırlatan Mountain, Küçüktahtafırlatan Hill, Kandilcik Hill, Oturum area and Osman Sivrisi Mountain and Bahçecik Village at the west (Figure 3). The unit consists of meta-sandstone dominated slate banded meta-clastic rocks.

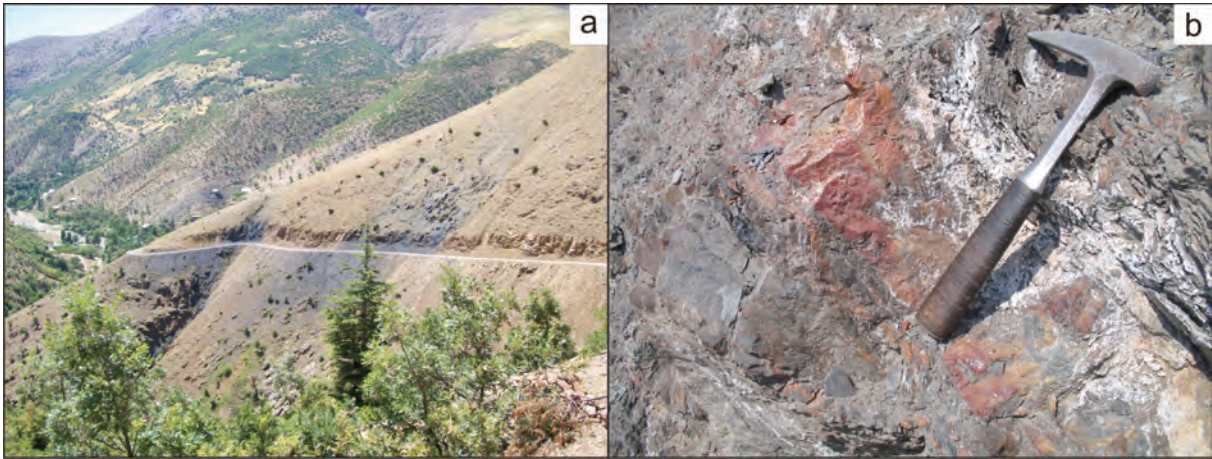


Figure 6- Field photographs (a) Bituminous schist observed at the bottom parts of the formation, (b) siderite lens transitional to the bituminous schist (NE of the Attepe iron deposit).

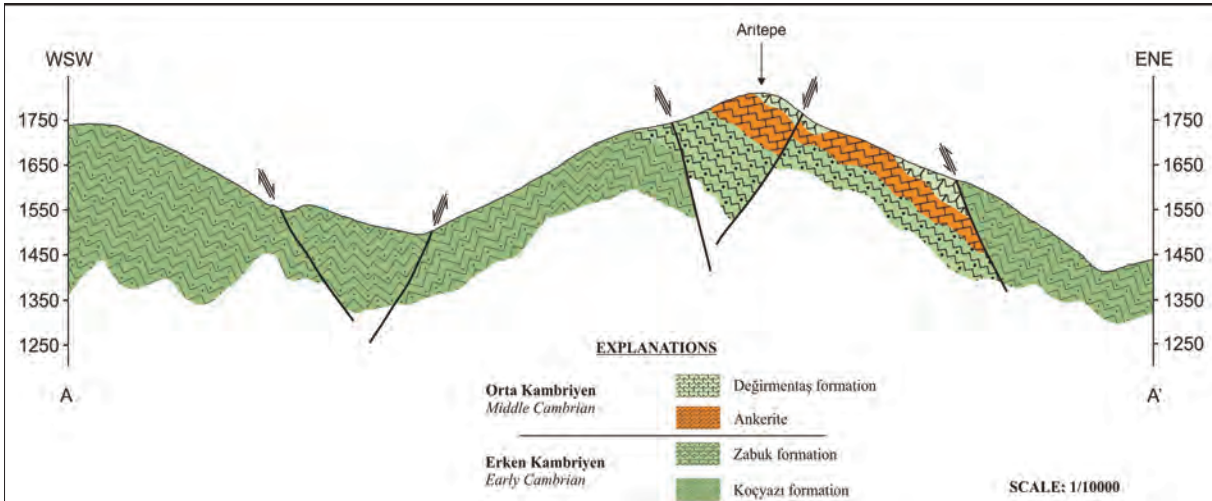


Figure 7- Cross-section showing the transitional contact between Koçyazı formation and Zabuk formation (W of Aritepe).

The lower part of the formation starts with quartzite and slate intercalation and continues with quartz-sandstone dominated clastic rocks. The angular/sub-angular detritic hematite minerals are observed in the quartzites having 1 to 2 mm grain size. The limonitized, partly specularized hematites and abundant specularites bearing quartz veins are observed in the meta-sandstones (Figure 8). Although there are no economic iron mineralization in the formation, these iron minerals might have been transported to the basin from the land and might have been resulted in the limited precipitation of the iron mineralization.

The unit is conformably overlain by the Middle Cambrian carbonate-dominated Değirmentaş formation (Özgül and Kozlu, 2002).

#### 2.4. Değirmentaş Formation (Middle Cambrian)

The outcrops are best exposed in Osman Sivrisi Mountain, Çaltepe-Oturum areas, and highlands of the northern part of Küçüktahtafırlatan Hill, Karaçat Hill and western part of Bahçecik Village (Figure 3).

The Değirmentaşı formation represented by neritic carbonates is composed of beige, pale brown clay bearing limestones, bluish-gray, gray and dirty white color medium to thick bedded dolomitic limestones and white to beige recrystallized limestones. Abundant calcite-quartz, hematite and siderite mineralization is developed along the fractures and joints of the formation (Figure 9).

Although the formation does not contain primary iron mineralization, a great majority of the second phase iron deposits have been hosted in the formation observed in the Mansurlu basin.

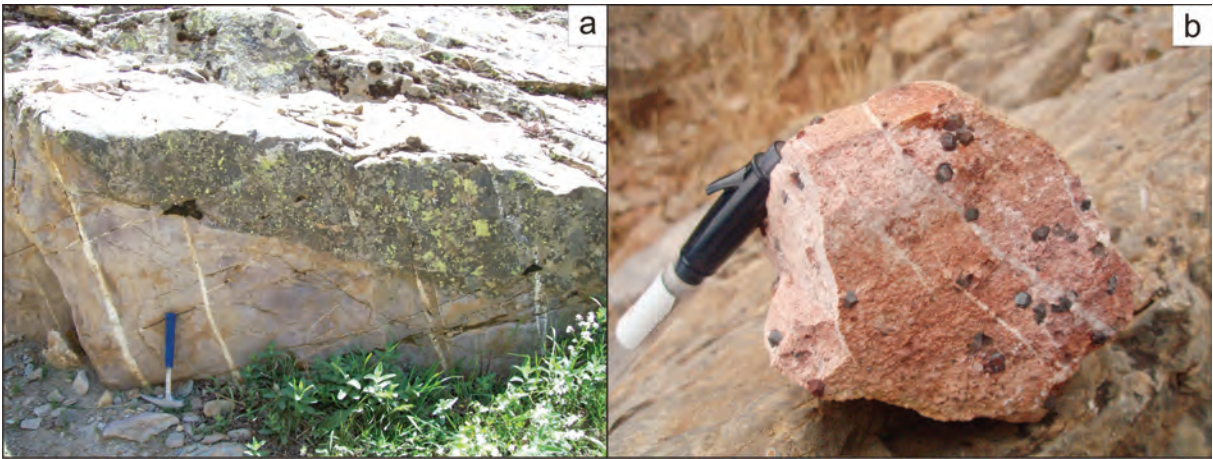


Figure 8- Field photographs; (a) meta-sandstone and quartzites of the Zabuk formation (Menteş dere), (b) detrital hematites deposited together with quartz grains.

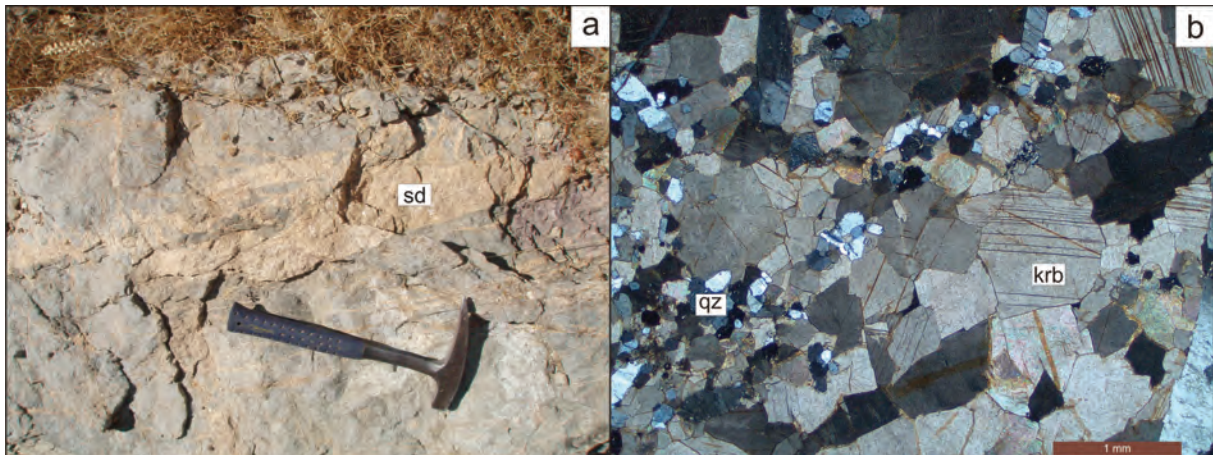


Figure 9- (a) Field photograph of the dolomitic limestone filled with the secondary siderite along the joints and fractures (Kozan-Okçulu area), (b) limonitized carbonates along the cleavage planes (sd: siderite, krb: carbonate, qz: quartz).

The settlement of the iron mineralizations in the formation were developed throughout the abundant fractures, faults, karstic spaces within the formation. The dolomitic lithology of the formation displays a convenient porosity for the ore-bearing solutions. Ore tenors after the settlement to the host rocks are extensively enriched by the active secondary processes (Tiringa, 2009; Tiringa et al., 2009, 2011).

The Değirmentaş formation is conformably overlain by nodular limestone layers in the lower parts of the Armutludere formation (Özgül and Kozlu, 2002).

### 2.5. Armutludere Formation (Late Cambrian-Ordovician)

The outcrops of the formation are observed in the Deveçökeği Hill in the north, Küçüktahtafırlatan Hill and northern hillside of the Sicim Mountain and Uğurunyurt Hill and Atkırı Hill in the west (Figure 3).

The base of the formation starts with beige, pink thin-middle bedded nodular limestone and continues with greenish, pale brown meta-siltstones.

Late-stage hematite mineralization near the lower part of the formation deposited in the calc-shists is widely observed. These mineralizations in the calc-shists lenses are limited as observed as small masses. The siderite lenses ( their thickness range from 10 cm to 1-2 m) are observed in southeastern part of the Karaçat Iron Deposits formed in the upper part of the Armutlu formation (Figure 10). 20-30 m thickness of

the siderite deposits in the formation is reported from the drilling studies.

The upper part of the Armutludere formation is not observed in the study area and is tectonically overlain by the Late Neoproterozoic Emirgazi formation of the Feke slice.

### 3. Ore Microscopy Studies

Ore microscopy studies were carried out on 268 samples collected either from ore or from the host rocks representing the mineralization of the different deposits observed in the basin. The results are discussed in the following.

#### 3.1. Precambrian-Early Cambrian Metasiltstones and Basic Rocks

Disseminated magnetites and marcasites were determined by the ore microscopy studies carried out in both of Precambrian and Early Cambrian siltstones. The magnetites are in the form of the euhedral-subhedral rectangle or triangle shape grains that are in different sizes. The martitizations are observed along the weak zones of the magnetites. The ilmenite, rutile and titanites as the forms of the cage structure are main alteration products of the ilmenomagnetite, pyrite (partly altered to goethite, hematite), chromite (partly replaced by magnetite along the weak zones), chalcopyrites and magnetites were determined in the ore microscopy studies of the basic volcanic rocks (Figure 11).

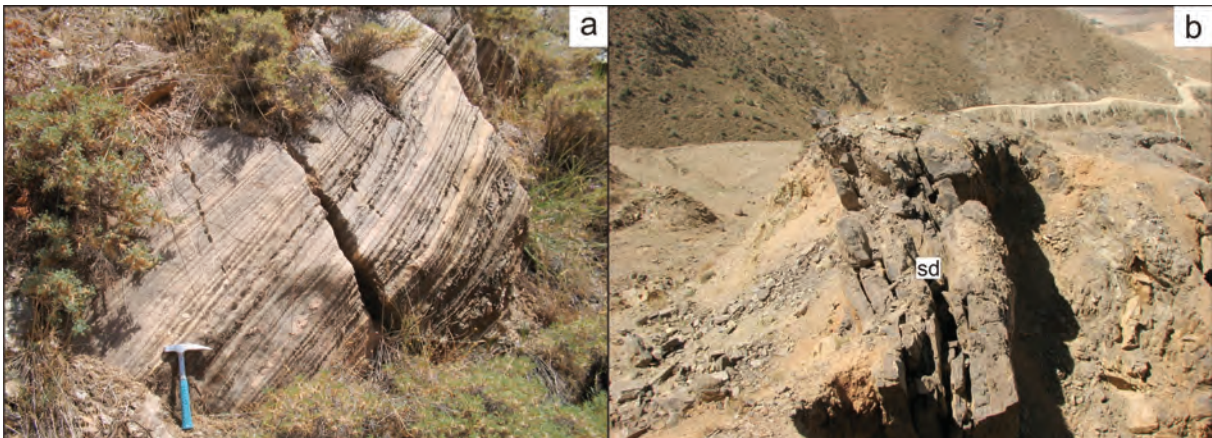


Figure 10- Field photographs: (a) Nodular limestone (NW of Alpseki creek), (b) siderite lens in the meta-siltstone (SE of Karaçat iron deposit) (sd: siderite).

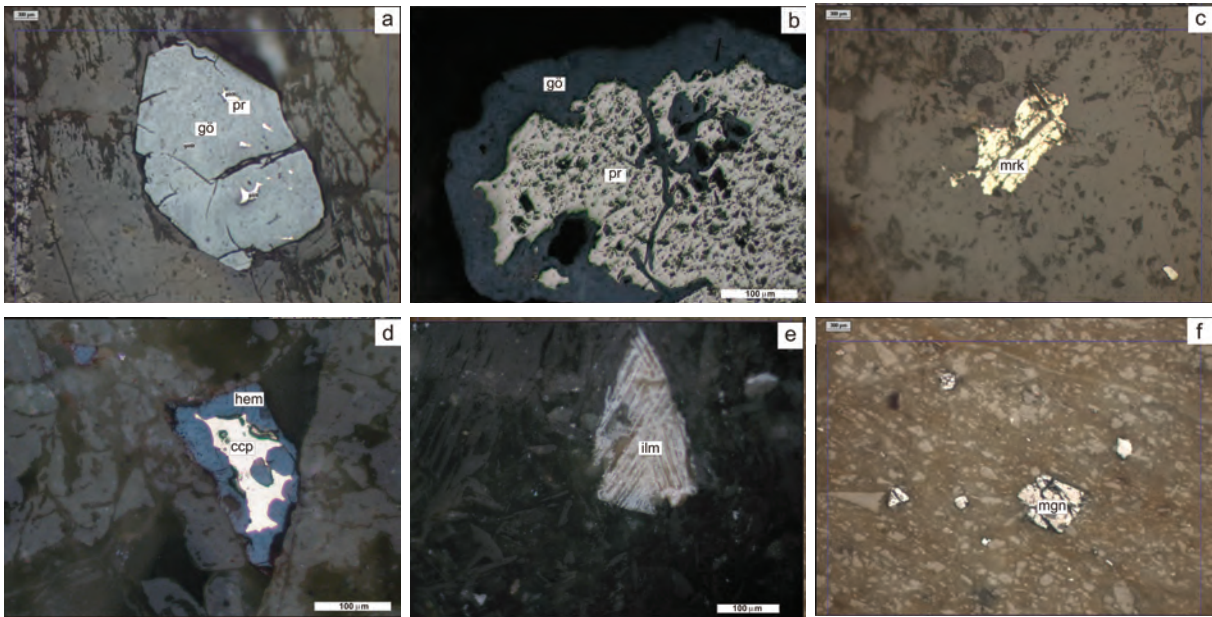


Figure 11- (a) Subhedral, goethite derived from pyrite (b) Goethite derived from pyrite along the cleavage planes (c) Marcasite within the meta-siltstone (d) Chalcopyrites observed within the hematite (e) Ilmenite lamella (f) Euhedral-subhedral magnetites partly replaced by martitite (pr: pyrite, gö: goethite, ccp: calcopyrite, ilm: ilmenite, hem: hematite, mgn: magnetite, mrk: marcazite)

### 3.2. Middle Cambrian Limestones

The limonites and limonitic stains are discovered in the Middle Cambrian dolomitic limestones and partly limonitized pyrites along the weak zones and sub-microscopic hematites are developed in the recrystallized limestones during the ore microscopy studies (Figure 12). Variated grain size of the carbonate minerals showing strain twins due to deformation were observed in the petrographic studies. In addition, abundant limonite strains and limonitization were detected throughout cleavage planes, grain boundaries and fractures (Figure 9).

### 3.3. Specularites

The different grain size of the goethites and specularites observed as lensoidal, detached, folded-bended due to cataclastic effects were determined in the polished sections. The specularites are also offset in some places in the form of rods having different thicknesses that display pronounced alignments. The red internal reflections of the hematites are distinctive in some sections. Specularite mineralization surrounding the goethite ores are tended to fill the cracks and fractures of the ore. Their relationships with host rocks are limited just in settlement into cracks and fractures. No substitution textures or traces in the Middle Cambrian recrystallized limestones are determined (Figure 13).

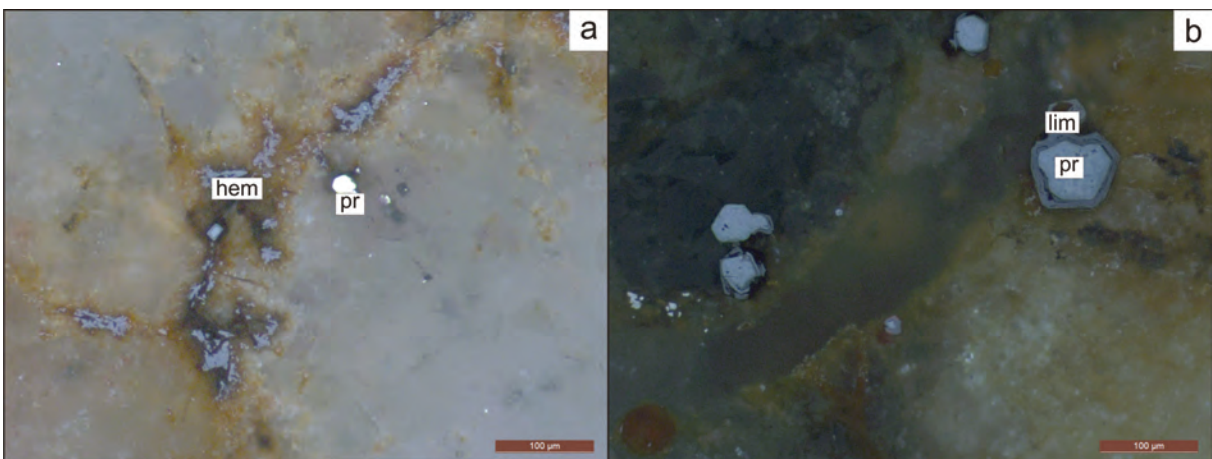


Figure 12- (a) Submicroscopic hematite and euhedral pyrite (b) Euhedral limonitized pyrite along the cleavage planes (hem: hematite, lim: limonite, pr: pyrite)

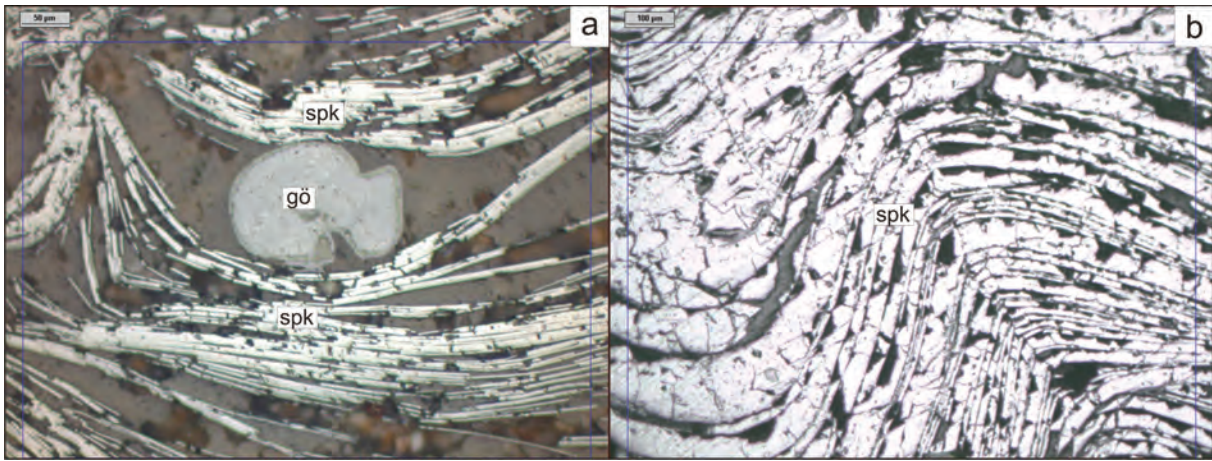


Figure 13- (a) Specularites surrounding the goethite (b) Folding structures in the specularites (spk: specularites, gö: goethite).

### 3.4. Hematites and Limonites

Abundant hematites and partly pyrite-formed limonites which filled up the cracks and spaces were determined in the polished samples. The hematites and limonites are partly developed as intergrowth grains. The forms of hematites are generally observed as in rhombohedral and sheets having different thicknesses and shows blood to red internal reflections, slightly bended structures with submicroscopic and stain. The

typical growing textures identified in the hematites and strain twins lamellae were observed in some sections. The limonitization throughout cracks/fractures, cleavage planes and grain boundaries were distinctively determined on the hematite mineral.

Limonites were observed as the pseudomorph of the pyrites and stains that filled along the cracks-fractures (Figure 14).

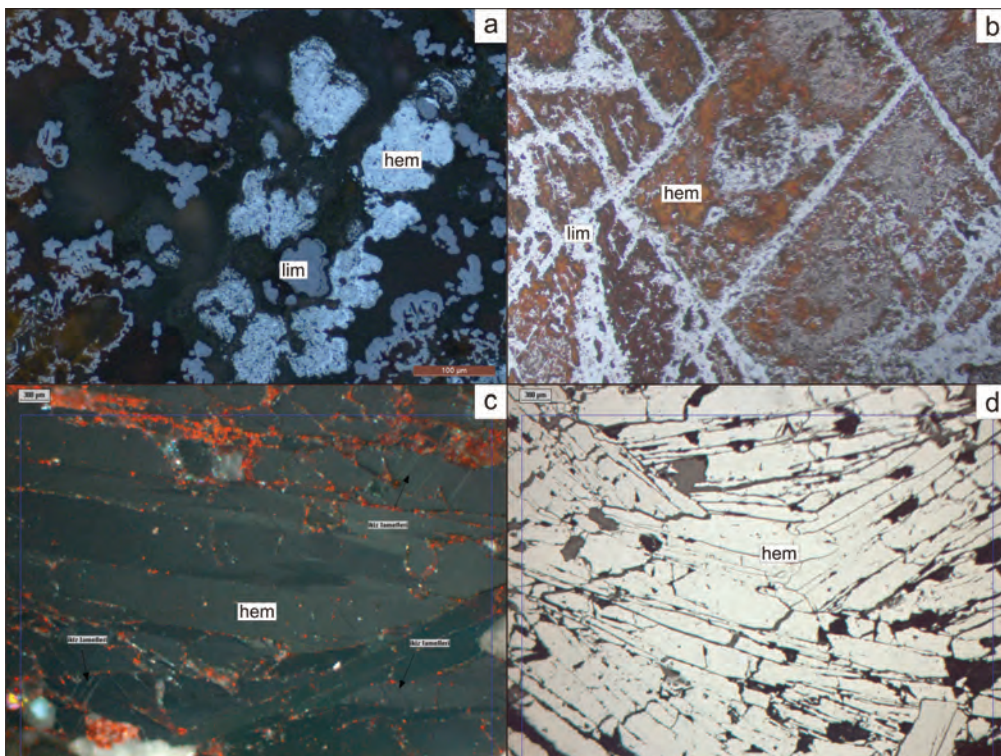


Figure 14- (a) Hematite within limonite (b) Limonitized hematite along the cleavage planes and mineral boundaries (c) Twin lamella in the hematite (d) Bended hematite plates (hem: hematite, lim: limonite).

### 3.5. Siderites

Siderites are the predominant mineral in the genesis of the iron deposits in the basin. Siderite may turn into hematite or magnetite depending on the change of the Eh and pH but may be easily converted to secondary siderite even at low temperatures in supergenetic enrichments (Bubenicek, 1964). In the petrographic studies, the rhombohedral forms as derived by the siderite alteration products in the hematites were determined from the samples taken from the different parts of the basin in the studied area. In this context, the siderites were largely altered to hematites and carbonate minerals or were substituted by hematites and then altered to the limonites along the grain boundaries.

Siderites were mineralogically and petrographically formed from the iron bearing carbonate minerals that

showed meso-micro crystalline grain size, cleavage planes, limonitized texture near the boundaries of the grains and strain twins due to the deformation (Figure 15). In addition, the limonites and limonitized strains with rarely subhedral/anhydral limonitized pyrites which occurred along the cleavage planes were observed in the siderite bearing samples (Figure 16).

### 4. SEM Studies

The ore microscopy studies on the hematite minerals showed that they have carbonate forms. Thus, SEM/EDX analyses were performed on the carbonate minerals to determine their chemistry. The analyses were done in the Mineralogy-Petrography Laboratory of the Department of Mineral Analysis, MTA using FEI Quanta 400 MK2 SEM instrument with EDAX Genesis XM4i EDS detector. The selected polished samples were prepared and coated with carbon before analyses.

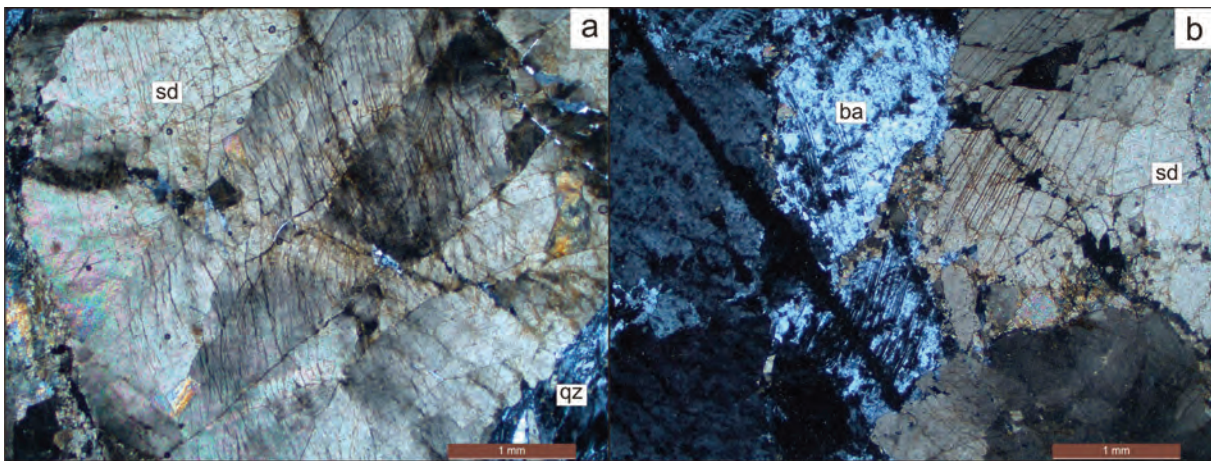


Figure 15- Microphotographs of the siderites, (a) limonitized siderites along the cleavage planes, (b) barite mineral associated with siderites (sd: siderite, qz: quartz, ba: barite).

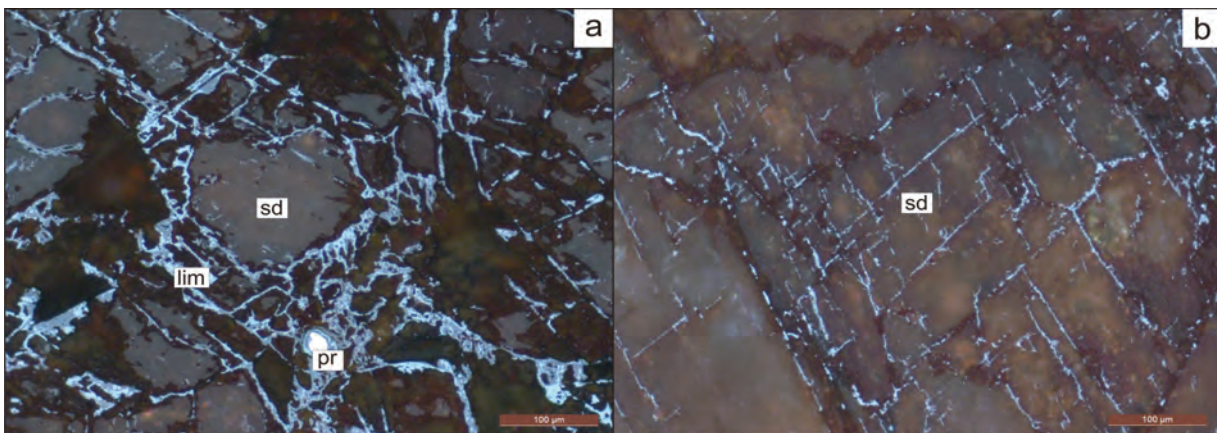


Figure 16- (a) limonitized siderites and pyrite minerals observed in the boundaries and fractures, (b) limonitized siderites along cleavage planes, (lim: limonite, sd: siderite, pr: pyrite)

The elemental analyses were carried out on the 25 spots of the samples by getting their back scatter electron and secondary electron signal images.

The elements Fe, Ca, Mg and Mn were primarily detected in the darker minerals than iron oxides minerals in the polished samples (Figure 17). S, K, Si and Al elements in these minerals were also detected. These elemental patterns clearly reveal that the host mineral associated with hematites is composed of siderite. It is known that Mn, Mg, P, Ca, Zn and Co elements are observed in their chemistry, although their chemical formula are  $FeCO_3$ . These data show that the carbonate forms observed within the hematites in the polished samples were composed of siderites and hematite formed by the alteration products of the siderites.

### 5. Geochemistry

A total of 89 samples (78 of which are hematite-goethite and 11 siderite) were collected and analyzed from the core drillings operated by MTA from open pit areas of Karaçat iron deposit, Taşlıkdere iron deposit, İnniktepe iron deposit, Menteşdere iron deposit, Kartalkaya iron deposit and Attepe iron deposit, Demirçoluğu creek in the north of Karaçat iron deposit and Karaköy village (Table 1). The major oxides and rare earth elements of the hematite-goethite and siderite samples taken from same and different parts of the iron deposits display similar elemental patterns.

The average major oxides, trace and rare earth elements of the studied samples normalized against chondrite (Sun et al., 1980) show that elemental patterns of the hematites-goethites and siderites present similar patterns (Figure 18, 19). These findings show that the ore minerals (hematites and goethites) in the studied area have the same origin and alteration products of the siderites.

### 6. Ore Type Distributions

The iron mineralizations in the Mansurlu Basin were generated in five different stratigraphical stages from Late Neoproterozoic to Early Ordovician. The iron mineralizations were formed as siderite and/or hematite, magnetite, pyrite and ankerite in the Late Neoproterozoic and Early Cambrian series (1), as siderite and/or hematite in the Early Cambrian quartzites and Middle Cambrian meta-carbonates (2), as hematite and specularite in the Middle Cambrian meta-carbonates (3), as hematite in the calc-schists in the Middle Cambrian meta-carbonates and Late Cambrian-Early Ordovician series (4) and as siderite and/or hematite in the Early Ordovician calc-schist lenses and shales (5) (Figure 20).

The results show that hematite mineralization observed in the iron deposits of the Mansurlu Basin was the primary alteration products of the Late Neoproterozoic-Early Cambrian iron ores.

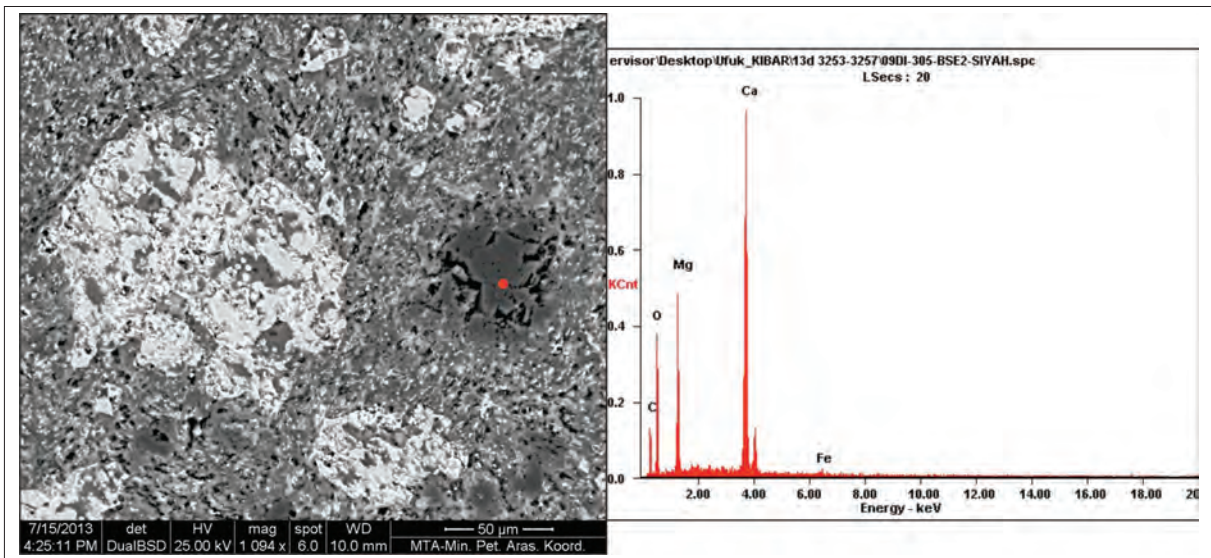


Figure 17- BSE images and EDAX graph of the hematite sample of the İnniktepe Iron Deposits (red spot mark the location of the analysis).

Table 1- Geochemical analyses of the iron deposits in the Mansurlu area (min: minimum value, max: maximum value, mean: arithmetic mean).

	Karaçat Iron Deposit						Taşlıktepe Iron Deposit						İnniktepe Iron Deposit		
	hematite+goethite n=36			siderite n=4			hematite+goethite n=13			siderite n=6			hematite+goethite n=14		
	min.	max.	mean	min.	max.	mean	min.	max.	mean	min.	max.	mean	min.	max.	mean
%															
SiO <sub>2</sub>	0,5	34,8	4,32	0,6	11,5	5,53	1,50	9,30	4,97	2,10	8,40	4,93	0,50	8,10	1,67
TiO <sub>2</sub>	0,07	0,1	0,07	0,07	0,07	0,07	0,07	0,07	0,07	0,07	0,07	0,07	0,07	0,07	0,07
Al <sub>2</sub> O <sub>3</sub>	0,07	1,9	0,21	0,1	0,6	0,28	0,10	1,40	0,60	0,30	1,40	0,77	0,07	0,20	0,10
Fe <sub>2</sub> O <sub>3</sub>	51,6	94,2	86,42	58,6	64,1	60,20	53,40	82,30	68,23	29,30	53,40	35,40	43,70	84,60	62,79
MnO	0,4	1,7	1,37	0,9	1,2	1,10	0,70	1,70	1,18	0,80	1,20	0,93	0,20	0,70	0,44
MgO	0,07	2,8	0,41	1,3	2,1	1,75	0,20	3,20	1,03	0,30	6,30	1,40	0,20	7,10	1,57
CaO	0,1	6,3	0,86	0,3	0,9	0,55	0,20	16,10	5,28	16,50	32,40	26,47	3,10	24,60	15,41
Na <sub>2</sub> O	0,07	0,1	0,07	0,07	0,07	0,07	0,07	0,07	0,07	0,07	0,07	0,07	0,07	0,07	0,07
K <sub>2</sub> O	0,07	0,4	0,09	0,07	0,2	0,11	0,07	0,20	0,12	0,07	0,40	0,19	0,07	0,07	0,07
P <sub>2</sub> O <sub>5</sub>	0,07	0,2	0,07	0,07	0,1	0,08	0,07	0,60	0,12	0,07	0,10	0,08	0,07	0,07	0,07
A.Z.	3,9	16,99	6,16	30	30,8	30,40	10,90	31,40	18,28	24,60	36,80	29,78	10,90	27,70	17,98
ppm															
Ba	6,759	3000	717,87	14	7500	1957,00	50,00	1540,00	464,16	231,14	1000,00	431,63	3,50	119,72	54,85
Rb	0,3	23	4,48	7	7	7,00	0,70	7,00	2,92	0,50	7,00	2,83	0,14	0,90	0,32
Sr	3,5	279	25,47	7	102	54,50	3,50	66,00	8,85	3,50	72,00	15,97	3,50	182,00	22,26
Zr	4	77	10,03	-	-	-	2,00	5,00	3,30	0,35	24,00	12,09	7,00	13,00	9,71
Nb	1	7	3,21	7	14	10,50	1,00	7,00	2,62	0,35	7,00	2,78	0,35	0,35	0,35
Ni	3,5	29	14,44	3,5	11	7,38	41,00	114,00	73,31	21,00	53,00	32,50	13,00	64,00	38,64
Co	4	210	47,89	7	14	10,50	6,00	14,00	9,15	4,00	7,00	5,50	2,00	10,00	7,07
Zn	20,598	89	38,99	30	41	35,50	14,32	29,00	21,20	14,21	43,00	20,29	3,98	26,93	17,28
Cr	3,5	248	17,49	7	21	14,00	3,50	7,00	4,31	3,50	7,00	4,67	3,50	3,50	3,50
La	0,2	7	1,97	7	28	17,50	0,30	7,00	2,75	1,30	7,00	3,35	1,10	4,90	2,35
Ce	0,6	5,9	2,12	-	-	-	0,80	6,20	3,71	3,90	5,00	4,53	1,70	12,00	4,95
Pr	0,1	1	0,39	-	-	-	0,20	1,40	0,81	1,00	1,20	1,10	0,40	2,00	0,86
Nd	0,8	29	7,56	14	19	16,25	1,00	19,00	7,68	5,60	10,00	7,08	2,10	8,20	3,50
Sm	0,4	2,9	1,13	-	-	-	0,50	3,90	2,34	3,00	3,50	3,33	0,80	3,70	1,70
Eu	1	4,4	2,34	-	-	-	0,50	7,20	2,81	2,00	2,70	2,30	0,20	3,60	1,74
Gd	0,5	3,3	1,37	-	-	-	0,80	5,00	3,06	3,60	4,50	4,18	0,60	4,20	2,34
Tb	0,07	0,5	0,22	-	-	-	0,10	0,80	0,45	0,60	0,70	0,65	0,07	0,70	0,38
Dy	0,6	3,1	1,47	-	-	-	0,80	3,90	2,42	3,40	3,80	3,60	0,30	3,20	1,86
Ho	0,2	0,6	0,32	-	-	-	0,20	0,70	0,43	0,60	0,70	0,65	0,07	0,40	0,27
Er	0,6	1,8	1,03	-	-	-	0,60	1,90	1,22	1,70	1,90	1,78	0,07	1,00	0,58
Tm	0,07	0,3	0,15	-	-	-	0,07	0,30	0,16	0,20	0,20	0,20	0,07	0,10	0,08
Yb	0,6	7	2,48	7	7	7,00	0,60	7,00	2,55	1,40	7,00	3,37	0,07	0,90	0,35
Lu	0,07	0,4	0,17	-	-	-	0,07	0,30	0,14	0,20	0,20	0,20	0,07	0,10	0,07
Y	3,1	13,2	6,59	7	7	7,00	3,10	12,80	7,81	7,00	12,20	10,00	1,20	7,80	4,64
Cs	0,07	0,07	0,07	-	-	-	0,07	1,30	0,29	0,07	0,10	0,09	0,07	0,10	0,07
Ta	0,35	5	1,64	-	-	-	0,35	2,00	0,78	0,35	1,00	0,51	0,35	0,35	0,35
Hf	0,35	3	1,84	-	-	-	0,35	4,00	2,44	2,00	3,00	2,25	2,00	4,00	3,00
Ag	0,7	0,7	0,70	-	-	-	0,70	0,70	0,70	0,70	0,70	0,70	0,70	0,70	0,70
Bi	3,5	16,801	9,79	-	-	-	13,42	36,43	20,09	16,51	18,64	18,05	0,35	20,16	11,23
Li	3,5	3,5	3,50	-	-	-	3,50	3,50	3,50	3,50	3,50	3,50	3,50	3,50	3,50
Se	7	7	7,00	-	-	-	7,00	7,00	7,00	7,00	7,00	7,00	0,70	7,00	1,15
Sn	3,5	3,5	3,50	-	-	-	3,50	3,50	3,50	3,50	3,50	3,50	3,50	3,50	3,50
Ti	14	14	14,00	-	-	-	14,00	14,00	14,00	14,00	14,00	14,00	1,40	14,00	2,30
Au	1,4	1,4	1,40	-	-	-	1,40	1,40	1,40	1,40	1,40	1,40	1,40	395,00	56,67
Cd	0,07	0,1	0,07	-	-	-	0,07	0,10	0,08	0,07	0,07	0,07	0,07	0,70	0,15
Ga	1,4	3,9	2,07	-	-	-	0,80	3,30	1,61	1,10	1,20	1,15	0,20	1,60	0,99
In	1,3	3,5	2,07	-	-	-	0,20	0,90	0,56	0,30	0,40	0,33	0,07	2,70	0,97
Sc	0,07	7	1,55	7	7	7,00	0,07	7,00	2,04	0,30	7,00	2,72	0,07	0,50	0,10
Th	1,4	260	50,11	150	160	155,00	1,40	180,00	36,46	1,40	70,00	22,60	1,40	1,40	1,40
Tl	0,14	0,14	0,14	-	-	-	0,14	0,14	0,14	0,14	0,14	0,14	0,14	11,00	2,30
U	1,4	70	13,68	38	39	38,50	1,40	62,00	12,42	2,70	75,00	25,62	1,40	26,90	9,36
As	11	33	19,26	-	-	-	14,00	27,00	18,10	3,00	18,00	9,00	0,35	4,00	1,39
Be	0,35	1	0,41	-	-	-	0,35	5,00	1,14	0,35	1,00	0,84	0,35	0,35	0,35
Cu	1	21	5,64	3,5	3,5	3,50	1,00	5,00	2,42	2,00	4,00	2,83	1,00	18,00	2,79
Ge	0,35	4	1,41	-	-	-	0,35	5,00	1,77	0,35	2,00	0,93	0,35	0,35	0,35
Mo	0,35	1	0,41	-	-	-	0,35	1,00	0,42	0,35	1,00	0,51	0,35	0,35	0,35
Pb	0,35	73	10,92	12	14	13,50	2,00	62,00	28,46	1,00	51,00	15,33	13,00	54,00	34,79
Sb	8	17	13,70	-	-	-	8,00	17,00	12,40	5,00	10,00	7,75	0,35	0,35	0,35
V	7	32	15,69	7	7	7,00	7,00	22,00	15,46	7,00	19,00	13,17	2,00	9,00	3,00

Iron Deposits of the Karaçat and Surrounding Area

Table 1- Geochemical analyses of the iron deposits in the Mansurlu area (min: minimum value, max: maximum vale, mean: aritmetic mean) (cont.).

	Menteşdere Iron Deposit			Karaköy drilling			Attepe Iron Deposit	Demirçoluğu creek	Kartalkaya Iron Deposit
	hematite+goethite n=5			hematite+goethite n=8			hematite+goethite n=1	siderit n=1	hematite+goethite n=1
%	min.	max.	mean	min.	max.	mean			
SiO <sub>2</sub>	1,20	2,60	1,80	1,80	22,60	6,93	7,7	3	2,5
TiO <sub>2</sub>	0,07	0,07	0,07	0,07	0,20	0,09	0,07	0,07	0,07
Al <sub>2</sub> O <sub>3</sub>	0,07	0,20	0,15	0,20	4,30	1,14	0,3	0,1	0,2
Fe <sub>2</sub> O <sub>3</sub>	77,30	85,10	81,60	42,60	61,10	54,49	80,3	60,2	73,9
MnO	1,30	1,90	1,58	0,60	1,00	0,81	1,3	0,07	1,2
MgO	0,10	0,40	0,28	0,10	0,80	0,45	0,4	3,2	0,4
CaO	0,10	7,20	2,94	0,10	0,50	0,23	1,4	0,9	6,1
Na <sub>2</sub> O	0,07	0,07	0,07	0,07	0,07	0,07	0,07	0,07	0,07
K <sub>2</sub> O	0,07	0,07	0,07	0,07	0,80	0,22	0,07	0,3	0,07
P <sub>2</sub> O <sub>5</sub>	0,07	0,20	0,10	0,07	0,10	0,07	0,07	0,07	0,07
A.Z.	10,35	12,00	11,46	7,95	16,40	10,88	8,19	31,88	15,4
ppm									
Ba	1000,00	2500,00	1700,00	70,00	54100,00	6952,50	1365	70	7000
Rb	7,00	7,00	7,00	-	-	-	10,5	10,5	7
Sr	7,00	42,00	19,20	70,00	800,00	161,25	10,5	10,5	102
Zr	-	-	-	-	-	-	21	21	-
Nb	7,00	7,00	7,00	-	-	-	-	-	7
Ni	3,50	12,00	5,20	-	-	-	21	21	30
Co	7,00	10,00	7,60	-	-	-	210	210	60
Zn	35,00	82,00	53,20	-	-	-	79	69	149
Cr	7,00	7,00	7,00	-	-	-	42	42	16
La	7,00	7,00	7,00	-	-	-	-	-	7
Ce	-	-	-	-	-	-	-	-	-
Pr	-	-	-	-	-	-	-	-	-
Nd	21,00	24,00	22,60	-	-	-	-	-	30
Sm	-	-	-	-	-	-	-	-	-
Eu	-	-	-	-	-	-	-	-	-
Gd	-	-	-	-	-	-	-	-	-
Tb	-	-	-	-	-	-	-	-	-
Dy	-	-	-	-	-	-	-	-	-
Ho	-	-	-	-	-	-	-	-	-
Er	-	-	-	-	-	-	-	-	-
Tm	-	-	-	-	-	-	-	-	-
Yb	7,00	7,00	7,00	-	-	-	-	-	7
Lu	-	-	-	-	-	-	-	-	-
Y	7,00	7,00	7,00	-	-	-	-	-	7
Cs	-	-	-	-	-	-	-	-	-
Ta	-	-	-	-	-	-	-	-	-
Hf	-	-	-	-	-	-	-	-	-
Ag	-	-	-	-	-	-	-	-	-
Bi	-	-	-	-	-	-	-	-	-
Li	-	-	-	-	-	-	-	-	-
Se	-	-	-	-	-	-	-	-	-
Sn	-	-	-	-	-	-	-	-	-
Ti	-	-	-	-	-	-	-	-	-
Au	-	-	-	-	-	-	-	-	-
Cd	-	-	-	-	-	-	-	-	-
Ga	-	-	-	-	-	-	-	-	-
In	-	-	-	-	-	-	-	-	-
Sc	7,00	7,00	7,00	-	-	-	-	-	7
Th	90,00	210,00	178,00	-	-	-	-	-	190
Tl	-	-	-	-	-	-	-	-	-
U	41,00	67,00	52,80	-	-	-	-	-	45
As	-	-	-	-	-	-	-	-	-
Be	-	-	-	-	-	-	-	-	-
Cu	3,50	3,50	3,50	-	-	-	21	21	26
Ge	-	-	-	-	-	-	-	-	-
Mo	-	-	-	-	-	-	-	-	-
Pb	7,00	28,00	12,80	-	-	-	14	14	41
Sb	-	-	-	-	-	-	-	-	-
V	7,00	7,00	7,00	-	-	-	10,5	16	20

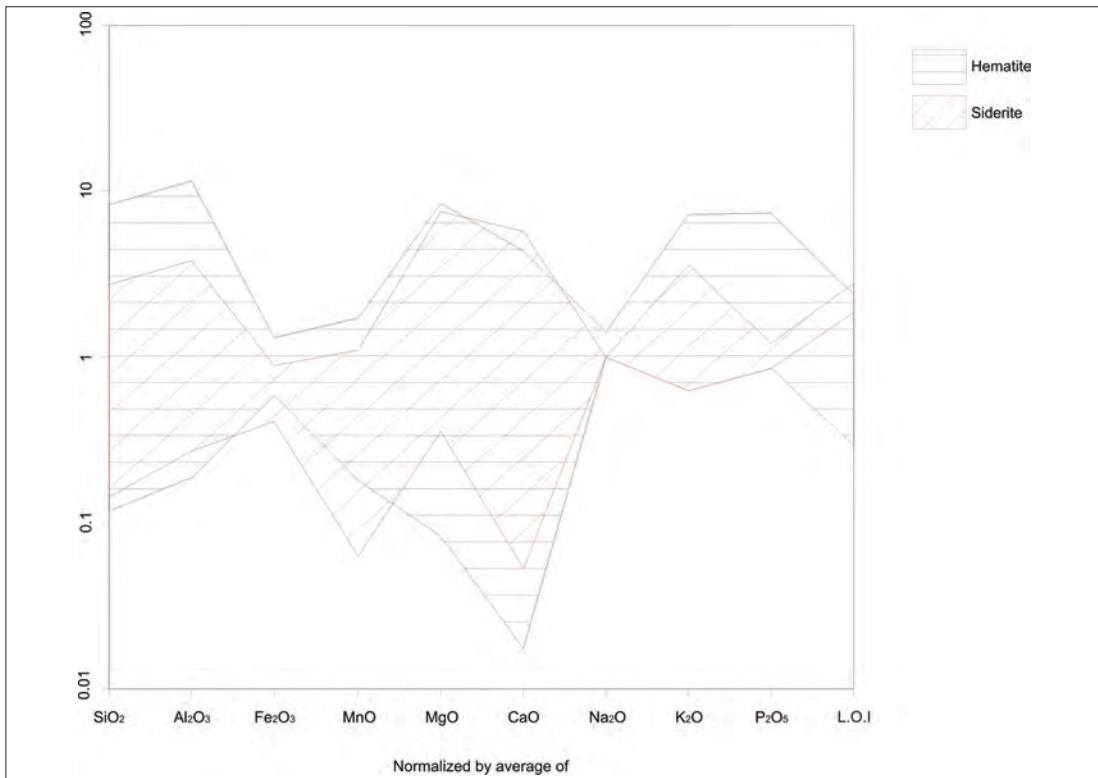


Figure 18- Major-oxides average-normalized diagrams of the hematites and siderites.

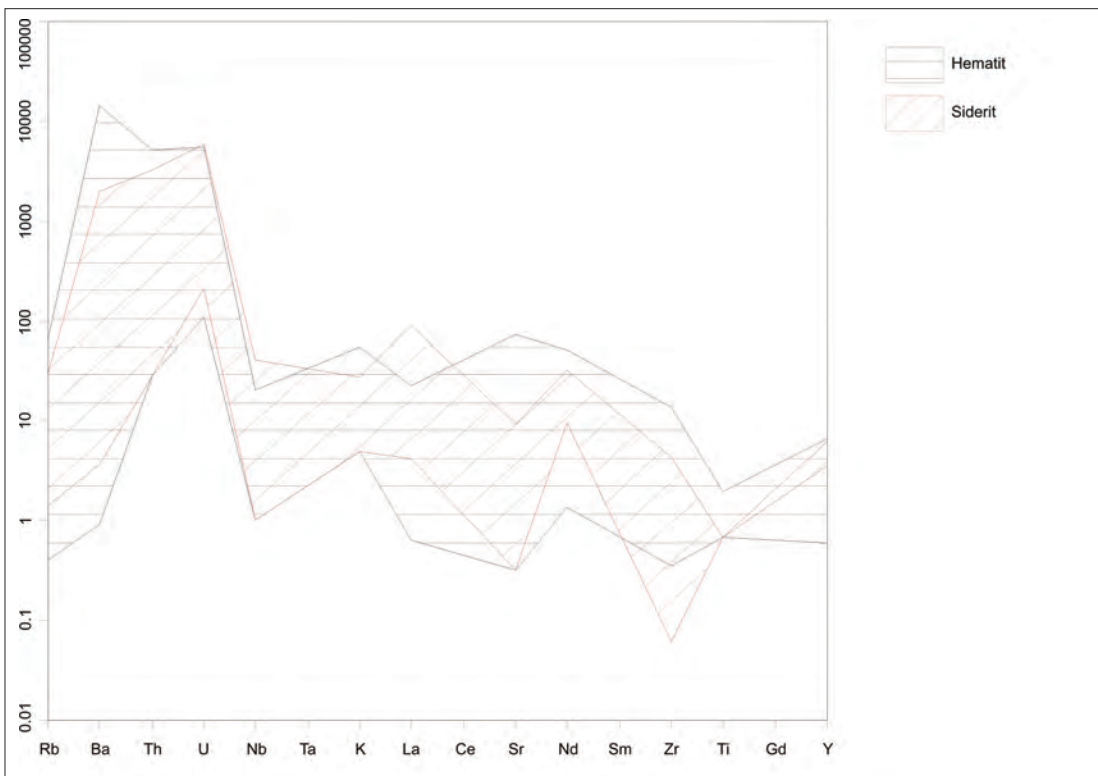


Figure 19- Trace elements chondrite-normalized diagrams of the hematites and siderites (normalization data from Sun et al., 1980).

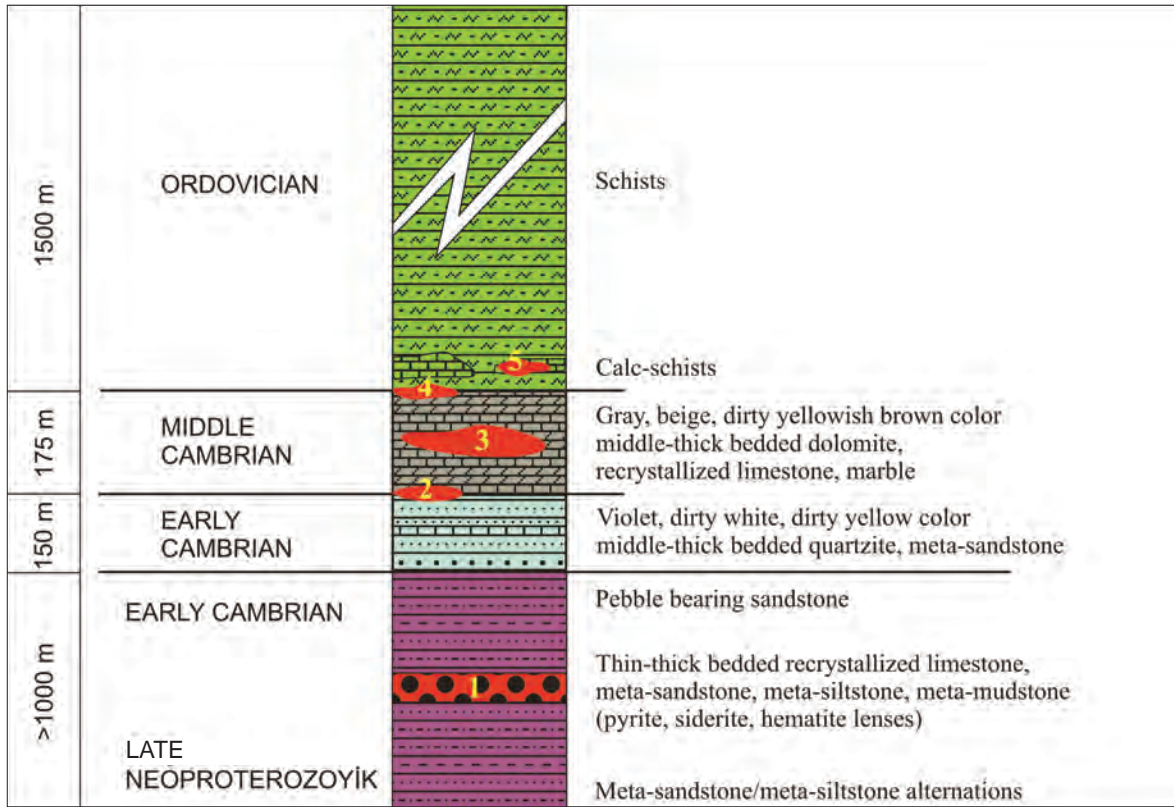


Figure 20- Stratigraphic columnar section of the iron mineralization.

## 7. Discussion, Correlation and Interpretation

The presence of the bimodal magmatism and rift related basin formed in the back-arc environment was previously discussed based on mineralogical, petrographical, geochemical and geostatistical methods in the earlier studies and in this study (Dayan, 2007; Dayan et al., 2008; Tiringa, 2009; Tiringa et al., 2009). The rift related sequence observed in the Early Cambrian Koçyazı formation in the eastern Taurides can be correlated with similar rock units cropping out in the central Taurides (Gürsu and Göncüoğlu, 2005a). Tringa et al. (2009) mentioned that first-stage of the rifting process observed in Sandıklı during the Early Cambrian might have been started during the Late Neoproterozoic period in the Kayseri-Adana Basin. İlinai et al. (2001) proposed a model about duration time of the rifting process and mentioned that the spreading rates in the intra-continental rifting are much higher than back-arc basins as showing the extension in the Arap Plate and opening of the Red Sea that occurred within the last 30 my. On the contrary, lithospheric thinning rates in the North Australian Craton was much slower than Arabian Plate and the continental breakdown continued nearly

140 my (Betts et al., 2003). Rapid extensional process is generally associated with the fast increase of the geothermal gradient and genesis of the large volume magmatism (Betts et al., 2003). The limited magmatic products in the studied area and lithological and magmatic correlations with the equivalent units in the Sandıklı (western Taurides) indicate that the back arc rifting process might have been formed during the Late Neoproterozoic to Early Cambrian.

There are different suggestions about the genesis of the iron mineralization in the Mansurlu basin in the previous studies. One part of these studies mentioned that the formation of the iron deposits might be related with the hydrothermal type epigenetic mineral deposits that may be in contact with deep-seated granitic rocks (Henden and Önder, 1980; Küpeli, 1991; Küpeli et al., 2006). However, recent studies suggest a metamorphosed volcanic syn-sedimentary and/or exhalative syn-sedimentary mineral deposit model for the genesis of the iron mineralization (Dayan et al., 2008; Tiringa et al., 2009, 2011). The presence of bimodal volcanism in the studied area also supports the volcanic syn-sedimentary and/or exhalative syn-sedimentary deposit models previously proposed by

the recent studies. Another approach against the other models is that the metals, which are the origin of ores, might have been transported from land into the basin and deposited by the chemical sedimentation.

As a result of subduction of the Proto-Tethys Ocean beneath the Tauride-Anatolide Platform (TAP) in the Late Neoproterozoic, the arc magmatism was developed on the continental margin of the TAP and arc-related basic and acidic volcanics and their tuffs bearing siliciclastic rocks (Emirgazi formation) were deposited at the fore-arc environment (Dayan, 2007; Dayan et al., 2008; Tiringa, 2009; Tiringa et al., 2009; Tiringa et al., 2011). The rifting process was developed in the continental crust by the extensional regime that resulted in the rollback of the subducted Proto-Tethys Ocean during the Early Cambrian (Gürsu and Göncüoğlu, 2005; Gürsu et al., 2015; Gürsu, 2016) (Figure 21a).

The thinning of the continental crust in the preliminary stages of rifting resulted in the genesis of the anatexis granites followed by the formation of the basic and intermediate submarine volcanic rocks and its derivatives along the fracture zones due to the mantle upwelling processes. They were deposited together with the coeval sediments and formed the volcanosedimentary sequences (Koçyazı formation) in the basin during the Early Cambrian (Figure 21b, c). In this tectonic environment, the areas having different Eh and pH values depending on the topography of the basin will lead to the formation of stratiform and stratabound type mineralizations there (Dayan, 2007; Dayan et al., 2008). The iron ore forming metals are accompanied either by solutions/melts enriched by ionic metals in marine water, which flows down through fractures into depths, then warms up and rises to the submarine environment, or by Fe<sup>+2</sup> included melts transported from the basic rocks cropped out in the land by the weathering processes. The solutions enriched with metals by discharging onto the sea bottom, can be deposited as magnetite, siderite and/or hematite and pyrite based on their Eh and pH characteristics.

The diversity of the mineralization and magmatism were directly related with the continuity of the subduction of the oceanic crust and breakoff process (Figure 21d). The succession and mineralizations affected by the active deformational phases and metamorphism processes were exhumed to the surface by the post-mineral faults and denudation processes.

These fault zones created suitable environments for the processes of karstification and resulted in the enrichment of the limonites and goethites by the alterations of the primary ore minerals of the siderites and/or hematites. The secondary coarse grain siderites which filled up the fractures cutting the sedimentary siderites in the Attepe Iron Deposits and goethite/limonite rich karstic fills observed in the base of the open-pit mine also support our model proposed above. Similar karst infilling mineralization is widely observed in the Karaçat and Kızıl Iron Deposits. Dayan et al. (2008) emphasized that metals dissolved from primary sedimentary origin iron minerals were formed by the late stage mineralized vein and veinlets, which pass through most of the rocks in the region along the fracture zones.

Iron mineralizations in the study area based on similar volcanic features can be correlated with Lahn-Dill in West-Central Germany, Zamora in Romania, Vares in Yugoslavia, Zarigan-Chahmir in Central Iran in the world and with Deveci Iron Deposit in Turkey. But, the metamorphosed type of exhalative sedimentary iron deposits of BIFs named as "Algoma Type" (Bottke, 1981) also presents similar features of the studied iron deposits.

## 8. Conclusions

The study area is located within the Mansurlu and Feke slices representing rock units of the Geyikdagi Unit in the Eastern Taurides of the Tauride-Anatolide platform (TAP) and are composed of outcrops of the Late Proterozoic Emirgazi formation, Early Cambrian Koçyazı and Zabuk formations, Middle Cambrian Değirmentaşı formation and Early to Late Ordovician Armutludere formation.

Iron mineralizations in the study area have tectonically contacted with host rocks today. The oblique and strike slip faults which had contact with the iron mineralizations were determined in the studied area and the deformational forces that affected the fault systems are concentrated in the NE-SW and NW-SE directions in the studied area.

The hematite-goethite-limonite, siderite-limonite, pyrite-limonite, chromite-magnetite and magnetite-ilmenite alterations and bended/broken parts on the specularites were determined in the ore microscopy. In addition, the rhombohedral forms of the carbonate minerals in the hematite are widespread in the studied area.

Iron Deposits of the Karaçat and Surrounding Area

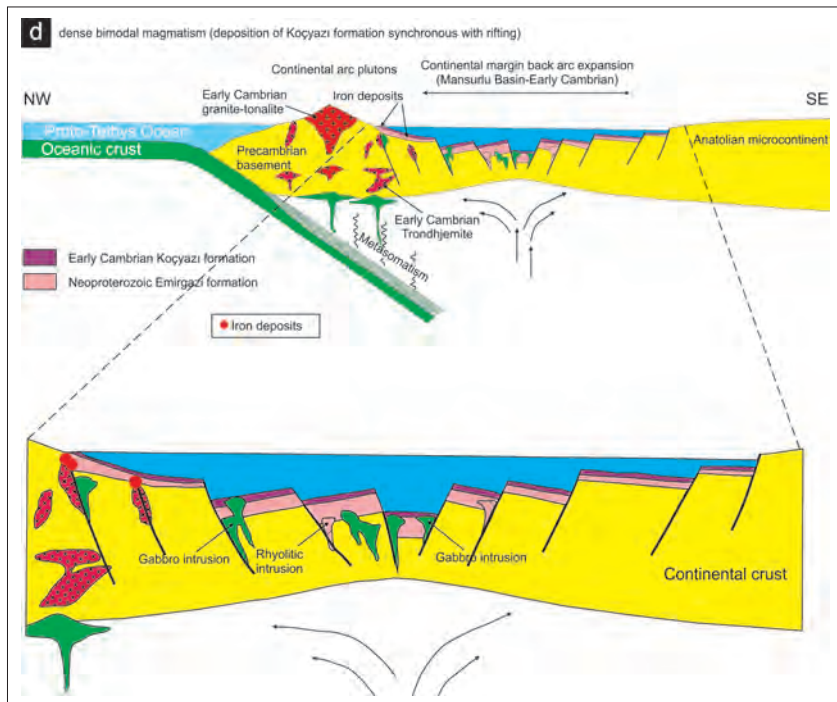
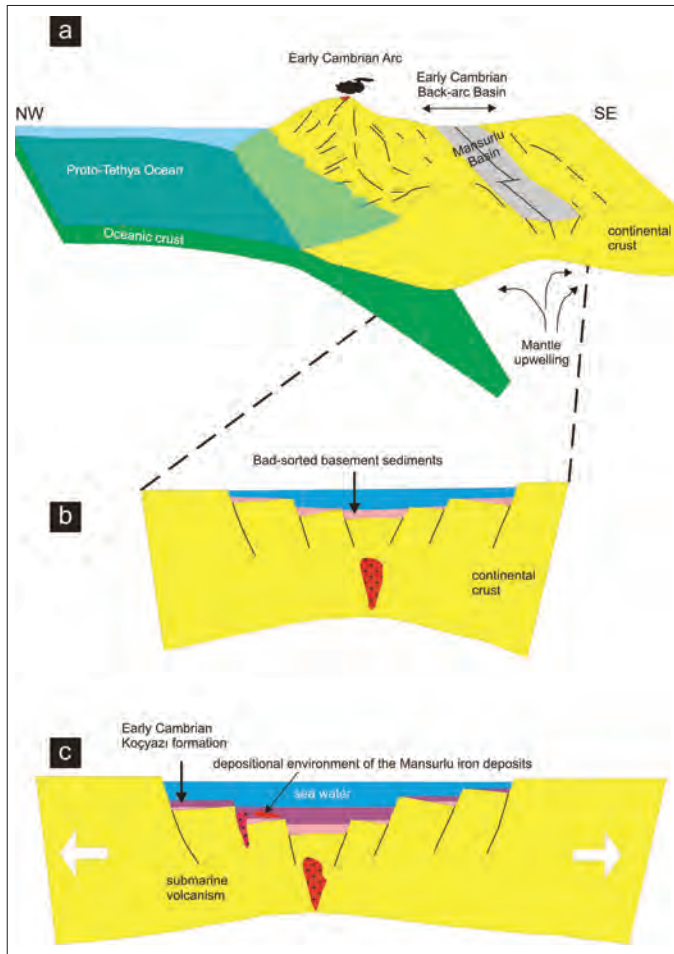


Figure 21- Geodynamic evolution of the genesis of the iron mineralization in the Mansurlu Basin (modified from Gürsu and Gönçüoğlu, 2005b; Rajabi et al., 2015).

The predominant Ca, Fe, Mn and Mg elements with S, K, Al and Si were determined on the rhombohedral forms of the hematites in SEM analyses. This data indicate that hematite with carbonate forms represent the alteration products of primary siderites.

The multi-elemental patterns of the hematite and siderite samples display similar trends in the major oxides and chondrite normalized trace element diagrams. This result geochemically supports that hematites were derived from the alteration products of primary siderites.

The field and ore microscopy studies show that the main ore minerals are composed of siderite and/or hematite, magnetite and pyrite as primary minerals. They are widely observed within the Late Neoproterozoic Emirgazi formation and Early Cambrian Koçyazı formation, where they are commonly placed within the contact of the sedimentary rocks of the formations. The field observations, ore microscopy, SEM/EDX results combined with the geochemical analyses show that the iron ores representing the late-stage of the mineralization were also formed within the Early Cambrian Zabuk formation, Middle Cambrian Değirmendere formation and Early to Late Ordovician Armutludere formation.

The primary source of the mineralization in the studied area might have been formed from volcanosedimentary-type or exhalative sedimentary-type (syn-sedimentary) deposits and the mineralization later have undergone metamorphism and tectonic events to exhume to the recent position.

### Acknowledgement

This study is the summary of PhD thesis of the first author under the supervisor of the second author at the Graduate School of Natural and Applied Sciences, Department of Geological Engineering of Ankara University. The authors thank to Şükrü Koç (Ankara University) for his contributions during ore microscopy studies, Okan Delibaş (Hacettepe University) for constructive comments and Emmanuel D. Sunkari for linguistic editing. The anonymous reviewers are acknowledged and improved the paper.

### References

- Arda, N., Tiringa, D., Ateşçi, B., Akça, A., Tufan, E. 2008. Yahyalı (Kayseri)-Mansurlu (Feke-Adana) Yöresi Demir Sahaları Maden Jeolojisi Ara Raporu. *Maden Tetkik ve Arama Genel Müdürlüğü Rapor No: 44437*, 75 s., Ankara (unpublished).
- Arıkan, Y. 1966. Adana İli, Kozan ve Feke İlçeleri Demir Zuhurları Hakkında Ön Rapor. *Maden Tetkik ve Arama Genel Müdürlüğü Rapor No: 859*, Ankara (unpublished).
- Arıkan, Y. 1968. Mansurlu Demir Zuhurları (Feke-Yahyalı; Adana-Kayseri). *Maden Tetkik ve Arama Genel Müdürlüğü Rapor No: 410*, Ankara ((unpublished).
- Betts, P. G., Giles, D., Lister, G. S. 2003. Tectonic Environment of Shale Hosted Massive Sulfide Pb-Zn-Ag Deposits of Proterozoic Northeastern Australia. *Economic Geology*, 98, 557-576.
- Bottke, H. 1981. Lagerstättenkunde des Eisens. *Verlag Glückauf GmbH*, Essen, 202.
- Brennich, G. 1961. Türkiye’de Demir Cevheri Zuhuratu. *Maden Tetkik ve Arama Genel Müdürlüğü Rapor No:3440*, Ankara (unpublished).
- Bubenicek, L. 1964. L’Oxydo-réduction en sédimentologie. *Bulletin BRGM*, 4, 1-36.
- Cihnioglu, M., İşbaşı, O., Ceyhan, Ü, Adıgüzel, O. 1994. Türkiye Demir Envanteri. *Maden Tetkik ve Arama Genel Müdürlüğü yayını*, Ankara.
- Çolakoğlu, A. R., Kuru, S. G. 2002. Attepe Demir Yatağı’nda Jeotermometrik Ölçüm Çalışmaları. *Maden Tetkik ve Arama Genel Müdürlüğü Dergisi*, 125, 1-11.
- Dağlıoğlu, C., Bahçeci, A. 1992. Adana-Feke-Mansurlu TDÇİ Ruhsat Sahalarının (Attepe, Koruyeri (Mağarabeli) Değerlendirme Raporu. *Maden Tetkik ve Arama Genel Müdürlüğü Rapor No: 9339*, Ankara (unpublished).
- Dağlıoğlu, C., Bahçeci, A., Akça, İ. 1998. Attepe, Koruyeri (Mağarabeli), Hanyeri Batısı (TDÇİ Genel Müdürlüğüne Ait) Demir Madenlerinin Değerlendirme Raporu. *Maden Tetkik ve Arama Genel Müdürlüğü Rapor No: 10101*, Ankara (unpublished).

- Dayan, S. 2007. Adana-Mansurlu Attepe Civarındaki Demir Yataklarının Jeolojik, Petrografik ve Yapısal Özelliklerinin İncelenmesi. *Ankara Üniversitesi Fen Bilimleri Enstitüsü Yüksek Lisans Tezi*, 125, Ankara (unpublished).
- Dayan, S., Ünlü, T., Sayılı, İ. S. 2008. Adana-Mansurlu Attepe Demir Yatağı'nın Maden Jeolojisi. *Jeoloji Mühendisliği Dergisi*, 32, 2, 1-44.
- Demirtaşlı, E. 1967. Pınarbaşı-Sarız-Mağara Civarının Jeoloji Raporu. *Maden Tetkik ve Arama Genel Müdürlüğü Rapor No: 1935*, 129, Ankara (unpublished).
- Göncüoğlu, M. C. 2010. Introduction to the Geology of Turkey: Geodynamic Evolution of the pre-Alpine and Alpine terranes. *General Directorate of Mineral Research and Exploration, Monography Series*, 5, 1-66.
- Göncüoğlu, M. C., Dirik, K., Kozlu, H. 1997. General Characteristics of pre-Alpine and Alpine Terranes in Turkey: Explanatory Notes to the Terrane Map of Turkey. *Annales Geologique de Pays Hellenique*, 37, 515-536.
- Gürsu, S. 2016. A new petrogenetic model for meta-granitic rocks in the central and southern Menderes Massif – W Turkey: Implications for Cadomian crustal evolution within the Pan-African mega-cycle. *Precambrian Research*, 275, 450-470.
- Gürsu, S., Göncüoğlu, M. C. 2005a. Batı Toroslar'ın (Sandıklı GB'si, Afyon) Geç Neoproterozoyik ve Erken Paleozoyik Yaşlı Birimlerinin Jeolojisi ve Petrografisi. *Maden Tetkik ve Arama Genel Müdürlüğü Dergisi*, 130, 29-55.
- Gürsu, S., Göncüoğlu, M. C. 2005b. Early Cambrian back-arc volcanism in the Western Taurides, Turkey: Implications for the rifting along northern Gondwanan margin. *Geological Magazine*, 142, 5, 617-631.
- Gürsu, S., Möller, A., Göncüoğlu, M. C., Köksal, S., Demircan, H., Köksal, F. T., Kozlu, H., Sunal, G. 2015. Neoproterozoic continental arc volcanism at the northern edge of the Arabian Plate, SE Turkey. *Precambrian Research*, 258, 208-233.
- Henden, İ., Önder, E., Yurt, M.Z. 1978. Adana-Kayseri, Mansurlu-Karaköy (Attepe, Elmadağ Beli, Kızıl Mevkii, Menteşdere, Uyuzpınarı) Demir Madenleri Jeoloji ve Rezerv Raporu. *Maden Tetkik ve Arama Genel Müdürlüğü Rapor No: 6394*, Ankara (unpublished).
- Henden, İ., Önder, E. 1980. Attepe (Mansurlu) Demir Madeni'nin Jeolojisi. *Türkiye Jeoloji Kurumu Bülteni*, 23, 1, 153-163.
- İlani, S., Harlavan, Y., Tarawneh, K., Rabba, I., Weinberger, R., Ibrahim, K., Peltz, S., Steinitz, G. 2001. New K-Ar Ages of Basalts from the Harrat Ash Shaam Volcanic Field in Jordan: Implications for the Span and Duration of the Upper Mantle Upwelling Beneath the Western Arabian Plate. *Geology*, 29, 171-174.
- Küpeli, Ş. 1986. Attepe (Mansurlu-Feke) Yöresinin Demir Yatakları. *Selçuk Üniversitesi Fen Bilimleri Enstitüsü, Yüksek Lisans Tezi*, 111, Konya (unpublished).
- Küpeli, Ş. 1991. Attepe (Mansurlu-Feke) Yöresi Demir Yataklarının Jeolojik, Petrografik ve Genetik İncelemesi. *Selçuk Üniversitesi Fen Bilimleri Enstitüsü, Doktora Tezi*, 227, Konya (unpublished).
- Küpeli, Ş. 1998. Attepe (Mansurlu-Feke-Adana) Yöresi Demir Yataklarının Jeolojisi ve Kökeni. *Cumhuriyet Üniversitesi Mühendislik Fakültesi Dergisi*, Seri A-Yerbilimleri, 15, 1, 101-118.
- Küpeli, Ş., Ayhan, A., Karadağ, M. M., Arık, F., Döyem, A., Zedef, V. 2006. Attepe (Feke-Adana) Demir Yataklarındaki Siderit Mineralizasyonunun C, O, S ve Sr İzotop Çalışmaları ve Genetik Bulgular. *Jeoloji Mühendisleri Odası 59. Türkiye Jeoloji Kurultayı Bildiri Özleri Kitabı*, 143-144, Ankara.
- Lucius, M. 1927. Antitoros Silsilesinde Zamantı Suyu ile Göksu Arasında Faraşa Demir Madeni Zuhurunda Yapılan Jeolojik Taharriyet Hakkında Rapor. *Maden Tetkik ve Arama Genel Müdürlüğü Rapor No: 421*, 84, Ankara (unpublished).
- Monod, O. 1977. Recherches Geologiques Dans le Taurus Occidentaleusud de Beyşehir-Turquie). Thesed'etat, *l'Univ. De Paris sud., Center d'Orsay*, 442, Paris (unpublished).

- Önder, E., Şahin, M. 1979. Adana-Feke-Mansurlu (Hanyeri, Çaldağı, Taşlık Tepe, Mursal Tepe, Bahçecik, Çandırlar, Kısacıklı) Demir Sahaları Jeoloji ve Kozan, Saimbeyli İlçeleri Prospeksiyon Raporu. *Maden Tetkik ve Arama Genel Müdürlüğü Maden Etüt ve Arama Dairesi Rapor No: 1636*, Ankara (unpublished).
- Özgül, N. 1976. Torosların Bazı Temel Jeoloji Özellikleri Türkiye Jeoloji Kurumu Bülteni, 19, 1, 65-78.
- Özgül, N. 1983. Stratigraphy and Tectonic Evolution of the Central Taurides, Tekeli, O. and Göncüoğlu, M. C. (Ed.), *International Symposium on the Geology of the Taurus Belt*. 77-90, Ankara.
- Özgül, N., Kozlu, H. 2002. Kozan-Feke (Doğu Toroslar) Yöresinin Stratigrafisi ve Yapısal Konumu ile İlgili Bulgular. *Türkiye Petrol Jeologları Derneği Bülteni*, 14, 1, 1-36.
- Rajabi, A., Canet, C., Rastad, E., Alfonso, P. 2015. Basin evolution and stratigraphic correlation of sedimentary-exhalative Zn-Pb deposits of the Early Cambrian Zarigan-Chahmir Basin, Central Iran. *Ore Geology Reviews*, 64, 328-353.
- Sun, S. S. 1980. Lead isotopic study of young volcanic rocks from mid-ocean ridges, ocean islands and island arcs. *Philos. Trans. R. Soc. Lond.*, 297, 179-202.
- Şenel, M., Usta, D., Metin, Y., Bedi, Y., Vergili, Ö., Usta, M., Balcı, V., Kuru, K., Tok, T., Özkan, M., K., Kop, A. 2004. Kozan-Tufanbeyli (Adana) Arasındaki Yapısal Birimlerin Jeolojik Özellikleri. *Jeoloji Mühendisleri Odası 57. Türkiye Jeoloji Kurultayı*, Bildiri Özleri, 275.
- Tiringa, D. 2009. Kayseri-Yahyalı-Karaköy, Karaçat Demir Yatağının Maden Jeolojisi. *Ankara Üniversitesi Fen Bilimleri Enstitüsü Yüksek Lisans Tezi*, 139, Ankara (unpublished).
- Tiringa, D., Ünlü, T., Sayılı, İ. S. 2009. Kayseri-Yahyalı-Karaköy, Karaçat Demir Yatağının Maden Jeolojisi. *Jeoloji Mühendisliği Dergisi*, 33, 1, 1-43.
- Tiringa, D., Çelik, Y., Ateşçi, B., Akça, İ., Keskin, S. 2011. Kayseri-Adana Havzası Demir Aramaları ve Menteş Dere (Yahyalı-Kayseri) Ruhsat Sahasının Maden Jeolojisi Raporu. *Maden Tetkik ve Arama Genel Müdürlüğü Rapor No: 11435*, 153, Ankara (unpublished).
- Ünlü, T. 2003. Attepe Demir Yatağı'nda Jeotermometrik Ölçüm Çalışmaları Makalesi Üzerine Eleştiri. *Maden Tetkik ve Arama Genel Müdürlüğü Dergisi*, 126, 87-88.
- Ünlü, T., Stendal, H. 1986. Divriği Bölgesi Demir Yataklarının Element Koreasyonu ve Jeokimyası (Orta Anadolu-Türkiye). *TMMOB Jeoloji Mühendisleri Odası Dergisi*, 28, 5-19.
- Ünlü, T., Stendal, H. 1989. Divriği Bölgesi Demir Cevheri Yatakları'nın Nadir Toprak Element (REE) Jeokimyası (Orta Anadolu-Türkiye). *Türkiye Jeoloji Kurumu Bülteni*, 32, 21-37.
- Ünlü, T., Yıldırım, M., Öztürk, M., Dağlıoğlu, C., Kırkoğlu, G., Hasarı, M. 1984. Feke-Mansurlu Yöresi Demir Yataklarının Oluşum Modeli Hakkında Bir Yaklaşım. *Maden Tetkik ve Arama Genel Müdürlüğü Maden Etüt Demir İzleme Destek 50225/1104*, 3, Ankara (unpublished).





# BULLETIN OF THE MINERAL RESEARCH AND EXPLORATION

<http://bulletin.mta.gov.tr>

BULLETIN OF THE MINERAL RESEARCH AND EXPLORATION	
CONTENTS	
DELINEATION OF THE CR MINERALIZATION BASED ON THE STREAM SEDIMENT DATA UTILIZING FRACTAL MODELING AND FACTOR ANALYSIS IN THE KHOY 1:100.000 SHEET, NW IRAN	Somayeh Momeni <sup>a,*</sup> , Seyed Vahid Shahrokhi <sup>a</sup> , Peyman Afzal <sup>b,c</sup> , Behnam Sadeghi <sup>b,d,e</sup> , Taher Farhadinejad <sup>a</sup> and Mohammad Reza Nikzad <sup>e</sup>
RESEARCH ARTICLE	143

## DELINEATION OF THE CR MINERALIZATION BASED ON THE STREAM SEDIMENT DATA UTILIZING FRACTAL MODELING AND FACTOR ANALYSIS IN THE KHOY 1:100.000 SHEET, NW IRAN

Somayeh Momeni<sup>a,\*</sup>, Seyed Vahid Shahrokhi<sup>a</sup>, Peyman Afzal<sup>b,c</sup>, Behnam Sadeghi<sup>b,d,e</sup>, Taher Farhadinejad<sup>a</sup> and Mohammad Reza Nikzad<sup>e</sup>

<sup>a</sup> Department of Geological, Khorramabad Branch, Islamic Azad University, Khorramabad, Iran

<sup>b</sup> Department of Mining Engineering, Faculty of Engineering, South Tehran branch, Islamic Azad University, Tehran, Iran

<sup>c</sup> Camborne School of Mines, University of Exeter, Penryn, UK

<sup>d</sup> Department of Earth and Oceans, James Cook University, Townsville, Queensland 4811, Australia

<sup>e</sup> Hampa Behineh Consultant Engineers Co., Tehran, Iran

Research Article

### ABSTRACT

Keywords:  
Stream Sediments,  
Fractal Analysis,  
Concentration-Number,  
Concentration-Area, Cr,  
Khoys, Iran

Fractal methods are regarded as a highly efficient method for more accurate separation of boundaries between mineralized zone in shallow and deep studies. In this research, concentration-number (C-N) and concentration-area (C-A) fractal methods were used in order to identify promising areas of the elements like Cr, Co and Ni in the Khoys 1:100.000 geological mapping sheet, NW Iran. The factor analysis was performed on the elements, and factors, which were related to the elements, were isolated and studied by both fractal methods. The current geological locations of the extreme anomalies were investigated and the results showed a very close relationship and overlapping. The results of the presented models show that the most elements under study are located in the central and southwestern parts of the sheet. From the point of view of the lithology, these areas correspond to the serpentinite ultramafic units of harzburgite and dunite, and as a result, there is a high probability of Cr mineralization. The achieved results are confirmed by factor analysis. This means that a factor accumulation of these elements is exactly the same as those of each element.

Received: 18.09.2014

Accepted: 01.06.2015

### 1. Introduction

Basically, the separation of the geochemical anomalies from background is very important in order to interpret the mineralized zones (Hassanpour and Afzal, 2013). Anomaly detection and separation are the most important aim in geochemical exploration. The analysis of the histogram is one of the methods which is used in these kinds of studies. Summary statistics such as mean, median, variance, maximum, minimum and standard deviation are calculated in addition to drawing the histograms of the stream sediment samples. The traditional methods can only show the frequency of the elements distribution without any information about the spatial variability and spatial correlation. Furthermore, conventional statistical methods e.g., histogram analysis or Q-Q plots assuming normality or lognormality and do not consider the shape, extent and magnitude of anomalous areas (Rafiee, 2005; Afzal et al., 2010).

The scientists were looking for a way to describe all processes in the nature because the Euclidean geometry uses the discrete and integer numbers which are not capable to the explanation of the most complications of the nature. Hence, Mandelbrot (1983) introduced fractal geometry as a suitable tool so as to describe these problems. Among various methods that have been proposed, the fractal geometry is one of the newest and applicable methods for separation of geochemical anomalies. Turcotte (1986) showed the fact that there is a fractal relationship between the cumulative amounts of a deposit and average grades in different parts of a deposit. Meng and Zhao (1991) expressed the existence of fractal structures in geology. In recent years, fractals and multifractal methods are being used in various branches of the earth sciences such as geophysics and geochemistry. In the analysis of the complex geological structures, especially in the field of economic geology and mining exploration,

\*Corresponding author: Somayeh Momeni, [somayeh\\_momeni10@yahoo.com](mailto:somayeh_momeni10@yahoo.com)  
<http://dx.doi.org/10.19111/bmre.89526>

the spatial distributions of the attributes are used. Fractal/multifractal theory may be interpreted as a theoretical framework that describes the power-law relations between areas enclosing concentrations below a given value and the actual concentrations itself. To demonstrate and prove that data distribution has a multifractal nature requires a rather extensive computation. There is not any relationship between data distribution and fractal/multifractal modelling (Mandelbrot, 1983; Afzal et al., 2010; Mohammadi et al., 2013).

In the fractal geometry, each shape and its complexity are shown in terms of decimal and continuous numbers, and consequently it is an appropriate tool to determine the thresholds. Some of the important and useful fractal methods used in the earth sciences are number-size (N-S: Mandelbrot, 1983; Agterberg, 1995; Monecke, 2005; Sadeghi et al., 2012a), concentration-volume (C-V: Afzal et al., 2011), concentration-distance (C-D: Li et al., 2003) concentration-area; concentration-perimeter (C-A and C-P: Cheng et al., 1994) and concentration-number (C-N: Hassanpour and Afzal, 2013).

## 2. Materials and Methods

### 2.1. Sampling and Analysis

To start geochemical studies in the Khoy 1:100,000 sheet, 1010 data samples (Figure 1) of the stream sediments were selected and analyzed for 44 elements by ICP-MS method by ALS Chemex (ALS Canada Ltd). Detection limits for Cr, Co and Ni are 10 ppm, 1 ppm and 2.5 ppm respectively. Moreover, 100 randomized samples were selected and analyzed for assay quality assurance and quality control with respect to Thompson-Howarth error analysis (1976; 1978). Based on the method, the error analysis for Cr is less than 10% and about 3%. Among these elements, Cr, Co and Ni were studied to identify the appropriate areas for Cr. In this study C-N and C-A fractal models were used. After considering the two methods, factor analysis is performed to evaluate the paragenesis and high grade anomalies.

### 2.2. Concentration-number (C-N) Fractal Method

The C-N method was established by Mandelbrot (1983) and developed by Hassanpour and Afzal (2013) to classify various natural phenomena. Agterberg (1995) and Monecke (2005) have developed this

method in the earth sciences. This model has the following general form (Deng et al., 2010; Mandelbrot, 1983; Sadeghi et al., 2012a):

$$N(\geq \rho) \propto \rho^{-\beta} \rho^{-\beta} \quad (1)$$

In this equation,  $\beta$  is the fractal dimension,  $\rho$  denotes element concentration, and  $N$  is the number of samples containing the concentration greater than or equal to  $\rho$ . This method is based on the inverse proportion between concentration and cumulative frequency of each grade and higher grades. In other words, when the concentration of the element is high, the number of the containing samples is low. The advantages of this method are using raw data (Mandelbrot, 1983; Deng et al., 2010).

### 2.3. Concentration-area (C-A) Fractal Method

The C-A fractal method was established by Cheng et al. (1994) who studied the area located in the Mitchel-Sulphurets porphyry copper deposit in the NW British Columbia, Canada. This method is based on the changes in the concentrations and contained area and higher grades. In other words, there is an inverse relationship between the concentration of the elements and the area occupied by them (Cheng et al., 1994). This means that if the concentrations of the elements are increased, the occupied area by them is reduced. This model has the following relationship (Cheng et al., 1994; Sadeghi et al., 2012b):

$$A(\rho \leq \rho \leq \nu) \propto \rho^{-\alpha_1} \propto \rho^{-\alpha_1} ; A_{\rho}(\rho \geq \rho \leq \nu) \propto \rho^{-\alpha_2} \propto \rho^{-\alpha_2} \quad (2)$$

where  $\alpha$  denotes the fractal dimension,  $\rho$  shows the element concentration, and  $A$  represents the area which is occupied by elements with concentration values less than or equal to and greater than or equal to the contour value  $\rho$ .

### 2.4. Factor Analysis

The purpose of factor analysis as one of the most popular multivariate analyses is to classify and reduce the number of geochemical variables. It is a useful tool for combining several correlated variables into a single variable and thus for reducing the dimensionality of datasets into uncorrelated principal components based on covariance or correlations of variables which represents the inter-relationships among the multi-dimensional variables. Based on this method, a large dataset of geochemical variables

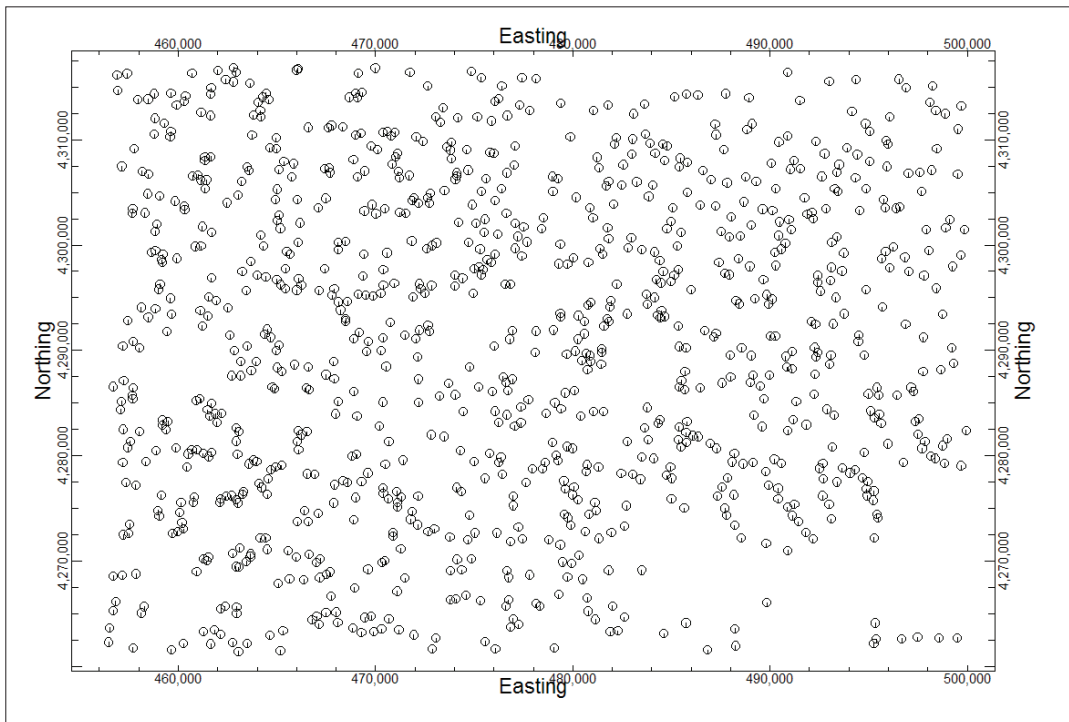
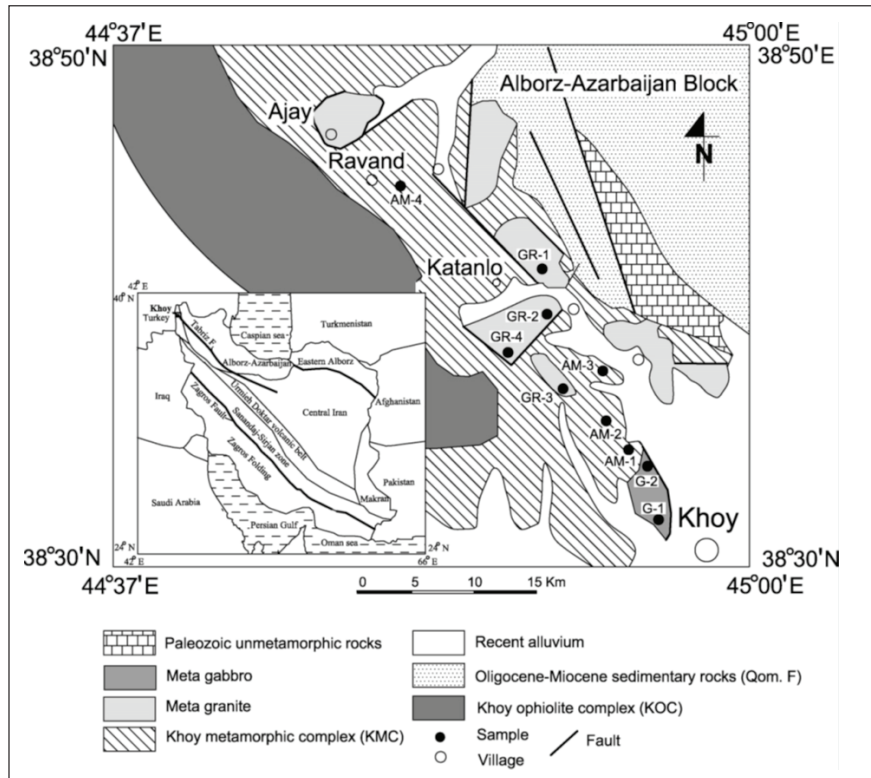


Figure 1- Geological map of Khoy 1:100,000 sheet and its situation in the geological setting of Iran (Alavi, 1994) within samples of chromite occurrences and stream sediments geochemical samples.

are combined in a few factors (Reimann et al., 2005; Shamseddin Meygoni et al., 2014). Factor analysis under a hypothetical model can find a specific relation between a series of various variables which seem unrelated together. The number of agents (linear combination of the main variables that means specific characteristic of relations between variables) is much less than the number of main variables. Hence, one of the main purposes of this method is to reduce the dimension of data. The basic hypothesis in this method is that there is a fundamental pattern or specific model in the determination of the relating complex concepts between variables. This relation reveals a factor in this hypothetical model and generally the main objective of this method is identification of the variables which are the main controller among a series of geochemical data (Afzal et al., 2013).

Moreover, the elements were classified using factor analysis by SPSS software package. It was carried out using principal component analysis (PCA) with varimax rotation. This classification has been evaluated in the form of the paragenesis factors. All existing elements were examined, and six factors were obtained. The amount of all elements in each factor was clear and higher than 0.6. There are three elements of Cr, Co and Ni in factor 1. In factor 2, the amount of Cu, Sc and V were above 0.6. In factor 3, the amount of Ba, Ga, Sr and Y were more than 0.6. In factors 4, 5 and 6, just the amounts of Pb, Be and Mo were above 0.6, respectively. The investigation of the all factors presents that factor 1 has the elements that they are paragenesis altogether. Statistical parameters of factor 1 (F1) show in the table 1.

Table 1- Summary statistics of Cr, Co, Ni and F1.

Statistical parameters	Cr (ppm)	Co (ppm)	Ni (ppm)	F1
Detection Limit	10	1	2.5	-
Mean	481.74	48.79	316.37	3.12
Median	350	38	138	2.25
Variance	184680.013	1803.87	224883.44	0.02
Maximum	2000	560	2000	10.8
Minimum	34	4.15	3.089	-2.21
Standard deviation	429.744	42.47	474.22	0.15

## 2.5. Geological Setting of the Khoy 1:100,000 Sheet

The Khoy 1:100,000 sheet is located in NW Iran. The study area is situated in the Alborz-Azerbaijan block which is in NE and SE parts of the Arabian Plate (Stocklin and Nabavi, 1972). The geological map of the study area shows that the KMC is positioned between the Khoy ophiolite complex (KOC) in the west that is overlain on the Arabian plate and Paleozoic unmetamorphosed sedimentary rocks of the AA Block in the east (Ghoraiishi and Arshadi, 1987; Radfar and Amini, 1999; Azizi et al., 2006). There are metamorphic rock units with a combination of gneiss, migmatites and quartzite. All regional faults have NW-SE trends with Late Cretaceous age and probably between Upper Cretaceous and Paleocene.

According to the division of the sedimentary structural blocks of Iran (Stocklin 1968), the building blocks are divided into two parts: 1- colored melange zones and 2- Alborz – Azerbaijan region that consists of two areas which are Zurabad (the colored *mélange* zones) and Ishgeh-su (the Alborz - Azerbaijan region). The area contains the outcrops of sedimentary rocks and metamorphic, volcanic lavas. The range can be observed of metallic and non-metallic minerals. Metallic elements such as Cu, Zn, Pb, Cr, Co and Ni and non-metallic minerals such as talc, asbestos, graphite, feldspar and magnesia. According to the elemental histogram, there is a similar distribution for Cr and Ni (Figure 2).

## 3. Discussion

Table 1 shows the mean, median, variance, maximum, minimum, and standard deviation. The distribution of each element is shown in figure 2. Concentrations of Cr, Co, and Ni have wide ranges and high standard deviations, as depicted in table 1.

In fractal modeling, the logarithmic plot is used for finding the threshold of host rocks and mineralized zones. The slope of the fitted line segments to the data points represents the fractal dimension. Using the obtained thresholds, high grade anomalies can be identified and distinguished easily. In table 2, threshold values of elements and factor analysis were calculated based on the C-N log-log graphs.

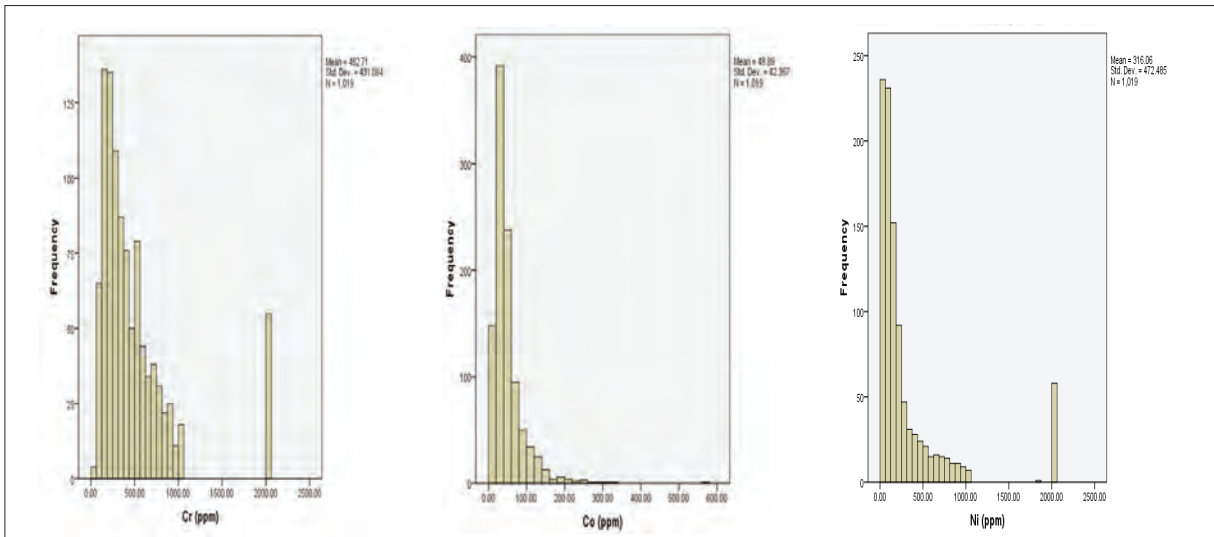


Figure 2- Histogram of Cr, Co and Ni in the study area.

Table 2- Threshold values based on C-N fractal models.

Very high intensity	High intensity	Moderate intensity	Low intensity	Element
threshold	threshold	threshold	threshold	
630.95	-	-	177.82	
123.02	-	40.73	17.78	Co (ppm)
954.99	-	602.55	125.89	Ni (ppm)
3.162	-	1.778	0.125	Factor 1 (ppm)

Based on the C-N log-log plots, there are two thresholds and three populations for Cr, as depicted in figure 3. The C-N log-log plots represent the three breakpoints and four concentration populations for Co, Ni and factor 1 (Figure 3). The factor 1 includes Cr, Ni and Co that fractal modelling for this factor shows Cr, Ni and Co anomalies with them. High intensive anomalies for Cr, Ni and Co commenced from 630.95, 954.99 and 123.02 ppm respectively, as depicted in table 2.

The Results of the C-A method display that the Cr and Co have two threshold values but Ni has three threshold values. However, the C-A log-log plot for factor1 reveals four threshold values (Figure 4). The characteristics of the anomalous thresholds are expressed in table 3.

Table 3- Threshold values based on C-A fractal model.

Element	Very high intensity	High intensity	Moderate intensity	Low intensity
	threshold	threshold	threshold	threshold
	1778.27	-	-	281.83
Cr (ppm)	501.18	-	-	35.48
Co (ppm)	1258.92	-	575.43	125.89
Ni (ppm)	9.12	5.011	3.162	0.794

Sudden changes in the C-A log-log plot shows that exchanging in the populations and anomalies. High in intensive anomalies of Cr, Co and Ni began from 1778.27, 501.18 and 1258.92 ppm respectively, as shown in table 3.

### 3.1. Comparison of the C-N and C-A Fractal Models

Comparison between results obtained by the fractal models reveals that the threshold values derived via the C-A method are higher than the C-N threshold values. On the other hand, the areas of high intensive anomalies obtained by C-N fractal modelling are greater than the C-A fractal modelling. It is worth to note that the discipline of the C-N method is based on irregularities, so calculations obtained from this

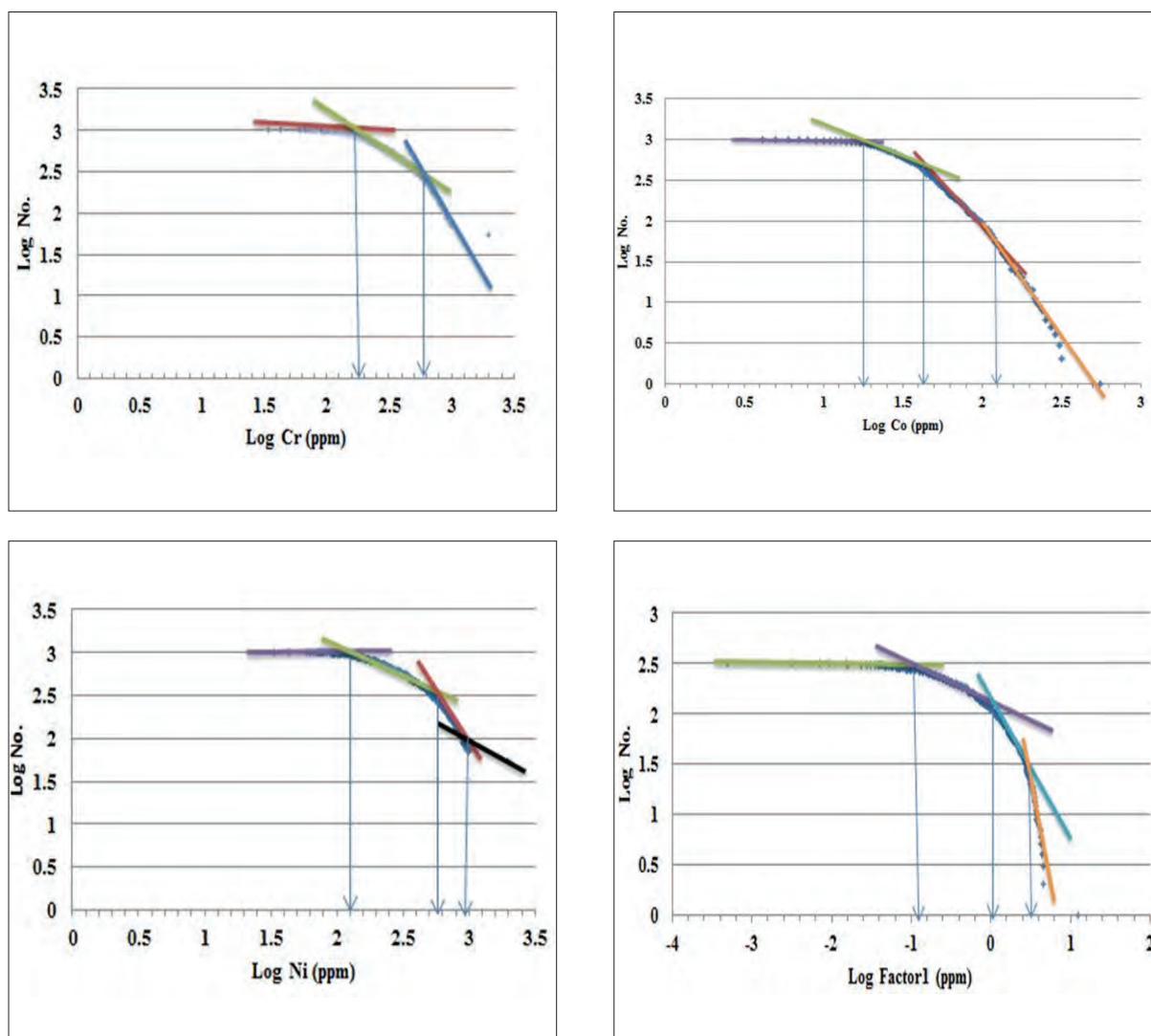


Figure 3- C-N log-log plots for Cr, Co, Ni and factor 1 in the Khoysheet.

method also follows the principle of this method. This fact leads to obtain a better logical estimation. On the other hand, in the C-A method because of the fact that certain irregularities are governing in obtaining the area and mineral aggregate are neither in order or regular, therefore this method cannot estimate exact and logical unless the network of surveyed data is organized and this means that the interval of sampling network is not less than or greater than other areas since this method estimates all areas and if the gap enlarged, the error increases as well.

### 3.2. Spatial Distribution of the Elements

Based on the obtained thresholds, the spatial distribution maps of the elements were generated using IDW algorithm by the Rockworks software. The high intensive anomalies derived by the both fractal

models are located in the central and SW parts of the area especially for Cr, Ni and factor1. The Co main anomalous parts occurred in the central part of the area based on the fractal modelling (Figure 5).

All three elements are in a good agreement with each other and they are aggregated in the central parts of the map in addition little in the SE. The detailed investigation of each map shows that a large amount of Cr is located in the center of the map and a little less in the southwest of the map. The accumulation of Co is in the central part of the map, and the dispersion of Ni is the same as Cr, which means it is located in the central and southwestern parts of the map. In the spatial distribution map of the factor analysis, based on the factor maps, it can be found that the accumulations of all three elements are in the central and SW parts of the study area (Figure 5).

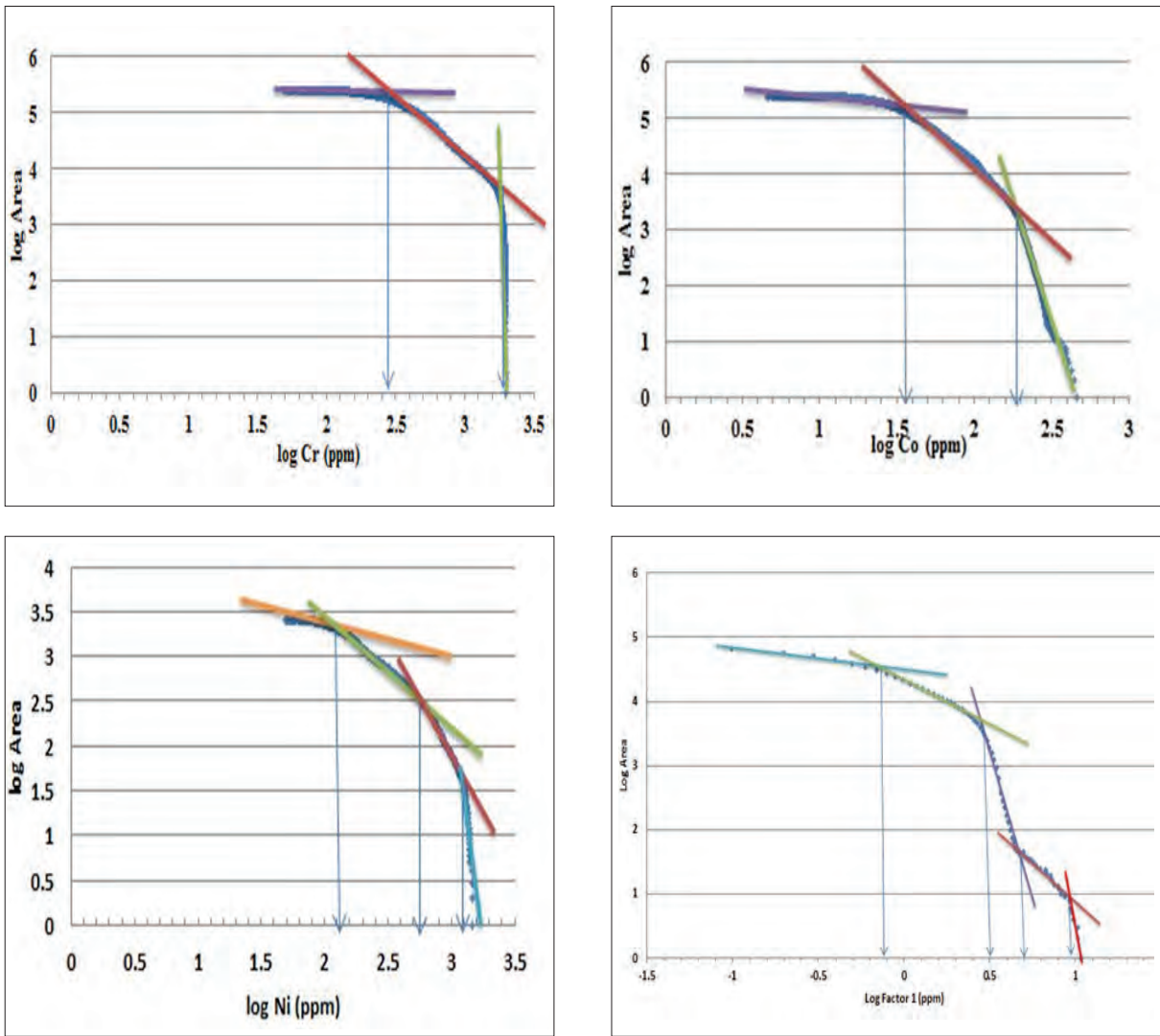


Figure 4- C-A log-log plat for Cr, Co, Ni and factor 1 in Khoy sheet.

#### 4. Conclusions

In conclusion, as far as the issue of economic geology, there are two identified areas which are more important than the other parts. These parts are located in the central and western parts of the Khoy geological sheet. In these areas, the accumulation of minerals contains Cr and its paragenesis, and therefore they are recognized as the high grade and promising areas of detailed exploration. Comparison between results derived via the fractal models indicates that the threshold values obtained by the C-A method are higher than the C-N threshold values. On the other hand, the areas of high intensive anomalies obtained by the C-N fractal modelling are greater than the C-A fractal modelling. The high intensive anomalies obtained by the both fractal models are situated in

the central and SW parts of the area especially for Cr and Ni. Besides, the evaluation of the factor analysis confirms the detailed analysis of the elements. Aggregation place of these elements is in accordance with the geological map. These places are mostly in the place of ultramafic rocks of serpentinite contain harzburgite and dunite that small amounts of the elements are related to the lithology of amphibolite rocks consistent with amphibolite schist, mica schist, marble cut by quartz-feldspathic veins and aplite. In assessing these two methods (C-N and C-A) it is realized that all obtained thresholds and populations were close to each other. It is identified in the factor analysis by both methods. It is pretty obvious in the histogram of the factor analysis that the aggregations of the paragenesis elements all together are exactly the same as those of each individual element.

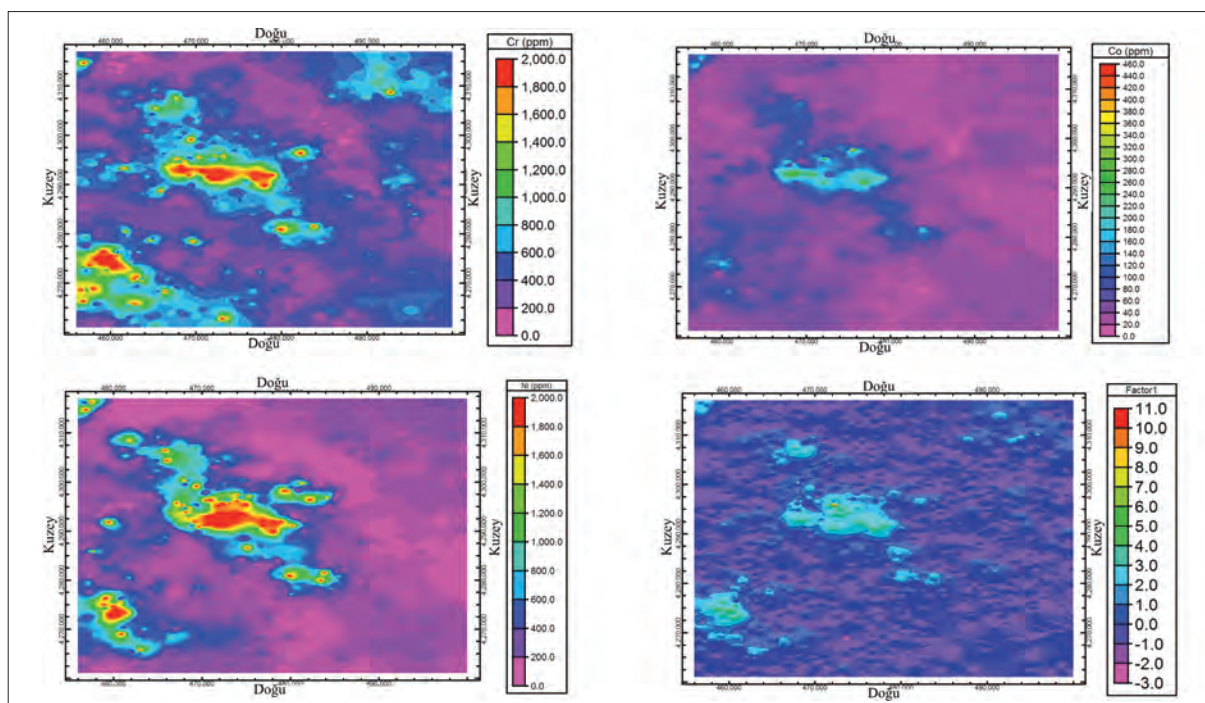


Figure 5- Geochemical maps obtained from the N-S fractal modelling for Cr, Co, Ni and factor 1.

## Acknowledgements

The authors would like to thank Mr. Seyed Ali Hosseini for his great helpful information in this research.

## References

- Afzal, P., Zia Zarifi, A., Sadeghi, B. 2013. Separation of Geochemical Anomalies Using Factor Analysis and Concentration-Number (C-N) Fractal Modeling Based on Stream Sediments Data in Esfordi 1:100000 Sheet, Central Iran, *Iranian Journal of Earth Sciences*, Vol. 5, p.p. 100-110.
- Afzal, P., Fadakar Alghalandis Y., Khakzad A., Moarefvand P., Rashidnejad, N. 2011. Delineation of mineralization zones in porphyry Cu deposits by fractal concentration–volume modeling. *Journal of Geochemical Exploration* 108: 220–232.
- Afzal, P., Khakzad, A., Moarefvand, P., Rashidnejad Omran, N., Esfandiari, B., Fadakar Alghalandis, Y. 2010. Geochemical anomaly separation by multifractal modeling in Kahang (GorGor) porphyry system, Central Iran. *Journal of Geochemical Exploration* 104: 34–46.
- Agterberg, FP. 1995. Multifractal modeling of the sizes and grades of giant and supergiant deposits. *Int Geol Rev* 37:1–8.
- Azizi, H., Moinevaziri, H., Mohajjel, M., Yagobpoor, A., 2006. PTt path in metamorphic rocks of the Khoy region (northwest Iran) and their tectonic significance for Cretaceous–Tertiary continental collision. *Journal of Asian Earth Science*, 27, 1–9.
- Azizi, H., Moinevaziri, H., Mohajjel, M., Yagobpoor, A. 2006. PTt path in metamorphic rocks of the Khoy region (northwest Iran) and their tectonic significance for Cretaceous–Tertiary continental collision. *Journal of Asian Earth Science* 27, 1–9.
- Cheng, Q., Agterberg FP, Ballantyn, SB. 1994. The separation of geochemical anomalies from background by fractal methods. *Journal of Geochemical Exploration* 51:109–130.
- Deng, J., Wang, Q., Yang, L., Wang, Y., Gong, Q., Liu, H. 2010. Delineation and explanation of geochemical anomalies using fractal models in the Heqing area, Yunnan Province, China. *Journal of Geochemical Exploration*. 105:95– 105.

- Ghoraishi, M., Arshadi, S. 1987. Geology Map of Khoy Quadrangle (1:250,000). Geological Survey of Iran.
- Hassanpour, S., Afzal, P. 2013. Application of concentration-number (C-N) multifractal modelling for geochemical anomaly separation in Haftcheshmeh porphyry system, NW Iran. *Arabian Journal of Geosciences*, vol. 6, pp. 957–970.
- Li, Changjiang Ma, Tuhua Shi, Junfa. 2003. Application of a fractal method relating concentrations and distances for separation of geochemical anomalies from background. *Journal of Geochemical Exploration*, 77: 167–175.
- Mandelbrot, B.B. 1983. The fractal geometry of nature. Freeman, San Francisco, pp 1–468.
- Meng, X., Zhao, P. 1991. Fractal method for statistical analysis of geological data, *Chinese Journal of Geosciences*, vol. 2, pp. 207-211.
- Mohammadi, A., Khakzad, A., Rashidnejad Omran, N., Mahvi, M.R., Moarefvand, P., Afzal, P. 2013. Application of number–size (N–S) fractal model for separation of mineralized zones in Dareh-Ashki gold deposit, Muteh Complex, Central Iran. *Arabian Journal of Geosciences*. 6: 4387-4398.
- Monecke, T., Monecke, J., Herzig, P.M., Gemmel, J.B., Monch, W. 2005. Truncated fractal frequency distribution of element abundance data: a dynamic model for the metasomatic enrichment of base and precious metals. *Earth and Planet. Sci. Lett.*, 232: 363–378.
- Radfar, J., Amini, B. 1999. Geology Map of the Khoy Quadrangle (1:100,000). Geological Survey of Iran.
- Rafiee, A. 2005. Separating geochemical anomalies in stream sediment media by applying combination of fractal concentration area model and multivariate analysis (Case study: Jeal-e-Barez 1:100,000 Sheet, Iran), 20<sup>th</sup> World Mining Congress Proceedings, Iran, 461–470.
- Reimann, C., Filzmoser, P., Garrett, R.G. 2005. Background and threshold: critical comparison of methods of determination. *Sci. Total Environ.*, 346, 1–16.
- Turcotte, D.L. 1986. A fractal approach to the relationship between ore grade and tonnage. *Econ. Geol.* 18: 1525–1532.
- Sadeghi, B., Moarefvand, P., Afzal, P., Yasrebi, A.B., Daneshvar Saein, L. 2012a. Application of fractal models to outline mineralized zones in the Zaghia iron ore deposit, Central Iran. *Journal of Geochemical Exploration* .Special Issue “fractal/multifractal modelling of geochemical data”, 122: 9–19.
- Sadeghi, B., Afzal, P., Moarefvand, P., Khoda Shenasi, N., 2012b. Application of concentration–area fractal method for determination of Fe geochemical anomalies and the background in Zaghia area, Central Iran. 34<sup>th</sup> International Geological Congress (IGC), Brisbane, Australia.
- Shamseddin Meigoony, M., Afzal, P., Gholinejad, M., Yasrebi, A.B., Sadeghi, B. 2014. Delineation of geochemical anomalies using factor analysis and multifractal modeling based on stream sediments data in Sarajeh 1:100000 sheet, Central Iran, *Arabian Journal of Geosciences*, 7, 5333–5343.
- Stocklin, J. 1968. Structural history and tectonics of Iran: a review. *AAPG Bulletin*, 52, 1229-1258.
- Stocklin, J., Nabavi, M. 1972. Tectonic Map of Iran. Geological Survey of Iran.
- Thompson, M., Howarth, R.J. 1976. Duplicate analysis in geochemical practice (2 parts). *Analyst*, 101, 690-709.
- Thompson, M., Howarth, R.J. 1978. A new approach to the estimation of analytical precision. *Journal of Geochemical Exploration* 9, 23-30.





# BULLETIN OF THE MINERAL RESEARCH AND EXPLORATION

<http://bulletin.mta.gov.tr>

BULLETIN OF THE MINERAL RESEARCH AND EXPLORATION	
CONTENTS	
OPAQUE MINERAL CONTENT OF DUTLUCA VOLCANICS (BURHANIYE - BALIKESİR): THE EFFECT OF HYDROTHERMAL ALTERATION ON THESE MINERALS	153
...	...

## OPAQUE MINERAL CONTENT OF DUTLUCA VOLCANICS (BURHANIYE - BALIKESİR): THE EFFECT OF HYDROTHERMAL ALTERATION ON THESE MINERALS

Şükrü KOÇ<sup>a</sup> and Nihal ÇEVİK<sup>a\*</sup>

<sup>a</sup>Ankara University, Faculty of Engineering, Dept. of Geological Eng., 06100, Tandoğan, Ankara

Research Article

### Keywords:

Hydrothermal Alteration,  
Pyrite, Enargite,  
High Sulfidation, Ore  
Microscopy

### ABSTRACT

Dutluca volcanics, which are known as Hallaçlar Formation in regional scale in the study area (Kurshensky, 1976), are composed of hydrothermally altered andesite and basaltic andesite. In these rocks, sulfidic minerals such as pyrite, enargite and chalcocite, and oxide and hydroxide minerals such as magnetite, hematite and goethite were detected as opaque minerals. The presence of enargite in opaque mineral paragenesis, and the changes observed in structures and textures of opaque and silicate minerals indicate that examined volcanics have been altered by highly sulfidic hydrothermal solutions. During the hydrothermal alteration process, which indicates at least in two phases, a diffuse pyritization rich in H<sub>2</sub>S in reducing conditions and enargite mineral, which is known as pathfinder minerals in such processes, formed in the first phase. Later on; the extensive martitization developed in oxidizing conditions.

Received: 28.02.2015

Accepted: 23.03.2015

## 1. Introduction

Tertiary volcanics, which are located in the study area, are regionally known as Hallaçlar formation (Kurshensky, 1976). This formation is composed of andesites and is affected from low and high sulfidic hydrothermal solutions. For instance; in volcanics around Küçükdere (Havran-Balıkesir) (Çolakoğlu, 2000; Çolakoğlu and Kuru, 2001) gold deposit, quartz ± calcite ± adularia ± illite paragenesis was detected indicating the low sulfidation (Hedenquist, 1985, Simmons et al., 2005). However; the high sulfidation alteration with quartz ± alunite ± prophyllite ± dickite ± kaolinite paragenesis is observed in Kirazlı and Ağı mineralization area (Yiğit, 2012). The purpose of this study is to obtain data on opaque mineral component of the volcanics which were affected from the alteration around Dutluca, the effects of hydrothermal solutions on opaque and ferrous silicate minerals (opacification), and the types of solutions which generated these effects. There are several methods that can be applied to reach

this goal. Here, it is just intended that the results obtained from ore microscopy would contribute to other methods. Andesites mostly consist of plagioclase (oligoclase, andesine, sometimes labradorite) and few amounts of mafic minerals such as; hornblende, biotite, pyroxene. As accessory minerals; magnetite, ilmenite and apatite are observed. Hornblende and biotite minerals in these rocks turn into chlorite, sphene and iron oxide by hydration. Plagioclase minerals turn into epidote, sericite, kaolinite and quartz. Besides; alterations such as silicification, albitization, kaolinitization and saussuritization can be seen in andesites.

Primary opaque and ferrous silicate minerals of which andesites contain could provide some new opaque minerals to occur by (mafic) alteration. For example; pyrite formations can be observed in many epithermal systems. Sulphur bearing solutions first enter into a region and precipitate, and form plenty of pyrite which react with iron in the rock. Other subsequent metals may form new sulfide minerals. (Krauskopf, 1987).

\*Corresponding author: Nihal Çevik, [ncevik@eng.ankara.edu.tr](mailto:ncevik@eng.ankara.edu.tr)  
<http://dx.doi.org/10.19111/bmre.85535>

Hematite, which is a stable mineral of iron in intermediate and strongly oxidizing environments, is frequently available in volcanic rocks. This occurs due to the oxidation during cooling events, and it is generally observed as martite lamellae. The alteration of pyrite into hematite is not rare in volcanic hydrothermal formations (Ramdohr, 1969).

Opaque minerals which the volcanics consist of, their relationships with mafic silicate minerals and the determination of associating and altering minerals may help reach some data about alterations. With this purpose, several volcanic rocks collected from the study area were polished and examined under the ore microscopy, and their opaque mineral components and alteration structures/textures were detected. Finally; the mineralogical results which could define the composition of hydrothermal solution that causes alteration and the type of the developing alteration have been discussed in this article. The type of hydrothermal alterations and types of solutions that cause alteration can guide mineral explorations in such fields.

## 2. Geological Setting

The region, which covers the study area, consists of Paleozoic, Mesozoic and Cenozoic rocks (Figure 1). The oldest rock assemblage in the region was named as the Kazdağ group and is composed of pre-Permian metadunite, metagabbro, pyroxenite, amphibolite, gneiss and marble (Bingöl et al., 1973). These rocks outcrop around Kozak pluton (Figure 1). The plutonism has become affective after Upper Cretaceous, and Eybek and Kozak plutonic massives have been emplaced. Both massives show big resemblance in terms of chemistry, mineralogy, location and age (Ercan et al., 1984). Ercan et al. (1984, 1990) determined Miocene lavas mostly as andesitic, occasionally dasitic and rarely rhyodasitic in the investigation they had carried out on widespread Tertiary rock units. However, Pliocene lavas were detected as basaltic type in their study. The same investigators also detected that Miocene lavas had totally been calcalkaline and had the character of crustal origin. Pliocene aged Dededağ basalt is observed as small outcrops in the region. These rocks have cut Tertiary units and flown over them (Akyürek and Soysal, 1978). Pliocene-Middle Miocene alluvial and lacustrine deposits widespread in the region are encountered as Neogene formations. Alluvials have

been formed by the erosion and transportation of old rocks in the area (Akyürek and Soysal, 1978).

Magmatic rocks in the Biga Peninsula are crustal origin, and the effects of upper mantle derived magma are occasionally observed. Most probably, these rocks were formed by the partial melting of lower parts of the increasingly thickening continental crust starting from Lower Eocene, after the collision of Anatolides with Pontides. Partial melting processes at depths have started in this thickening continental crust, and the metamorphism has become effective in the region. Kozak and Eybek granodioritic plutons and Hallaçlar – Dedetepe - Yuntdağ volcanics can be the products of the same calcalkaline magma, and have been formed within small time difference. However, the material of the rising upper mantle have intruded into the crust and formed hybrid magma, thus Yuntdağ volcanics have become hybridized towards its final stages and acquired partially shoshonitic character. Later on; mantle effects have increased and much siliceous, hybrid Alibey and Dededağ basalts have formed. Actually; the formation of alkali basaltic volcanism (Kula example), which is the product of primary magma, starting from Upper Pliocene in West Anatolia also indicate this situation due to the increase in mantle effect and depletion in melting crustal material in time (Ercan, 1982, Ercan et al., 1983).

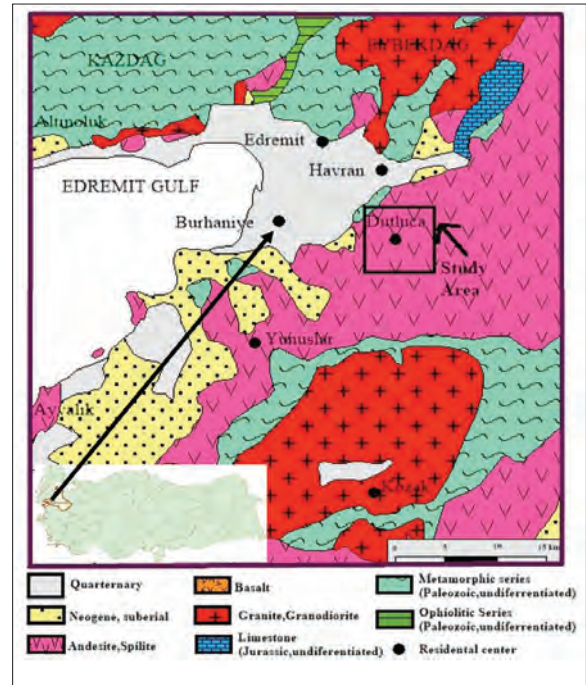


Figure 1- Geological map of the study area (from Çolakoğlu, 2002).

Volcanics outcropping in NE of Dutluca village (Figure 1) are composed of andesite and basaltic andesites. These rocks were named as Hallaçlar formation by Kurshensky (1976) in the northern part of the study area. Rocks are generally hypocrySTALLINE and porphyritic texture, and are composed of plagioclase, pyroxene, biotite, amphibole and opaque minerals. Plagioclase minerals in samples exhibit zoning or polysynthetic twinning. It is also possible to encounter plagioclase microliths in some samples of which their matrices are unaltered. Biotite, amphibole and pyroxene phenocrysts, which generally exhibit opacitization in circumferences, have also full opacified forms. While extensive argillization and carbonation were observed in rocks, the chloritization, sericitization and epidotization were also encountered. Using biotite minerals in andesite rocks belonging to Hallaçlar formation, dating by K/Ar method was also performed, and the age of andesites were determined as Early Neogene ( $23.6 \pm 0.6$  my, Middle Miocene) (Kurshensky, 1976). However; the K/Ar age of andesite bearing whole rock sample was found as  $26.5 \pm 11$  my in other investigation carried out by MTA. Thus, the volcanism started to become effective in Late Oligocene and has continued its effectiveness until Early Miocene (Yüzer and Tunay, 2012).

### 3. Opaque Mineral Contents of Volcanics

Several polishing were performed for field and drill samples during field studies and they have different macroscopic views to examine under ore microscope. Thus; sulfide minerals like; pyrite, enargite and chalcocine, and oxide and hydroxide minerals like; magnetite, hematite and goethite were detected in Dutluca volcanics which had been affected from the hydrothermal solution.

### Pyrite (FeS)

In volcanics, two pyrite formations were detected which are different from each other. These are disseminated pyrites in the rock (Figure 2) and pyrites which are the alteration mineral of ferrous silicate minerals like amphibole and biotite (Figure 3).

1. There are two types of pyrites as disseminated within rock. These are defined as; “Pyrite 1” and “Pyrite 2” because they have different grain sizes and the matrix in which they are located.

Pyrite 1: Located in fine grained, pale gray matrix and are disseminated throughout the rock (Figure 2). In some samples they are also encountered as fully limonitized pyrite pseudomorphs (Figure 4).

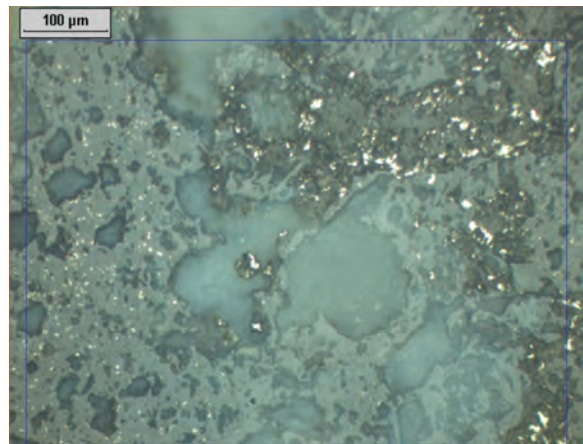


Figure 2- Disseminated pyrites in the rock. Pale gray colored pyrites on the left in matrix are finer grained. Gray and black colored pyrites are gangue minerals.

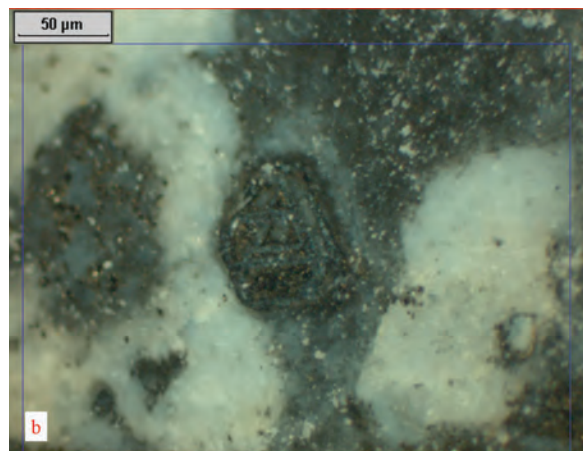
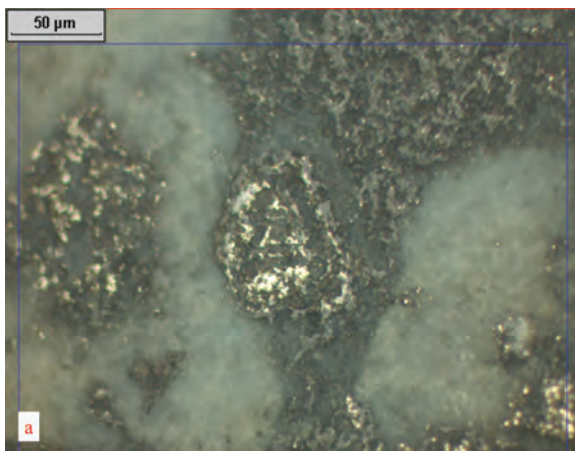


Figure 3- The pyritized amphibole on edges and crystallographical directions. Triangular shaped pyrite with zoning structure and surrounding silicates are seen at the center (b:+N).

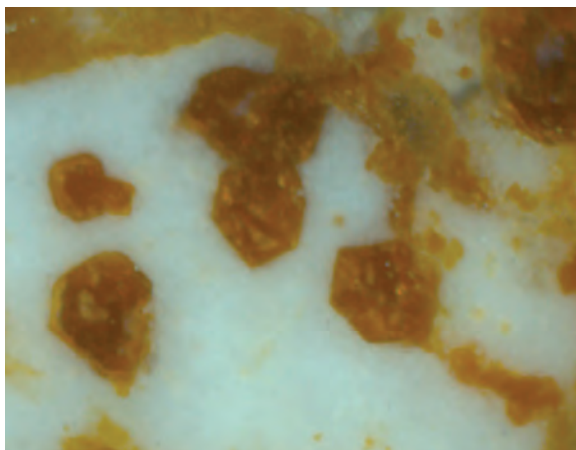


Figure 4- Euhedral and subhedral pyrites fully altered into geothite (+N).

**Pyrite 2:** They are much coarser grained than Pyrite 1 as disseminated within dark gray matrix and abundant. Dark gray matrix surrounds the pale gray matrix and occasionally intakes (Figure 5). This situation and the intrusion of coarse grained pyrite bearing dark gray matrix into Pyrite 1 bearing pale gray matrix indicate that first Pyrite 1 then Pyrite 2 have formed (Figure 6).

2. Pyrite minerals (alteration product of ferrous silicate minerals)

Pyrites have formed due to the alteration of silicates like amphibole and biotite minerals. These pyrites, of which their formations depend on silicates (Figure 3), exhibit various structural and textural characteristics. Some pyrites, which were categorized in this group, are located at inner parts of the ferrous silicate minerals encircling grains partly or fully on the edges (Figure 7) and as emplaced in crystallographical directions (Figure 8). It is seen that such alterations of silicates cause zoning structures (Figure 3). However; other pyrites are located in the form of seriates with respect to the boundaries of silicate minerals (Figure 7). Besides; the secondary pyrites are also available which emplaced into cracks and fractures close to these formations (Figures 7 and 9).

### **Enargite ( $\text{Cu}_3\text{AsS}_4$ )**

Enargite, in studied samples, are pale pinkish, brown and gray colored, and exhibit strong anisotropy. The colors of anisotropy are yellowish, brownish, orange like and greenish gray. Although enargite is confused with luzonite and stibioluzonite in its group, these two minerals have very strong twin lamellae and much orange colors.

As it was in pyrites, two different formations of enargite were detected too. Enargite 1 is seen as disseminated in altered volcanic rocks and is very fine

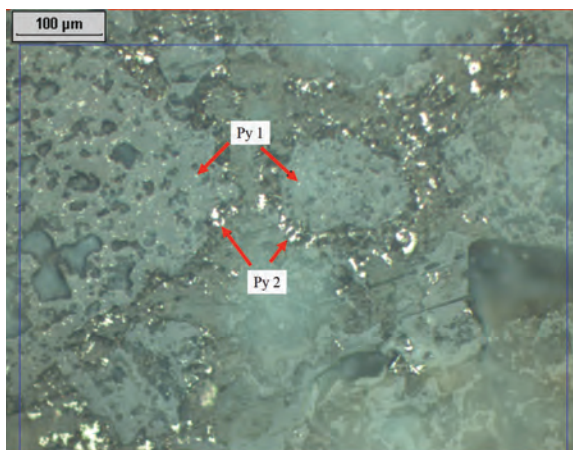


Figure 5- Two different matrices, two different pyrites. Fine grained “Pyrite 1” within pale gray matrix, and “Pyrite 2” coarser and more abundant than dark gray colored Pyrite 1 in matrix. Matrix with Pyrite 2 completely surrounds the other.



Figure 6- Central part: dark gray matrix which contains coarse grained “Pyrite 2” penetrates into “Pyrite 1” bearing dark gray matrix.

grained (Figure 10). Enargite 2, on the other hand, are the alteration products of ferrous silicate minerals like amphibole and biotite. These enargites, which formed by silicates, are encountered together with hematites (Figures 11, 12, 13, 14, 15). In figure 13, there are observed hematite and enargite formations in the outer and inner parts of amphibole mineral, respectively. There were also detected enargites which emplaced into cracks and fractures and these are associated with silicates. For example; the enargites which accumulated on the edge of cavity is seen in figure 15. There is also seen that this enargite turns into another yellow colored sulfide mineral starting from edges. This is probably a pyrite mineral, and it is known that enargite could change into various sulfide minerals like chalcocite, pyrite, chalcopyrite, covellite and galenite (Ramdohr, 1969).

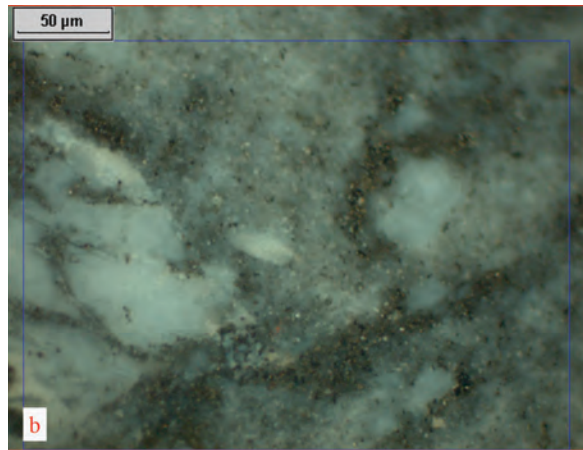
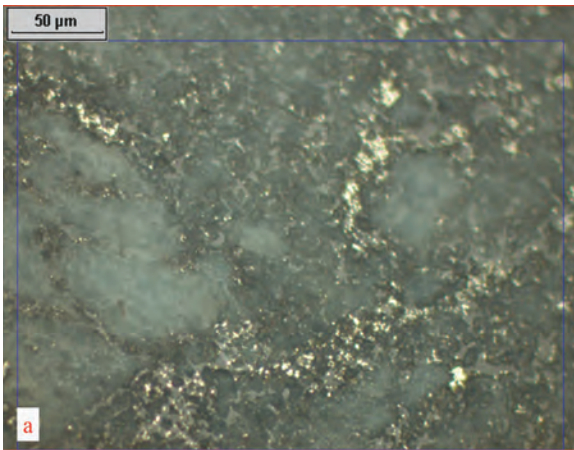


Figure 7- Pyrites placed around bluish gray gangue mineral in the form of "S" shape and into the fracture of matrix along a line.

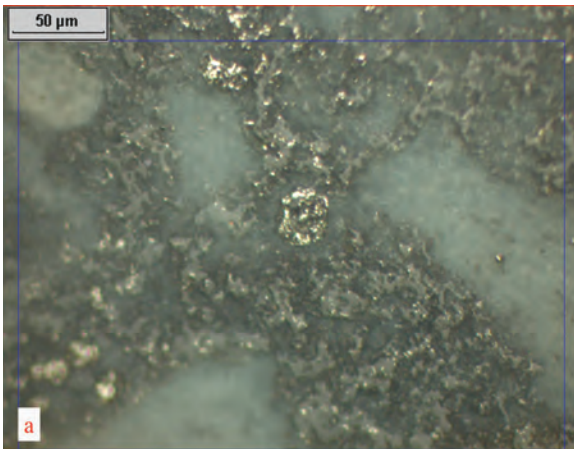


Figure 8a- Pyritized amphibole (b: +N).

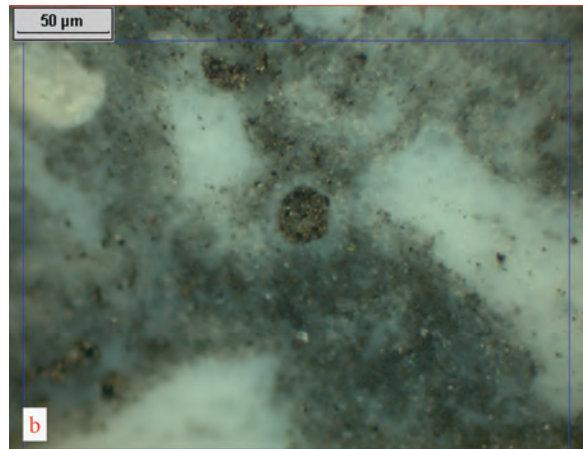


Figure 8b- Pyritized amphibole (b: +N).

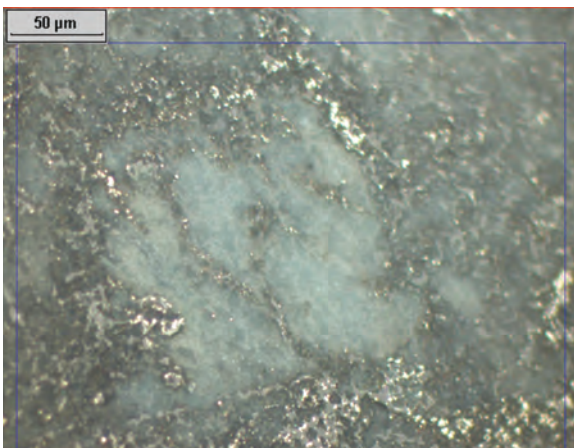


Figure 9- Pyrites placed around the edges of matrix and fractures.

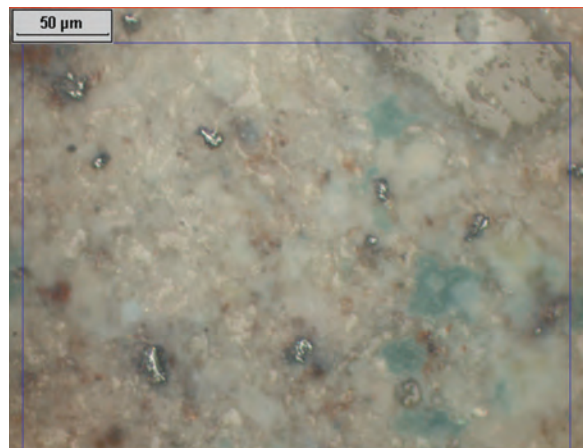


Figure 10- Very fine enargite grains dispersed in the rock.

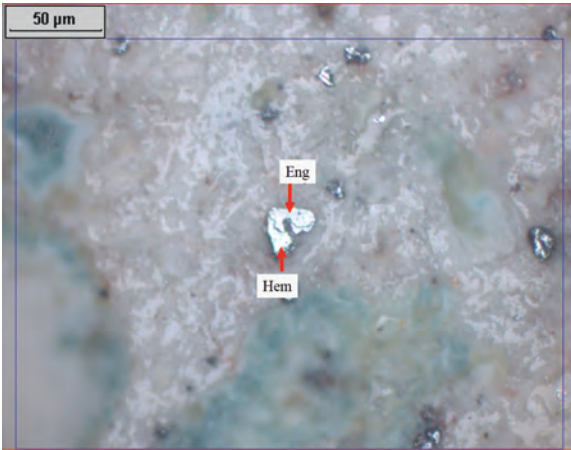


Figure 11- Hematite and enargite.

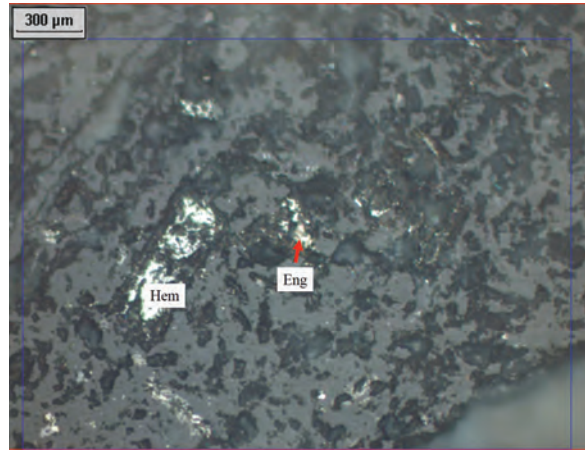


Figure 12- Hematite and enargite.

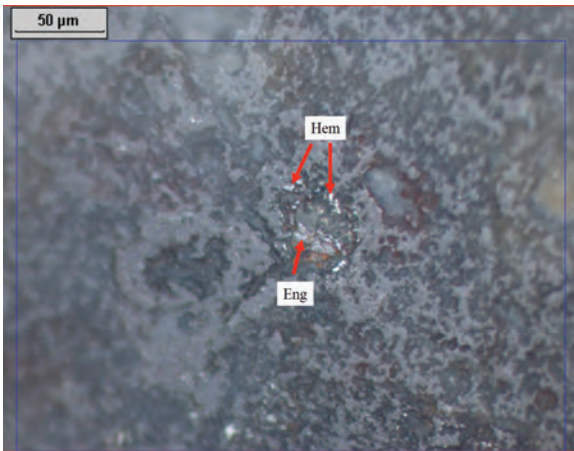


Figure 13- Formation of hematite around highly altered amphibole and enargite formation in the interior part.

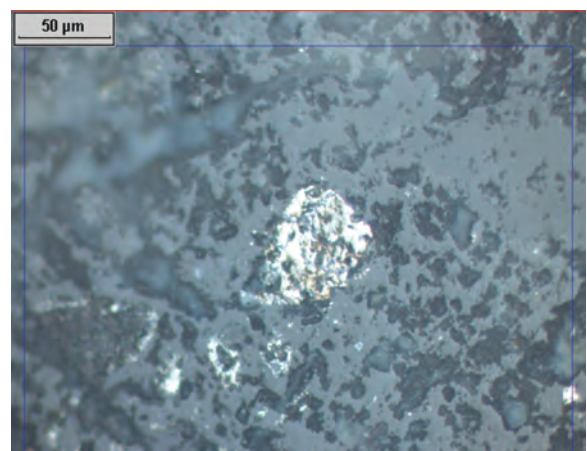


Figure 14- Enargite.

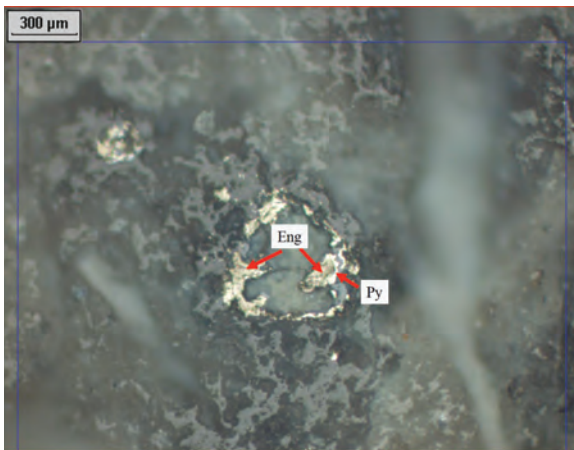


Figure 15- Enargite which precipitated around the edges of void. Enargite has turned into another sulfide mineral starting from the edges of enargite. The void has then been filled by matrix.

### Chalcosine (CuS)

Chalcosine, which was observed only in one of all the polished samples in the study area, is seen as associated with hematites (Figure 16). This chalcosine exhibits anisotropy and is a secondary mineral. It is probably the alteration product of enargite.

### Magnetite (FeOFe<sub>2</sub>O<sub>3</sub>)

In samples, subhedral magnetites are seen less than pyrite as disseminated in the rock (Figures 17 and 18). In these magnetites, the magnetizations (hematizations) are encountered in various degrees (Figure 19). Magnetites have mostly been hematitized starting from edges (Figures 19a and 19b). Besides, the rod like hematizations, which developed along crystallographical directions of the magnetite, are not seldom (Figure 19a). In figure 20, the hematitization

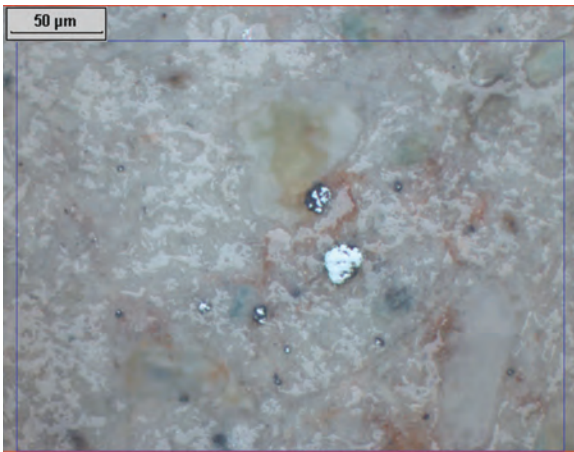


Figure 16- Chalcosine (coarse, whitish gray) and hematite (grayish white).

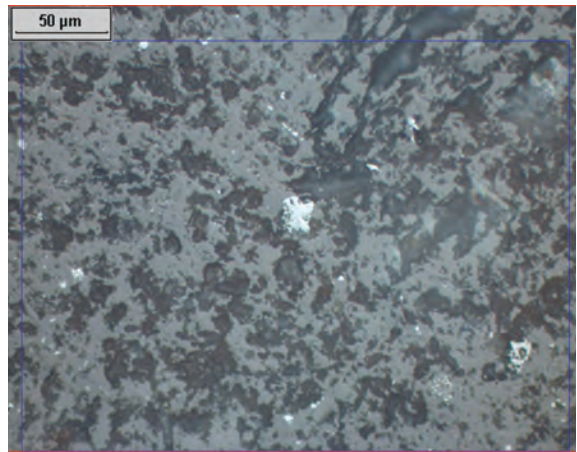


Figure 17- Subhedral magnetite in the center.

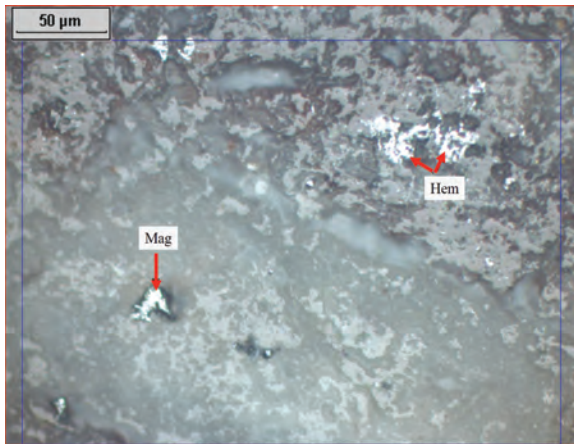


Figure 18- Euhedral (triangle) and subhedral magnetite and hematites in upper right. Both minerals were substituted by the matrix.

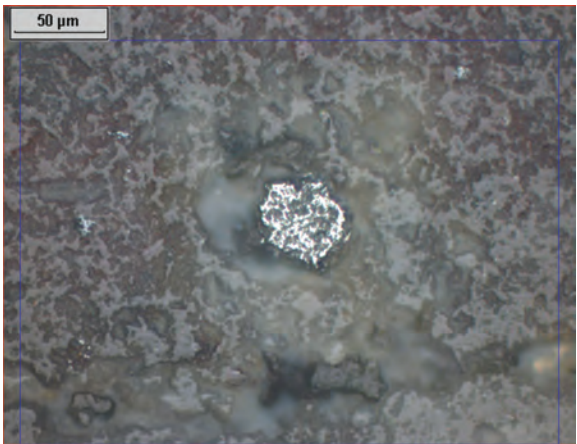


Figure 20- The hematitization of a euhedral magnetite.

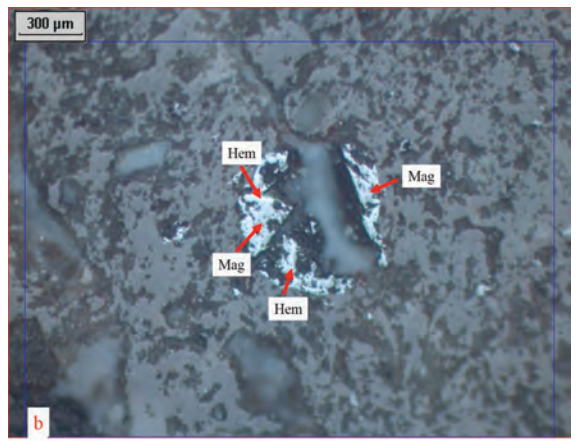
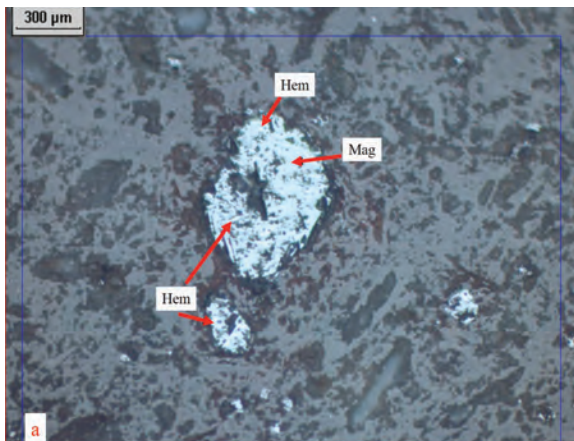


Figure 19- Hematitized (martitized) and highly substituted magnetite mineral by matrix (a, b).

of euhedral magnetite is seen. In samples, where magnetite mineral was hematitized then limonitized, these three minerals associate with each other.

### Hematite (Fe<sub>2</sub>O<sub>3</sub>)

The most abundant opaque mineral after pyrite is hematite, and is secondary origin. Some hematites are the alteration product of opaque minerals. Many amphibole grains in samples turned into hematite in various shapes by the effect of alteration. In figure 21, the alteration in which the cleavages of hornblends are seen is observed. It is frequently seen that the amphibole alters into hematite from edges and inner parts (Figure 22). As an alteration product of amphibole, the association of hematite and enargite is also observed (Figures 12 and 13). Besides, the pseudomorphs in which euhedral amphibole fully hematitized were also detected (Figure 23). Hematizations were also observed starting from edges in biotites in ferrous silicates (Figure 24).

The iron, which is dissolved from mafic minerals during the alteration of volcanics, has substituted

carbonates in the form of hematite (Figure 25). A significant portion of secondary hematite formations are associated with opaque minerals. Pseudomorphic euhedral and subhedral hematites, which are observed as disseminated (Figure 26), are bonded to the primary origin opaque minerals. Triangular and rectangular shaped hematites can be given as examples to this phenomenon (Figure 27). The hematitization of a euhedral magnetite is seen in figure 20. The partly (Figure 28) or fully (Figure 29) limonitization of secondary hematites is a frequent situation.

### Goethite (FeOOH)

Goethite minerals were encountered as an alteration product of opaque or ferrous silicate minerals in many polished samples. Goethites formed by opaque minerals are in the form of hematite-magnetite-goethite mineral association (Figure 22), or as hematite-goethite mineral association (Figure 29). However; goethites formed by ferrous silicates only associate with hematite (Figures 30 and 31), and the formation of temporal limonite and iron staining are seen in the form of fracture in samples (Figure 4).

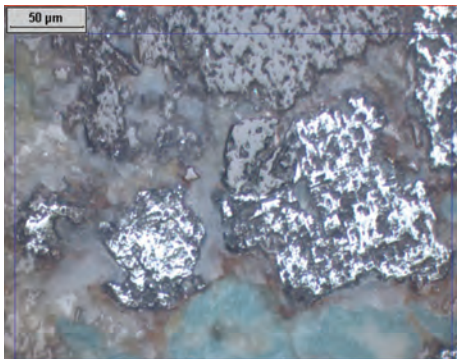


Figure 21- Hematite formed by hornblende (white). Typical cleavage traces of the hornblende can be seen.

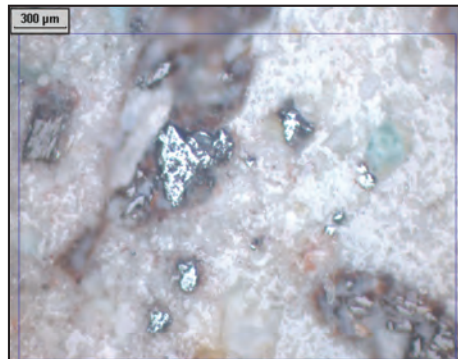


Figure 22- Hematite, magnetite and goethite: Partly hematitized goethite in the upper right, goethite around a coarse amphibole in the central part and a belt formed by very fine grained hematites and hematite in interior parts of amphibole.



Figure 23- Fully hematitized euhedral ferrous silicate mineral (amphibole) (pseudomorphose).

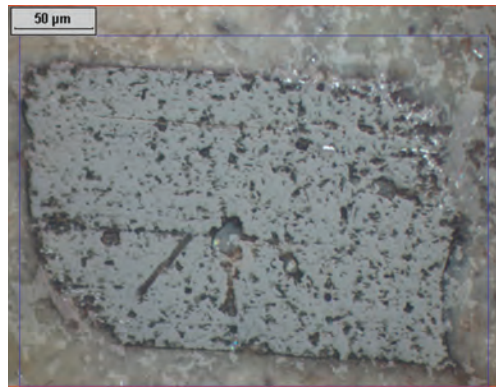
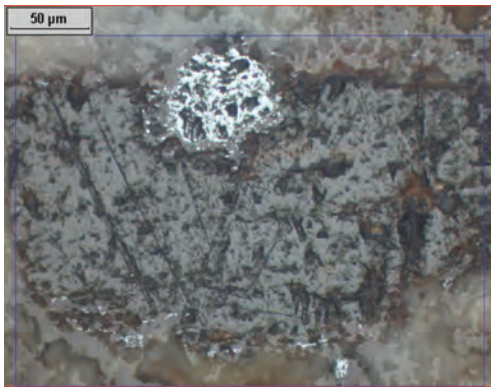


Figure 24- Hematitization starting from the circumference of euhedral biotite grain.

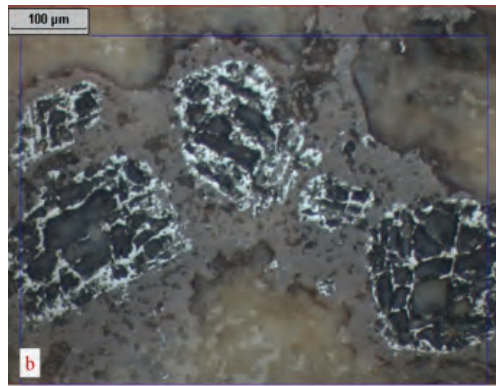
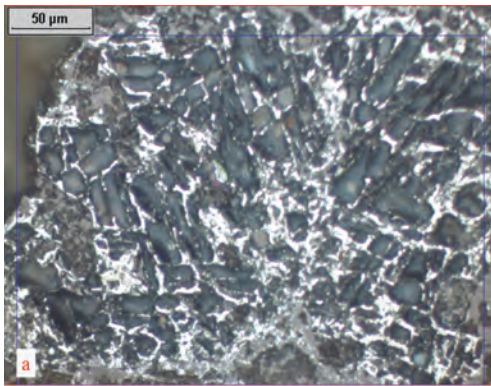


Figure 25- Hematites which substitute carbonates. Hematizations that form along 75° cleavage, which is a typical characteristic of carbonates, display a cell texture (a, b).

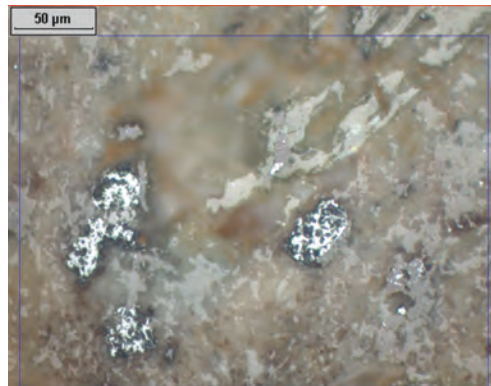


Figure 26- Anhedral hematites in the rock.

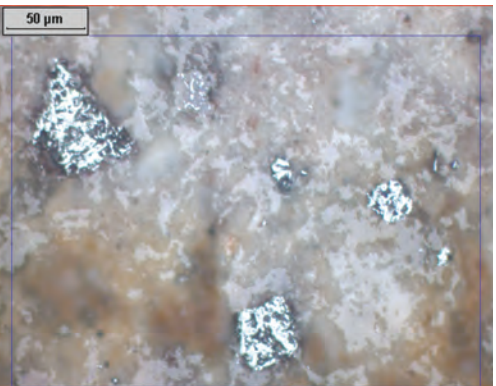


Figure 27- Hematite minerals in variable shapes (triangle, rectangle and amorphous) and sizes dispersed in the rock.

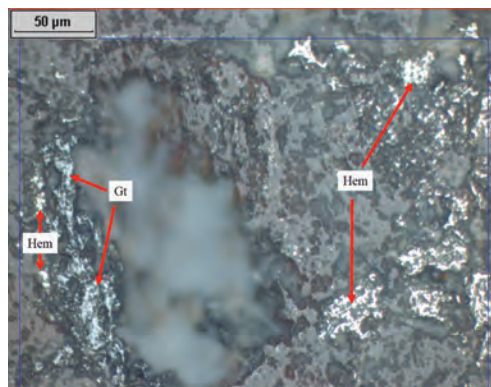


Figure 28- Hematite and goethite. On the left, hematites have altered into goethite.

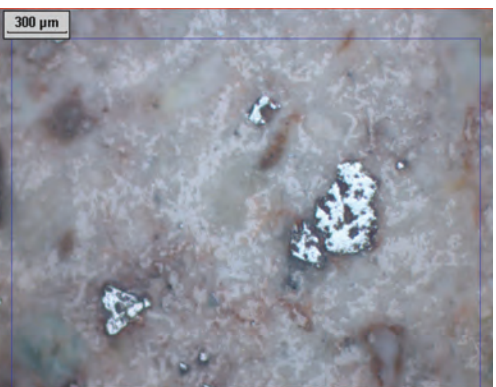


Figure 29- Hematite fully altered into goethite.

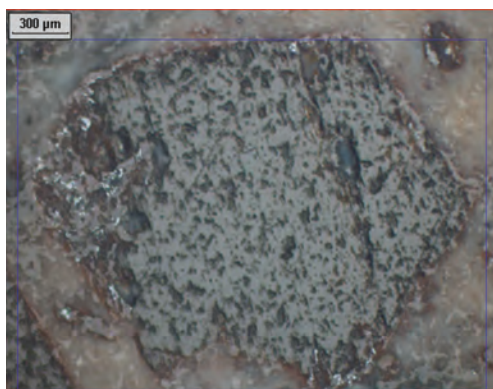


Figure 30- Hematite (white) and goethite (gray) formations observed on the circumference of an opacified amphibole grain.



Figure 31- Highly opacified amphibole; hematite (white), goethite (gray).

#### 4. Discussion and Results

Dutluca volcanics in sulfidic minerals consist of pyrite, enargite and chalcocite and in oxide minerals; magnetite, hematite and goethite. Magnetite is associated with the primary process, and the others are associated with secondary processes.

The most abundant opaque mineral in samples is pyrite; then goethite, hematite, magnetite and enargite minerals are observed in decreasing amount. Sulfur bearing solutions form abundant pyrite minerals reacting with iron which is present in the composition of the rock. The latter forming ore metals can substitute ferrous minerals and form new sulfide minerals (Krauskopf, 1987). Metals and sulfur may remain until low temperatures within excessively saturated solutions and continue to interact with the rock. Variable forms of pyritizations in studied volcanics approve this fact. Pyrite 1 and Pyrite 2 show at least in two stages that solutions with  $H_2S$  caused pyritization. Pyrite 3 has formed as a result of hydrothermal alteration of mafic minerals such as amphibole and biotite. As a result of reaction of some portion of iron which is dissolved from mafic minerals with solution enriched in sulfide pyrites in the form of fracture infilling have formed. These alterations might have formed in Pyrite 1 or Pyrite 2 or at an earlier stage. This relationship was not detected in microscope.

The type of formation of enargite in volcanics shows a parallelism with pyrite. Enargite is an important mineral of paragenesis, because enargite mineral indicates the high sulfidation. Mineralizations, which are defined as sulfidic or acidic sulfate type and show typical alteration as alunite±kaolinite±prophyllite, always contain enargite and differentiate from

adularia-sericite type mineralization (low sulfur) due to this characteristic (Silberman, 1982; Giles and Nelson, 1983).

The presence of few anisotropic chalcocite in samples indicates the formation of secondary sulfide minerals. The occurrence of magnetites is usual. Ramdohr (1969) states that magnetite mineral formed in many basalt, andesite and diabases. In studied samples, subhedral magnetites in fewer amounts than pyrite are seen. Martitizations in variable degrees have formed in many of these magnetites. There was not encountered any magnetite mineral which had been formed by the alteration of minerals such as biotite and hornblende. Hematite is the most abundant mineral in samples after pyrite. Hematite minerals are the secondary products associated with the alteration of opaque and ferrous silicate minerals.

Hematite is the stable mineral of iron in intermediate and oxidic environments. However; in reducing environments pyrite, siderite and magnetite become stable due to the concentration of sulfur and carbonate in solution. The transformation of minerals to each other by oxidizing occurs by means of basic solutions (Krauskopf, 1987). The martitization of magnetites in various degrees shows oxidic conditions and the non-presence of magnetite by hydrothermal alteration from silicates also supports this phenomena. The association of hematite-sulfur is not observed when the solution contains low sulfur. The association of hematite and enargite in studied samples indicates high sulfur concentration (Krauskopf, 1987).

Consequently; the opaque mineral paragenesis (occurrence of enargite in paragenesis), structures and textures reflecting the alteration of opaque and silicate

minerals, which show opacification, indicate that studied volcanics have been altered by highly sulfidic hydrothermal solutions. Hydrothermal alteration process has developed in at least two phases.

Primary magnetite bearing volcanics have firstly caused a widespread pyritization under reducing conditions rich in H<sub>2</sub>S, and the formation of enargite which is known as pathfinder mineral in such processes. Later on; the oxygen in the environment has increased and intensive martitizations in oxidic conditions have developed.

### Acknowledgement

This study has been carried out at the Ankara University, within scope of Scientific Investigation Projects (BAP) numbered as 13B4343012. We would like to thank to executives of BAP and to MTA (General Directorate of Mineral Research and Exploration) who helped during the collection of drill samples.

### References

- Akyürek, B., Soysal, Y. 1978. Kırkağaç-Soma (Manisa), Savaştepe-Korucu-Ayvalık (Balıkesir). Bergama (İzmir) civarının jeolojisi. *Maden Tetkik ve Arama Genel Müdürlüğü Raporu*, no.6432, Ankara (unpublished).
- Bingöl, E., Akyürek, B., Korkmazer, B. 1973. Biga Yarımadasının jeolojisi ve Karakaya formasyonunun bazı özellikleri. *Cumhuriyetin 50. yılı Yerbilimleri Kongresi Tebliğleri Kitabı*, pp.70-76, Ankara.
- Çolakoğlu, A.R. 2000. Küçükdere (Havran-Balıkesir) epitermal altın damarlarının özellikleri. *Türkiye Jeoloji Bülteni*, c. 43, sayı 2, 99-110p.
- Çolakoğlu, A.R., Sezerer Kuru, G. 2001. Küçükdere (Havran-Balıkesir) epitermal altın damarlarında sıvı kapanım çalışmaları. *Yerbilimleri Dergisi*, 24, pp.1-11.
- Ercan, T. 1982. Batı Anadolu'nun Genç Tektoniği ve Volkanizması. Batı Anadolu'nun Genç Tektoniği ve Volkanizması Paneli, *TJK Yayını*, pp.5-14.
- Ercan, T., Günay, E., Savaşçın, M. Y. 1983. Simav ve çevresindeki Senozoyik yaşlı volkanizmanın bölgesel yorumlanması. *Maden Tetkik ve Arama Genel Müdürlüğü Dergisi* 97/98, pp.86-101.
- Ercan, T., Günay, E., Türkecan, A. 1984. Edremit-Korucu yöresinin (Balıkesir) Tersiyer Stratigrafisi magmatik kayaların petrolojisi ve kökensele yorumu. *Türkiye Jeoloji Kurumu Bülteni*, C. 27, pp.21-30.

- Ercan, T., Ergül, E., Akçören, F., Çetin, A., Granit, S., Asutay, J. 1990. Balıkesir-Bandırma arasının Tersiyer volkanizmasının petrolojisi ve bölgesel yayılımı. *Maden Tetkik ve Arama Genel Müdürlüğü Dergisi* 110, pp.113-130.
- Giles, D. L., Nelson, C. E. 1983. Principal features of epithermal lode gold deposits of the circum-pacific rim: circum pacific. *Energy Mineral Resource Conference*, 3rd, Honolulu, Hawaii, August 22-28, Trans., pp.273-278.
- Hedengvist, J.W. 1985. Hydrothermal eruptions in the Waiotapu geothermal system, New Zealand: origin, breccia deposits and effects on precious metal mineralization. *Economic Geology*, 80, pp.1640-1666.
- Krauskopf, K. B. 1987. Introduction to Geochemistry. Mc Graw-Hill Book Company, 667p.
- Krushensky, R.D. 1976. Neogene calcalkaline extrusive and intrusive rocks of the Karalar-Yeşiller area, north-west Anatolia. *Bull. Volcan.*, 40, pp.336-360.
- Ramdohr, P. 1969. The Ore Minerals and Their Intergrowths. *Pergamon Press*, 1174p.
- Silberman, M.L. 1982. Hot-spring type, large tonnage, low grade gold deposit. *U.S. Geol. Survey Open File Rept.* 82-795, pp.131-143.
- Simmons, S.F., White, N.C., John, D.A. 2005. Geological characteristics of epithermal precious and base metal deposits. *Economic Geology*, 100th Anniversary Volume, pp.485-522.
- Şengör, A.M.C., Yılmaz, Y. 1981. Tethyan evolution of Turkey: A plate tectonic approach. *Tectonophysics*, v. 75, pp.181-241.
- Yiğit, Ö. 2012. A prospective sector in the Tethyan Metallogenic Belt: Geology and geochronology of mineral deposits in the Biga Peninsula, NW Turkey. *Ore Geology Reviews*, pp.118-148.
- Yüzer, E., Tunay, G. 2012. Biga Yarımadasının Genel ve Ekonomik Jeolojisi. *Maden Tetkik ve Arama Genel Müdürlüğü Özel yayın serisi* 28., 326p., Ankara





and paleoenvironment properties of diatomites in the Çiftlik Basin (Niğde) region are studied by Yıldız and Gürel (2005) and diatom assemblage and lithofacies characteristics of diatomites in the Ihlara-Selime region are investigated by Gürel and Yıldız (2006).



Figure 1- Location map of study area with measured stratigraphic section sites.

Physicochemical properties and the area of use of diatomite levels within late Miocene-Quaternary volcanogenic units exposing in the study area are first discussed in this study in detail. The Cappadocian Volcanic Province (CVP) is one of diatomite-rich regions in Turkey. In this respect, determining the physicochemical properties and the area of use of diatomites of Karacaören region within CVP is important to contribute to science and industry.

**2. Material and Method**

In the study area, 2 stratigraphic sections were measured; one is in Quaternary lacustrine deposits (K1) (thickness 9 m) and another is in lacustrine deposits of Bayramhacılı member of Miocene Ürgüp formation (K2) (thickness 50 m). A total of 12 diatomite samples were collected along both sections and were photographed in the field (Figures 2-5). Scanning electron microscope (SEM) (FEI Quanta 400 MK2 model) photographs of diatomite assemblage of a diatomite-rich sample (sample K2-5) were taken at laboratories of General Directorate of Mineral Research and Exploration in Ankara (Figure 6).

To determine physicochemical properties and the area of use of diatomites, samples collected from the field were subjected to several analyses at laboratories of General Directorate of Mineral Research and Exploration (MTA) including X-ray diffractometry (XRD) analysis (Cu X-ray tube Bruker D8 Advanced XRD device), loss on ignition (at 1050°C), thermal conductivity analysis (using Unitherm Model 2022

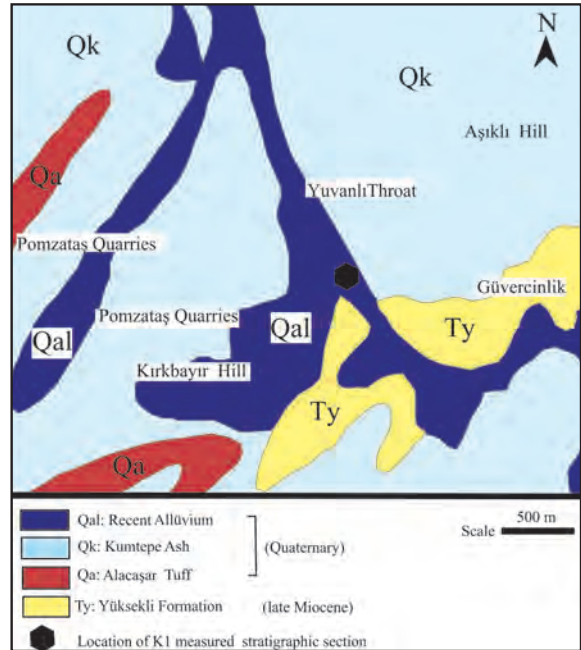


Figure 2- Location of K1 measured stratigraphic section and geology map (compiled from Pasquare, 1968; MTA, 1989).

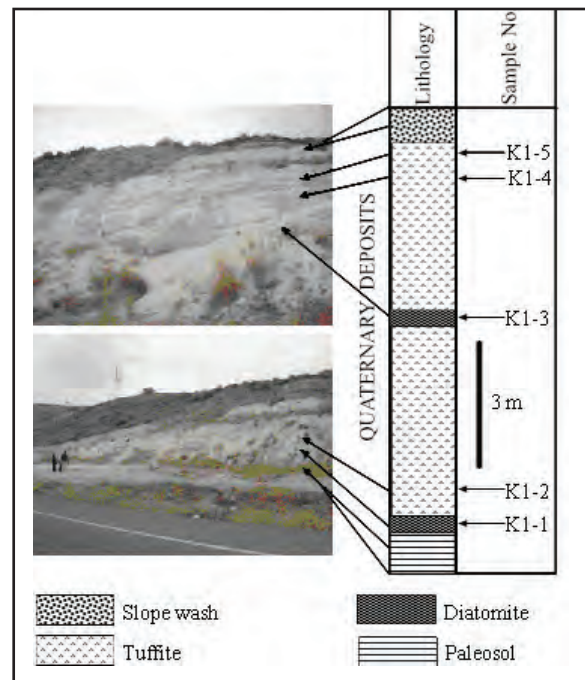


Figure 3- K1 measured stratigraphic section.

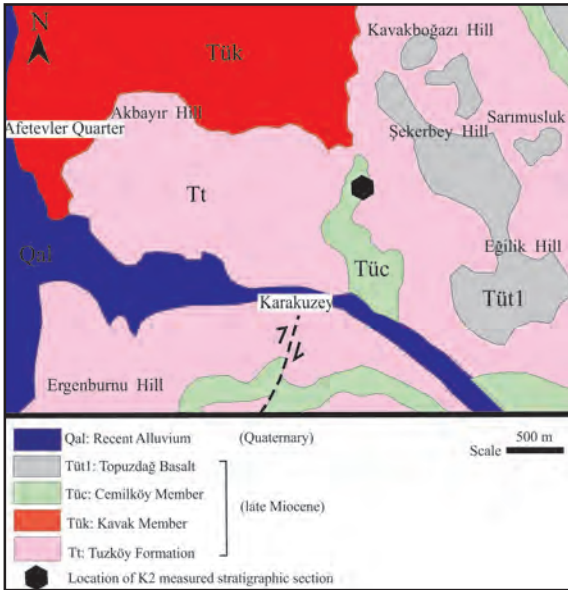


Figure 4- Location of K2 measured stratigraphic section and geology map (compiled from Pasquare, 1968; MTA, 1989).

Thermal Conductivity Instrument 101; at 150°C and  $\pm 10^\circ\text{C}$ ), X-ray fluorescence spectrometer (XRF) analysis (samples were dried at 105°C and analysis was made with Thermo ARL brand XRF device equipped with UQ program), pH analysis (pH analysis of 10% solution of samples was made with wet method), amount of acid and water-insoluble matter (chemical analysis was made drying samples at 105°C), total porosity and density (since samples fall apart during absorption, porosity tests were not performed by water absorption method but their apparent density was determined with mercury-method), whiteness analysis (using Minolta Chroma Meter CR 300 device), specific surface area, pore volume, pore size analysis (with Nova Station B device) and grain size analysis (with wet method on Malvern Mastersizer 2000 device) (Tables 1–5). Results obtained were compared to those from standardized analysis of diatomites in Turkey and various parts of the world and the area of use of diatomites was assessed.

### 3. Regional Geology and Stratigraphy

The study area is located in the Cappadocian Volcanic Province (CVP). The CVP is a NE-SW extending province with length of 250–300 km and width of 60 km lying about 1400-1500 m above the sea level (Aydar et al., 2012). CVP is a calc-alkaline volcanic terrain which was formed as a result of collision between Eurasia and Africa-Arabian plates (Batum, 1978). The study area was

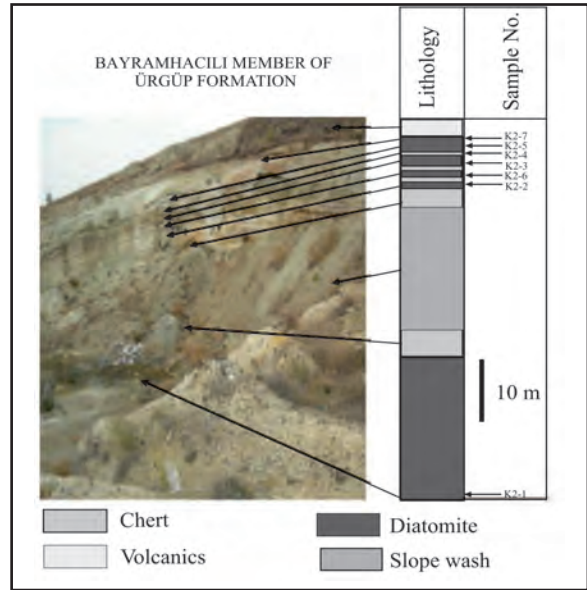


Figure 5- K2 measured stratigraphic section geology map (compiled from Pasquare, 1968; MTA, 1989).

undergone a complex neotectonic deformation during late Miocene-Pliocene and consequently several faults and within plate basins were formed and the region witnessed intense volcanism (Dirik, 2001). The Cappadocian Volcanic Province is bordered by Central Anatolian Fault Zone at east, Tuz Gölü Fault Zone at west and Orta Kızılırmak Fault Zone to the north. Derinkuyu Fault and Niğde Fault Zone are at the south. CVP is grouped into three rock units comprised by volcanic complexes corresponding to main eruption centers, volcanoclastic rocks and cinder cone areas. A total of 19 volcanic centers were determined. The highest ones are Erciyes Mountain (3917 m) and Hasandağ (3268 m) (Ekingen, 1982). Based on paleontological, palynological and radiometric age data, tectonic depression area at north of CVP was filled during late Miocene-Quaternary time by lacustrine and fluvial sediments that are intercalated with volcanic units. Volcano-sedimentary rocks in the region unconformably overlie the Paleozoic-Cretaceous basement rocks of Niğde massif at south and Kırşehir massif at north (Schumacher et al., 1990; Toprak, 1996). These deposits in the Ürgüp basin are described by Pasquare (1968) and Viereck-Goette et al. (2010) as Ürgüp formation. This stratigraphic level corresponds to Messinian salinity crisis that took place in the late Miocene. The deposits of Ürgüp formation which are interlayered with lacustrine and fluvial sediments are widely distributed within CVP and host several ignimbrite, andesitic and basaltic lava levels.

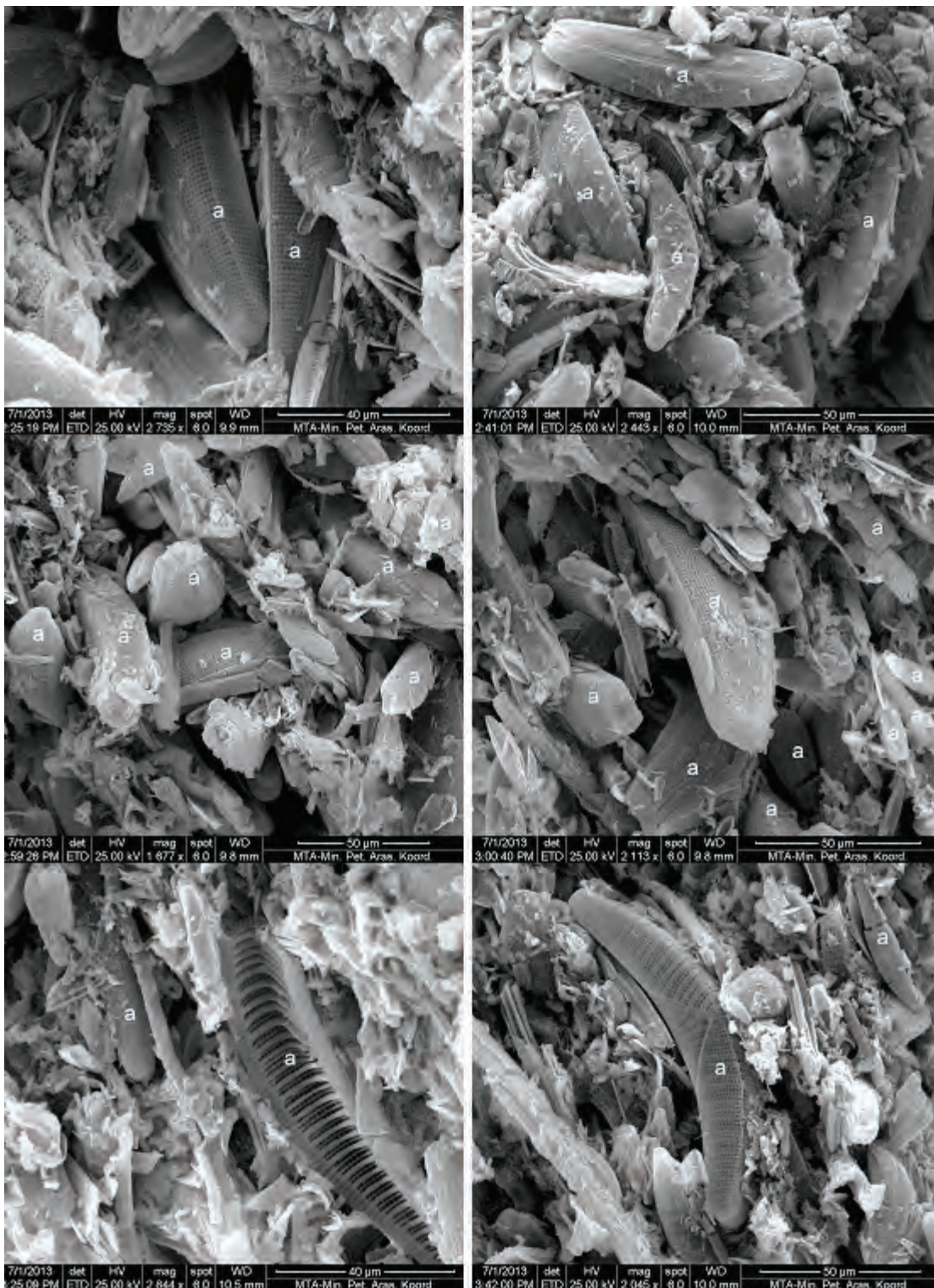


Figure. 6- Scanning electron microscope (SEM) images of sample K2-5 from K2 measured section, (a) bulk pennate diatome forms.

Table 1- Results of XRD analysis of the studied samples.

Sample No.	Analysis Results
K1-1	1- Smectite 2- Feldspar 3- Opal-CT 4- Opal A
K2-1	1- Smectite 2-Feldspar 3- Opal- CT. 4-Quartz (trace) 5- Opal A
K2-4	1- Smectite 2-Feldspar 3- Opal- CT.
K2-7	1- Smectite 2- Opal- CT.

They are namely Kavak, Zelve, Sarımaden Tepe (or Sofular), Cemilköy, Tahar, Gördeles, Kızılkaya and İncesu ignimbrites, Topuzdağ and Çataltepe basalts and Bayramhacılı and Kışladağ members. Radiometric age data indicate that these rocks are of late Miocene-Pliocene age (Besang et al., 1977). The Bayramhacılı member is composed of lacustrine and fluvial sediments consisting of conglomerate, sandstone, limestone, marl and diatomite. The Kışladağ member is composed of lacustrine limestone and diatomite. Lacustrine limestone contains ostracode and gastropod fossils. Kavak, Zelve and Sarımaden Tepe ignimbrites are generally white-gray while Cemilköy ignimbrite is dull gray colored. The pinkish colored Tahar ignimbrite, dull gray colored Gördeles ignimbrite and red-pinkish colored Kızılkaya ignimbrite are have a wide distribution and show columnar joint structures (Le Pennec et al., 1994). The Ürgüp formation is overlain by Quaternary alluvium. The age ignimbrite series within the formation is found as 1 to 9 Ma ( $^{40}\text{Ar}/^{39}\text{Ar}$  plagioclase and U-Pb zircon dating methods) (Aydar et al., 2012).

Table 2 – Results of thermal conductivity analysis.

Sample No.	At Temperature of $\pm 10^\circ\text{C}$		At Temperature of 101; 150 $^\circ\text{C}$	
	Average Sample Temperature ( $^\circ\text{C}$ )	Thermal Conductivity Value (W/mK)	Average Sample Temperature ( $^\circ\text{C}$ )	Thermal Conductivity Value (W/mK)
K1-1	- 4,63	0,891	101,08	0,193
	2,10	0,785	126,28	0,198
	11,81	0,738	151,53	0,221
K2-1	- 5,79	0,984	101,04	0,223
	1,71	0,860	126,21	0,220
	11,42	0,790	151,36	0,225
K2-4	- 6,20	0,590	100,90	0,164
	1,17	0,503	126,08	0,155
	11,00	0,452	151,09	0,140
K2-7	- 5,42	0,742	100,90	0,136
	1,31	0,595	125,99	0,137
	10,98	0,484	151,05	0,134

Table 3- Total porosity, whiteness, acid and water-insoluble matter contents of diatomite samples from studied area.

Sample No.	Total Porosity (%)	Results of Whiteness Analysis				Acid-Insoluble Matter Content (%)	Water-Insoluble Matter Content (%)
		L	a	b	Y		
K1-1	69,40	84,29	+0,94	+6,66	64,63		
K2-1	64,89	92,62	+0,62	+4,29	82,29		
K2-4	76,90	87,14	+0,22	+15,04	70,30		
K2-7	76,56	83,93	+1,60	+11,97	63,94		
K2-5						90,20	98,85

Diatomites in the Karacaören

Table 4 – Results of specific surface area, pore volume and pore size analysis.

Methods	Sample No.			
	K1-1	K2-1	K2-4	K2-7
<b>Specific Surface Area</b>				
Multiple Point BET	2,027 e <sup>+02</sup> m <sup>2</sup> /g	4,315 e <sup>+01</sup> m <sup>2</sup> /g	1,678 e <sup>+01</sup> m <sup>2</sup> /g	1,558 e <sup>+01</sup> m <sup>2</sup> /g
Cumulative Absorption Specific Surface BJH	1,200 e <sup>+02</sup> m <sup>2</sup> /g	3,337 e <sup>+01</sup> m <sup>2</sup> /g	1,938 e <sup>+01</sup> m <sup>2</sup> /g	1,956 e <sup>+01</sup> m <sup>2</sup> /g
Cumulative Desorption Specific Surface BJH	1,985 e <sup>+01</sup> m <sup>2</sup> /g	4,485 e <sup>+01</sup> m <sup>2</sup> /g	2,574 e <sup>+01</sup> m <sup>2</sup> /g	2,600 e <sup>+01</sup> m <sup>2</sup> /g
Cumulative Absorption Specific Surface DH	1,217 e <sup>+01</sup> m <sup>2</sup> /g	3,387 e <sup>+01</sup> m <sup>2</sup> /g	1,967 e <sup>+01</sup> m <sup>2</sup> /g	1,985 e <sup>+01</sup> m <sup>2</sup> /g
Cumulative Desorption Specific Surface DH	2,011 e <sup>+01</sup> m <sup>2</sup> /g	4,550 e <sup>+01</sup> m <sup>2</sup> /g	2,610 e <sup>+01</sup> m <sup>2</sup> /g	2,638 e <sup>+01</sup> m <sup>2</sup> /g
<b>Pore Volume</b>				
Cumulative Absorption Pore Volume BJH		8,124 e <sup>-02</sup> cc/g	4,626 e <sup>-02</sup> cc/g	4,334 e <sup>-02</sup> cc/g
Cumulative Desorption Pore Volume BJH	3,190 e <sup>-01</sup> cc/g	7,245 e <sup>-02</sup> cc/g	4,133 e <sup>-02</sup> cc/g	3,747 e <sup>-02</sup> cc/g
Cumulative Absorption Pore Volume DH	2,865 e <sup>-01</sup> cc/g	7,916 e <sup>-02</sup> cc/g	4,508 e <sup>-02</sup> cc/g	4,225 e <sup>-02</sup> cc/g
Cumulative Desorption Pore Volume DH	3,109 e <sup>-01</sup> cc/g	7,064 e <sup>-02</sup> cc/g	2,029 e <sup>-01</sup> cc/g	3,654 e <sup>-02</sup> cc/g
<b>Pore Diameter</b>				
Absorption Pore Diameter BJH	3,125 e <sup>+01</sup> A	3,141 e <sup>+01</sup> A	3,141 e <sup>+01</sup> A	4,038 e <sup>+01</sup> A
Desorption Pore Diameter BJH	3,703 e <sup>+01</sup> A	3,671 e <sup>+01</sup> A	3,716 e <sup>+01</sup> A	3,687 e <sup>+01</sup> A
Absorption Pore Diameter DH	3,125 e <sup>+01</sup> A	3,141 e <sup>+01</sup> A	3,141 e <sup>+01</sup> A	4,038 e <sup>+01</sup> A
Desorption Pore Diameter DH	3,703 e <sup>+01</sup> A	3,671 e <sup>+01</sup> A	3,716 e <sup>+01</sup> A	3,687 e <sup>+01</sup> A

Table 5- Standardized compositions of various diatomites used in different areas and comparison of XRF, loss on ignition, grain size, density and pH analyses on samples 1) Spain, raw, 2) France, calcined, beer filtration, 3) Italy, raw, light construction material, 4) W. Germany, fertilizer carrier, 5) W. Germany, calcined, beer filtration, 6) W. Germany, calcined and fill material, 7) W. Germany, filter matter, 8) Brazil, insulation matter, 9) USA, calcined filtration diatomite, 10) Basalt-Nevada (modified from Uygun, 2001).

	1	2	3	4	5	6	7	8	9	10	KARACAÖREN			
											K1-1	K2-1	K2-4	K2-7
%SiO <sub>2</sub>	86,6	89,9	88,6	69,7	82,9	92,1	94,4	86	88,4	83,13	68,3	84,2	88,9	87,1
%TiO <sub>2</sub>	0,1	0,6	0,2	0,4	0,1	0,2	0,1	0,7	0,2		0,4	0,1	< 0,1	< 0,1
%Fe <sub>2</sub> O <sub>3</sub>	0,4	2,2	8,3	3,1	10,1	0,6	4	1,4	1,5	2,00	4,6	1,1	1,8	3,3
%Al <sub>2</sub> O <sub>3</sub>	0,9	3,9	1,7	4,9	1,8	2,6	2,3	9,4	4,1	4,60	11,5	3,8	0,7	0,9
%CaO	5,2	0,8	0,6	0,4	2,5	0,1	0,2	0,1	0,6	2,50	2,4	1,6	1,1	1,1
%MgO	0,6	0,2	0,1	0,1	0,4	0,1	0,2	0,4	0,8	0,64	2,7	0,8	0,3	0,3
%Na <sub>2</sub> O	0,2				1,1	0,9	3,2		2,9	1,60	1	0,6	0,1	0,3
%K <sub>2</sub> O	0,1	0,2	0,3	1,2	0,3	0,3	0,6	0,2	0,7	0,44	0,7	0,3	< 0,1	< 0,1
%P <sub>2</sub> O <sub>5</sub>	0,2	0,3	0,1		0,1	0,1	0,1		0,2	4,92	0,1	0,6	0,5	0,4
%V <sub>2</sub> O <sub>5</sub> + TiO <sub>2</sub>										0,23				
%SiO <sub>3</sub>											0,20	0,35	0,10	0,08
%SrO											0,03	0,02	< 0,01	< 0,01
%BaO											0,03	< 0,01	< 0,01	< 0,01
%ZrO <sub>2</sub>											0,02	< 0,01	< 0,01	< 0,01
%V <sub>2</sub> O <sub>5</sub>											0,02	0,03	0,01	0,03
%ZnO											0,01	< 0,01	< 0,01	< 0,04
%CuO											0,01	< 0,01	< 0,01	< 0,01
%MnO											0,2	< 0,1	0,1	< 0,1
Loss on Ignition % (at 850 °C)	5,5	0,7	0,5	19,1	0,5	3	5,9	2	0,3	5,30	7,65(1050 °C)	6,20(1050 °C)	6,20(1050 °C)	6,10(1050 °C)
Average Grain Size (µ)	3,4	2,7	2,4	4,7	4,5	1,2	6,8	2,7	14,7		550	15	15	20
Grain Smaller than 20 µ (%)	3,7	0,8	1,6	23,4	6,8	2,7	20	4,6	31,8		< 1	< 5,5	< 7,5	< 7
Wet Density (g/cm <sup>3</sup> )	4,17	2,44	2,44	3,00	2,17	2,50	2,50	2,08	2,44		2,43	2,26	2,29	2,30
Filtration Rate (ml/min)	12	52	30	18	70	10	190	50	740					
pH	8,3							8,5		8,8	8,65	9	8,7	9,85
Quartz (%)				18										

Table 6- Comparison of analyses values of various commercially used diatomites in Turkey with those of studied diatomites 1) Turkey – Kayseri, 2) Kayseri-Kırka, 3) Aydın-Dedeler, 4) Ürgüp, 5) Denizli-Sarayköy, 6) Kütahya-Alayunt, 7) Balıkesir-Balya, 8) Niğde-Belısırma, 9) Afyon-Incehisar, 10) Afyon-Tınaztepe, 11) Ankara-Kızılcahamam, 12) Çankırı-Çerkeş (modified from Sariz and Nuhoğlu, 1992; Aruntaş et al., 1998; Bozkurt, 1999; Nuhoğlu and Elmas, 1999; Bentli, 2001; 8 th Five-Year Development Plan, 2001; Uygun.2001).

	1	2	3	4	5	6	7	8	9	10	11	12	KARACAÖREN			
													K1-1	K2-1	K2-4	K2-7
%SiO <sub>2</sub>	90,2	90,0	89,6	88,7	85,0	84,42	79,5	72,1	81,86	84,15	88,62	83,25	68,3	84,2	88,9	87,1
% TiO <sub>2</sub>	0,1	0,2	0,01	0,06	0,01	0,05		0,2					0,4	0,1	< 0,1	< 0,1
% Fe <sub>2</sub> O <sub>3</sub>	0,8	1,1	14	3,38	2,8	1,55	3,24	4,4	1,87	3,36	0,57	1,20	4,6	1,1	1,8	3,3
% Al <sub>2</sub> O <sub>3</sub>	3,3	2,9	21	1,11	5,0	5,02	6,14	13,1	3,91	4,50	3,30	5,50	11,5	3,8	0,7	0,9
% CaO	0,6	0,7	0,01	1,35	0,01	0,96	12	0,9	0,86	1,07	0,74	1,30	2,4	1,6	1,1	1,1
% MgO	0,3	0,5	12	0,38	1,6	0,74	1,19	3,7	0,15	1,03	0,80	1,90	2,7	0,8	0,3	0,3
% Na <sub>2</sub> O		0,6	0,06	0,28	0,13	0,62		17		0,47	0,77	0,95	1	0,6	0,1	0,3
% K <sub>2</sub> O	0,1	0,2	0,15	0,32	0,4	0,60		0,1		0,44	0,71	1,30	0,7	0,3	< 0,1	< 0,1
% P <sub>2</sub> O <sub>5</sub>			0,01	0,42	0,01			1,7					0,1	0,6	0,5	0,4
% V <sub>2</sub> O <sub>5</sub> + TiO <sub>2</sub>								1,9								
% SiO <sub>3</sub>													0,20	0,35	0,10	0,08
% SrO													0,03	0,02	< 0,01	< 0,01
% BaO													0,03	< 0,01	< 0,01	< 0,01
% ZrO <sub>2</sub>													0,02	< 0,01	< 0,01	< 0,01
% V <sub>2</sub> O <sub>5</sub>													0,02	0,03	0,01	0,03
% ZnO													0,01	< 0,01	< 0,01	< 0,04
% CuO													0,01	< 0,01	< 0,01	< 0,01
% MnO													0,2	< 0,1	0,1	< 0,1
Loss on Ignition % (at 850 °C)	4,2	4,6	5,5	2,7	5,25	6,09	8,35	4,2	11,31	4,92	4,24	5,54	7,65(1050 °C)	6,20(1050 °C)	6,20(1050 °C)	6,10(1050 °C)
Average Grain Size (µ)	3,3					10					145	90	550	15	15	20
Grain Smaller than 20 µ (%)	2,7												<1	< 5,5	< 7,5	< 7
Wet Density (g/cm <sup>3</sup> )	2,94					1,9 2,4					1,95	1,90	2,43	2,26	2,29	2,30
Filtration Rate (ml/min)	48															
pH		8,0									7,87	7,28	8,65	9	8,7	9,85
Color						White					White	White	White	White	White	White

Stratigraphic units in the study area, from bottom to the top, are composed of late Miocene Tuzköy formation (Tt), Yüksekli formation (Ty) and Kavak member (Tük), Cemilköy member (Tüc), Topuzdağ basalt (Tüt1), Quaternary Alacaşar tuff (Qa), Kumtepe Ash (Qk) and recent alluvium deposits (Qal) within the Ürgüp formation (Bayramhacılı member) (Figure 7).

*Tuzköy Formation (Tt)*: It was named by Atabey et al. (1988). It consists of yellow colored, thin bedded, bioturbated siltstone, laminated silicified claystone, thin bedded and laminated sandstone and tuff alternation. Limestone and claystone host gypsum crystals. The unit has thickness of 100 m It is unconformable with underlying Kızılöz formation. Based on *Cyprideis* sp., *Chara*, *Ilyocyris* cf. *gibba*

(Ranbohr) fossils in marl samples and stratigraphic relations, the age of Tuzköy formation is late Miocene.

*Yüksekli Formation (Ty)*: It was named by Aydın (1984). It consists of whitish-gray colored, medium-fine grained, trough cross bedded sandstone, pebbly sand, tuffite, siltstone, claystone and coarse sandstone and conglomerate. Pebbles show sorting and orientation. The unit that represents a lacustrine environment has thickness of 200 m and is concordant with underlying Tuzköy formation.

*Bayramhacılı Member of Ürgüp Formation (Tü)*: It was named by Pasquare (1968). This member is found at the base of Ürgüp formation. It consists of lacustrine and fluvial sediments that are made up by conglomerate, limestone, clay, marl, volcanic ash,

Table 7- Comparison of physicochemical properties of diatomites in the study area with standardized compositions of diatomites commercially used in various industrial sectors (modified from Özbey and Atamer,1987; Açıklan, 1991; Aruntaş et al., 1998; Bentli, 2001).

	COMMERCIAL	DIATOMITES USED IN SUGAR PLANTS IN TURKEY	FILTER		FILL			ABRASIVE AUTOMOBILE POLISH	REGULATORY FERTILIZER	KARACAÖREN			
			WINE	SUGAR	PAPER	PAINT	PLASTIC			K1-1	K2-1	K2-4	K2-7
%SiO <sub>2</sub>	>85,0	87,3								68,3	84,2	88,9	87,1
% TiO <sub>2</sub>										0,4	0,1	< 0,1	< 0,1
% Fe <sub>2</sub> O <sub>3</sub>	<1,5	1,95								4,6	1,1	1,8	3,3
% Al <sub>2</sub> O <sub>3</sub>	<5,0	3,23								11,5	3,8	0,7	0,9
% CaO	<1,0	1,09								2,4	1,6	1,1	1,1
% MgO	<0,5	0,45								2,7	0,8	0,3	0,3
% Na <sub>2</sub> O	<1,0	0,47								1	0,6	0,1	0,3
% K <sub>2</sub> O	<1,0	0,44								0,7	0,3	< 0,1	< 0,1
% P <sub>2</sub> O <sub>5</sub>										0,1	0,6	0,5	0,4
% SiO <sub>3</sub>										0,20	0,35	0,10	0,08
% SrO										0,03	0,02	< 0,01	< 0,01
% BaO										0,03	< 0,01	< 0,01	< 0,01
% ZrO <sub>2</sub>										0,02	< 0,01	< 0,01	< 0,01
% V <sub>2</sub> O <sub>5</sub>										0,02	0,03	0,01	0,03
% ZnO										0,01	< 0,01	< 0,01	< 0,04
% CuO										0,01	< 0,01	< 0,01	< 0,01
% MnO										0,2	< 0,1	0,1	< 0,1
Loss on Ignition % (at 850 °C)	< 6,0	4,43								7,65(1050 °C)	6,20(1050 °C)	6,20(1050 °C)	6,10(1050 °C)
Average Grain Size (µ)			2,5	22		6,8	5,1	5,5		550	15	15	20
Grain Smaller than 20 µ (%)										<1	< 5,5	< 7,5	< 7
Wed Density (g/cm <sup>3</sup> )			2,3	2,0	2,4	2,2	2,8	2,4	1,7	2,43	2,26	2,29	2,30
Water Absorption(%)	>280 >180												
pH		4,49	7,0	10	7,0	10	7,0	9,4	7,0	8,65	9	8,7	9,85
Moisture (%)	<15												
	White	Dirty White	Pink	White	Grey	White	Pink	White	Yellowish	White	White	White	White

siltstone and diatomite and volcanic material-bearing sandy and fine grained deposits interbedded with epiclastic, lateritic and sandy soils (Pasquare, 1968; Le Pennec et al., 1994).

*Kavak Member (Tük):* It was named by Pasquare (1968). The member has ignimbritic character and contains light brown, whitish homogeneous ignimbrite and pumice. In the Kavak member, white-dirty white colored, glassy tuff-bearing angular pumice ash levels are also observed. The member with thickness of 100 m represents the first ignimbrite occurrence in the Ürgüp region. It is transitional to Tuzköy formation.

*Cemilköy Member (Tüc):* It was named by Pasquare (1968). According to Pasquare (1968), the member is pure white colored, pumice-bearing a volcano-sedimentary unit with a lithic character. It locally contains ophiolitic rock and basaltic lava pebbles. The unit with thickness of 80 m is conformable with underlying Kavak and Sarımaden Hill members. In the member following fossils were determined:

*Hipparion gracile* de Christol, *Samotherium majori* Bohlin, *antilope* sp., *gazella* sp. and *Hipparion meditarreneum* Hansel, *Rhinoceras* sp. (Şenyürek, 1953, İzbırak and Yalçınlar, 1951).

*Topuzdağ Basalt (Tüt1):* Volcanites of basic composition exposing at west of Tekkedağ are named by Dönmez et al. (2003) as Topuzdağ Volcanite. The same rock unit is called as Topuzdağ basalt by Atabey (1989). The main eruption center is at northeast of Ürgüp. It is composed of dark black-gray colored, banded, platy altered lava and pyroclastics of basic composition having little or no phenocrystal (Dönmez et al., 2003). It is described as pyroxene andesite.

*Alacaşar Tuff (Qa):* It is exposed in the area between Nevşehir, Alacaşar, Gülşehir and Çat. It is widely distributed in Alacaşar village, Baçlın, Çat and Sulusaray counties and at south of Gülşehir. It is composed of pink colored, obsidian-rich, glassy and pumice-bearing tuffs interbedded with gray ash deposits (Atabey, 1989). Brecciated tuff and sand

Upper System	System	Series	Million Year (Ma)	Formation	Member	Thickness (m)	Symbol	Lithology	Remarks		
Cenozoic	Quaternary						Qal		Recent alluvium, diatomite.		
							Qk		Kumtepe ash.		
							Qa		Alacaşar tuff.		
	Neogene	Miocene	6.3 - 7.0 - 6.7 - 13.7	Ürgüp	Bayramhacılı	12	Tüt1		Topuzdağ basalt.		
						80	Tüc		Pumice, lahar, Sediment, diatomite.		
						100	Tük		White colored ignimbrite, lahar, sediment.		
					Yüksekli			200	Ty		Trough cross bedded sandstone, conglomerate, sandy silt, siltstone.
					Tuzköy			100	Tt		sandstone, siltstone tuffite, gypsum.

Figure 7- Generalized stratigraphic section of the study area (compiled from Pasquare, 1968; MTA, 1989; Lepetit et al., 2014), No scale.

interlayers are locally observed. Boğazköy obsidian, Taşkesik hill, Villa hill and Tepeköy rhyolites are covered by the Alaşar tuff (Dönmez et al., 2003).

*Kumtepe Ash (Qk)*: It is composed of pumice-rich glassy ashes. Fragmented pumice, obsidian, vitrophyre, plagioclase crystals and (oligoclase and andesine) and hornblende are observed within the vitrified cement. Based on vertebrate fossils such as *Sus* sp., *Antilope* sp., *Cervus* sp., *Equus* sp. within clays at Hanyerininbaşı hill, the age of Kumtepe ash is accepted as Holocene (Ozansoy, 1964).

*Recent Alluvium (Qal)*: Recent alluviums in the study area are composed of pebble, sand and soils distributed along the Kızılırmak River.

#### 4. Results

##### 4.1. Stratigraphic Sections Measured in the Study Area

In the study area two stratigraphic sections were measured; one is in Quaternary lacustrine sediments (K1) and another is in lacustrine sediments of Bayramhacılı member of Miocene aged Ürgüp formation (K2) (Figures 2–5).

*K1 measured stratigraphic section*: In 1/25.000 scaled Kayseri K33-d3 quadrangle, K1 section has start coordinates of longitude: 0651683, latitude: 4269138, elevation: 1311 m and end coordinates of longitude: 0651645, latitude: 426917, elevation: 1320 m. The thickness of section is 9 m and 5 samples were collected (Figures 2 and 3). The section starts at the bottom with a light brown paleosol level. Towards the upper part of section, following units are observed: 50 cm-thickened white colored diatomite level, 4.5 m-thickened light gray tuffites and 30 cm-thickened white diatomite level. The second diatomite level is overlain by a gray colored tuffite level of 3.7 m thickness and a slope wash comprises the uppermost part of section (Figure 3).

*K2 measured stratigraphic section*: In 1/25.000 scaled Kayseri K33-d3 quadrangle, K2 section has start coordinates of longitude: 0670278, latitude: 4278081, elevation: 1175 m and end coordinates of longitude: 0670351, latitude: 4278360, elevation: 1233 m. The thickness of section is 58 m and 7 samples were collected (Figures 4 and 5). The K2 section starts at the bottom with a white diatomite

level of 23 m thickness. It is overlain by light brown chert level of 4 m thickness and slope wash of 10 m thickness. It is covered with another light brown chert level of 4 m thickness and 4 different white diatomite levels of about 1 m alternating with cherts (Figure 5). Diatomites at both locations are light and soft and easily fall apart within hand.

#### 4.2. Results of Analysis for Samples Collected From the Study Area

In order to determine physicochemical properties and the area of use of diatomites in the study area, XRD analysis was carried out on samples collected from the field. Results indicate that smectite is the main clay mineral in both sections (K1 and K2) and feldspar and opal are the secondary phases. A sample from K2 section (sample K2-1) contains little quartz (Table 1). It is known that smectite is an authigenic mineral occurring in alkali environments (Gürel and Kadir, 2006). This might show that diatomites in the area were formed in an alkali environment.

As a result of thermal conductivity analysis, samples from both sections (K1 and K2) are found to have thermal conductivity values in the range from 0.452 to 0.984 W/mK at  $\pm 10^\circ\text{C}$  and from 0.134 to 0.225 W/mK at  $150^\circ\text{C}$ . It is noticeable that conductivity values of samples are decreased as temperature is increased (Table 2).

It was determined that samples have extremely high porosity values between 64.89 and 76.90%, whiteness between 63.93 and 82.29%, acid-insoluble matter of 94.20% and water-insoluble matter of 98.85% showing that they behave as inert chemical reactions. Diatomites may be white, light yellow, beige and gray in color while organic matter-rich ones are green, brown and black in color (Cummins, 1960; Uygun, 1976; Brady and Clauser, 1991). Studied diatomites are white colored and therefore it can be said that they do not contain any organic matter and may be nearly pure (Table 3).

As a result of specific surface area, pore volume and pore size analyses, cumulative absorption specific surface area of studied diatomites is found to change from  $1200 \text{ e}^{+2} \text{ m}^2/\text{g}$  to  $3,387 \text{ e}^{+2} \text{ m}^2/\text{g}$ , cumulative desorption specific surface area value is between  $1.985 \text{ e}^{+1} \text{ m}^2/\text{g}$  and  $4.485 \text{ e}^{+1} \text{ m}^2/\text{g}$ , cumulative absorption pore volume values change from  $2.865 \text{ e}^{+1} \text{ cc/g}$  to  $8.124 \text{ e}^{-02} \text{ cc/g}$ , cumulative desorption pore

volume values are between  $2.029 \text{ e}^{-01} \text{ cc/g}$  and  $7.245 \text{ e}^{-02} \text{ cc/g}$ , absorption pore diameter value is between  $3.125 \text{ e}^{+01} \text{ \AA}$  and  $4.038 \text{ e}^{+01} \text{ \AA}$  and desorption pore diameter value ranges from  $3.671 \text{ e}^{+01} \text{ \AA}$  to  $3.716 \text{ e}^{+01} \text{ \AA}$ . These findings indicate that samples have high porosity (Table 4).

As a result of XRF, loss on ignition, grain size, density and pH analyses, diatomite samples are determined to have following range of chemical compositions:  $\text{SiO}_2$ : 68.3-88.9%,  $\text{TiO}_2$ : < 0.1-0.4%,  $\text{Fe}_2\text{O}_3$ : 1.1- 4.6%,  $\text{Al}_2\text{O}_3$ : 0.7-11.5%,  $\text{CaO}$ : 1.1-2.4%,  $\text{MgO}$ : 0.3-2.7%,  $\text{Na}_2\text{O}$ : 0.1-1%,  $\text{K}_2\text{O}$ : < 0.1-0.7%,  $\text{P}_2\text{O}_5$ : 0.1-0.6%,  $\text{SiO}_3$ : 0.03-0.35%,  $\text{SrO}$ : < 0.01-0.03%,  $\text{BaO}$ : < 0.01-0.03%,  $\text{ZrO}_2$ : < 0.01-0.02%,  $\text{V}_2\text{O}_5$ : 0.01-0.03%,  $\text{ZrO}_2$ : 0.3-2.7%,  $\text{ZnO}$ : < 0.01-0.01%,  $\text{CuO}$ : < 0.01-0.01% and  $\text{MnO}$ : < 0.1-0.2%. Loss on ignition values of samples are between 6.10 and 7.65% at  $1050^\circ\text{C}$ , grain size values of samples from K1 section are 0.4-3000  $\mu$  with an average of 550  $\mu$  and those of samples from K2 section are 0.4-100  $\mu$  with an average of 15-20  $\mu$ . Regarding average grain size, grain size of samples from K2 section are under sand size while samples from K1 section contain sand-size material. Density of samples from both sections is between 2.26 and 2.43  $\text{g/cm}^3$  and pH values are between 8.65 and 9.85 showing that samples reflect a basic environment (Table 5).

Assessment of scanning electron microscope images of diatomite assemblage in a sample from K1 section (sample no K2-5) reveals that diatomite samples in the study area are generally composed of coarse, elongate and pennate diatom forms (mostly species of *Epithemia*) (Figure 6).

## 5. Results and Discussion

The diatomite which is used in various sectors such as toothpaste, newspaper, automobile tire, coffee cup, headache tablet and wall paint, is one of important raw materials required by modern technology. The areas of use of diatomites are 1) filtration material, 2) fill material, 3) construction material, 4) absorbent, 5) carrier, 6) catalyst and catalyst carrier, 7) silicate production, 8) mild abrasive and cleaner and 9) isolation material. In industry diatomite is mostly used for filtration material (58%), fill material (19%), isolation material (4%) and various purposes (19%) (Uygun, 2001).

Regarding their physicochemical properties, commercialized diatomites should meet the following

composition spectrum (Özbey and Atamer, 1987; Aruntaş et al., 1998):  $\text{SiO}_2$ : > 85%,  $\text{Fe}_2\text{O}_3$ : < 1.5%,  $\text{Al}_2\text{O}_3$ : < 5.0%,  $\text{CaO}$ : < 1.0%,  $\text{MgO}$ : < 0.5%,  $\text{Na}_2\text{O}$ : < 1.0%,  $\text{K}_2\text{O}$ : < 1.0%, loss on ignition value (at 850°C): < 6.0%, water absorption: > 180 to > 280%, moisture content: < 15% and their color is to be white (Table 7). In the study area diatomites at K2 location have following compositions:  $\text{SiO}_2$ : 84.2-88.9%,  $\text{Fe}_2\text{O}_3$ : 0.1-1.6%,  $\text{Al}_2\text{O}_3$ : 1.1-1.8%,  $\text{MgO}$ : 0.3-0.8%,  $\text{Na}_2\text{O}$ : 0.1-1.6%,  $\text{K}_2\text{O}$ : < 0.1-0.3% and loss on ignition value (at 1050°C): 6.1-6.2% and they have white color. These characteristics are conformable with standardized physicochemical properties of commercial raw diatomites. Only  $\text{CaO}$  value is slightly higher (0.1-2.4%) which can be reduced by processing (Tables 5-7). Standardized analysis values of studied diatomites and diatomites that are used commercially in various fields are given in table 5 for comparison. Commercially used diatomites are represented by the following compositions:  $\text{SiO}_2$ : 83.13-94.0%,  $\text{TiO}_2$ : 0.1-0.7%,  $\text{Fe}_2\text{O}_3$ : 0.4-10.1%,  $\text{Al}_2\text{O}_3$ : 0.9-9.4%,  $\text{CaO}$ : 0.1-5.2%,  $\text{MgO}$ : 0.1-0.8%,  $\text{Na}_2\text{O}$ : 0.2-1.60%,  $\text{K}_2\text{O}$ : 0.1-0.7%,  $\text{P}_2\text{O}_5$ : 0.1-4.92%, loss on ignition value (at 850°C) between 0.3-19.1%, the average grain size of 1.2-14.7  $\mu$ , wet density value of 2.08-4.17  $\text{g/cm}^3$ , rate of filtration of 10-740 ml/min and pH value of 8.3-8.8. In table 6 commercially used diatomites in Turkey are compared to those from study area. Commercially used diatomites have the following compositions:  $\text{SiO}_2$ : 72.1-90.2%,  $\text{TiO}_2$ : 0.01-0.2%,  $\text{Fe}_2\text{O}_3$ : 0.20-14%,  $\text{Al}_2\text{O}_3$ : 1.1-13.1%,  $\text{CaO}$ : 0.01-12%,  $\text{MgO}$ : 0.15-12%,  $\text{Na}_2\text{O}$ : 0.06-17%,  $\text{K}_2\text{O}$ : 0.1-0.71%,  $\text{P}_2\text{O}_5$ : 0.01-1.7%, loss on ignition value (at 850°C) between 2.7-11.31%, the average grain size of 3.3-145  $\mu$ , wet density value of 1.9-2.94  $\text{g/cm}^3$ , rate of filtration of 48 ml/min and pH value of 7.28-8.0. Diatomites in the study area are represented by  $\text{SiO}_2$  contents of 68.3% (at location of K1 section) and 84.2-88.9% (at location of K2),  $\text{TiO}_2$  contents of < 0.1-0.4%,  $\text{Fe}_2\text{O}_3$  contents of 1.1-4.6%,  $\text{Al}_2\text{O}_3$  contents of 0.7-3.8% (at location of K2 section) and 11.5% (at location of K1 section),  $\text{CaO}$  contents of 0.1-2.4%,  $\text{MgO}$  contents of 0.3-0.8% (at location of K2 section) and 2.7% (at location of K1 section),  $\text{Na}_2\text{O}$  contents of 0.1-1.0%,  $\text{K}_2\text{O}$  contents of < 0.1-0.7%,  $\text{P}_2\text{O}_5$  contents of 0.1-0.6%, loss on ignition values of 6.10-7.65%, average grain sizes of 15-20  $\mu$  (at location of K2 section) and 550  $\mu$  (at location of K1 section), wet density values of 2.26-2.43  $\text{g/cm}^3$ , pH values of 8.65-9.85. These values indicate that, except for grain size, diatomites particularly at K2 section

are similar to those of other commercial diatomites in the world. Diatomites in the K2 location can be used commercially if their grain size is minimized. It was found that analysis values of diatomites at both locations (K1 and K2) are consistent with those of various commercial diatomites in Turkey and that diatomites only in the K2 location could be used commercially if their grain size is minimized (Tables 5 and 6).

Based on results of analysis conducted on studied diatomites, their areas of use can be categorized as follows:

*As filtration material:* Due to its high porosity, resistance to chemical effects and purity, filtration is the most common area of use of diatomite (Köktürk, 1997). Diatomite increases rate and efficiency of filtration because of its porous structure and providing wide filtration surface and absorbing oil and some microorganisms. Diatomite is utilized for purification of liquids that contain suspended undesirable materials such as raw sugar syrup (glucose), beer, whisky, wine, fruit juice, metallic and vegetable oil, pharmacy products, polluted waters, dry cleaning solvents, industrial wastes, chemical materials and varnish. In order for diatomite to be used in filtration, it has to contain minimum 84%  $\text{SiO}_2$  (Bozkurt, 1999). In percolators pure, elongate and coarse diatom species are desired (Uygun, 2001).

Diatomites in the study area are characteristic with their high porosity (porosity: 64.89–76.90%, pore volume: 2.865e-01cc/g – 8.124e-01cc/g; pore size: 3.125e-01–4.038e-01 Å), resistance to chemical effects (amount of acid-insoluble matter: 94.20%, amount of water-insoluble matter: 98.85%), purity (with their white color and whiteness values of 63.94-82.29%),  $\text{SiO}_2$  values up to 88.9% (particularly samples from K2 section) and pure, elongate and coarse diatom species (especially *Epithemia* species) and therefore, they are suitable to be used in percolators (Tables 3, 4, 5, 7) (Figure 6). For wine filtering process, diatomites with pink color, grain size of 2.5  $\mu$ , wet density of 2.3  $\text{g/cm}^3$  and pH value of 7.0 are used while for sugar filtering process, diatomites with white color, grain size of 22  $\mu$ , wet density of 2.0  $\text{g/cm}^3$  and pH value of 10 are utilized (Açıkalın, 1991) (Table 7). In addition, sugars that are processed at sugar plants in Turkey are in white color and have the following compositions: 87.3%  $\text{SiO}_2$ , 1.95%  $\text{Fe}_2\text{O}_3$ , 3.23%  $\text{Al}_2\text{O}_3$ , 1.09%  $\text{CaO}$ ,

0.45% MgO, 0.47% Na<sub>2</sub>O and 0.44% K<sub>2</sub>O with loss on ignition of 4.43% (at 850 °C) and pH of 4.49-10 (Bentli, 2001) (Table 7). Diatomite samples from K2 section with their white color, grain size of 15-20 μ, wet density of 2.26–2.30 g/cm<sup>3</sup>, pH value of 9.85 – 9.0 and composition of 84.2-88.9% SiO<sub>2</sub>, 1.1-3.3% Fe<sub>2</sub>O<sub>3</sub>, 0.7-3.8% Al<sub>2</sub>O<sub>3</sub>, 1.1-1.6% CaO, 0.3-0.8% MgO, 0.1-0.6% and Na<sub>2</sub>O, <0.1-0.3% K<sub>2</sub>O are similar to diatomites used in sugar filtering process but differ from these diatomites with their loss on ignition (at 1050°C) which ranges from to 6.10 to 6.20% (Tables 3,5,6,7).

*As fill material:* Diatomite is used for production of paper, plastic, match, paint, pesticides, polish, toothpaste, cleaning supplies, some chemical materials and improving and increasing the performance of products of drug and cosmetic industries. For diatomites to be used as fill material purity, fine grained texture, high porosity, lightness, and resistance to chemicals, ability to insulate sound and heat and high absorptance and minimum 80% SiO<sub>2</sub> are required. In paint sector, diatomite with grain size of 200–300 μ is added to paint in an amount of 2–3%. Moreover, it is shown in table 7 that diatomites used in paper industry are required to have wet density of 2.4 g/cm<sup>3</sup>, pH value of 7.0 and gray color while those used in paint industry are required to have an average grain size of 6.8 μ, wet density of 2.2 g/cm<sup>3</sup>, pH value of 10 and white color and finally diatomites used in plastic industry are required to have an average grain size of 5.1 μ, wet density of 2.8 g/cm<sup>3</sup>, pH value of 7.0 and pink color (Diatomite Inventory of Turkey, 1968; Bentli, 2001; Açıkalın, 1991; DPT, 2001; Uygun, 2001). Diatomites in the study area, particularly samples from K2 section, are represented by high whiteness character (63,94–82,29%), grain size of 15-20 μ, high porosity (porosity: 64.89–76.90%, pore volume: 2.865e-01 cc/g – 8.124e-01 cc/g, pore size: 3.125e-01 – 4.038e-01 Å) and low density (2.26–2.43 g/cm<sup>3</sup>), high resistance to chemicals (amount of acid-insoluble matter: 94.20%, amount of water-insoluble matter: 98.85%), high ability to insulate heat (thermal conductivity values at ±10 °C are between 0.452 and 0.984 W/mK, 101; thermal conductivity values at 150 °C are 0.134-0.225 W/mK), high absorptance character (since samples are easily fall apart in water, their absorptance property could not be determined experimentally. However, their high porosity and low density may be indicative of their high absorptance

character) and high SiO<sub>2</sub> contents (84.2-88.9%) and therefore, they may be used as fill material (Tables 2, 3, 5, 6, 7). Results of analyses of the studied diatomites indicate that particularly those from K2 section may be suitable to be used in paint industry if coarse grains within them are removed (Table 7).

*As construction material:* In the construction industry diatomite is used as admixture for cement, mortar and bentonite-bearing light bricks. It is shown that 3% diatomite addition to concrete increases compressive strength 20% and tensile strength 10%. In this industry low-quality diatomites may also be utilized (MTA, 1968; DPT, 2001; Uygun, 2001). Diatomites in the study area can be used as construction material if required. In addition, diatomite is used as mineral admixture in Portland-cement concretes if SiO<sub>2</sub>+Al<sub>2</sub>O<sub>3</sub>+Fe<sub>2</sub>O<sub>3</sub> total is at least 70% and loss on ignition is maximum 10% (Aruntaş et al., 1998). SiO<sub>2</sub>+Al<sub>2</sub>O<sub>3</sub>+Fe<sub>2</sub>O<sub>3</sub> total of studied diatomites 70.1-105% and loss on ignition (at 1050 °C) is 6.10-7.65% and therefore diatomites at both locations may be used as mineral admixture in Portland-cement concretes (Tables 5-7).

*As carrier:* Diatomite may also be utilized to carry nitrogen-bearing fertilizers. Under dry climate conditions, diatomite can absorb even little amount of moisture in the air thus providing fertilizer is easily blended with the soil. In addition, grinded diatomite may be directly used as fertilizer in silica-deficient soils (MTA 1968; DPT, 2001; Uygun, 2001). Diatomites which are preferred as regulator in fertilizer industry 1.7 g/cm<sup>3</sup> wet density and pH of 7.0 are required. Because studied diatomites have wet densities of 2.26-2.43 g/cm<sup>3</sup> and pH values between 8.65 and 9.85, they are not suitable to be used as carrier (Tables 5-7).

*In silicate production:* Diatomite is utilized in production of ceramic, glazer and ultramarine and various glass materials (MTA 1968; DPT, 2001; Uygun, 2001). Diatomites in the study area, particularly those in the area of K2 section, have high SiO<sub>2</sub> contents (84.2–88.9%) and therefore can be used for silicate production (Tables 5-7).

*As mild abrasive and cleaner:* Diatomite is used as mild abrasive and cleaner in laundry detergent, stain absorber and automobile polisher (MTA, 1968; DPT,

2001; Uygun, 2001). Diatomites used as abrasive in automobile polishers are white colored and have an average grain size of 5.5  $\mu$ , wet density of 2.4 g/cm<sup>3</sup> and pH value of 9.4 (Açıklan, 1991). Because diatomites in the study area are white colored and represented by wet density of 2.26-2.43 g/cm<sup>3</sup> and pH values of 8.65-9.85, they are suitable to be used as mild abrasive and cleaner. However regarding grain size they are not suitable and therefore grain size is required to be minimized (Tables 3, 5-7).

*As isolation material:* Due to its high porosity, diatomites are good insulators for heat and sound. They are used in walls and flooring by injecting asbestos-mixed plates into lime or cement. Diatomite coating in vapor and gas pipes and diatomite bricks in outer wall of blast furnace prevent heat loss. In addition, it is also used for production of firebrick as isolation material (Uygun, 2001). In order for diatomite to be used as isolation material it should contain minimum 94% SiO<sub>2</sub> (Bentli, 2001).

Considering low thermal conductivity values (thermal conductivity values at  $\pm 10$  °C are 0.452-0.984 W/mK, 101; thermal conductivity values at 150°C are 0.134-0.225 W/mK), high porosity values (porosity: 64.89–76.90%, pore volume: 2.865e-01–8.124e-01 cc/g, pore size: 3.125e-01–4.038e-01 Å) and low density values (2.26–2.43 g/cm<sup>3</sup>), diatomites in the study area can be used as isolation material. However, diatomites at both locations with SiO<sub>2</sub> contents of 68.3-88.9% are needed to be enriched to be used for isolation (Tables 2-5).

### Acknowledgements

This study was financially supported by Aksaray University Scientific Research Unit under grand no. 2012/16. Also, we thank you to geological engineer Zafer Ertosun for his assistance in obtaining the necessary geological maps during our study.

### References

Açıklan, N. 1991. Dünya'da ve Türkiye'de Diatomit. *Maden Tetkik ve Arama Genel Müdürlüğü*, Ankara.

Aruntaş, H.Y., Albayrak, M., Saka, H.A., Tokyay, M. 1998. Ankara-Kızılcahamam ve Çankırı-Çerkeş yöresi diatomitlerinin özelliklerinin belirlenmesi. *Turkey Journal of Engineering and Environmental Science* 22, 337-343.

Atabey, E. 1989. 1/100.000 ölçekli açınsama nitelikli Türkiye jeoloji haritaları serisi, Kayseri-H19 paftası. *Maden Tetkik ve Genel Müdürlüğü*, Ankara.

Atabey, E., Papak, İ., Tahran, N., Aksu, B., Taşkiran, M., Adil, A. 1987. Ortaköy (Niğde)-Tuzköy (Nevşehir)-Kesikköprü (Kırşehir) yöresinin jeolojisi raporu. *Maden Tetkik ve Arama Genel Müdürlüğü Rapor No: 8156* Ankara (unpublished).

Atabey, E., Tarhan, N., Yusufoglu H., Canpolat, M. 1988. Hacıbektaş, Gülşehir, Kalaba (Nevşehir)-Himmetdede (Kayseri) arasının jeolojisi raporu. *Maden Tetkik ve Arama Genel Müdürlüğü Rapor No: 8523* (unpublished).

Aydar, E. 1992. Etude volcano-structurale et magmatologique du strato-volcan Hasandağı (Anatolie Centrale-Turquie). *These de Doctorat, Universite Blaise Pascal*, 200 pp. France.

Aydar, E., Gourgaud, A. 1998. The geology of Mount Hasan stratovolcano, Central Anatolia, Turkey. *Journal of Volcanology and Geothermal Research* 85, 129–152.

Aydar, E., Çubukçu, H.E., Şen, E., Akın, L. 2012. Central Anatolia'n Plateau, Turkey: incision and paleoaltimetry recorded from volcanic rocks. *Turkish Journal of Earth Sciences* 22, 739–746.

Aydın, N. 1984. Orta Anadolu Masifi'nin Gümüşkent (Nevşehir) dolayında jeolojik-petrografik incelemeler. *Doktora tezi, Ankara Üniversitesi, Fen Fakültesi*, 400 s. Ankara.

Ayhan, A., Papak, İ., Atabey, E. 1988. Göçlük (Misli)-Derinkuyu-Sulucaova civarının jeolojisi raporu. *Maden Tetkik ve Arama Genel Müdürlüğü Rapor No: 8345* Ankara (unpublished).

Ayrancı, B. 1970. Orta Anadolu'da Kayseri civarında Erciyes Volkanik Bölgesi'nin kantitatif incelemelerine istinaden petrolojisi ve jeolojisi. *Maden Tetkik ve Arama Genel Müdürlüğü Dergisi* 74, 13–24.

Batum, I. 1978. Geology and petrography of Acıgöl and Göllüdağ volcanics at southwest of Nevşehir Central Anatolia (Turkey). *Yerbilimleri* 4, 1–2, 70–88.

Beekman, P. H. 1963. İncesu bölgesinin (Kayseri) jeolojik ve volkanolojik etüdü raporu. *Maden Tetkik ve Arama Genel Müdürlüğü Rapor No: 6880*. Ankara (unpublished).

- Beekman, P.H. 1966. The Pliocene and Quarternary volcanism in The Hasandağ-Melendizdağ Region, *Maden Tetkik ve Arama Genel Müdürlüğü Bülteni* 66, 99–106.
- Besang, C., Eckhardt, F.J., Harre, W., Kreuzer, H., Müller, P. 1977. Radiometrische altersbestimmungen an Neogen Eruptivgesteinen der Türkei. *Geol. Jb.* B-25, 3-36.
- Bentli, İ. 2001. Kütahya-Alayunt diatomit cevherinin zenginleştirilebilirliğinin araştırılması. *4.Endüstriyel Hammaddeler Sempozyumu*, 2001, Köse, H., Arslan, V., Tanrıverdi, M. (Ed.), İzmir, 119-126.
- Bigazzi, G., Yeğingil, Z., Boztuğ, D., Ercan, T., Norelli, P., Özdoğan, M. 1997. Studi di Provenienza della obsidiana con il metodo tracce di fissione: nuovi dati sulle Potenziali fonti Anatoliche. IV. Giornata "Le Scienze della Terra e l' Archeometria", *Neaples*, 20–21 February 1997, 33.
- Bozkurt, R. 1999. Diatomit, Türkiye'de Endüstriyel Mineraller Envanteri. *İstanbul Maden İhracatçıları Birliği (İMİB), Yurt Madenciliği Geliştirme Vakfı* Önal, Y., Özpeker, G., (Ed.), İstanbul, 42-47.
- Brady, G. S., Clauser, H. R. 1991. *Materials Handbook. Mc Graw-Hill.*
- Cummins, A. B., 1960. Diatomite, Industrial Minerals and Rocks (Nonmetallics other than fuels). *The Am. Inst. of Mining and Metallurgical Engineers*, New York.
- Dhont, D., Chorowicz, J., Yürür, T., Froger, J.L., Köse, O., Gündoğdu, N. 1998. Emplacement of volcanic vents and geodynamics of Central Anatolia, Turkey. *Journal of Volcanology and Geothermal Research* 85, 33–54.
- Dirik, K. Göncüoğlu, M.C., Kozlu, H. 2001. Ecemiş Fay Zonu Orta Kesiminin (Sultansazlığı-Tuzlagölü arası) stratigrafisi ve tektoniği. *Niğde Üniversitesi, Mühendislik Fakültesi Dergisi*, 73–90.
- Dönmez, M., Türkecan, A., Akçay, E.A. 2003. Kayseri-Niğde-Nevşehir yöresi Tersiyer volkanikleri raporu. *Maden Tetkik ve Arama Genel Müdürlüğü Rapor No: 10575*. Ankara (unpublished).
- DPT. 2001. Sekizinci beş yıllık kalkınma planı madencilik özel İhtisas komisyonu raporu, endüstriyel hammaddeler alt komisyonu genel sanayi mineralleri IV. çalışma grubu raporu, Ankara.
- Duritt, T. H., Brenchley, P.J., Gökten, Y. E., Francaviglia, V. 1995. Late Quaternary rhyolitic eruptions from the Acıgöl complex, Central Turkey. *Journal of Geological Society of London* 152, 655–667.
- Ekingen, A. 1982. Nevşehir Kalderasında jeofizik prospeksiyon sonuçları. *Türkiye Jeolojisi Kurultayı*, 1982, 82.
- Ercan, T., Yıldırım, T. 1988. Maar volkanizmasının özellikleri ve Anadolu'dan örnekler, *Akdeniz Üniversitesi, İsparta Mühendislik Fakültesi Dergisi*, 4, 36–52.
- Ercan, T., Fujitani T., Matsuda, J., Tokel, S., Notsu, K, Ul, T., Can, B., Selvi, Y., Yıldırım, T., Fişekçi, A., Ölmez, M., Akbaşlı, A. 1990. The origin and evolution of the Cenezpic volcanism of Hasandağı-Karacadağ area (Central Anatolia). *Jeomorfoloji Dergisi* 18, 39–54.
- Froger, J.L., Lenat, J.F., Chorowicz, J., Le Penneç, J.L., Bourdier, J.L., Köse, O., Zimitoglu, O., Gündoğdu, N.M., Gourgaud, A. 1998. Hidden calderas evidenced by multisource geophysical data; example of Cappadocian Calderas, Central Anatolia. *Journal of Volcanology and Geothermal Research* 85, 99–128.
- Gevrek, A. İ., Kazancı, N. 1994a. Occurrence and evolution of Narköy maar in SE Cappadocia. *AVCE*, 1994, Ankara.
- Gevrek, A.İ., Kazancı, N. 1994b. Material-rich and poor maars with examples from central Anatolia, Turkey. *AVCE*, 1994, Ankara.
- Göncüoğlu, M.C., Toprak, V. 1992. Neogene and Quaternary volcanism of Central Anatolia: a volcano structural evolution. *Bulletin de la Section de Volcanologie* 26,1–6.
- Güner, Y., Emre, Ö. 1983. Erciyes Dağı'nda Pleyistosen buzullaşması ve volkanizma ile ilişkisi. *Jeomorfoloji Dergisi* 11, 23–34, Ankara.
- Gürel, A., Yıldız, A. 2006. Diatom communities, lithofacies characteristics and paleoenvironmental interpretation of Pliocene diatomite deposits in the Ihlara-Selime plain (Aksaray, Central Anatolia, Turkey). *Journal of Asian Earth Science* 30, 170–180.

- Gürel, A., Kadir, S. 2006. Geology and mineralogy and origin of clay minerals of the Pliocene fluvial-lacustrine deposits in the Cappadocian Volcanic Province, Central Anatolia, Turkey. *Clay and Clay Minerals* 54, 555–570.
- Gürel, A., Kadir, S., Kerey, E.İ. 2007. Orta Anadolu volkanik bölgesinin (CAVP) güneydoğu bölümündeki erken Miyosen yaşlı killi kayaların sedimantolojisi ve mineralojisi. *Kapadokya Bölgesi'nin Jeolojisi Sempozyumu*, 2007, Niğde, 133–147.
- Gürel, A., Kadir, S. 2008. Geology and mineralogy of Late Miocene clayey sediments in the southeastern part of the Central Anatolian Volcanic Province, Turkey. *Clay and Clay Minerals* 56, 3, 307–321.
- Gürel, A., Kerey, E.İ., Özcan, S. 2008. Sedimentology and mineralogy of late Miocene paleotopraks and calcrete rich sediments in the western part of Central Anatolian Volcanic Province (CAVP), Turkey. *SGEM Conference*, 2008, Bulgaria, 25.
- Göz E., Kadir S., Gürel A., Eren M. 2014. Geology, minerology, geochemistry, and depositional environment of a late Miocene/Pliocene fluvial-lacustrine succession, Cappadocian Volcanic Province Central Anatolia, Turkey. *Turkish Journal of Earth Sciences* 23, 386–411.
- Innocenti, F., Mazzuoli, G., Pasquare, F., Radicati Di Brozolo, F., Villari, L. 1975. The Neogene calcalkaline volcanism of Central Anatolia geochronological data on Kayseri-Niğde area. *Geological Magazine* 112, 4, 349–360.
- İzbrak, R., Yalçınlar, İ. 1951. Kayseri kuzeyinde Üst Miosen'e ait omurgalılar. *Türkiye Jeoloji Kurumu Bülteni* III, 1, 153–154, Ankara.
- Kadir, K., Gürel, A., Lepetit, P., Davarcıoğlu, B. 2006. Preliminary approach to mineralogy and depositional environment of upper Miocene Cappadocian Volcanic Province, Ürgüp-Başköy-Güzelöz (Nevşehir, Central Anatolia, Turkey). *Fourth Mediterranean Clay Meeting*, 2006, Ankara, 1, 73.
- Kayalı, R., Gürel A., Davarcıoğlu, B., Çiftçi, E. 2005. Orta Anadolu Bölgesi'ndeki endüstriyel ham maddelerinden kil ve diyatomitlerin spektroskopik yöntemlerle nitelik ve niceliklerinin belirlenmesi raporu. TÜBİTAK Rapor No: ÇAYDAG-101Y067, 157 s.
- Koçyiğit, A., Beyhan, A.A. 1998. New Intracontinental transcurrent structure: The Central Anatolian Fault Zone, Turkey. *Tectonophysics* 284, 317–336.
- Köktürk, U. 1997. Endüstriyel Hammaddeler. *Dokuz Eylül Üniversitesi Mühendislik-Mimarlık Fakültesi Yayınları* 205, İzmir, 64-68.
- Kürkçüoğlu, B., Şen, E., Aydar, E., Gourgaud, A., Gündoğdu, M.N. 1998. Geochemical approach to magmatic evolution of Mt. Erciyes stratovolcano Central Anatolia, Turkey. *Journal of Volcanology and Geothermal Research* 85, 473–494.
- Le Pennec, J.L., Bourdier, J.L., Froger, J.L., Temel, A., Camus, G., Gourgaud, A. 1994. Neogene ignimbrites of the Nevşehir plateau (Central Turkey): stratigraphy, distribution and source constraints. *Journal of Volcanology and Geothermal Research* 63:59–87.
- Le Pennec, J.L., Temel, A., Froger, J.L., Şen, Ş., Gourgaud A., Bourdier, J.L. 2005. Stratigraphy and age of the Cappadocia ignimbrites, Turkey: reconciling field constraints with paleontologic, radiochronologic, geochemical and paleomagnetic data. *Journal of Volcanology and Geothermal Research* 141, 45–64.
- Lepetit, P., Viereck, L., Piper John, D.A., Sudo, M., Gürel, A., Çopuroğlu, İ., Gruber, M., Mayer, B., Koch, M., Tatar, O., Gürsoy, H. 2014. 40Ar/39Ar dating of ignimbrites and plinian air-fall layers from Cappadocia, Central Turkey: Implications to chronostratigraphic and Eastern Mediterranean palaeoenvironmental record. *Research Gate Elsevier* 74, 471–488.
- MTA. 1989. 1/100.000 ölçekli Türkiye Jeoloji Haritası, Kayseri-H 19 Paftası. *Maden Tetkik ve Arama Genel Müdürlüğü*, Ankara.
- MTA. 1968 Türkiye Diyatomit Envanteri, *Maden Tetkik ve Arama Enstitüsü* 138, Ankara.
- Nuhoğlu, İ., Elmas, N. 1999. Alayunt diyatomit yataklarının oluşumu ve ekonomik olarak incelenmesi. *I. Batı Anadolu Hammadde Kaynakları Sempozyumu*, 1999, İzmir, 82-95.
- Ozansoy, F. 1964. Fauni-zon bilimleri ışığında Çanakkale çevresi Neojen stratigrafisi ve Neojen paleocoğrafyasında bölgede tabii rejimler problemi: karasal-denizel-somatr. *Ankara Üniversitesi, Dil ve Tarih Coğrafya Fakültesi, Antropoloji Dergisi* 1, 2, Ankara.

- Özbey, G., Atamer, N. 1987. Kızılirmur (Diyatomit) Hakkında Bazı Bilgiler. *10. Türkiye Madencilik Bilimsel ve Teknik Kongresi*, 1987, Ankara, 493-502.
- Özkuzey, S., Önemli, Ö., F. 1977. Acıgöl (Nevşehir) perlitlerinin petrografisi ve ekonomik jeolojisi. *I. Ulusal Perlit Kongresi*, 1977, Ankara, 137-147.
- Pasquare, G. 1968. Geologie of the Senozoic volcanic area of Central Anatolia. *Atti della Acad. No. Delinca, Menorie Serie*, 1968, Roma, VIII, IX, 55-204.
- Pasquare, G., Poli, S., Venzolli, L., Zanchi, A. 1988. Continental arc volcanism and tectonic setting in Central Anatolia, Turkey. *Tectonophysics* 146, 217-230.
- Sarız, K., Nuhođlu, İ. 1992. Endüstriyel Hammadde Yatakları ve Madenciligi. *Anadolu Üniversitesi Yayını*, No:636, 452 s.
- Sassano, G. 1964. Acıgöl bölgesinde Neojen ve Kuvaterner volkanizması raporu. *Maden Tetkik ve Arama Genel Müdürlüğü Rapor No: 6841*. Ankara (unpublished).
- Schumacher, R., Keller, J., Bayhan, H. 1990. Depositional characteristics of ignimbrites in Cappadocia, Central Anatolia, Turkey. In: M.Y. Savaşçın and A.H. Eronat (Eds.), *International Earth Science Congress on Aegean Regions*, 1990, 2, 435-449.
- Schumacher, R., Mues, U., Kobeski, U. 1992. Petrographical and geochemical aspects and K/Ar-dating of ignimbrites in Cappadocia, Turkey. *6th Congress of the Geological Society of Athens*, 1992.
- Schumacher, R., Schumacher, U.M. 1996. The Kızılkaya İgnimbrite an unusual low-aspect-ratio ignimbrite from Cappadocia, Central Turkey. *Journal of Volcanology and Geothermal Research* 70. 107-121.
- Şenyürek, M. 1953. A note on a new species of Gazella from the Pontian of Küçük Yozgat. *Rev. Fac. Langue, Hist. Geogr.*, University of Ankara, pp. 16, 14.
- Temel, A. 1992. Kapadokya eksplosif volkanizmasının petrolojik ve jeokimyasal özellikleri. Doktora Tezi, Hacettepe Üniversitesi, 209 s. Ankara.
- Temel, A., Gündođdu, M. N., Gourgaud, A. 1998a. Petrological and geochemical characteristics of Cenozoic high-K calc-alkaline volcanism in Konya, Central Anatolia, Turkey. *Journal of Volcanology and Geothermal Research* 85, 327-354.
- Temel, A., Gündođdu, M.N., Gourgaud, A., Le Penneç, J. L. 1998b. İgnimbrites of Cappadocia Central Anatolia, Turkey petrology and geochemistry. *Journal of Volcanology and Geothermal Research* 85, 447-471.
- Toprak, T. 1996. Kapadokya Volkanik Çöküntüsü'nde gelişmiş Kuvaterner yaşlı havzaların kökeni, Orta Anadolu. *30. Yıl Sempozyumu*, 1996, Trabzon, 327-329.
- Toprak, V. 1998. Vent distribution and its relation to regional tectonics, Cappadocian Volcanics, Turkey. *Journal of Volcanology and Geothermal Research* 85, 55-67.
- Uygun, A. 1976. Geologie und Diyatomit - Vorkommen des Neogen - Beckens vorc Emmiler-Hırka (Kayseri-Türkei). *Doktora Tezi, Bonn Üniversitesi*, 137 s (unpublished).
- Uygun, A. 2001. Diyatomit jeolojisi ve yararlanma olanakları. *Maden Mühendisleri Odası Dergisi* 15, 31-39.
- Viereck-Götte, L., Gürel, A. 2003. Klima-und Vegetationswechsel dokumentiert in obermiozaenen Paläoböden Kappadokiens, Zentralanatolien', *Berichte der Deutschen Mineralogischen Gesellschaft. Beihefte zum European. Journal of Mineralogy* 15, 211, 211pp.
- Viereck-Goette, L., Lepetit, P., Gürel, A., Ganskow, G., Çopurođlu, İ., Abratis, M. 2010. Revised volcanostratigraphy of the upper Miocene to lower Pliocene Ürgüp Formation, Central Anatolian Volcanic Province, Turkey. *Geological Society of Amsterdam* 464, 85-112.
- Yavuz-İşık N., Toprak, V. 2010. Palynostratigraphy and vegetation characteristics of Neogene continental deposits interbedded with the Cappadocia ignimbrites (Central Anatolia, Turkey). *International Journal of Earth Science* 99, 1887-1897.
- Yıldırım, T. 1984. Acıgöl volcanism and hot dry rock, possibilities, Nevşehir, Turkey; Sern.in.ar on. *Utilization of Geothermal Energy for electric, power production and space Heating*, 1981, Florence-İtalya.
- Yıldırım, T., Özgür, R. 1981. Acıgöl Kalderası. *Jeomorfoloji Dergisi* 10, 59-70.
- Yıldız, A., Gürel, A. 2005. Diyatomit community and palaeoenvironmental interpretation of Pleistocene-Holocene lacustrine diyatomite deposits in the Çiftlik Basin (Niğde, Central Anatolia, Turkey). *12 th RCMNS Congress*, 2005, Vienna, 82.



characteristics that develop based on geochemical conditions of the depositional environment. Gradually increasing oil prices in the world have impelled countries to explore new alternative energies. Within this context, the need for the alternative energy has again revived bituminous rocks. With this purpose, intensive exploration related to bituminous rocks (especially bituminous shales) and investigations related to hydrocarbon production are carried out in our country as well as in all over the world. Thus; drilling exploration and studies about reservoir estimation continue in Hatıldağ/Göynük (Ankara) and Beydilli/Nallıhan (Ankara) bituminous shale license areas within the scope of a project conducted by TKİ and TPAO. Considering mining costs, the oil is extracted either by excavating bituminous shale from surface (by retort method) or by in situ electrofrac process (Symington et al., 2008). In this process, the thickness of bituminous shales, the amount of organic material and especially the kerogen type to be in Type-I kerogen are significant.

In this study, the depositional environments of Lower Eocene bituminous rocks and source rock potentials were assessed in detail using pyrolysis analyses (TOC %, HI, OI, Tmax, S1, S2, S3), methods of gas chromatography (GC) and gas chromatography–mass spectrometer (GC-MS), stable carbon isotope analysis ( $\delta^{13}\text{C}$ ) and organic petrographic analyses. Bituminous rocks have excellent source rock potential according to S1 (average 1.28 mg HC/g rock) and S2 (average 45.51 mg HC/g rock) hydrocarbons in addition to TOC values ranging between 2.52-8.38 %. According to hydrogen index (HI)/oxygen index (OI), Hydrogen Index (HI)/Tmax, S2/TOC diagrams, and Hydrocarbon Type Index (S2/S3) and Hydrogen Index limit values, the kerogen type is Type-I and Type-II (only in two samples). With respect to organic petrographic methods, samples are composed of 100% Algal+Amorph organic material. The organic material type is lacustrine algal considering the ternary diagram of C27, C28, C29 steranes. According to CV values estimated by  $\delta^{13}\text{C}$  (saturated) and  $\delta^{13}\text{C}$  (aromatic) hydrocarbon data the organic material type is terrigenous in some samples and is marine origin in others. However; it should be kept in mind that the results of isotope analysis present values in very large ranges. Nevertheless; these results show compatibility with Type I and Type II kerogen when it is considered that the depositional environment is lagoon partly

connected with sea. It is seen that bituminous rock samples are still in immature stage based on biomarker studies, Tmax, production index (PI) and SCI values. Besides; it was determined that samples were immature by m/z 191 triterpane and m/z 217 sterane biomarker data (Ts/(Ts+Tm), 22S/(22S+22R),  $\alpha\beta\beta/(\alpha\beta\beta+\alpha\alpha\alpha)$ , 29Ts/ (29Ts+norhopane), 20S/(20S+20R)). According to genetic potential values (S1+S2) (18400-70250 ppm) bituminous rocks have a good source rock potential. However; according to S2/S3 ratio, Hydrogen Index (HI) – TOC and S2 – TOC diagrams, the studied samples possess a hydrocarbon potential that can produce oil.

## 2. Material and Method

Pyrolysis analyses (Rock Eval-VI), gas chromatography (GC) and gas chromatography–mass spectrometry (GC-MS), stable carbon isotope analyses ( $\delta^{13}\text{C}$ ) and Spore Color Index (SCI) studies were performed in Geochemistry Laboratories of TPAO Research Group. Pyrolysis estimations were carried out by IFP 160000 standard (Behar et al., 2001) using Rock Eval-VI type instrument (Institut Français du Pétrole). TOC % values were estimated automatically by TOC module mounted in the device. When applying the pyrolysis analysis (Espitalie et al., 1977; Peters, 1986) 100 g pulverized rock sample is heated 3 minutes under 300°C temperature under helium atmosphere in anoxic environment. Later on; the temperature is increased up to 600°C with 25°C increments each minute. During this heating period the peaks of S1 (mg HC/g rock), S2 (mg HC/g rock), S3 (mg CO<sub>2</sub>/g rock), S4 (mg CO<sub>2</sub>/gr rock) and Tmax come out. With these hydrocarbon peaks the following parameters are calculated;

$$\text{Hydrogen Index [HI = (S2 / TOC) x 100]}$$

$$\text{Oxygen Index [OI = (S3 / TOC) x 100]}$$

$$\text{Production Index [PI = S1 / (S1+S2) ]}$$

$$\text{Genetic Potential (S1 + S2)}$$

$$\text{Kerogen Type Index (S2 / S3)}$$

Gas Chromatography (GC) analyses are carried out in Agilent 6850 instrument using the Norwegian Oil Standard. GC-MS analysis is performed in Agilent 5975C quadrupole mass spectrometer device using the Norwegian Oil Standard. This device is used as combined with 7890A gas chromatograph and 7683B automatic liquid sampler. Stable carbon isotope analysis was performed in GV instruments Isoprime EA-IRMS device.

### 3. Geological Setting

The study area is located along Sakarya Zone in the western part of Pontides. Sakarya Zone is surrounded by İzmir-Ankara-Erzincan suture belt in south and by Ankara-Erzincan suture zone in north (Şengör and Yılmaz, 1981). The zone consists of a metamorphic basement at the bottom and clastics overlying with an angular unconformity, carbonate rocks and volcanics. Volcanics, clastic rocks and carbonates of this zone are observed within formations located in the general geology map of the study area (Figure 1). The study area, which is situated between the Northwestern Anatolian Mountains rising with the effect of Alpine Orogeny and the Central Anatolian massive, and basins in its close vicinity were folded and faulted in several cases. As a result of these tectonical movements strike slip faults, thrust faults, anticlinal and synclinal structures and overturned layers are observed.

The oldest unit observed in the study area is Carboniferous aged Sarıcakaya granitoids (Csg). Bakırköy formation (Jba), which is composed of sandstone, mudstone, conglomerate and limestone, is Liassic in age and unconformably overlies Sarıcakaya granitoids. This formation is unconformably overlain by Callovian-Hauterivian neritic limestones of Bilecik

formation (JKb) and by Callovian-Aptian aged limestones of Soğukçam formation. This formation is then overlain by Albian-Maestrichtian aged Yenipazar formation. Yenipazar formation in the study area is divided into three members as; Değirmenözü (Kyed), Bayat (KyeB) and Taraklı (Kyet) members (Gedik and Aksay, 2002). Yenipazar formation, which is transitional with Soğukçam formation, consists of sandstone, shale, limestone and tuff units. Lower Paleocene Selvipınar formation, which is formed by reefal limestones, is overlain by Paleocene-Lower Eocene Kızılçay formation consisting of conglomerate, sandstone and mudstone units in nearby regions of the study area. However; the Lower Eocene Kabalar member (Tpekk) of the Kızılçay formation encountered in our study area is the member in which bituminous rocks are observed. Lutetian aged Güvenç formation (Teg), which is observed outside the study area and consists of sandstone, conglomerate and marl, unconformably overlies Kızılçay formation. This formation is then unconformably overlain by Upper Eocene-Lower Miocene Gemiciköy formation (Temg). The unit is generally composed of pale red, loosely consolidated, cross bedded conglomerate and sandstone. This formation is then unconformably overlain by Lower-Middle Eocene Hançılı formation

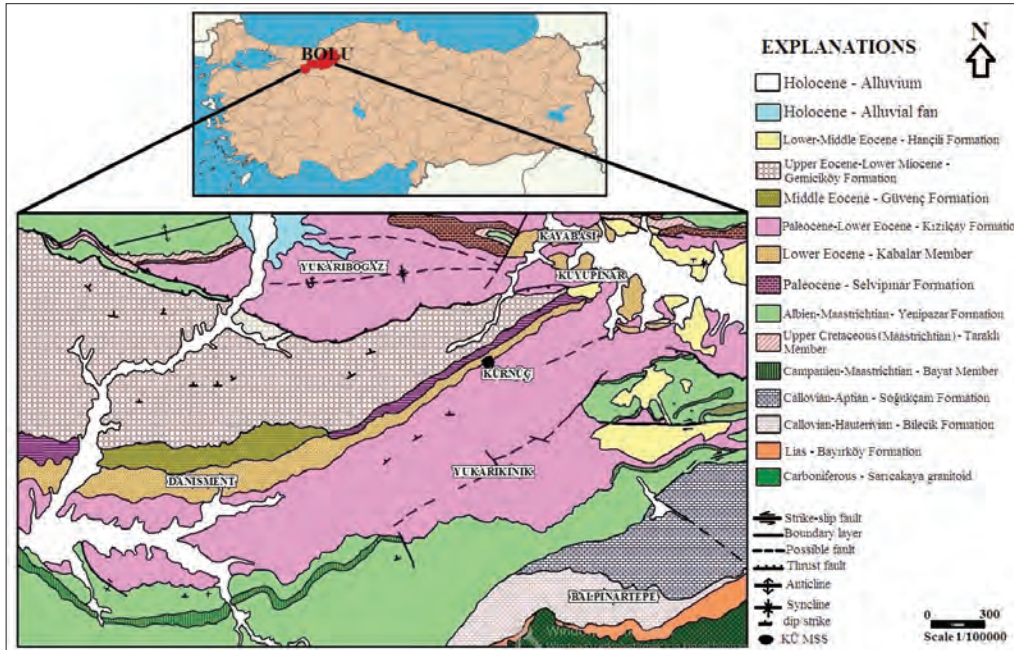


Figure 1- General geological map of the study area (modified from Gedik and Aksay, 2002).

(Tmh) (Gedik and Aksay, 2002). Hançılı formation is composed of sandstone, claystone, clayey limestone, diatomite, chert, tuffite and conglomerate units, and is unconformably overlain by Quaternary alluvial deposits (Qal) (Figure 2).

**4. Findings and Discussion**

**4.1. Biomarker Studies**

According to GC and GC-MS analyses significant data on organic material type, maturation, rock lithology and depositional environment are obtained. Within this scope, m/z 217 sterane and m/z 191 terpane lists defined in GC-MS analyses were given in table 1 and table 2, respectively.

In this study, GC analyses were carried out on 4 samples from which were subjected to pyrolysis analysis (Figure 3a,b), In each studied sample

n-alkanes and prenoids were defined. N-alkanes in each studied sample range from n-C9 to n-C36. N-alkane peaks of n-C23, n-C-25, n-C27 and n-C31 are abundant in samples KÜ-19, KÜ-41 and KÜ-50. N-C27 is the n-alkane, which is the most abundant component belonging to terrigenous plants. Besides, fitan is the most abundant isoprenoid in samples. Slight increases from n-C15 to n-C25 in studied samples mainly indicate an increase in the biomasses of algae and planktons (Peters and Moldowan, 1993).

The aquatic source of n-alkanes is defined by carbon atoms varying from 16 to 18, because these are typically derived from aquatic algae and cyanobacteria. However, the terrigenous plant origin n-alkanes are defined as n-alkanes with n-C27 and n-C33 carbon atom, because these are typically derived from waxes' of terrigenous plants (Peters et al., 2005a).

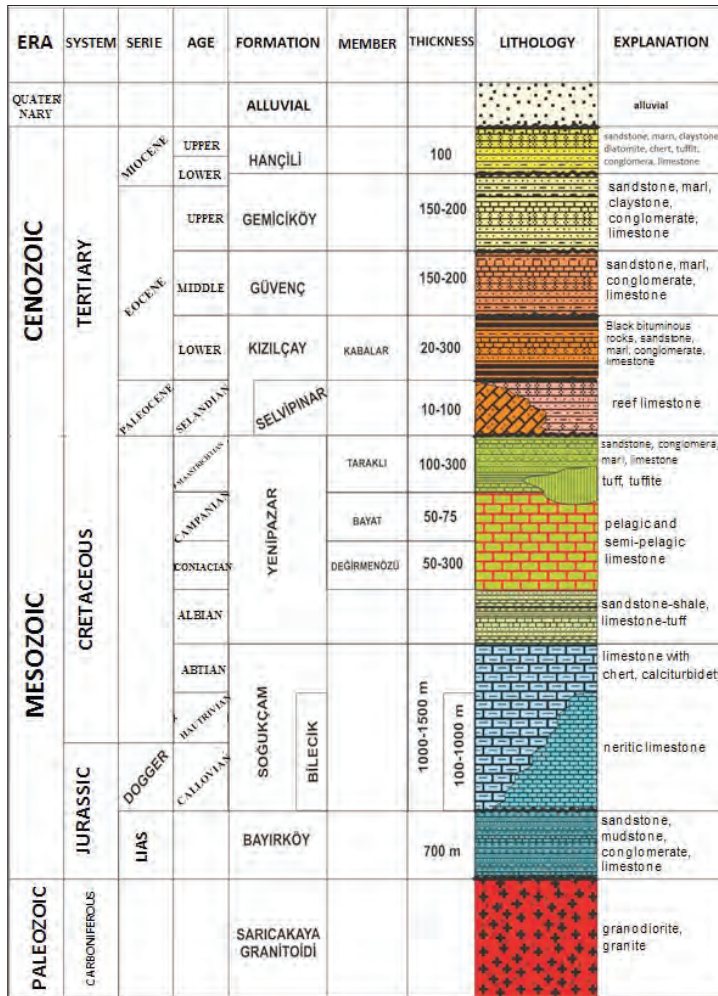


Figure 2- Generalized stratigraphic columnar section of the study area (modified from Gedik and Aksay, 2002).

Table 1- List of defined m/z 217 steran ions used in GC-MS analyses.

COMPONENT NO	COMPONENT NAME
9	C27 5α (H), 14β (H), 17β (H)-Steran (20R)+C29 13β (H), 17α (H)-Diasteran (20S)
10	C27 5α (H), 14β (H), 17β (H)-Steran (20S)+C28 13α (H), 17 β (H)-Diasteran (20R)
11	C27 5α (H), 14α (H), 17α (H)-Steran (20R)
12	C29 13β (H), 17α (H)-Diasteran (20R)
13	C29 13α (H), 17β (H)-Diasteran (20S)
14	C28 5α (H), 14α (H), 17α (H)-Steran (20S)
15	C28 5α (H), 14β (H), 17β (H)-Steran (20R)+C29 13α (H), 17β (H)-Diasteran (20R)
16	C28 5α (H), 14β (H), 17β (H)-Steran (20S)
17	C28 5α (H), 14α (H), 17α (H)-Steran (20R)
18	C29 5α (H), 14α (H), 17α (H)-Steran (20S)
19	C29 5α (H), 14β (H), 17β (H)-Steran (20R)
20	C29 5α (H), 14β (H), 17β (H)-Steran (20S)
21	C29 5α (H), 14α (H), 17α (H)-Steran (20R)
22	C30 5α (H), 14α (H), 17α (H)-Steran (20S)

Table 2- List of defined m/z 191terpan ions used in GC-MS analyses.

COMPOUND NO	COMPOUND NAME
1	C <sub>19</sub> TRICYCLICTERPANE
2	C <sub>20</sub> TRICYCLICTERPANE
3	C <sub>21</sub> TRICYCLICTERPANE
4	C <sub>22</sub> TRICYCLICTERPANE
5	C <sub>23</sub> TRICYCLICTERPANE
6	C <sub>24</sub> TRICYCLICTERPANE
7	C <sub>25</sub> (22S+22R) TRICYCLICTERPANE
8	C <sub>24</sub> TETRACYCLICHOPANE (SECO)
9	C <sub>26</sub> 22 (S) TRICYCLICTERPANE
10	C <sub>26</sub> 22(R) TRICYCLICTERPANE
11R	C <sub>28</sub> TRICYCLICTERPANE ( R )
11S	C <sub>28</sub> TRICYCLICTERPANE ( S )
12R	C <sub>29</sub> TRICYCLICTERPANE ( R )
12S	C <sub>29</sub> TRICYCLICTERPANE ( S )
13	C <sub>27</sub> 18α(H)-22,29,30-TRISNORHOPANE (Ts)
14	C <sub>27</sub> 17α (H)-22,29,30-TRISNORHOPANE (Tm)
15	17 α (H)-29,30-BISNORHOPANE
16R	C <sub>30</sub> TRICYCLIC TERPANE ( R )
16S	C <sub>30</sub> TRICYCLIC TERPANE ( S )
17	17 α (H)- 28,30- BISNORHOPANE
18	C <sub>29</sub> 17α (H), 21β(H)-30- NORHOPANE
19	C <sub>28</sub> Ts (18α (H)-30-NORHOPANE
20	C <sub>30</sub> (17α (H)-DIAHOPANE)
21	C <sub>29</sub> 17β (H), 21α (H)-30 NORMORETANE
22	OLEANANE
23	C <sub>30</sub> 17α (H), 21β (H)-HOPANE
24	C <sub>30</sub> 17β (H), 21α (H)-MORÉTANE
25	C <sub>31</sub> 17α (H), 21 β (H)-30-HOMOHOPANE (22S)
26	C <sub>31</sub> 17α (H), 21 β (H)-30-HOMOHOPANE (22R)
27	GAMMACERANE
28	HOMOMORETANE
29	C <sub>32</sub> 17 α (H), 21β (H)-30,31-BISHOMOHOPANE (22S)
30	C <sub>32</sub> 17 α (H), 21β (H)-30,31-BISHOMOHOPANE (22R)
31	C <sub>33</sub> 17α (H), 21β (H)-30,31,32-TRISHOMOHOPANE (22S)

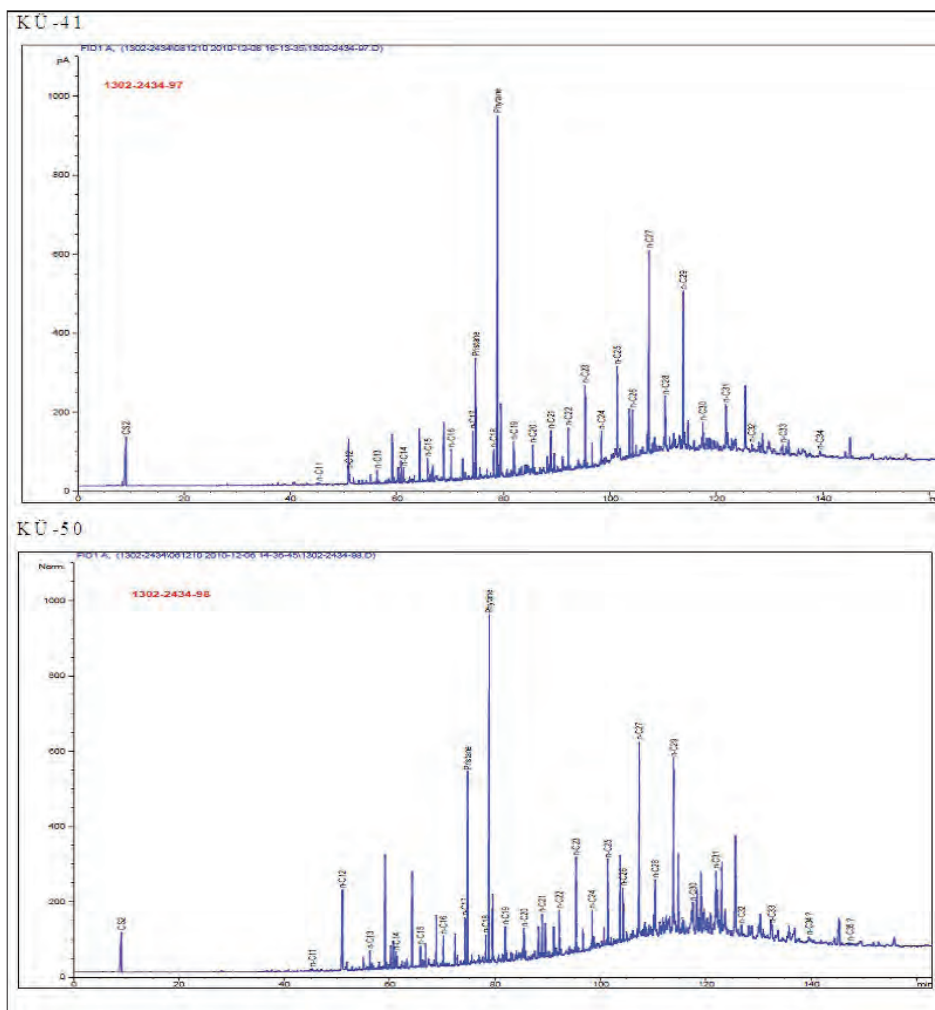


Figure 3a- Results of gas chromatography (GC) analysis.

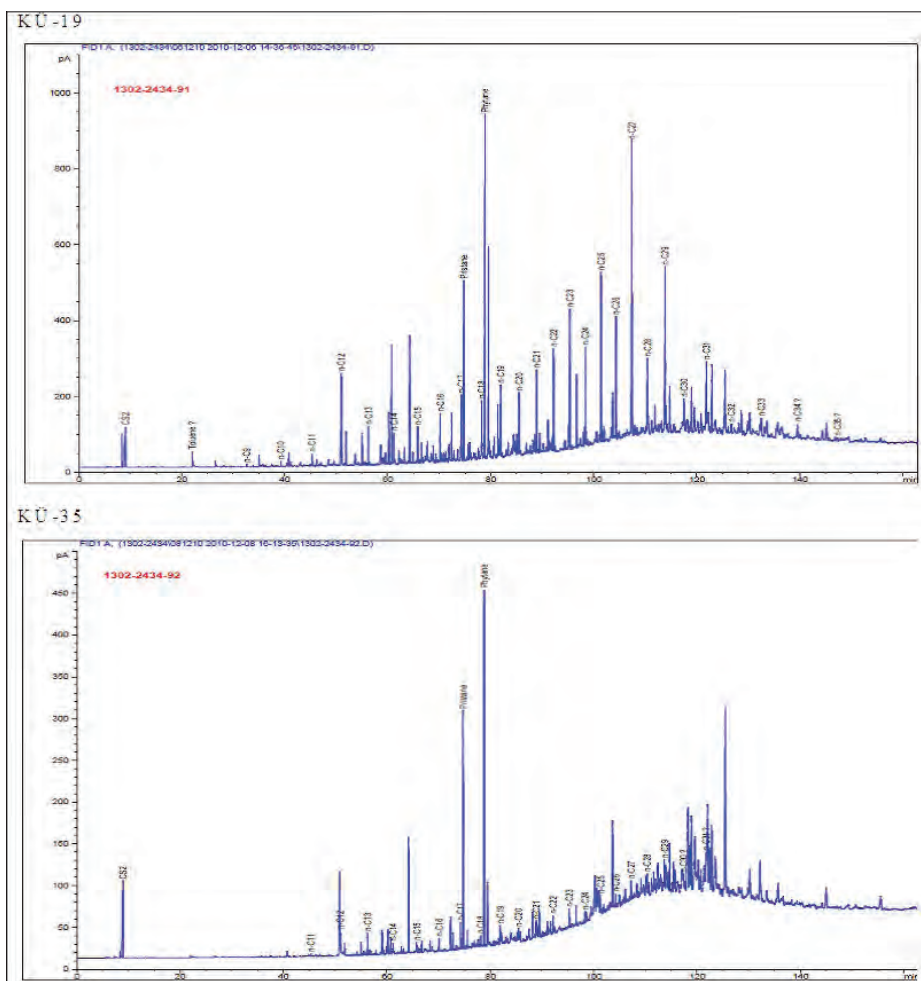


Figure 3b- Results of gas chromatography (GC) analysis.

Pr/Ph ratios for bituminous samples of KÜ-19, KÜ-35, KÜ-41 and KÜ-51 are 0.4, 0.6, 0.25 and 0.45, respectively. The depositional environment of samples according to isoprenoid ratios reflects anoxic reducing conditions (Didyk et al., 1978; Tissot and Welte, 1984; Leythaeuser and Schwarzkopf, 1986). Again, according to Pr/n-C17 and Ph/n-C18 ratios from isoprenoid/n-alkane ratios, the redox conditions of the depositional environment is reducing, organic material type is Type I and Type II kerogen and samples are yet in immature stage (Tissot and Welte, 1984, Moldowan et al., 1985, Hunt, 1995) (Figure 4).

The ratio of n-C17/n-C31 indicates that the source of organic material is marine algal or terrigenous plant. Values higher than 2 ( $>2$ ) indicate terrigenous plant source is more than marine algae (Forster et al., 2004). However; the alteration of organic material within sedimentary system breaks down the n-alkane

distribution and causes the increase of some more stable terrigenous n-alkanes and the loss of algal based n-alkanes. This situation may cause errors in n-C17/n-C31 ratio. The ratio of n-C17/n-C31 in samples KÜ-19, KÜ-41 and KÜ-50 changes between 0.7-0.9 and indicates terrigenous organic materials. According to pyrolysis analyses and organic petrographic data the kerogen types of the samples KÜ-19, KÜ-41 and KÜ-50 are Type-I, Type II and Type I, respectively. Accordingly; the organic materials to be terrigenous material according to n-C17/n-C31 can be concluded as the alteration of the organic material within sedimentary system.

Sterane mass chromatography (m/z 217) of the bituminous shale sample KÜ-35 is seen in figure 5. In order to determine the source of organic material a regular sterane distribution from C27 to C29 is used too. C27 steranes mostly are derived from marine

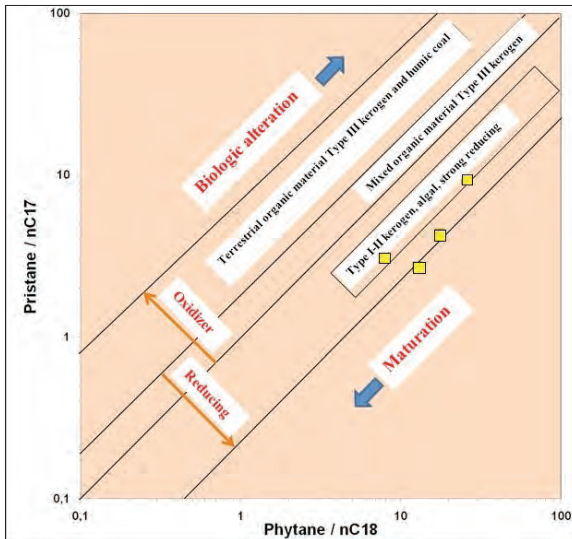


Figure 4- Kerogen type according to Pr/n-C17 and Ph/n-C18 values (Hunt, 1995).

algae, however; C28 steranes are derived from barm, fungi, bacterial plankton and algae; and C29 steranes are derived from terrigenous plants (Peters et al., 2005b).

The abundancy percentages of C27, C28 and C29 steranes in sample KÜ-35 were determined as 21.5%, 41.3% and 37.2%, respectively (Figure 6).  $C29/C27 < 1$  indicates that marine algae are more dominant than terrigenous plants (Peters et al., 2005b). When studied in this manner, it can be said that the rational value of terrigenous plants in sample KÜ-35 are more dominant than marine algae. The dominance of C29 steranes against C27 and C28 steranes in sterane

distribution indicates that terrigenous organic material income into depositional environment is much despite the marine organic material contribution. However; C29 steranes may also come from blue-green algae and marine diatoms (Nichols et al., 1990).

Terpane mass chromatography ( $m/z$  191) of bituminous shale sample KÜ-35 was given in figure 7. According to  $C29NH/C30H$  ratio (0.31), the bitumen was derived from a clastic clayey source rock (Mello et al., 1988, Clark and Philip, 1989).  $C24$  tetracyclic/ $C26$  tricyclic (S+R) ratio is 0.25, and indicates shale source rock. Also, the mineralogical data of the sample KÜ-35 show that the studied sample is bituminous shale. Gammacerane index value of the same sample was found as 0.17. Therefore; the salinity of water in a depositional environment cannot be talked about, even the presence of gammacerane molecule can be associated with an algal growth in a lacustrine environment (Hunt, 1995, Sinnighe Damsté et al., 1995, Peters et al., 2005a). In general, the presence of gammacerane may indicate the marine, lacustrine, near shore or a deltaic depositional environment (Waples and Machihara, 1991).

The distribution from C27 to C29 can also be used to determine the changes of sedimentary depositional environments from deep marine (>150 m) to shallow marine and to lacustrine depositional environments. Thus, the abundancy percentages of C27 and C29 steranes in sample KÜ-35 are 21.5% and 37.2%, respectively, and C29 steranes are dominant. This situation indicates that Kürnüç basin depositional environment cannot be a deep marine.

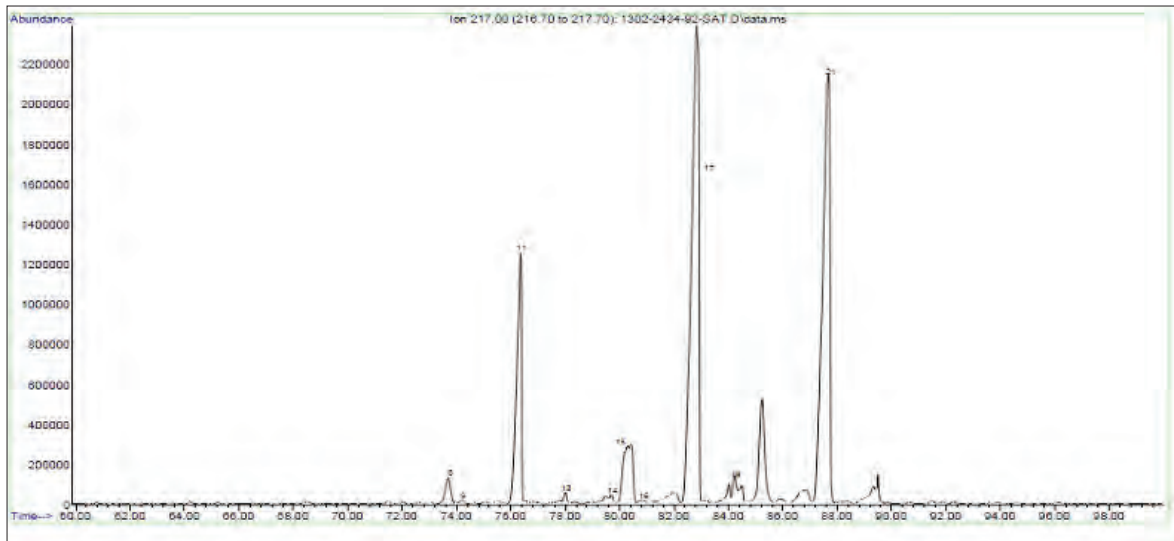


Figure 5- Sterane mass chromatograph of the sample number KÜ-35 ( $m/z$  217).

And according to the ratio of C25/C26 tricyclic tripane (0.32), it is understood that the depositional environment of Kürnüş bituminous rocks is not marine environment (Burwood et al., 1992, Hanson et al., 2000). Besides; according to pyrolysis analyses and lithological data the investigated basin can be regarded as a lagoon partly connected with the sea.

#### 4.2. Source Rock Potential

Results of pyrolysis analyses of Kürnüş (Göynük/Bolu) bituminous rocks (bituminous shale, bituminous marl) was given in table 3. TOC contents vary between 2.52-8.38% with a mean value of 6.13%. Considering TOC values of bituminous rocks they possess excellent source rock potential (Tissot and Welte, 1984; Peters, 1986; Jarvie, 1991; Peters and Cassa, 1994).

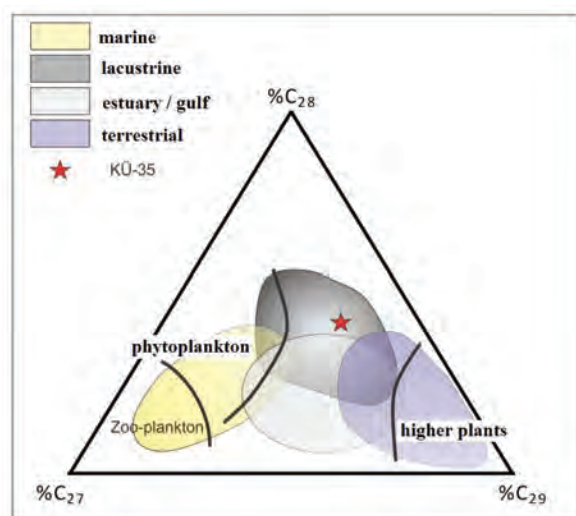


Figure 6- Basin determination by means of C<sub>27</sub>, C<sub>28</sub> and C<sub>29</sub> steranes (Huang and Meinchein, 1979).

According to carbon average in medium shales (Wedepohl, 1971) the total organic carbon amounts of bituminous rocks in the study area is quite rich (Figure 8). When a frequency interval for the total organic carbon amount for studied bituminous rocks is formed, it is seen that most of the samples concentrate between 5-8% TOC values (Figure 9). S1 hydrocarbon values of Lower Eocene bituminous rocks is between 0.37-2.84 mg HC/g rock with a mean value of 1.28 mg HC/g rock. The source rock potential according to S1 hydrocarbon values is good (Peters, 1986; Peters and Cassa, 1994). S2 hydrocarbon values range between 18.03-69.23 mg HC/g rock with a mean value of 45.51 mg HC/g rock. Source rock potential is good for S2 hydrocarbon value according to Espitalie (1982), very good according to Peters (1986) and excellent according to Peters and Cassa (1994).

#### 4.3. Organic Material Type

The determination of organic material or kerogen type was assessed also using other parameters. Hydrogen Index values (HI) vary between 476-891 mg HC/g rock (Table 3) in studied samples, and the kerogen type is Type I and Type II according to Peters and Cassa (1994). However; according to Hydrogen Index (HI)–Oxygen Index (OI) diagram the organic material type is mostly Type I kerogen. When the kerogen type is assessed according to Hydrogen Index (HI)-Tmax diagram, Type I kerogen is mostly observed and only in 2 samples Type II kerogen is observed (Figure 10 a, b). According to S2-TOC diagram associated with Hydrogen Index (HI) values, the kerogen type is mostly Type I and in some samples it is Type II (Figure 11).

Table 3- Results of pyrolysis analysis.

Sample No	TOC %	*S <sub>1</sub>	*S <sub>2</sub>	**S <sub>3</sub>	T <sub>max</sub> , °C	HI	OI	PI	S <sub>2</sub> /S <sub>3</sub>	GP
KÜ-19	8,38	0,52	67,36	3	439	804	36	0,01	22,45	67,88
KÜ-35	5,61	0,67	48,77	1,1	437	869	20	0,01	44,34	49,44
KÜ-37	2,52	0,37	18,03	0,51	432	715	20	0,02	35,35	18,40
KÜ-38	7,77	1,02	69,23	1,08	430	891	14	0,01	64,10	70,25
KÜ-39	5,21	1,35	35,41	2,08	425	680	40	0,04	17,02	36,76
KÜ-40	4,78	1,61	30,45	1,25	419	637	26	0,05	24,36	32,06
KÜ-41	5,61	2,00	29,48	1,86	402	525	33	0,06	15,85	31,48
KÜ-50	6,15	1,22	53,99	0,84	438	878	14	0,02	64,27	55,21
KÜ-51	7,91	1,22	67,35	1,21	437	851	15	0,02	55,66	68,57
KÜ-52	7,36	2,84	35,00	4,55	403	476	62	0,08	7,69	37,84

\*mg HC/g rock), \*\*mg CO<sub>2</sub>/g rock

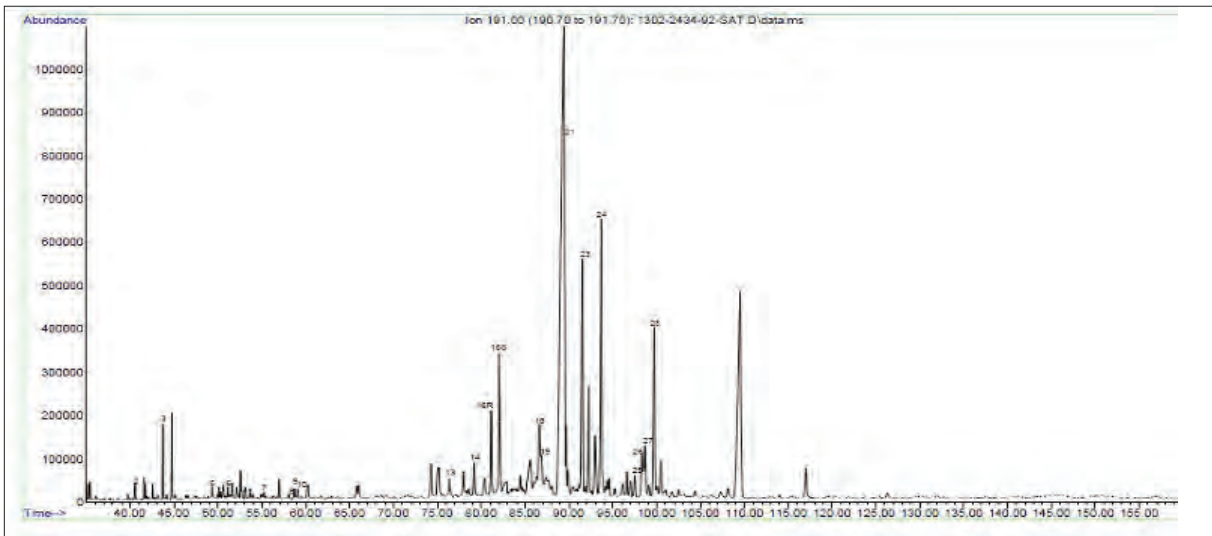


Figure 7- Terpene mass chromatograph of the sample number KÜ-35 (m/z 191).

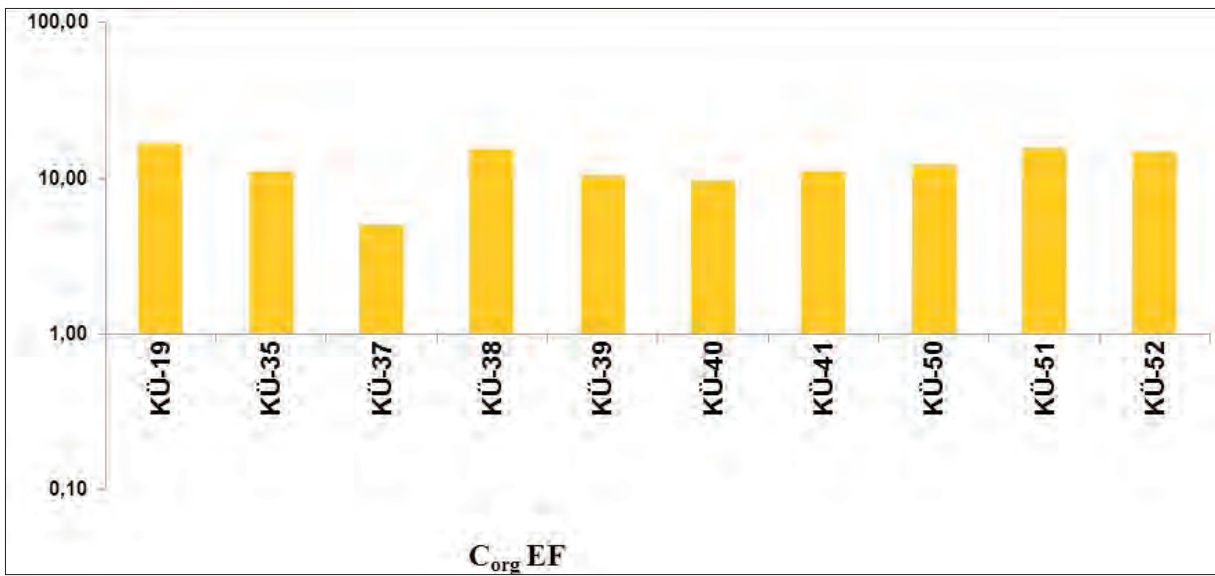


Figure 8- Total Organic Carbon (TOC) enrichments with respect to normal shales.

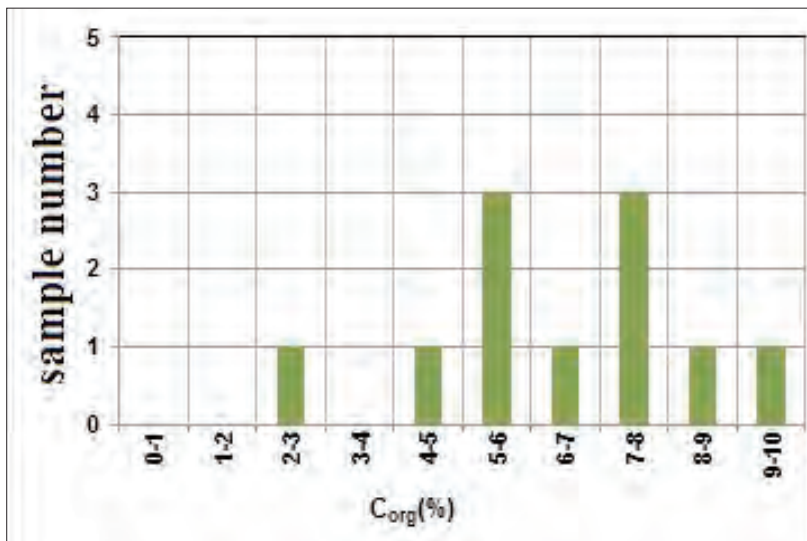


Figure 9- Total % organic carbon amount frequency interval.

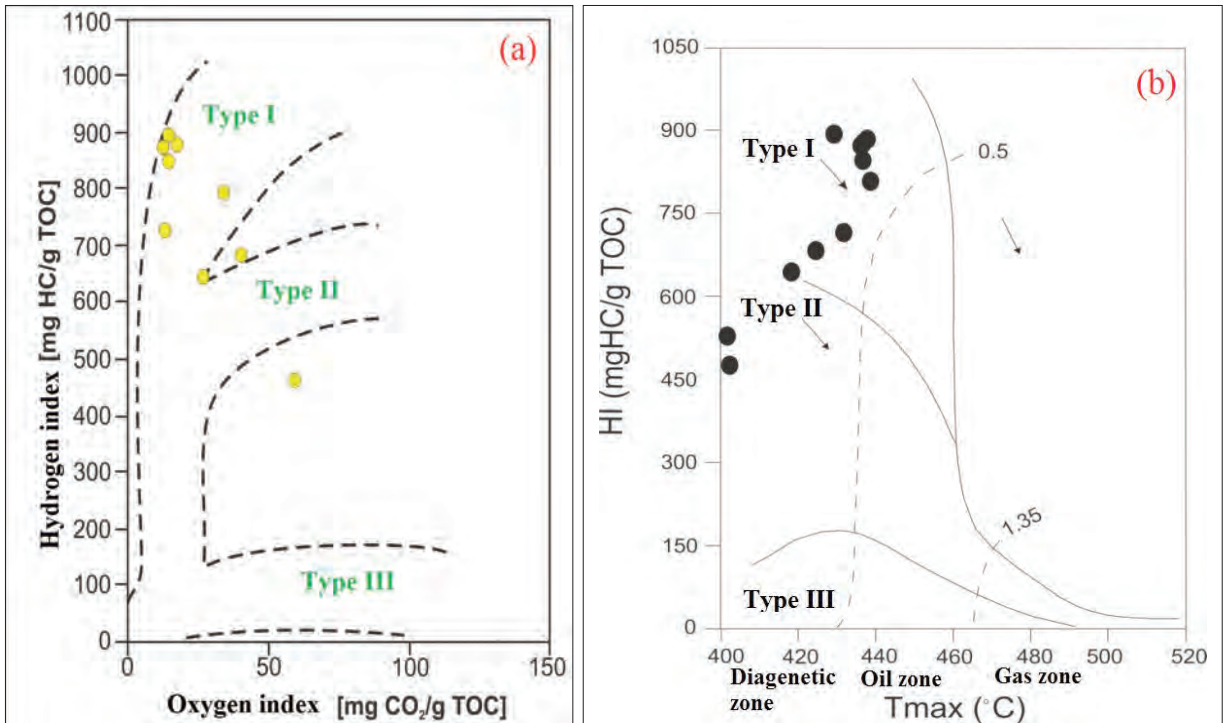


Figure 10 a, b- Kerogen types according to HI-OI and HI-Tmax diagrams (Pratt, 1984; Espitalie et al., 1977).

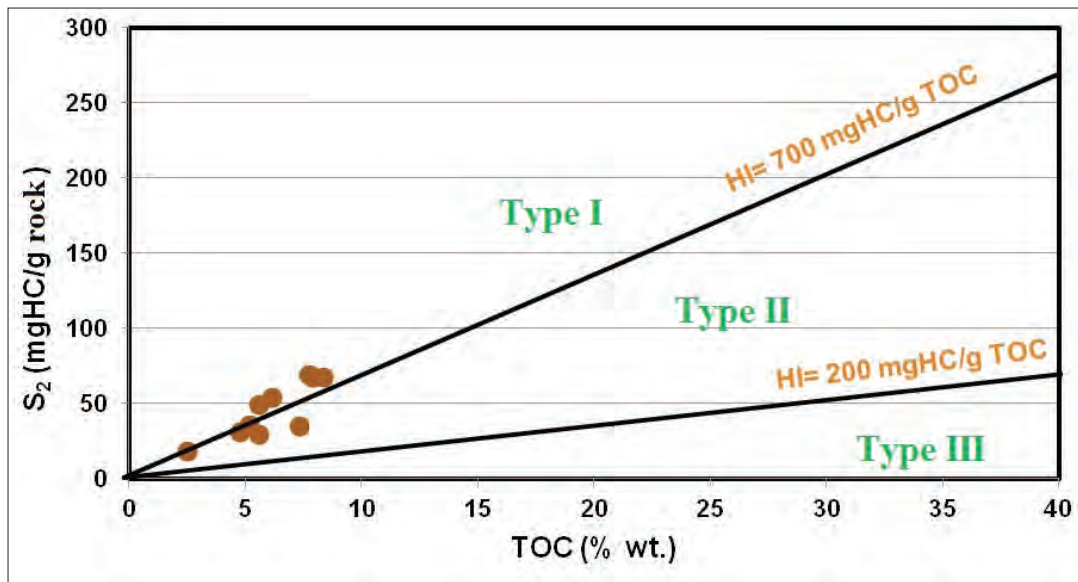


Figure 11- Kerogen types according to S<sub>2</sub> and TOC values (Langford, and Blanc-Valleron, 1990).

The ratio of S<sub>2</sub>/S<sub>3</sub> is 7.69 only in sample KÜ-52 and the kerogen type is Type II/III. The organic material type in the other samples according to S<sub>2</sub>/S<sub>3</sub> ratio is Type I kerogen (Peters and Cassa, 1994). The organic material type of bituminous rocks according to organic petrographic studies is 100% Amorph+Algal (Table 4), and is compatible with results of pyrolysis analysis. The abundancy percentages of C<sub>27</sub>- C<sub>28</sub>-

C<sub>29</sub> steranes in sample KÜ-35 were determined as 21.5%, 41.3% and 37.2%, respectively (Figure 6). The dominance of C<sub>28</sub> steranes with 41.3% abundancy over C<sub>27</sub> and C<sub>29</sub> steranes indicate the presence of bacterial plankton and/or algae in this sample. C<sub>29</sub>/C<sub>27</sub><1 shows that marine algae are more dominant than terrigenous plants (Peters et al., 2005b). Thus, it can be said that the rational value of terrigenous

Table 4- Results of organic petrography analysis

Sample No	% Amorp+ Alg	SCI
KÜ-19	100	2,5 - 3
KÜ-35	100	3
KÜ-37	100	3
KÜ-38	100	3
KÜ-39	100	-
KÜ-40	100	3
KÜ-41	100	-
KÜ-50	100	-
KÜ-52	100	-

plants in sample KÜ-35 is more dominant than marine algae. The dominance of C29 steranes against C27 and C28 steranes in sterane distribution indicates that terrigenous organic material income into depositional environment is much despite the marine organic material contribution. However; C29 steranes may also come from blue-green algae and marine diatoms (Nichols et al., 1990).

#### 4.4. Organic Maturation

The maturation assessments of organic materials in studied samples were examined in different methods. Tmax values vary between 402°C (min) and 439°C (max). According to Tmax values, bituminous rocks are not mature (Éspitalié et al., 1985). The Production Index (PI) values of the rocks are in between 0.01-0.08 mg HC/g rock and yet not mature (Peters and Cassa, 1994). Spore Color Index (SCI) values range in between 2.5-3.0 and are in immature stage.

17  $\alpha$  (H)-22, 29, 30-trisnorhopane (Tm) is biologically produced and turns into 18  $\alpha$  (H)-22, 29, 30 trisnorhopane (Ts) by burial and maturation (Peters et al., 2005b). Therefore; Ts/(Ts+Tm) ratio increases as thermal maturation rises. Ts/(Ts+Tm) ratio reaches 1.0 in late mature oil formation phase (Peters et al., 2005b). Ts/(Ts+Tm) ratio in studied sample KÜ-35 is 0.33, and can be regarded as immature.

R configuration is biologically produced in C-22 (22R) in 22S/(22S+22R) ratio, and gradually turns into 22R and 22S isomers by burial and maturation (Peters et al., 2005b). Therefore; 22S/(22S+22R)

also increases by maturation. Thermal equilibrium value of 22S/(22S+22R) reaches 0.5 in oil formation zone (Peters et al., 2005b). 22S/(22S+22R) ratio to be 0.34 in the same sample indicates the beginning of immature/maturation.

Another maturation method is the ratio of 5 $\alpha$ (H), 14 $\beta$ (H), 17 $\beta$ (H) isomers ( $\alpha\beta\beta$ ) to 5 $\alpha$ (H), 14 $\alpha$ (H), 17 $\alpha$ (H) ( $\alpha\alpha\alpha$ ), and is expressed as;  $\alpha\beta\beta/(\alpha\beta\beta+\alpha\alpha\alpha)$ . As the thermal maturation increases ( $\alpha\alpha\alpha$ ) isomers are biologically produced and gradually turn into mixture of  $\alpha\beta\beta$  and  $\alpha\alpha\alpha$  isomers (Peters et al., 2005b). This ratio increases as the thermal maturation rises. The value of C28- $\alpha\beta\beta/(\alpha\beta\beta+\alpha\alpha\alpha)$  ratio indicates the thermal maturation and is 0.72 in oil formation zone (Peters et al., 2005b). Values lower and higher than 0.7 indicate early and late mature oil phase, respectively. In sample KÜ-35,  $\alpha\beta\beta/(\alpha\beta\beta+\alpha\alpha\alpha)$  value is 0.02 and may indicate that the maturation has just started.

C30 17 $\beta$  (H), 21 $\alpha$  (H)- moretan/ C 30 17 $\alpha$  (H), 21 $\beta$  (H)- hopan ratio is again used as the maturity parameter. This value in the studied sample is 1.17 and may indicate that the immature/partly maturation has just started.

C29 Ts 18 $\alpha$  (H)-30- norhopane/ C29 Ts 18 $\alpha$  (H)-30- norhopane+ C29 17 $\alpha$  (H), 21 $\beta$ (H)-30- norhopane ratio is again used as the maturity parameter. The stability of 29 Ts component is relatively higher than norhopane. It means that 29Ts/ (29Ts+norhopane) ratio will increase with rising temperature and maturation (Hughes et al., 1995). Again, this ratio for the sample KÜ-35 was determined as 0.49 and indicates immature stage.

The ratio of 20S/(20S+20R) starts to increase from 0 value with the increase in thermal maturation, and this increase continues with maturation until 0.52-0.55 interval (Seifert and Moldowan, 1981). This ratio is 0.44 in sample KÜ-35 and indicates that the maturation has just started.

According to all maturity assessment results, it is seen that the organic maturity in Lower Eocene bituminous rocks in Kürnüç area has not yet occurred.

#### 4.5. Hydrocarbon Production Potential

It was assessed whether or not Lower Eocene aged bituminous rocks possess a hydrocarbon production potential using several parameters. S2/S3 ratio changes in between 7.69-64.27 and shows that rocks

can produce oil (Clementz et al., 1979; Peters, 1986). Genetic Potential (S1+S2) values vary in between 18400-70250 ppm and bituminous rocks possess good source rock potential (Tissot and Welte, 1984). According to Hydrogen Index (HI)-TOC % diagram, again bituminous rocks indicate the excellent oil source (Figure 12). Also, according to S2-TOC diagram these rocks hold excellent oil generation potential except for one sample (Figure 13). Hydrocarbons were produced by Lower Eocene bituminous rocks according to S1-TOC diagram, and there is not any evidence showing that there had been any organic contamination in bituminous rocks (Figure 14). According to results of hydrocarbon production potential assessment, it is seen that Lower Eocene bituminous rocks in Kürnüş area have excellent oil production potential and the produced hydrocarbons are in situ.

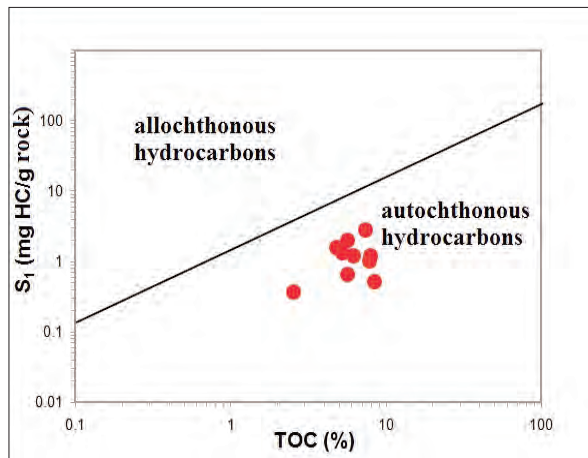


Figure 14- Hydrocarbon characterization according to S1-TOC values (Hunt, 1995).

4.6. Isotope Studies

In this study, pyrolysis analyses, GC and GC-MS analyses, and also the carbon isotope analyses were carried out. Carbon isotope analyses were performed on 3 samples selected from which organic petrographic investigations had been made. According to carbon isotope analyses carried out it was detected that  $\delta^{13}C$  (Saturated Hydrocarbon) isotope values and  $\delta^{13}C$  (Aromatic Hydrocarbon) ranged in between ‰(-) 32.07, (-)31.31 and ‰(-)32.59, (-)30.39, respectively (Table 5). If Canonical Variable (CV) value calculated from carbon isotope analyses is greater than 0.47, then it shows non-marine origin oil; if it is less than 0.47, then it shows marine origin oil (Sofer, 1984).

$$CV (\text{Canonical Variable}) = -2.53 * \delta^{13}C_{\text{saturated}} + 2.22 * \delta^{13}C_{\text{aromatic}} - (11.65)$$

According to CV results, sample KÜ-35 falls into areas of non-marine and some lacustrine oils. However; samples KÜ-19 and 50 fall into areas of marine and other lacustrine oils (Figure 15).

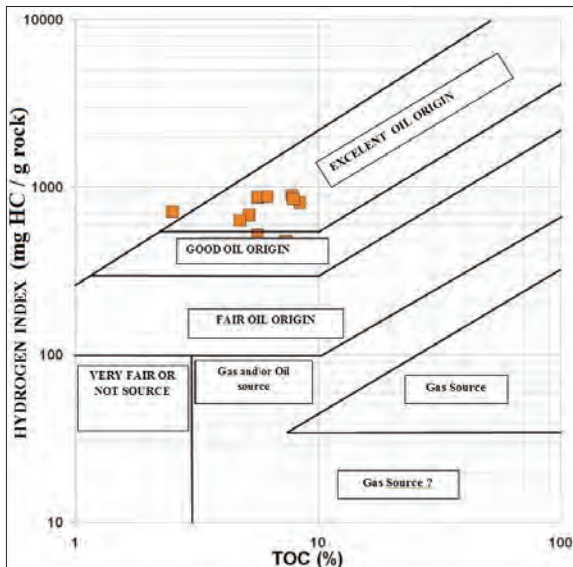


Figure 12- Hydrocarbon potential according to HI and TOC values (Jackson et al., 1985).

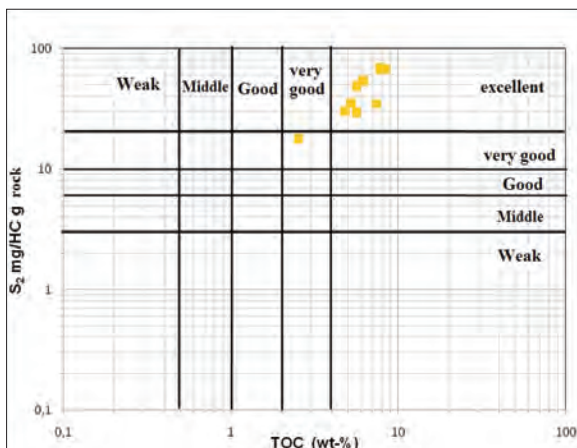


Figure 13- Hydrocarbon potential according to S2 and TOC values (Peters and Cassa, 1994).

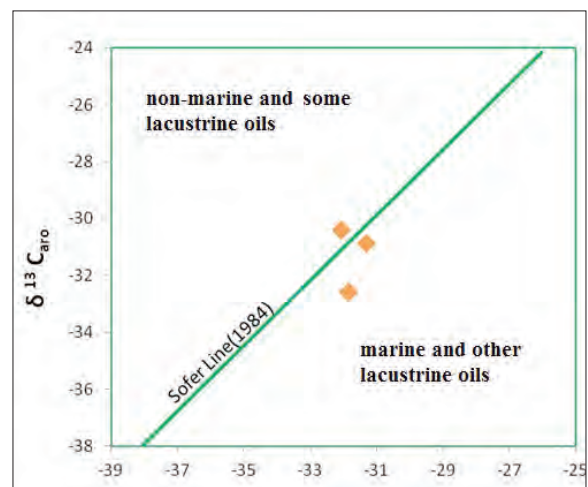


Figure 15-  $\delta^{13}C$  Aromatic and  $\delta^{13}C$  mature hydrocarbon diagram (Sofer, 1984).

Table 5- Saturated, aromatic  $\delta^{13}\text{C}$  and CV values of bituminous rocks.

Sample No	$\delta^{13}\text{C}$		CV
	Saturated Hydrocarbon	Aromatic Hydrocarbon	
KÜ-19	-31.85	-32.59	-4,3748
KÜ-35	-32.07	-30.39	1,0592
KÜ-50	-31.31	-30.88	-1,9286

## 5. Results

According to mean TOC % (6.13%) values and S1 (1.28 mg HC/g rock) and S2 (45.51 mg HC/g rock) hydrocarbon averages, the bituminous rocks have very good-excellent source rock potential. Kerogen types are Type I and very few Type II based on Hydrogen Index (HI) limit values. This result is also supported by Hydrogen Index (HI)-Oxygen Index (OI), Hydrogen Index (HI)-Tmax, S2-TOC diagrams and data of Hydrocarbon Type Index (S2/S3). Organic petrographic results imply 100% Algal+Amorph organic material. According to Tmax, PI, SCI, Pr/nC17 and Ph/nC18 ratios, all samples are in immature stage. Besides, m/z 191 triterpane and m/z 217 sterane biomarker data carried out in some samples [Ts/(Ts+Tm), 22S/(22S+22R)],  $\alpha\beta\beta/(\alpha\beta\beta+\alpha\alpha\alpha)$ , 29Ts/(29Ts+norhopane), 20S/(20S+20R) as well indicate that Lower Eocene bituminous rocks in Kürnüş area are immature.

Genetic potential (S1+S2) values show that samples possess good source rock potential. According to S2/S3 ratio, HI-TOC and S2-TOC diagrams, Lower Eocene bituminous rocks have excellent oil generation potential. According to S1-TOC diagram, hydrocarbons produced by Lower Eocene bituminous rocks are in situ and were not subjected to any contamination. According to C29 17 $\alpha$ (H)-hopan and C24 tetracyclic/C26 tricyclic (S+R) ratio, source rock lithology is of clastic source and imply bituminous shale. Mineralogical data also support this result.

## Acknowledgment

This study has been carried out with the cooperation of General Directorate of Turkish Coal Enterprise. We would like to thank to Vice General Director Dr. Abdurrahman Murat, to Mustafa Özdingiş and to all other staffs who contributed in this study.

## References

- Aliyev, S., Sari A., Koç, S. 2006. Investigation of Organic Carbon and Iron Group Elements in the Bituminous Rocks. *Energy Sources*, part A. 28,1461-1472pp.
- Behar,F., Beaumont,V., Penteado, H.L. De B. 2001. Rock-Eval 6 Technology: Performances and Developments. *Oil & Gas Science and Technology – Rev. IFP*, 56, 2, pp. 111-134pp.
- Burwood, R., Leplat, P., Mycke, B., Paulet, J. 1992. Rifted margin source rock deposition: carbon isotope and bio-marker study of a West African Lower Cretaceous "lacustrine" section. *Organic Geochemistry*. 19, 41-52pp.
- Büyüktoku, A.G., Sari, A., Karaçam, A. 2005. The reservoir potential of the Eocene carbonates in the Bolu Basin, West of Turkey. *Journal of Petroleum Science and Engineering* 49, 79-91pp.
- Clark, J.P., Philp, R.P. 1989. Geochemical Characterization of Evaporite and Carbonate Depositional Environments and Correlation of Associated Crude Oils in the Black Creek Basin, Alberta, *Bulletin of Canadian Petroleum Geology*, 37, 401-416pp.
- Clementz, D.M., Demaison, G.J., Daly, A.R. 1979. Well site geochemistry by programmed pyrolysis. *Proceedings of the 11th Annual Offshore Technology Conference*, Houston, OTC 3410, 1, 465-470pp.
- Didyk, B.M., Simoneit, B.R.T., Brassell; S.C., Eglinton, G. 1978. Organic geochemical indicators of paleoenvironmental conditions of sedimentation. *Nature*. 272, 216-222pp.
- Espitalié, J. 1982. Institute Francis du Petrole, *Syntheses Geologiques et Geochimie*. 7020 dated April 18.
- Espitalié, J., Madec, M., Tissot, J., Menning, J., Leplat, P. 1977. Source rock characterization method for petroleum exploration. *Proceedings, 9th Annual Offshore Technology Conference*, 3, 439-448pp.
- Espitalié, J., Deroo, G., Marquis, F. 1985. La pyrolyse Rock-Eval et ses applications. Partie 1. *Rev. Inst. Fr. Pet.* 40, 563-579pp.
- Forster, A., Sturt, H., Meyers, P.A., the Leg 207 Shipboard Scientific Party. 2004. Molecular biogeochemistry of Cretaceous black shales from the Demerara Rise:Preliminary shipboard results from sites 1257 and 1258, Leg 207: *In* Erbacher, J., Mosher, D.C., Malone, M.J., et al., *Proceedings of the Ocean Drilling Program, Initial Reports*: v. 207, p. 1-22.

- Gedik, İ., Aksay, A. 2002. Geological maps (scale: 1/100.000) of Turkey. No: 32, Adapazarı G25. *Maden Tetkik ve Arama Genel Müdürlüğü*, 40p.
- Hanson, A. D., Zhang, S. C., Moldowan, J. M., Liang, D. G.; Zhang, B. M. 2000, Molecular organic geochemistry of the Tarim basin, Northwest China. *Bulletin of the American Association of Petroleum Geologists*. 84, 1109–1128pp.
- Huang, W.Y., Meinschein, W.G. 1979. Sterols as ecological indicators. *Geochimica et Cosmochimica Acta* 43, 739–745pp.
- Hughes, W.B., Holba, A.G., Dzou, L.I.P. 1995. The ratios of dibenzothiophene to phenanthrene and pristane to phytane as indicators of depositional environment and lithology of petroleum source rocks. *Geochimica et Cosmochimica Acta*, 59, 3581-3598pp.
- Hunt, J. M., 1995. Petroleum geochemistry and geology. *W.H. Freeman and Company*, New York. 743 p.
- Jackson, K. S., Hawkins, P. J., Bennett, A. J. R. 1985. Regional facies and geochemical evolution of the southern Denison Trough. *APEA Journal* 20, 143-158pp.
- Jarvie, D. M. 1991. Total organic carbon (TOC) analysis; in, Source Migration Processes and Evaluation Techniques, R. K. Merrill, ed.: *Bulletin of the American Association of Petroleum Geologists, Treatise of Petroleum Geology Handbook of Petroleum Geology*, p. 113-118.
- Kara, G.R., Korkmaz S. 2008. Element contents and organic matter-element relationship of The Tertiary oil shale deposits in Northwest Anatolia, Turkey”. *Energy & Fuels*, 22, 3164-3173.
- Leythaeuser, D., Schwarzkopf, T. 1986. The pristane/n-heptadecane ratio as an indicator for recognition of hydrocarbon migration effects. *Org. Geochem.* 10, 191-197pp.
- Mello, M. R., Telnaes, N. Gaglianone, P. C., Chicarelli, M. I., Brassell, S. C.; Maxwell, J. R. 1988. Organic Geochemical Characterization of Depositional Paleoenvironments of Source Rocks and Oils in Brazilian Marginal Basins. In, *Advances in Organic Geochemistry* 1987 (L. Mattavelli ve L. Novelli, eds.), Oxford, Pergamon Press, 31-45.
- Moldowan, J.M., Seifert, W.K., Gallegos, E.J. 1985. Relationship Between Petroleum Composition and Depositional Environment of Petroleum Source Rocks. *Bulletin of the American Association of Petroleum Geologists*, 69, 1255-1268.
- Nichols, P. D., Palmisano, A. G., Rayner, M. S., Smith, G. A., White, D. C. 1990. Occurrence of novel C30 sterols in Antarctic sea-ice diatom communities during a spring bloom: *Organic Geochemistry*, v. 15, p. 503-508.
- Peters, K.E. 1986. Guidelines for Evaluating Petroleum Source Rock Using Programmed Pyrolysis, *Bulletin of the American Association of Petroleum Geologists*. 70, 3, 318-329pp.
- Peters, K. E., Moldowan, J. M. 1993. The Biomarker Guide, Interpreting molecular fossils in petroleum and ancient sediments, Prentice Hall, 363p.
- Peters, K. E., Cassa, M.R. 1994. Applied Source Geochemistry. In: Magoon, L.B. and Dow, W.G. (Eds), The Petroleum System-from Source to Trap. *Bulletin of the American Association of Petroleum Geologists*, 70, p.329.
- Peters, K.E., Walters, C.C., Moldowan, J.M. 2005a. The Biomarker Guide: Volume 1 Biomarkers and Isotopes in the Environment and Human History: New York, Cambridge University Press.
- Peters, K.E., Walters, C.C., Moldowan, J.M. 2005b. The Biomarker Guide volume 2: Biomarkers and Isotopes in Petroleum Exploration and Earth History. Cambridge, Cambridge University Press.
- Pratt, L.M. 1984. Influence of paleoenvironmental factors on preservation of organic matter in Middle Cretaceous Greenhorn formation, Pueblo, Colorado. *AAPG Bull.* 68, 1146–1159pp.
- Sarı, A., Sonel, N. 1995. Kayabaşı (Göynük-Bolu) Yöresinin Bitümlü Şeyl İncelemeleri. *Türkiye Jeoloji Bülteni*. 2, 39-49pp.
- Sarı, A., Aliyev, S.A. 2005. Source rock evaluation of the lacustrine oil shale bearing deposits: Göynük/Bolu, Turkey. *Energy Sources*, 27, 279-298pp.

- Sarı, A., Aliyev, S.A., Koralay, B. 2007. Source Rock Evaluation of the Eocene Shales in the Gökçeşu Area (Bolu/Turkey). *Energy Sources*, Part A. 29, 1025-1039pp.
- Sarı, A., Geze, Y. 2008. Organic Geochemical Evaluations of Bituminous Rock and Coals in Miocene Himmetoğlu Basin (Bolu, Turkey). *Petroleum Science and Technology*. 26, 649-664pp.
- Seifert, W.K., Moldowan, J.M. 1981. Paleoreconstruction by biological markers. *Geochimica et Cosmochimica Acta*. 45, 783-794pp.
- Sinninghe Damsté, J.S., Hayes, J.M., Kenig, F., Koopsman, M.P., Koster, J., Schouten, S. 1995. Evidence for gammacerane as an indicator of water column stratification. *Geochim. Cosmochim. Acta*. 59, 1895-1900pp.
- Sofer, Z. 1984. Stable carbon isotope compositions of crude oils: Application to source depositional environments and petroleum alteration. *Bulletin of the American Association of Petroleum Geologists*, 68, 31-49pp.
- Symington, W. A., Olgaard, D. L., Otten, G. A., Phillips, T. C., Thomas, M.M., Yeakel, J. D. 2008. *ExxonMobil's Electrofrac Process for In Situ Oil Shale Conversion*. AAPG Annual Convention. San Antonio: American Association of Petroleum Geologists. Retrieved 2009-04-12.
- Şeker, H., Kesgin, Y. 1991. Geology and petroleum possibilities of around Nallıhan - Mudurnu-Seben-Beypazarı regions. *TPAO* report no: 2907.
- Şener, M., Sengüler, I. 1998. Geological, mineralogical and geochemical characteristics of oil shale bearing deposits in the Hatıldag oil shale field, Göynük, Turkey. *Fuel*, 8, 871-880pp.
- Şengör, A.M.C., Yılmaz, Y. 1981. Tethyan evolution of Turkey: A plate tectonic approach. *Tectonophysics*, 75, 181-241pp.
- Şengüler, İ. 2012. Hatıldag ve Himmetoğlu (Göynük/Bolu) Civarının Stratiğrafisi ve Bitümlü Şeyl Oluşumları. *TPJD Bülteni*, 24, 7-21pp.
- Tissot, B.P., Welte, D.H. 1984., *Petroleum Formation and Occurrence*, Springer Verlag, Berlin, Heidelberg, New York Tokyo.
- Waples, D. W., Machihara, T. 1991. Biomarkers for geologists. A practical guide to the application of steranes and triterpanes in petroleum geology. *AAPG Methods in Exploration Series*, No. 9, 91 p.
- Wedepohl, K.H. 1971. Environmental influences on the chemical composition of shales and clays. In: Ahrens, L.H., Press, F., Runcorn, S.K., Urey, H.C. (Eds.), *Physics and Chemistry of the Earth*, vol. 8. Pergamon, Oxford, pp. 305- 333.





# BULLETIN OF THE MINERAL RESEARCH AND EXPLORATION

<http://bulletin.mta.gov.tr>

BULLETIN OF THE MINERAL RESEARCH AND EXPLORATION	
CONTENTS	
1. PRODUCTION OF AN INSULATION MATERIAL FROM CARPET AND BORON WASTES	197
2. ...	...
3. ...	...
4. ...	...
5. ...	...
6. ...	...
7. ...	...
8. ...	...
9. ...	...
10. ...	...
11. ...	...
12. ...	...
13. ...	...
14. ...	...
15. ...	...
16. ...	...
17. ...	...
18. ...	...
19. ...	...
20. ...	...
21. ...	...
22. ...	...
23. ...	...
24. ...	...
25. ...	...
26. ...	...
27. ...	...
28. ...	...
29. ...	...
30. ...	...
31. ...	...
32. ...	...
33. ...	...
34. ...	...
35. ...	...
36. ...	...
37. ...	...
38. ...	...
39. ...	...
40. ...	...
41. ...	...
42. ...	...
43. ...	...
44. ...	...
45. ...	...
46. ...	...
47. ...	...
48. ...	...
49. ...	...
50. ...	...
51. ...	...
52. ...	...
53. ...	...
54. ...	...
55. ...	...
56. ...	...
57. ...	...
58. ...	...
59. ...	...
60. ...	...
61. ...	...
62. ...	...
63. ...	...
64. ...	...
65. ...	...
66. ...	...
67. ...	...
68. ...	...
69. ...	...
70. ...	...
71. ...	...
72. ...	...
73. ...	...
74. ...	...
75. ...	...
76. ...	...
77. ...	...
78. ...	...
79. ...	...
80. ...	...
81. ...	...
82. ...	...
83. ...	...
84. ...	...
85. ...	...
86. ...	...
87. ...	...
88. ...	...
89. ...	...
90. ...	...
91. ...	...
92. ...	...
93. ...	...
94. ...	...
95. ...	...
96. ...	...
97. ...	...
98. ...	...
99. ...	...
100. ...	...

## PRODUCTION OF AN INSULATION MATERIAL FROM CARPET AND BORON WASTES

Yasin ERDOĞAN<sup>a\*</sup>

<sup>a</sup> *Iskenderun Technical University, Faculty of Mechanical, Department of Petroleum & Natural Gas Engineering, 31200, Iskenderun, Hatay-Turkey*

Research Article

### ABSTRACT

Keywords:  
Boron, Carpet Wastes,  
Halibor, Turkey

Received : 04.03.2015  
Accepted : 23.06.2015

Buildings are large consumers of energy in all countries. In regions with harsh climatic conditions, a substantial share of energy goes to heat and cool buildings. This paper reports an investigation of the insulation materials made from mixing carpet wastes with a solution with added crude colemanite ore, one of boron minerals, and a solution with added colemanite wastes from a barrage. A new building insulation material was produced which is name, Halibor. Optimum mixing ratios were determined for mass production and the physical properties of the product were established. In addition, the material produced was compared with similar products used in buildings in terms of physical properties. As a result of the investigations, it was established that the product provides high heat and sound insulation and can be used easily in building and construction industry.

### 1. Introduction

Of the total energy produced in the world, 25% is consumed during industrial production, 25% during use of motor vehicles, and 50% in buildings. A very large proportion of the energy consumed in buildings is used for heating or cooling buildings. The efficient use of energy makes a significant contribution to preventing negative environmental impacts. The emission of greenhouse gases, primarily CO<sub>2</sub>, causes global warming and along with it, climate change. Thermal insulation enables heating or cooling of buildings with less fuel so greenhouse gases, such as carbon dioxide (CO<sub>2</sub>), sulfur dioxide (SO<sub>2</sub>), will also be reduced, thus contributing to mitigation of greenhouse effect in the atmosphere, global warming and climate change (Demir and Orhan 2006; Enek, 2012, Erdoğan and Yaşar, 2005).

According to building census of 2000, there are 7.8 million buildings in Turkey. This number is increasing every day in proportion to the rate of population growth and urbanization. According to the census, the area occupied by residential and commercial buildings is 913 million m<sup>2</sup>, 400 million m<sup>2</sup> of which is heated. In terms of resource consumption and environmental

damage, buildings are responsible for 13.6% of water use, 70% of electricity consumption, 60% of solid waste generation, and 33-39% of greenhouse gas emissions. From the perspective of building life cycle, it is seen that 83% of the total energy is consumed during use of the building. 80% of the energy consumed in households is spent on heating. The efficiency of use of a building and environmental damage caused by it vary depending on its design, the materials used during its construction and efficiency in its operation. Therefore, it is possible to lower energy consumption values and support sustainability by insulation to be implemented in buildings as well as increasing efficiency of building energy systems (Keskin, 2010).

In other words, thermal insulation appears to be an important factor. Reducing building energy demand, thus reducing energy consumption by applying insulation material with high thermal resistance means reducing fossil fuels used for heating as well as fossil fuel-based carbon emissions. In this way, energy-related air pollution can be reduced (Yaşar et al., 2004). In addition, urbanization, industrialization, technological development and population growth

\*Corresponding author: Yasin Erdoğan, [yasin.erdogan@iste.edu.tr](mailto:yasin.erdogan@iste.edu.tr)  
<http://dx.doi.org/10.19111/bmre.74700>

in our developing world requires an increasingly noisy way of life. Today, noise is expressed as an environmental problem as well as a health issue. To get rid of this problem, people are seeking a quiet and peaceful life as much as possible. In order to reduce noise pollution, living areas with high sound insulation and less noise should be developed. For this reason, the product developed in this study has heat conduction as well as sound insulation properties, providing great advantages in terms of marketing the product (Erdoğan and Yaşar, 2012; Erdoğan, 2007).

A number of research projects have investigated about insulation materials. Aspiras and Manalo (1995) analyzed composites made from textile waste cuttings and Portland cement; and Fisher et al. (2001) studied the suitability of cellulose fibers, Kriker et al. (2004) of palm fibers, Perry (2003) of long and short synthetic fibers, Wong (2004), Meyer et al. (2002) of different kinds of specific and waste fibers, Schmidt and Cieslak (2007) analyzed concrete with carpet recycles.

In this study has been reported on the development of insulation materials from carpet waste fibers with comparable properties as that of conventional materials. Two different insulating materials were produced by mixing carpet wastes with a solution with added crude colemanite ore, a boron derivative, and a solution with added colemanite wastes from a barrage. The name, HaliBor, was chosen as the designation for the resultant insulation material for use in patent applications. The product (HaliBor) is a low-cost material with high heat and sound insulation values, whose physical and mechanical properties comply with standards in building and construction industry.

Moreover, mineralogical advantages of boron and use of idle raw materials enabled the product to be both a fire-resistant and an environmentally friendly material.

## 2. Materials and methods

### 2.1. Material

Carpets are complex composite material structures often made from a number of natural or synthetic materials. A typical carpet has four main layers or components. The top layer, or face fiber, represents the main component in the carpet waste and is usually made of wool, nylon or polypropylene (Olivares-Marin and Maroto-Valer, 2011). Weft yarn, warp yarn and pile yarn are used to manufacture carpets. In the province of Gaziantep, where almost half of Turkey's carpet production takes place, it was determined that total wastage and loss of yarns per year amounts to 6-16% for weft yarn, 10-15% for warp yarn and 15-20% for pile yarn. According to information obtained from carpet factories and studies in the literature, annual total amount of carpet waste is approximately 600.000 tonnes. For the national economy, such high amount of carpet waste is a significant loss. Furthermore, carpet edges, threads ripped away from rug underlay and jute yarn generated in carpet factories or plants for cutting carpets are important wastes which are sustainable wastes waiting to be utilized. Main theme of this study was to utilize constantly increasing carpet wastes and use boron, a valuable resource of Turkey, in this sector (Kozak, 2010). During preliminary studies, the state of the carpet wastes of a company operating in carpet making in the province of Gaziantep, was examined and these wastes were found to be generated consistently (Figure 1).



Figure 1- Kinds of carpet waste

Boron is a chemical element shown with symbol B in the periodic table and its atomic number is 5. Other properties of boron are as follows: atomic weight: 10.81, density: 2.84 gr/cm<sup>3</sup>, melting point: 2300°C and boiling point: 2550°C. It is a metalloid with semiconductor properties. It is found in the form of compounds with other elements and is not found naturally on Earth. There are about 230 varieties of boron in nature. Since it is susceptible to bonding with oxygen, there is a wide variety of boron-oxygen compounds. Boron-oxygen compounds are generally called borate. Turkey has 72.2% of the world's boron deposits, and mining and processing of high grade boron ores is very easy and cost-effective.

In the study, carpet wastes were mixed with two individual solutions with different concentrations. The first solution contains concentrated colemanite ore with 36.19% of B<sub>2</sub>O<sub>3</sub>, and the other contains concentrated colemanite waste with 25.77% of B<sub>2</sub>O<sub>3</sub>. Colemanite ore and concentrated wastes were supplied by Emet Boron Works attached to Directorate- General of Eti Mining, and their chemical composition is given in table 1. Concentrated colemanite wastes are stored in barrage pools inside the facility and are not used. Efforts were made to also use these idle concentrated wastes, which pose an environmental problem, to produce the resultant HaliBor material. After completion of all these procedures, the mixture was pressed and the insulation material was dried (Batar et al., 2009; Yılmaz, 2004). Furthermore, an adhesive called Carboxy Methyl Cellulose (CMC), commonly used in the industry, was used in order to obtain a more robust insulation material, produced from a mixture of carpet wastes and colemanite ore solution.

Table 1- Espey concentrate colemanite ore and chemical analysis of colemanite waste.

Chemical Composition	Concentrate Ore (%)	Espey Colemanite Waste (waste of old dam) (%)
B <sub>2</sub> O <sub>3</sub>	36,19	25,77
SiO <sub>2</sub>	14,6	22,46
Fe <sub>2</sub> O <sub>3</sub>	1,04	1,51
Al <sub>2</sub> O <sub>3</sub>	3,84	5,83
CaO	19,83	15,9
MgO	2,46	5,02
TiO <sub>2</sub>	3,54	4,84
As(ppm)	205	400
SO <sub>4</sub>	0,13	0,18

## 2.2. Method

Flow diagram for the production of insulation material with added boron from carpet wastes is given in figure 2. As seen in figure 2, first, carpet wastes were cut and torn into pieces. Then, pre-determined amounts of water, colemanite, and CMC and carpet wastes were placed inside a mixer and mixed, after which the resultant product was placed inside a mold, pressed and shaped. Following the pressing procedure, the product was oven-dried at 35°C for 4 hours and became ready for use.

## 3. Results and Discussion

As a result, two different products which gave optimal values were obtained. The product with added crude colemanite ore was designated as HaliBor-1, and the other with added colemanite barrage waste was designated as HaliBor-2. The resultant materials were designed in dimensions of 40 x 40 x 10 cm (width x length x height).

Physical and mechanical properties of the product (density, thermal conductivity, flame retardancy properties and sound insulation values) were determined. In addition, HaliBor-1 and HaliBor-2 were compared with other insulation and construction materials used in building and construction industry. A classification of materials by flame retardancy values was made according to the DIN 4112 standard and the results are given in table 2 (DIN 4112, 1960, <http://www.termolnumara.com>). In view of table-2, it is clear that HaliBor insulation materials gave considerably good results when compared with other materials used in the industry. A density value ranging between 185 and 200 kg/m<sup>3</sup> was obtained.

The insulation material with values comparable to those of HaliBor-1 in the industry is glass wool. HaliBor-1 with added crude ore turned out to be a new insulation material with the lowest density value used in the industry (Figure 3).

Thermal conductivity tests were performed according to TS 825. The results showed that HaliBor-1 and HaliBor-2 gave values of 0.035 λW/(mK) and 0.04 λW/(mK), respectively. When HaliBor with added boron and carpet waste was compared with other materials, it was seen that HaliBor-1 with added crude ore also gave the highest heat insulation value (Figure 4).

Production of an Insulation Material From Carpet and Boron Wastes

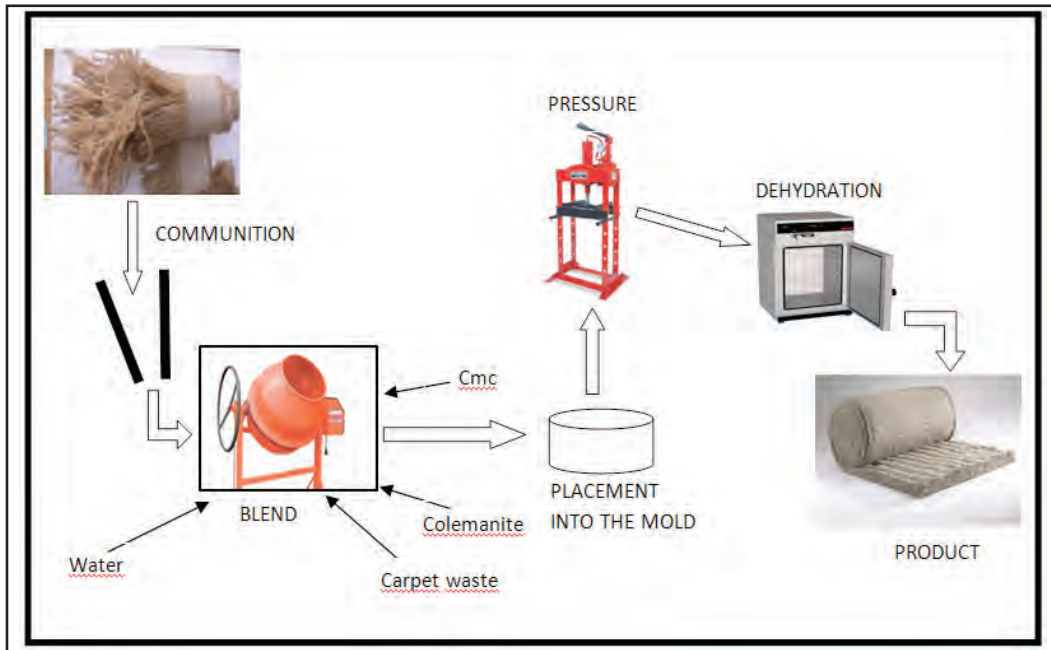


Figure 2- HaliBor production plan.

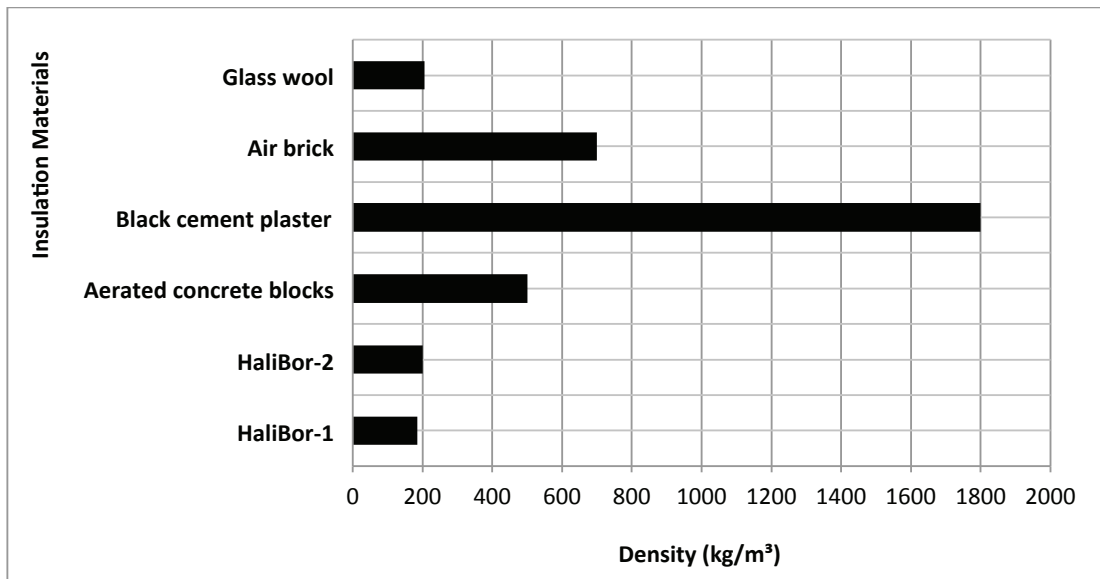


Figure 3- Density values of the sealing materials.

Table 2- Comparison Table of Various Structural Elements (<http://www.termo1numara.com>).

Insulation Material	Density(kg/m³)	Thermal Conductivity λ.W/(mK)	Flammability (DIN 4112)	Sound Insulation (dB) (10cm/500hz)
HaliBor-1	185	0,035	B1- Difficult Flaming	38
HaliBor-2	200	0,04	B1- Difficult Flaming	38
Aerated concrete blocks	500	0,14	B1- Difficult Flaming	38
Black cement plaster	1800	0,87	A- Fireproof	35
Air brick	700	0,24	A- Fireproof	37
Glass wool	205	0,04	B1- Difficult Flaming	36

Sound insulation is given by the amount of sound absorbed by the materials to provide insulation in a room with sound insulation where sound is emitted by an amplifier at a certain distance (TS EN ISO 10140-3, 2011). Considering the results obtained, it is clear that HaliBor-1 and 2 were the materials offering the highest insulation along with aerated concrete (Figure 5).

#### 4. Conclusions

In this study, it was understood that carpet wastes with limited use in the industry and concentrated colemanite ore and wastes can be used to generate

insulation materials. The insulation material with added crude colemanite ore was designated as HaliBor-1, and the other with added concentrated colemanite wastes was designated as HaliBor-2.

Physical properties of HaliBors were determined and comparisons were made with other insulation materials used in the industry. As a result of such comparisons, it was seen that HaliBors can be used quite easily in building and construction industry. Importance and value of the work was further increased by the fact that waste materials were recycled to obtain a different product.

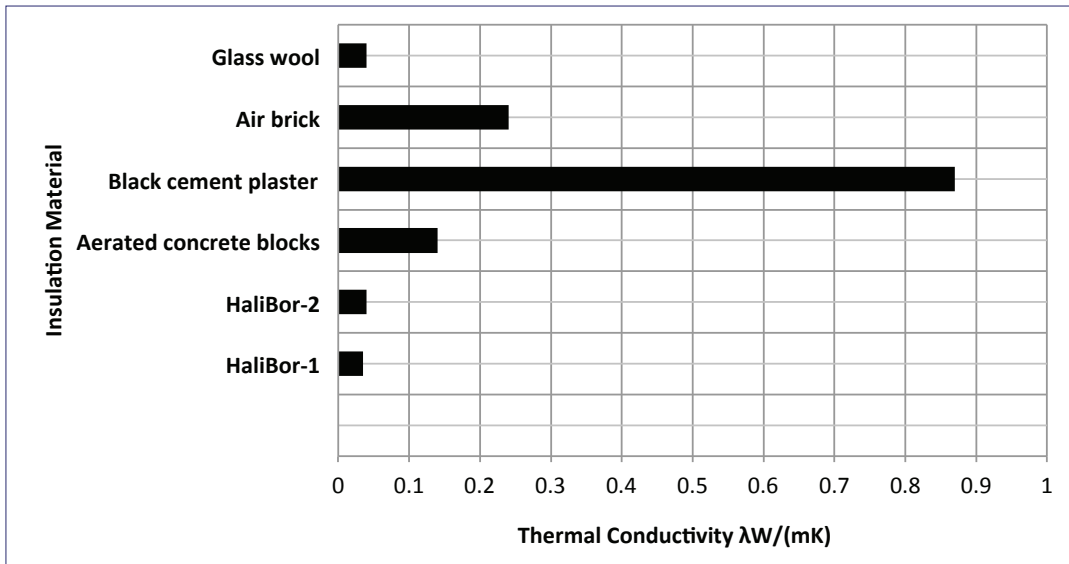


Figure 4- Thermal insulation value of insulation materials.

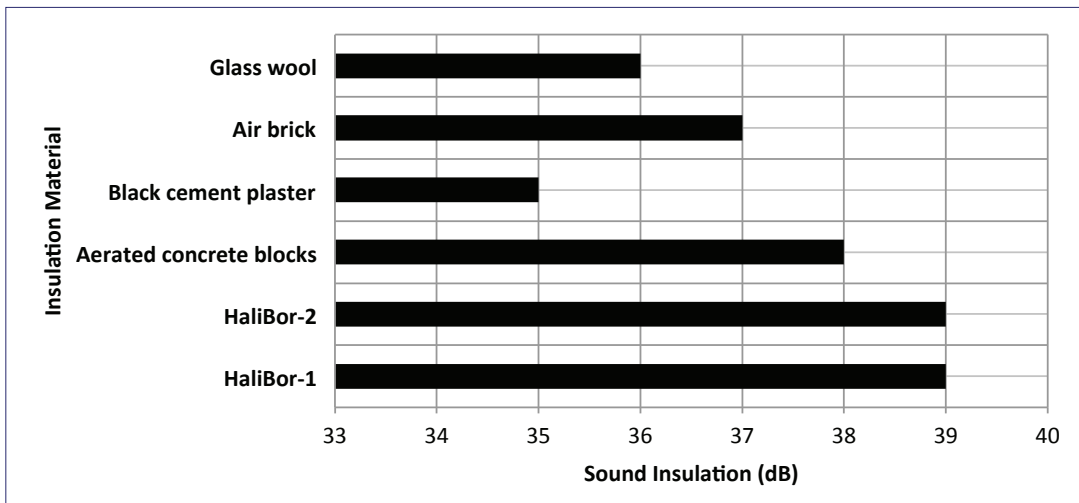


Figure 5- Sound insulation values of insulation materials.

## References

- Aspiras, F.F., Manalo, J.R.I. 1995. Utilization of textile waste cuttings as building material. *Journal of Materials Processing Technology* 48, 379–384.
- Batar, T., Köksal, N. S., Yersel E., Ş. 2009. Waste boron doped waste paper and plaster perlite production and characterization of materials, *Ecology*, 18, 72, 45-53
- Demir, I., Orhan, M. 2006. Building materials in the production of Boron waste assessment. *1st International Symposium on Boron Book*. Ankara.
- DIN 4112. 1960. Temporary structures, code of practise for design and construction, *German National Standard*. <http://www.termo1numara.com>
- Eken, M. 2012. Use of waste materials in the Production of insulation material, Sütçü İmam University, *Master's Thesis, Department of Civil Engineering, Kahramanmaraş*.
- Erdoğan, Y. 2007. Produced from acidic and basic Pumice Investigation of characteristics of Building Materials Engineering, *Cukurova University, Institute of Science, PhD thesis*, 301 p. Adana
- Erdoğan, Y., Yasar, E. 2005. Pumice briquette produced from Nevşehir in terms of the evaluation of the heat and sound conductivity, *19th International Mining Congress and Exhibition - IMCET2005, The Chamber of Mining Eng.*, İzmir.
- Erdoğan Y., Yaşar E. 2012. Nevşehir pumice produced from acidic lightweight concrete examination of the sound insulation value. *8th International Symposium on Industrial Minerals*, p. 89-97, Istanbul
- Fisher, A.K., Bullen, F., Beal, D. 2001. The durability of cellulose fiber reinforced concrete pipes in sewage applications. *Cement and Concrete Research*, 31, 543–553.
- Keskin, T. 2010. The current state of the building sector assessment report, Turkey's national climate change action plan to develop the project report, *Ministry of Energy and Natural Resources*. Ankara
- Kozak, M. 2010. Investigation of The Usage of Textile Waste as Construction Materials. *Electronic Journal of Construction Technologies*, 2010, 6(1) 62-70.
- Kriker, A., Debicki, G., Bali, A., Khenfer, M.M., Chabannet, M. 2004. Mechanical properties of date palm fibers and concrete reinforced with date palm fibers in hot-dry climate. *Cement and Concrete Composites*, 27, 554–564.
- Meyer, C., Shimanovich, S., Vilkner, G. 2002. Precast concrete wall panels with glass concrete. Final Report for The New York State Energy Research and Development Authority (NYSERDA), Albany, NY.
- Olivares-Marin, M., Maroto-Valer, M.M. 2011. Preparation of a highly microporous carbon from a carpet material and its application as CO<sub>2</sub> sorbent, *Fuel Processing Technology*, 92, 322–329.
- Perry, B. 2003. Reinforcing external pavements with both large and small synthetic fibers. *Concrete*, 37 (8), 46–47.
- Schmidt, H., Cieslak, M. 2007. Concrete with carpet recyclates: Suitability assessment by surface energy evaluation, *Waste Management*, 28, 1182–1187.
- TS 825, 2011. Thermal insulation requirements for buildings. *Turkish Standards Institution*. Ankara.
- TS En ISO 10140-3, 2011. Acoustics - Laboratory measurement of sound insulation of building elements - Part 3: Measurement of impact sound insulation, *Turkish Standards Institution*. Ankara.
- Wong, Ch.M. 2004. Use of short fibers in structural concrete to enhance mechanical properties. A Dissertation. University of Southern Queensland.
- Yaşar E., Erdoğan Y., Kilic A. 2004. Effect of limestone aggregate type and water-cement ratio on concrete strength, *Material Letters*, 58 (5), 772-777.
- Yılmaz, A. 2004. Energy Saving Boron and Perlite, *Eti Mine Works General Directorate*, Ankara

# **BULLETIN OF THE MINERAL RESEARCH AND EXPLORATION NOTES TO THE AUTHORS**

## **1. Aims**

The main aims of the journal are

- To contribute to the providing of scientific communication on geosciences in Turkey and the international community.
- To announce and share the researches in all fields of geoscience studies in Turkey with geoscientists worldwide.
- To announce the scientific researches and practices on geoscience surveys carried out by the General Directorate of Mineral Research and Exploration (MTA) to the public.
- To use the journal as an effective media for international publication exchange by keeping the journal in high quality, scope and format.
- To contribute to the development of Turkish language as a scientific language

## **2. Scope**

At least one of the following qualifications is required for publishing the papers in the *Bulletin of Mineral Research and Exploration*.

### **2.1. Research Articles**

#### **2.1.1. Original Scientific Researches**

- This type of articles covers original scientific research and its results related to all aspects of disciplines in geoscience.

#### **2.1.2. Development Researches**

- The studies using new approaches and methods to solve any problems related to geosciences and/or the researches using new approaches and methods to solve any problems related to the science of engineering performed in the General Directorate of Mineral Research and Exploration.

#### **2.1.3. Review articles**

- This type of papers includes comprehensive scholarly review articles that summarize and critically assess previous geoscience research with a new perspective and it also reveals a new approach.

## **2.2. Discussion/Reply**

- This type of article is intended for discussions of papers that have already been published in the latest issue of the Bulletin.
- The discussion/reply type articles that criticize all or a part of a recently published article, are published in the following first issue, if it is submitted within six months after the distribution of the Bulletin.
- The discussions are sent to the corresponding author of the original paper to get their reply, before publication. So that, the discussion and reply articles can be published at the same time, if they can be replied within the prescribed period. Otherwise, the discussion is published alone. Re-criticising of the replies is not allowed. The authors should keep the rules of scientific ethics and discussions in their discussion/reply papers. The papers in this category should not exceed four printed pages of the journal including figures and tables etc. The format of the papers should be compatible with the "Spelling Rules" of the Bulletin.

## **2.3. Short Notes**

- Short notes publishing in the Bulletin covers short, brief and concisely written research reports for papers including data obtained from ongoing and/or completed scientific researches and practices related to geoscience and new and/or preliminary factual findings from Turkey and worldwide.
- The short notes will follow a streamlined schedule and will normally published in the following first or second issue shortly after submission of the paper to the Bulletin. To meet this schedule, authors should be required to make revisions with minimal delay.
- This type of articles should not exceed four printed pages of the journal including figures, tables and an abstract.

## **3. Submission and Reviewing of Manuscripts**

Manuscript to be submitted for publishing in the Journal must be written clearly and concisely in Turkish and/or English and it should be prepared in the *Bulletin of Mineral Research and Exploration* style

guidelines. All submissions should be made online at the <http://bulletin.mta.gov.tr> website.

The authors, having no facility for online submission can submit their manuscript by post-mail to the address given below. They should submit four copies of their manuscript including one original hard copy, and CD. The files belonging to manuscript should be clearly and separately named as “Text”, “Figures” and “Tables” at the CD.

*Address:*

*Maden Tetkik ve Arama Genel Müdürlüğü*

*Redaksiyon Kurulu Başkanlığı*

Üniversiteler Mah. Dumlupınar Bulvarı, No: 139

06800 Çankaya-Ankara

- The manuscript submitted for reviews has not been partially or completely published previously; that it is not under consideration for publication elsewhere in any language; its publication has been approved by all co-authors.
- The rejected manuscripts are not returned back to author(s) whereas a letter of statement indicating the reason of rejection is sent to the corresponding author.
- Submitted manuscripts must follow the *Bulletin* style and format guidelines. Otherwise, the manuscript which does not follow the journals' style and format guidelines, is given back to corresponding author without any reviewing.
- Every manuscript which passes initial Editorial treatise is reviewed by at least two independent reviewers selected by the Editors. Reviewers' reports are carefully considered by the Editors before making decisions concerning publication, major or minor revision or rejection.
- The manuscript that need to be corrected with the advices of reviewer(s) is sent back to corresponding author(s) to assess and make the required corrections suggested by reviewer(s) and editors. Authors should prepare a letter of well-reasoned statement explaining which corrections are considered or not.
- The Executive editor (Editorial Board) will inform the corresponding author when the manuscript is approved for publication. Final version of

text, tables and figures prepared in the *Bulletin of Mineral Research and Exploration* style and format guidelines, will need to be sent online and the corresponding author should upload all of the manuscript files following the instructions given on the screen. In the absence of online submission conditions, the corresponding author should send four copies of the final version of the manuscript including one original hard copy, and CD by post-mail. The files belonging to manuscript should be clearly and separately named as “Text”, “Figures” and “Tables” at the CD.

- To be published in the *Bulletin of Mineral Research and Exploration*, the printed length of the manuscript should not exceed 30 printed pages of the journal including an abstract, figures and tables. The publication of longer manuscripts will be evaluated by Editorial Board if it can be published or not.

#### **4. Publication Language and Periods**

- *The Bulletin of Mineral Research and Exploration* is published at least two times per year, each issue is published both in Turkish and English. Thus, manuscripts are accepted in Turkish or English. The spelling and punctuation guidelines of Turkish Language Institution are preferred for the Turkish issue. However, technical terms related to geology are used in accordance with the decision of the Editorial Board.

#### **5. Spelling Draft**

Manuscripts should be written in word format in A4 (29.7 x 21 cm) size and double-spaced with font size Times New Roman 10-point, margins of 25 mm at the sides, top and bottom of each page. Authors should study carefully a recent issue of the *Bulletin of Mineral Research and Exploration* to ensure that their manuscript correspond in format and style.

- The formulas requiring the use of special characters and symbols must be submitted on computer.
- Initial letters of the words in sub-titles must be capital. The first degree titles in the manuscript must be numbered and left-aligned, 10 point bold Times New Roman must be used. The second degree titles must be numbered and left-aligned, they must be written with 10 point normal Times New Roman. The third degree titles must be

numbered and left-aligned, they must be written with 10 point italic Times New Roman. The fourth degree titles must be left-aligned without having any number; 10 point italic Times New Roman must be used. The text must continue placing a colon after the title without paragraph returns (See:Sample article: <http://bulletin.mta.gov.tr>).

- Line spacing must be left after paragraphs within text.
- Paragraphs must begin with 0.5 mm indent.
- The manuscript must include the below sections respectively;
  - o Title Page
  - o Abstract
  - o Key Words
  - o Introduction
  - o Body
  - o Discussion
  - o Conclusion
  - o Acknowledgements
  - o References

### 5.1. Title Page and Author's Address

The title page should include:

A short, concise and informative title

The name(s) of the author(s)

The affiliation(s) and address(es) of the author(s)

The e-mail address, telephone and fax numbers of the corresponding author

The title must be short, specific and informative and written with capital letters font size Times New Roman 10-point bold. The last name (family name) and first name of each author should be given clearly. The authors' affiliation addresses (where the actual work was done) are presented below the names and all affiliations with a lower-case superscript letter is indicated immediately after the author's name and in front of the appropriate address. Provide the full postal address of each affiliation, including the country name and, if available, the e-mail address of each author.

The author who will handle correspondance at all stages of refereeing and publication, also post-publication are to be addressed (the corresponding author) should be indicated and the telephone, FAX and e-mail address given.

Please provide a running title of not more than 50 characters for both Turkish and English issue.

### 5.2. Abstract

- The article must be preceded by an abstract, which must be written on a seperate page as one paragraph, preferably. Please provide an abstract of 150 to 200 words. The abstract should not contain any undefined or non-standard abbreviations and the abstract should state briefly the overall purpose of the research, the principle results and major conclusions. Please omit references, criticisms, drawings and diagrams.
- Addressing other sections and illustrations of the text or other writings must be avoided.
- The abstract must be written with 10-point normal Times New Roman and single-spaced lines.
- "Abstract" must not be given for the writings that will be located in "Short Notes" section.
- English abstract must be under the title of "Abstract".

### 5.3. Key Words

Immediately after the abstract, please provide up to 5 key words and with each word seperated by comma. These key words will be used for indexing purposes.

### 5.4. Introduction

- The introduction section should state the objectives of the work, research methods, location of the study area and provide an adequate and brief background, avoiding a detailed literature survey.
- Non-standard or un-common classifications or abbreviations should be avoided but if essential, they must be defined at their first mention and used consistently thereafter.
- When needed reminder information for facilitating the understanding of the text, this section can also be used (for example, statistical data, bringing out the formulas, experiment or application methods, and others).

### 5.5. Body

- In this chapter, there must be data, findings and opinions that are intended to convey the reader about the subject. The body section forms the main part of the article.
- The data used the other sections such as “Abstract”, “Discussions”, and “Results” is caused by this section.
- While processing subject, care must be taken not to go beyond the objective highlighted in “Introduction” section. The knowledge which do not contribute to the realization of the purpose of the article or are useless for conclusion must not be included.
- All the data used and opinions put forward in this section must prove the findings obtained from the studies or they must be based on a reference by citation.
- Guidance and methods to be followed in processing subjects vary according to the characteristics of the subjects dealt with. Various phased topic titles can be used in this section as many as necessary.

### 5.6. Discussions

- This section should explore the significance of the results of the work, not repeat them. This must be written as a separate section from the results.

### 5.7. Conclusions

- The main conclusion of the study provided by data and findings of the research should be stated concisely and concretely in this section.
- The subjects that are not mentioned sufficiently and/or unprocessed in the body section must not be included in this section.
- The conclusions can be given in the form of substances in order to emphasize the results of the research and be understandable expression.

### 5.8. Acknowledgements

Acknowledgement of people, grants, funds, etc should be placed in a separate section before the reference list. While specifying contributions, the attitude diverted the original purpose of this section away is not recommended. Acknowledgments must be made according to the following examples.

- This study was carried out under the.....project.
- I/we would like to thank to ..... for contributing the development of this article with his/her critiques.
- Academic and / or authority names are written for the contributions made because of ordinary task requirement.

For example:

- o “Prof. Dr. İ. Enver Altınlı has led the studies”.
- o “The opinions and warnings of Dr. Ercüment Sirel are considered in determining the limits of İlerdiyen layer.”
- The contributions made out of ordinary task requirement:

**For example:**

- o “I would like to thank to Professor Dr. Melih Tokay who gives the opportunity to benefit from unpublished field notes”; “I would like to thank to State Hydraulic Work 5. Zone Preliminary-Plan Chief Engineer Ethem Göğçer.” Academic and /or task-occupational titles are indicated for this kind of contributions.
- The contributions which are made because of ordinary task requirement but do not necessitate responsibility of the contributor must be specified.

**For example:**

- o Such sentences as “I would like to thank to our General Manager, Head of Department or Mr. / Mrs. President .....who has provided me the opportunity to research” must be used.

### 5.9. References

- All references cited in the text are to be present in the reference list.
- The authors must be sure about the accuracy of the references. Publication names must be written in full.
- Reference list must be written in Times New Roman, 9-point type face.
- The reference list must be alphabetized by the last names of the first author of each work.

- If an author's more than one work is mentioned, ranking must be made with respect to publication year from old to new.
- In the case that an author's more than one work in the same year is cited, lower-case alphabet letters must be used right after publication year (for example; Saklar, 2011a, b).
- If the same author has a publication with more than one co-author, firstly the ones having single author are ranked in chronological order, then the ones having multiple authors are ranked in chronological order.
- In the following examples, the information related to works cited is regulated in accordance with different document/work types, considering punctuation marks as well.
- If the document (periodic) is located in a periodical publication (if an article), the information about the document must be given in the following order: surnames of the author/authors, initial letters of author's/ authors' first names. Year of publication. Name of the document. Name of the publication where the document is published (in italics), volume and/ or the issue number, numbers of the first and last pages of the document.

**For example:**

- o Pamir, H.N. 1953. Türkiye'de kurulacak bir hidrojeoloji enstitüsü hakkında rapor. *Türkiye Jeoloji Bülteni* 4, 1, 63-68.
- o Barnes, F., Kaya, O. 1963. İstanbul bölgesinde bulunan Karbonifer'in genel stratigrafisi. *Maden Tetkik ve Arama Dergisi* 61,1-9.
- o Robertson, A.H.F. 2002. Overview of the genesis and emplacement of Mesozoic ophiolites in the Eastern Mediterranean Tethyan region. *Lithos* 65, 1-67.
- If more than one document by the same authors is cited, firstly the ones having single name must be placed in chronological order, then the ones having two names must be listed in accordance with chronological order and second author's surname, finally the ones having multiple names must be listed in accordance with chronological order and third author's surname.

- If the document is a book, these are specified respectively: surnames of the author/authors, initial letters of author's/authors' first names. Year of publication. Name of the book (initial letters are capital). Name of the organization which has published the book (in italics), name of the publication where the document is published, volume and/ or the issue number, total pages of the book.

**For example**

- o Meric, E. 1983. Foraminiferler. *Maden Tetkik ve Arama Genel Müdürlüğü Eğitim Serisi* 23, 280p.
- o Einsele, G. 1992. Sedimentary Basins. *Springer-Verlag*, p 628.
- If the document is published in a book containing the writings of various authors, the usual sequence is followed for the documents in a periodic publication. Then the editor's surname and initial letters of their name /names are written. "Ed." which is an abbreviation of the editor word is written in parentheses. Name of the book containing the document (initial letters are capital ). Name of the organization which has published the book (*in italics*). Place of publication, volume number (issue number, if any) of the publication where the document is published, numbers of the first and last page of the document.

**For example:**

- o Göncüoğlu, M.C., Turhan, N., Şentürk, K., Özcan, A., Uysal, Ş., Yalınız, K. 2000. A geotraverse across northwestern Turkey. Bozkurt, E., Winchester, J.A., Piper, J.D.A. (Ed.). *Tectonics and Magmatism in Turkey and the Surrounding Area. Geological Society of London Special Publication* 173, 139-162.
- o Anderson, L. 1967. Latest information from seismic observations. Gaskell, T.F. (Ed.). *The Earth's Mantle*. Academic Press. London, 335-420.
- If name of a book where various authors' writings have been collected is specified, those must be indicated respectively: book's editor/editors' surname/surnames, and initial letters of their name/names. "Ed." which is an abbreviation of the editor word must be written in parentheses. Year

of Publication. Name of the book (initial letters are capital). Name of the organization which has published the book (*in italics*), total pages of the book.

**For example:**

- o Gaskel, T.F.(Ed.)1967. The Earth's Mantle. *Academic Press*, 520p.
- If the document is an abstract published in a Proceedings Book of a scientific activity such as conference/symposium/workshop ...etc., information about the document must be given in the following order: surnames of the author/authors, initial letters of author's/authors' first names. Year of publication. Title of the abstract. Name (*in italics*), date and place of the meeting where the Proceedings Book is published, numbers of the first and last pages of the abstract in the Proceedings Book.

**For example:**

- o Yılmaz, Y. 2001. Some striking features of the Anatolian geology. 4. *International Turkish Geology Symposiums*, 24-28 September 2001, London, 13-14.
- o Öztunalı, Ö., Yenişol, M. 1980. Yunak (Konya) yöresi kayaçlarının petrojenezi. *Türkiye Jeoloji Kurumu 34. Bilim Teknik Kurultayı*, 1980, Ankara, 36
- If the document is unpublished documents as report, lecture notes, and so on., information about the document must be given by writing the word "unpublished" in parentheses to the end of information about the document after it is specified in accordance with usual order which is implemented for a document included in a periodic publication.

**For example:**

- o Özdemir, C. Biçen, C. 1971. Erzincan ili, İliç ilçesi ve civarı demir etütleri raporu. *General Directorate of Mineral Research and Exploration Report No: 4461*, 21 p. Ankara (unpublished).
- o Akyol, E. 1978. Palinoloji ders notları. *EÜ Fen Fakültesi Yerbilimleri Bölümü*, 45 p., İzmir (unpublished).

- The followings must be specified for the notes of unpublished courses, seminars, and so on: name of the document and course organizer. Place of the meeting. Name of the book, corresponding page numbers.

**For example:**

- o Walker, G. R. Mutti, E. 1973. Turbidite facies and facies associations. Pacific Section Society for Sedimentary Geology Short Course. Anaheim. Turbidites and Deep Water Sedimentation, 119-157.
- If the document is a thesis, the following are written: surname of the author, initial letter of the author's first name. Year of Publication. Name of the thesis. Thesis type, the university where it is given, the total number of pages, the city and "unpublished" word in parentheses.

**For example:**

- o Seymen, İ. 1982. Kaman dolayında Kırşehir Masifi'nin jeolojisi. Doçentlik Tezi, İTÜ Maden Fakültesi, 145 s.İstanbul (unpublished).
- Anonymous works must be regulated according to publishing organization.

**For example:**

- o MTA. 1964. 1/500.000 ölçekli Türkiye Jeoloji Haritası, İstanbul Paftası. Maden Tetkik ve Arama Genel Müdürlüğü, Ankara.
- The date, after the name of the author, is not given for on-printing documents; "in press" and / or "on review" words in parenthesis must be written. The name of the article and the source of publication must be specified, volume and page number must not be given.

**For example:**

- o Ishihara, S. The granitoid and mineralization. *Economic Geology 75th Anniversary* (in press).
- Organization name, web address, date of access on web address must be indicated for the information downloaded from the Internet. Turkish sources must be given directly in Turkish and they must be written with Turkish characters.

**For example:**

- o ERD (Earthquake Research Department of Turkey). <http://www.afad.gov.tr>. March 3, 2013.
- While specifying work cited, the original language must be used; translation of the title of the article must not be done.

## 6. Illustrations

- All drawings, photographs, plates and tables of the article are called “illustration”.
- Illustrations must be used when using them is inevitable or they facilitate the understanding of the subject.
- While selecting and arranging the illustrations’ form and dimensions, page size and layout of the *Bulletin* must be considered, unnecessary loss of space must be prevented as much as possible.
- The pictures must have high quality, high resolution suitable for printing.
- The number of illustrations must be proportional to the size of the text.
- All illustrations must be sent as separate files independent from the text.
- While describing illustrations in the text, abbreviations must be avoided and descriptions must be numbered in the order they are mentioned in the text.
- Photographs and plates must be given as computer files containing EPS, TIFF, or JPEG files in 600 dpi and higher resolutions (1200 dpi is preferred) so that all details can be seen in the stage of examination of writing.

### 6.1. Figures

- Drawings and photos together but not the plate in the text can be evaluated as “Figure” and they must be numbered in the order they are mentioned in the text.
- The figures published in the *Bulletin of Mineral Research and Exploration* must be prepared in computing environment considering the dimensions of single-column width 7.4 cm or double-column width 15.8 cm. Figure area together with the writing at the bottom should not exceed a maximum 15.8x21.

- Figures must not be prepared in unnecessary details or care must be taken not to use a lot of space for information transfer.
- Figures must be arranged to be printed in black-and-white or colored. The figure explanations being justified in two margins must be as follows:

Figure 1 -Sandıklı Town (Afyon); a) Geological map of the south-west, b) general columnar section of the study area (Seymen 1981), c) major neotectonic structures in Turkey (modified from Koçyiğit 1994).

- Drawings must be drawn by well-known computer programs painstakingly, neatly and cleanly.
- Using fine lines which can disappear when figures shrink must be avoided. Symbols or letters used in all drawings must be Times New Roman and not be less than 2 mm in size when shrink.
- All the standardized icons used in the drawings must be explained preferably in the drawing or with figure caption if they are very long.
- Linear scale must be used for all drawings. Author’s name, figure description, figure number must not be included into the drawing.
- Photos must have the quality and quantity that will reflect the objectives of the subject.

### 6.2. Plates

- Plates must be used when needed a combination of more than one photo and the publication on a special quality paper.
- Plate sizes must be equal to the size of available magazine pagespace.
- Figure numbers and linear scale must be written under each of the shapes located on the Plate.
- The original plates must be added to the final copy which will be submitted if the article is accepted.
- Figures and plates must be independently numbered. Figures must be numbered with Latin numerals and plates with Roman numerals (e.g., Figure1, Plate I).
- There must be no description text on Figures.

### 6.3. Tables

- Tables must be numbered consecutively in accordance with their appearance in the text.
- All tables must be prepared preferably in word format in Times New Roman fonts.
- Tables together with table top writing must not exceed 15x8 cm size.
- The table explanations being justified in two margins must be as follows:

Table 1- Hydrogeochemical analysis results of geothermal waters in the study area.

### 7. Nomenclature and Abbreviations

- Non-standard and uncommon nomenclature abbreviations should be avoided in the text. But if essential, they must be described as below: In cases where unusual nomenclatures and unstandardized abbreviations are considered to be compulsory, the followed way and method must be described.
- Full stop must not be placed between the initials of words for standardized abbreviations (MER, SHW, etc.).
- Geographical directions must be abbreviated in English language as follows: N, S, E, W, NE ...etc.
- The first time used abbreviations in the text are presented in parenthesis, the parenthesis is not used for subsequent uses.
- The metric system must be used as units of measure.

- Figure, plate, and table names in the article must not be abbreviated. For example, “as shown in generalized stratigraphic cross-section of the region (Figure 1.....)”

#### 7.1. Stratigraphic Terminology

Stratigraphic classifications and nomenclatures must be appropriate with the rules of International Commission on Stratigraphy and/or Turkey Stratigraphy Committee. The formation names which has been accepted by International Commission on Stratigraphy and/or Turkey Stratigraphy Committee should be used in the manuscript.

#### 7.2. Paleontologic Terminology

Fossil names in phrases must be stated according to the following examples:

- o For the use authentic fossil names:

e.g. Calcareous sandstone with *Nummulites*

- o When the authentic fossil name is not used.

e.g. nummulitic Limestone

- o Other examples of use;

e.g. The type and species of *Alveolina*/ *Alveolina* type and species

- Taxonomic ranks must be made according to following examples:

Super family: <i>Alveolina</i> Ehrenberg, 1939 Family: <i>Borelidae</i> Schmarda, 1871 Type genus: <i>Borelis</i> de Montfort, 1808 Type species: <i>Borelis melenoides</i> de Montfort, 1808; <i>Nautilus melo</i> Fitchel and Moll, 1789	<i>Not reference, Not stated in the Reference section</i>
<i>Borelis vonderschmitti</i> (Schweighauser, 1951) (Plate, Figure, Figure in Body Text)	<i>Schweighauser, 1951 not reference</i>
1951 <i>Neoalveolina vonderschmitti</i> Schweighauser, page 468, figure 1-4	<i>Cited Schweighauser (1951), stated in the Reference section.</i>
1974 <i>Borelis vonderschmitti</i> (Schweighauser), Hottinger, page, 67, plate 98, figure 1.7	<i>Cited Hottinger (1974), stated in the Reference section.</i>

- The names of the fossils should be stated according to the rules mentioned below:
- o For the first use of the fossil names, the type, species and the author names must be fully indicated

*Alveolina aragoensis* Hottinger

*Alveolina cf. Aragoensis* Hottinger

- o When a species is mentioned for the second time in the text:

A.aragoensis

A.cf.aragoensis

A.aff.aragoensis

- o It is accepted as citation if stated as *Alveolina aragoensis* Hottinger (1966)
- The statement of plates and figures (especially for articles of paleontology):
- o for statement of the species mentioned in the body text

*Borelis vonderschmitti* (Schweighauser, 1951).

(plate, figure, figure in the body text).

- o When citing from other articles

1951 *Neoalveolina vonderschmitti* Schweighauser, page 468, figure 1-4, figure in body text

1974 *Borelis vonderschmitti* (Schweighauser), Hottinger, page 67, plate 98, figure 1-7

- For the citation in the text
- (Schweighauser, 1951, page, plate, figure, figure in the body text) (Hottinger, 1974, page, plate, figure 67, plate 98, figure 1-7, figure in the bodytext.)

## 8. Citations

All the citations in the body text must be indicated by the last name of the author(s) and the year of publication, respectively. The citations in the text must be given in following formats.

- For publications written by single author:
- It is known that fold axial plain of Devonian and Carboniferous aged units around Istanbul is NS oriented (Ketin, 1953, 1956; Altınlı, 1999).

-Altınlı (1972, 1976) defined the general characteristics of Bilecik sandstone

- For publications written by two authors:

- The upper parts of the unit contain Ilerdian fossils (Sirel and Gündüz, 1976; Keskin and Turhan, 1987, 1989).

- For publications written by three or more authors:

According to Caner et al. (1975) Alıcı formation reflects the fluvial conditions.

The unit disappears wedging out in the East direction (Tokay et al., 1984).

- If reference is not directly obtained but can be found in another reference, cross-reference should be given as follows:

- It is known that Lebling has mentioned the existence of Lias around Çakraz (Lebling, 1932: from Charles, 1933).

## 9. Reprints

The author(s) will receive 5 free reprints and two hard copies of the related issues

## 10. Copyright and Conditions of Publication

- It is a condition of publication that work submitted for publication must be original, previously unpublished in whole or in part.
- It is a condition of publication that the authors who send their publications to the *Bulletin of Mineral Research and Exploration* hereby accept the conditions of publication of the Bulletin in advance.
- All copyright of the accepted manuscripts belong to MTA. The author or corresponding author on behalf of all authors (for papers with multiple authors) must sign and give the agreement under the terms indicated by the Regulations of Executive Publication Committee. Upon acceptance of an article, MTA can pay royalty to the authors upon their request according to the terms under the “Regulations of Executive Publication Committee” and the “Regulations of Royalty Payment of Public Office and Institutions”

All the information and forms about the *Bulletin of Mineral Research and Explorations* can be obtained from <http://bulletin.mta.gov.tr>